

Engineering Materials

Sarawut Rimdusit
Chanchira Jubsilp
Sunan Tiptipakorn

Alloys and Composites of Polybenzoxazines

Properties and Applications

 Springer

Engineering Materials

For further volumes:
<http://www.springer.com/series/4288>

Sarawut Rimdusit · Chanchira Jubsilp
Sunan Tiptipakorn

Alloys and Composites of Polybenzoxazines

Properties and Applications

 Springer

Sarawut Rimdusit
Department of Chemical Engineering
Chulalongkorn University
Bangkok
Thailand

Sunan Tiptipakorn
Department of Chemistry
Kasetsart University
Nakhon Pathom
Thailand

Chanchira Jubsilp
Department of Chemical Engineering
Srinakharinwirot University
Nakhon Nayok
Thailand

ISSN 1612-1317

ISSN 1868-1212 (electronic)

ISBN 978-981-4451-75-8

ISBN 978-981-4451-76-5 (eBook)

DOI 10.1007/978-981-4451-76-5

Springer Singapore Heidelberg New York Dordrecht London

Library of Congress Control Number: 2013941503

© Springer Science+Business Media Singapore 2013

This work is subject to copyright. All rights are reserved by the Publisher, whether the whole or part of the material is concerned, specifically the rights of translation, reprinting, reuse of illustrations, recitation, broadcasting, reproduction on microfilms or in any other physical way, and transmission or information storage and retrieval, electronic adaptation, computer software, or by similar or dissimilar methodology now known or hereafter developed. Exempted from this legal reservation are brief excerpts in connection with reviews or scholarly analysis or material supplied specifically for the purpose of being entered and executed on a computer system, for exclusive use by the purchaser of the work. Duplication of this publication or parts thereof is permitted only under the provisions of the Copyright Law of the Publisher's location, in its current version, and permission for use must always be obtained from Springer. Permissions for use may be obtained through RightsLink at the Copyright Clearance Center. Violations are liable to prosecution under the respective Copyright Law. The use of general descriptive names, registered names, trademarks, service marks, etc. in this publication does not imply, even in the absence of a specific statement, that such names are exempt from the relevant protective laws and regulations and therefore free for general use.

While the advice and information in this book are believed to be true and accurate at the date of publication, neither the authors nor the editors nor the publisher can accept any legal responsibility for any errors or omissions that may be made. The publisher makes no warranty, express or implied, with respect to the material contained herein.

Printed on acid-free paper

Springer is part of Springer Science+Business Media (www.springer.com)

Preface

In the past 30 years, only few polymers, that have been developed, are able to reach the commercial stage. Polybenzoxazines are one of those few. Their ease of synthesis with tremendous molecular design flexibility allows tailor-made properties with a broad range of applications. Their unique characteristics such as self-polymerizability upon heating without a need for a catalyst or curing agent, very low A-stage viscosity, near-zero volumetric shrinkage, fire resistant behaviors, as well as their outstanding thermal and mechanical properties make the polymer highly attractive for various applications including electronic packaging or aerospace.

Demand for high performance multicomponent polymeric materials based on existing polymers continues to be increasingly important from stringent requirements from a variety of industrial sectors. This book provides an introduction to the unique and fascinating properties of alloys and composites from novel commercialized thermosetting resins based on polybenzoxazines. Their outstanding properties such as processability, thermal, mechanical, electrical properties, as well as ballistic impact properties of polybenzoxazine alloys and composites are discussed and reviewed in the monograph. [Chapter 1](#) of this book presents an introduction to major and commercially available benzoxazine resins, their commercialized polymeric products, and their outstanding properties. [Chapter 2](#) presents major alloy systems based on polybenzoxazines and some synergistic behaviors observed in these alloys, whereas [Chap. 3](#) discusses the fundamentals of highly filled polybenzoxazine composite systems that render, e.g., very high thermomechanical and thermophysical composite materials. High thermal conductivity of filled polymers is one essential property desired for an application such as electronic packaging encapsulation and very high thermally conducting polybenzoxazine composites for such applications will be discussed in [Chap. 4](#). [Chapter 5](#) summarizes natural fiber-reinforced polybenzoxazine composites as a newly high performance wood-substituted material from the ability of polybenzoxazines to strongly adhere to lignocelulosic materials. An ability of polybenzoxazines to form polymer alloys with various types of other resins or polymers are demonstrated in [Chap. 6](#) on their applications as lightweight ballistic composites with high performance fibers such as KevlarTM. The last chapter of this book presents electrical properties of filled polybenzoxazine composites with those

conductive fillers such as carbon black and graphite. The composites are investigated for promising applications such as a bipolar plate in fuel cell, etc. Although [Chap. 2](#) and part of [Chap. 4](#) resemble original research articles, the information from these chapters is up-to-date and highly cited by researchers and thus worthy to be included in this book.

One of the authors, S. Rimdusit, would like to acknowledge the hard work by Manunya Okhawalai to help prepare this book ([Chap. 1](#)), and Isala Dueramae ([Chap. 3](#)). Finally, Dr. Ramesh N. Premnath of Springer is gratefully acknowledged from his continuous support and comments on the preparation of this book.

Contents

1 Introduction to Commercial Benzoxazine and Their Unique Properties	1
1.1 An Overview of Polybenzoxazines	1
1.2 Synthesis of Distinguished Benzoxazines and Their Properties.	3
1.2.1 Bisphenol-A- and Aniline-Based Benzoxazine Resin.	4
1.2.2 Bisphenol-F- and Aniline-Based Benzoxazine Resin	9
1.2.3 Thiobiphenol- and Aniline-Based Benzoxazine Resin	10
1.2.4 Phenolphthalein- and Aniline-Based Benzoxazine Resins.	11
1.2.5 Dicyclopentadiene- and Aniline-Based Benzoxazine Resins.	16
1.3 Major Producers of Benzoxazine Resins and Related Products	18
1.3.1 Huntsman Advanced Materials	18
1.3.2 Henkel Corporation	20
1.3.3 Gurit	21
1.3.4 Shikoku Chemical Corporation	22
1.4 Conclusion	23
References	24
2 Polybenzoxazine Alloys	29
2.1 Introduction	29
2.2 Benzoxazine/Epoxy Copolymers	30
2.3 Benzoxazine/Epoxy/Phenolic Ternary System	30
2.4 Poly(Benzoxazine-Urethane) Alloys	32
2.5 Polybenzoxazine/Poly(N-Vinyl-2-Pyrrolidone) Alloy	35
2.6 Polybenzoxazine/Poly(ϵ -Caprolactone) Blends.	36
2.7 Polybenzoxazine/Poly(Imide-Siloxane) Alloys.	38
2.8 Polybenzoxazine/Polyimide Blends	39
2.9 Polybenzoxazine/Dianhydride Copolymer.	40
2.10 Polybenzoxazine/Lignin Alloys	42

2.11	Potential Applications of Polybenzoxazine Blends and Alloys	43
	References	44
3	Highly Filled Systems of Polybenzoxazine Composites	47
3.1	Introduction	47
3.2	High Processability Characteristics of Benzoxazine Resins	49
3.3	Fundamentals of Particle Packing Characteristics	50
3.4	Highly Filled Polybenzoxazine Microcomposite	54
3.4.1	Highly Filled Wood-Substituted Composites from Polybenzoxazine	54
3.4.2	Boron Nitride-Filled Polybenzoxazine for Electronic Packaging Application	57
3.4.3	Highly Filled Systems of Alumina and Polybenzoxazine	57
3.4.4	Graphite-Filled Polybenzoxazine Composites	59
3.5	Highly Filled Polybenzoxazine Nanocomposites	61
	References	63
4	High Thermal Conductivity of BN-Filled Polybenzoxazines	67
4.1	Introduction	67
4.2	High Thermal Conductivity Electronic Packaging Materials Obtained by Boron Nitride-Filled Polybenzoxazine	70
4.3	Conclusions	81
	References	81
5	Newly High-Performance Wood-Substituted Composites Based on Polybenzoxazines	83
5.1	Introduction	83
5.2	High-Performance of Para-Woodflour-Filled Polybenzoxazine Composites	86
5.3	Fire-Retardant Para-Woodflour-Filled Polybenzoxazine Alloy Composites	96
5.4	Ternary System Based on Benzoxazine, Epoxy, and Phenolic Resins Filled with Para-Rubber Woodflour	101
5.5	Novel Cardanol-Benzoxazine-Based Wood Composites	108
5.6	Conclusions	112
	References	113
6	Polybenzoxazine Composites for Ballistic Impact Applications	117
6.1	Introduction	117
6.2	Polybenzoxazine/Urethane Polymer Alloys	123
6.3	Novel Kevlar TM Fiber-Reinforced Polybenzoxazine/Urethane Composites	127

6.4	Ballistic Properties of Kevlar™ Fiber-Reinforced Benzoxazine/Urethane Composites	129
6.5	Conclusions	136
	References	137
7	Electrical Conductivity of Filled Polybenzoxazines	139
7.1	Introduction	139
7.2	Types of Materials Classified Based on Electrical Resistivity	140
7.3	Conductive Path and Percolation Threshold	141
7.4	Inherently Conductive Polymer Filler.	143
7.5	Carbon-Based Electrically Conductive Fillers and Their Polymer Composites	150
	7.5.1 Carbon Nanotube Filled Composites	150
	7.5.2 Graphene- and Graphene-Based Polymer Nanocomposites	152
7.6	Metal Fillers and Their Polymer Composites	153
7.7	Potential Applications of Electrically Conductive Polybenzoxazine Composites	153
	References	154
	Index	157

Chapter 1

Introduction to Commercial Benzoxazine and Their Unique Properties

Abstract Since World War II, only few polymers, which have been developed, are able to reach the commercial stage. Polybenzoxazines are one of those few. Their ease of synthesis with tremendous molecular design flexibility allows tailor-made properties with broad range of applications. Their unique characteristics such as self-polymerizability upon heating without a need for a catalyst or curing agent, very low A-stage viscosity, near-zero volumetric shrinkage, fire-resistant behaviors, as well as their outstanding thermal and mechanical properties, make the polymer highly attractive for various applications including electronic packaging or aerospace. As a consequence, some companies start to commercialize the resins and their composites. This chapter summarizes benzoxazine resins and their related products recently commercialized by some major companies. The key properties of the polymers for engineering applications are also concisely discussed.

Keywords Commercialized polybenzoxazine • ARALDITE[®] MT • Epsilon resin • PB1000 prepreg

1.1 An Overview of Polybenzoxazines

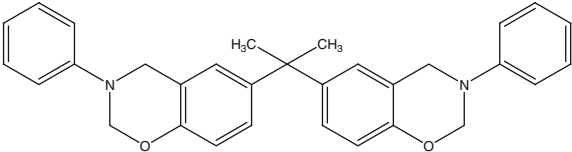
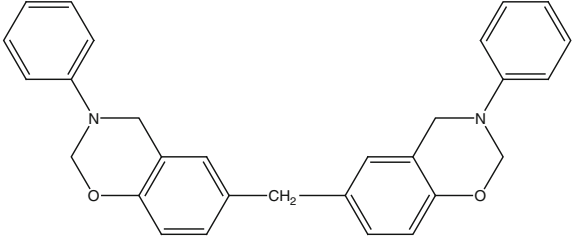
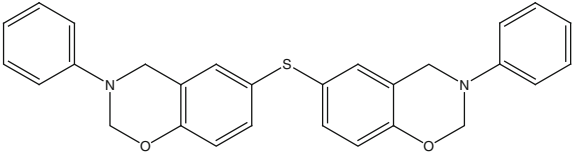
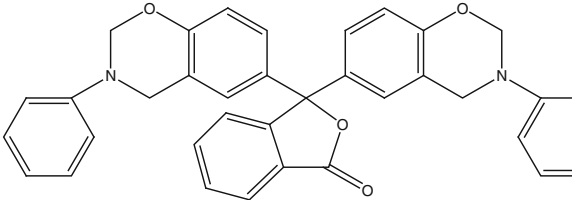
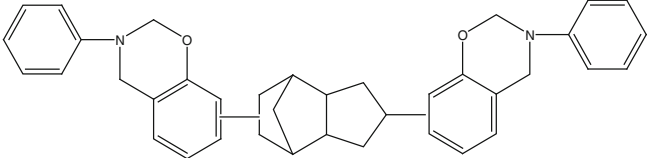
Polybenzoxazines are heterocyclic macromolecules possessed nitrogen and oxygen in their cyclic molecular structure and fuse to another benzene ring. Polybenzoxazine can be prepared through the ring-opening polymerization at oxazine ring by thermal activation with no further addition of initiator or catalyst, consequently is called self-polymerization. Benzoxazine resins are basically synthesized from formaldehyde, amine functional group, and phenoxide group, thus rendering them tremendous flexibility in their molecular design. The various molecular structures of benzoxazine resins are obtained by incorporation of different amine and phenoxide structures. The molecular design flexibility of benzoxazine resins is of crucial advantages of being tailored their versatile properties to

suit specific requirements and leads to the solutions of several shortcomings of conventional phenolic resins. Upon polymerization, polybenzoxazines provide various outstanding characteristics of no catalytic needed for curing, near-zero volumetric change (near-zero shrinkage) upon thermal curing rendering dimensional stability, and no by-product released during polymerization leading to no additional removal of volatile by-product. Moreover, polybenzoxazines offer a number of attractive properties such as low melt viscosity, high glass transition temperature, high thermal stability, good mechanical strength and modulus, low water absorption, low dielectric constant, good adhesive properties, and high resistance to burning and chemical. Consequently, polybenzoxazines have gained much attention from scientists in the field of polymer research as well as from the industrial researchers. In addition, multicomponent polymeric materials based on the reaction of benzoxazine resins with other polymers or resins have been reported to further enhance the properties of the resulting polymer hybrids with even broader range of applications, for example epoxy/polybenzoxazine copolymers [1–3], bismaleimide/polybenzoxazine copolymers [4], polycarbonate/polybenzoxazine hybrids [5, 6], poly(ϵ -caprolactone)/polybenzoxazine hybrids, [7, 8], polyurethane/polybenzoxazine copolymers [9, 10], polyimide/polybenzoxazine alloys [11]. Additionally, polybenzoxazines were successfully demonstrated to provide composite materials with various outstanding characteristics both in particulate-filled polybenzoxazine composites [12–16], and fiber-reinforced polybenzoxazine composites [17–20]. Several applications including conductive polymeric systems [21, 22], polymer electrolyte membrane [23, 24], coatings [25], electronic packaging [26], aerospace composites [27], and wear-resistant composites [28] are some examples reported in the literatures.

Polybenzoxazines could be classified by their functionality into monofunctional benzoxazine monomers, bifunctional benzoxazine monomers, and multifunctional benzoxazine monomers. Several structures of benzoxazine resins have intensively been synthesized by scientists to tailor their properties. Although much technical information of polybenzoxazines has been reported, to date, no engineering information specifically on commercial polybenzoxazines has been reviewed. In this book chapter, we discuss in detail the key properties of polybenzoxazine based on bifunctional type to be attentively commercialized by Huntsman Advanced Materials, Gurit, Henkel Corporation, and Shikoku Chemical Corporation.

In the following section, five principal types of polybenzoxazines based on bisphenol-A, bisphenol-F, thiobiphenol, phenolphthalein, and dicyclopentadiene (DCPNO) commercialized by Huntsman Advanced Materials are mainly discussed. For simplicity, abbreviation will be used throughout this book chapter. The structures and the abbreviations are shown in Table 1.1.

Table 1.1 Five principal monomeric benzoxazines commercialized by Huntsman Advanced Materials

Benzoxazine monomer structure	Abbreviation	Reference
	BA-a	[29]
	BF-a	[30]
	TD-a	[31]
	Boz-BP	[32]
	DCP-a	[33]

1.2 Synthesis of Distinguished Benzoxazines and Their Properties

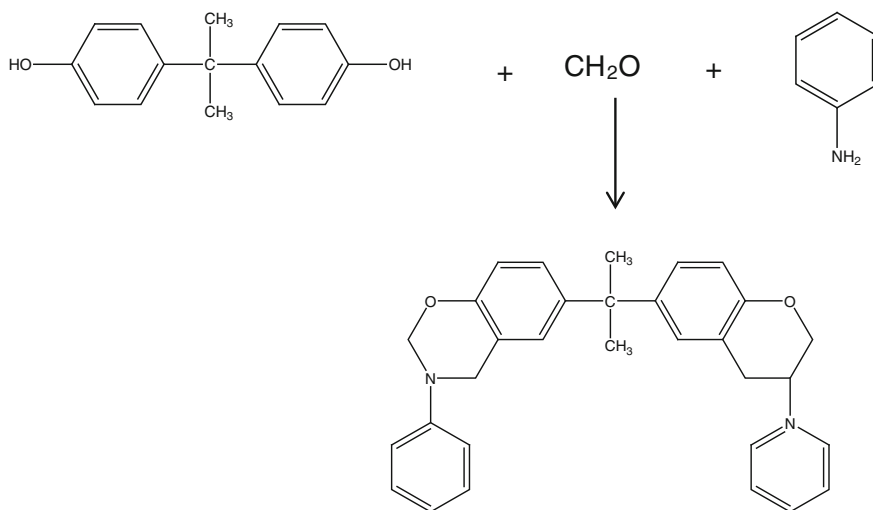
As stated in the previous section, benzoxazine resins can be classified by their functionality into mono-functional benzoxazine, bifunctional benzoxazine, and multifunctional benzoxazine resins. Mono-functional benzoxazines are less attractive to researchers. The molecular structure of mono-functional polybenzoxazine is reported as a linear low molecular weight polymer, in contrast to the bifunctional polybenzoxazine which is a crosslinked structure [29–34]. The formation of small molecule of oligomeric structures with an average molecular

weight of 1,000 from curing process is a main reason for the limited applications of the mono-functional-type benzoxazine resins [35]. Therefore, in this chapter, we are focusing on bifunctional types of benzoxazine resins which show various tailor-made properties and have been successfully commercialized.

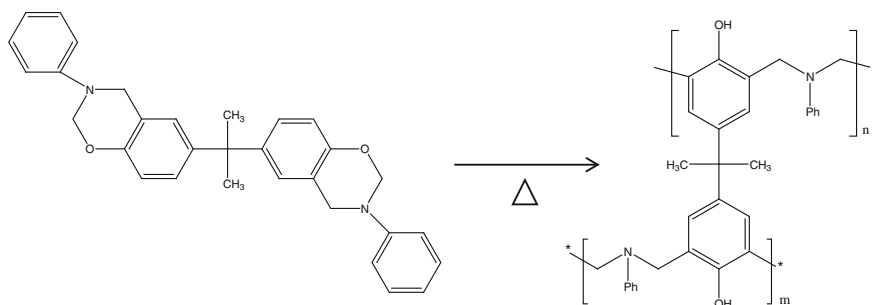
1.2.1 Bisphenol-A- and Aniline-Based Benzoxazine Resin

Bisphenol-A and aniline-based benzoxazine resin (BA-a) or bis(3,4-dihydro-2H-3-phenyl-1,3-benzoxazinyl)isopropane is the most investigated and utilized type of benzoxazine resins due to ease of synthesis and wide range of acceptable properties. The benzoxazine resin is synthesized from the reaction of bisphenol-A, paraformaldehyde, and aniline at 1:4:2 mol ratio at 110 °C without the use of any solvent as disclosed by Ishida in 1996 [36]. This solvent-less synthesis method is a convenient, cost competitive, and environmentally friendly method for preparation of various types of benzoxazine monomers and is one reason for a successful introduction of the benzoxazine resin into the market. The synthesis path of this monomer is shown in Scheme 1.1. The obtained benzoxazine resin can, then, be polymerized by the ring-opening polymerization of cyclic monomers via thermal cure without an addition of any catalyst or curing agent. The structural change in benzoxazine monomer to polybenzoxazine via thermal polymerization is illustrated in Scheme 1.2.

Among various outstanding properties of BA-a resin, its low melt viscosity before curing is one of those useful properties, rendering the ability of BA-a to



Scheme 1.1 Synthesis route of BA-a-type benzoxazine resin



Scheme 1.2 Formation of polybenzoxazine network by thermal curing process

easily wet the filler or reinforcement in a compounding process. This property is desirable and crucial in various composite applications. Moreover, the low melt viscosity of BA-a is also reported to help facilitate the mixing of BA-a with other resins or polymeric materials to form copolymers or alloys [2, 9, 17, 19]. Figure 1.1 illustrates processing window of BA-a resin, revealing its liquefying temperature and its gel point. From the figure, after the temperature is raised to its liquefying point at 70 °C, the solid BA-a resin is transformed into low viscosity and remained at this stage to the temperature of about 180 °C. After that, the resin underwent crosslinking reaction past its gel point, resulting in a sharp increase in its complex viscosity as a result of chemical network formation. The gel temperature or gel point under dynamic heating determined from the processing window of BA-a in Fig. 1.1 was reported to be about 196 °C [9].

The curing profile of BA-a benzoxazine resin is normally investigated by differential scanning calorimetry analysis (DSC) as shown in Fig. 1.2. The curing behavior observed using dynamic DSC at a heating rate of 10 °C/min of the

Fig. 1.1 Processing window of BA-a resin (adapted from Rimdusit et al. (2011) [9])

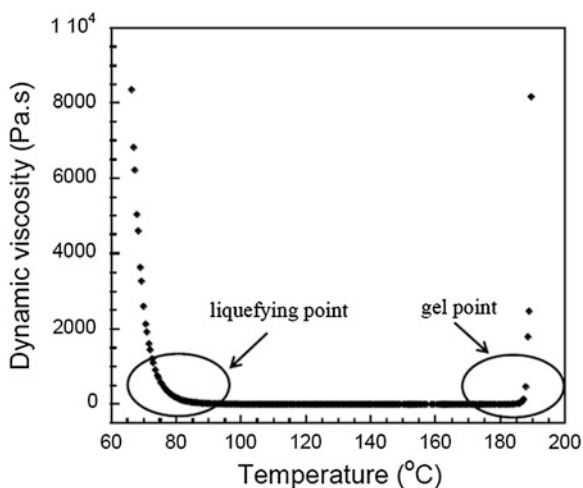
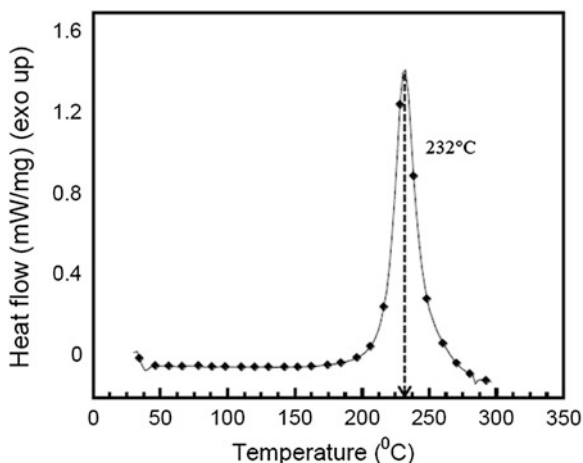


Fig. 1.2 DSC thermogram of BA-a resin (adapted from Rimdusit et al. (2008) [37])



as-synthesized BA-a exhibited a relatively symmetric exothermic peak with the peak temperature at about 232 °C and the onset temperature of 190 °C which is the characteristic of the oxazine ring-opening reaction [37]. However, the purified BA-a shows slightly higher curing temperature of about 240 °C [32, 33].

In terms of mechanical properties, the changes in mechanical behavior of materials as a function of temperature are conveniently investigated by dynamic mechanical analysis (DMA) due to the high sensitivity of this technique to even minor transitions or relaxations. The DMA analysis of the fully cured BA-a was investigated, e.g., by Rimdusit et al. [17]. As seen in Fig. 1.3, the storage modulus under bending mode at a glassy state of BA-a polybenzoxazine was found to be about 5.7 GPa. The modulus value starts to decrease at elevated temperature and then reaches its rubbery plateau at about 200 °C. The T_g observed from maxima peak of loss modulus curve of BA-a polybenzoxazine was observed at 173 °C which is its α -transition.

Fig. 1.3 Storage and loss modulus of BA-a resin (adapted from Rimdusit et al. (2011) [17])

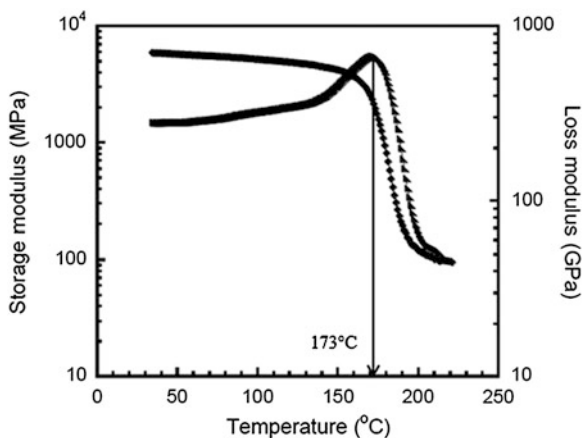


Fig. 1.4 TGA thermogram of BA-a resin (adapted from Rimdusit (2011) [9])

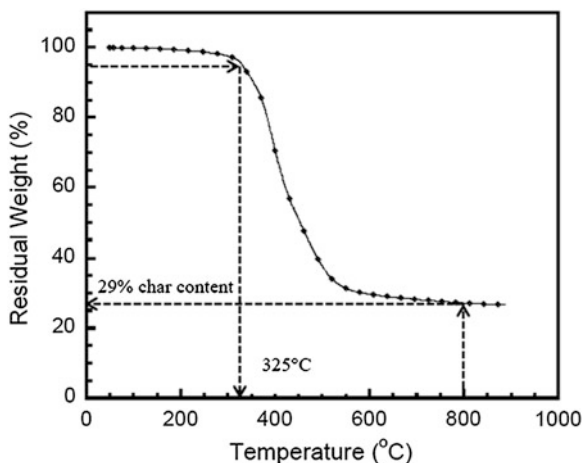
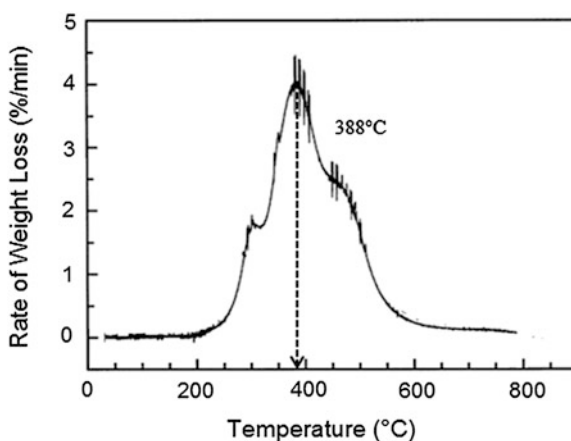


Fig. 1.5 Derivatives TGA thermograms of BA-a under nitrogen atmosphere (adapted from Low et al. (1999) [31])



In principle, thermal stability of polymeric materials can be indicated by their thermal degradation temperature. The thermal degradation of BA-a in nitrogen atmosphere has been studied by thermogravimetric analysis (TGA) as exhibited in Fig. 1.4. Rimdusit et al. [9] reported that the T_d at 5% weight loss of BA-a polymer was observed to be 325 °C with the char content at 800 °C of about 29%. A limiting oxygen index (LOI) is one key parameter needed to be considered for flame-resistant properties of material. The larger the LOI value of the material is, the less susceptible it is to burn. In general, the material is regarded as flammable when its LOI is below 22. The material with LOI equal to or greater than 26 is classified as self-extinguishable [38]. The LOI of the BA-a polybenzoxazine was reported to be 23.5. Though this polymer is not classified as self-extinguishable materials by the above criteria, its simple modification with compounds such as phenolic novolac [12], dianhydrides [39], or triphenyl phosphate flame retardant

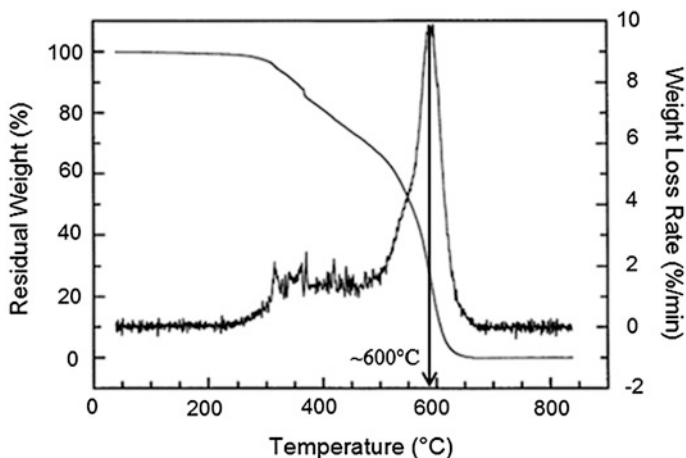


Fig. 1.6 TGA thermogram of BA-a under oxidative environment (adapted from Low et al. (1999) [31])

[40] can provide BA-a polybenzoxazine with the LOI up to 26 which meets the self-extinguishable criteria.

The mechanism of thermal degradation of BA-a was thoroughly observed by Low et al. [31]. The derivative thermogram of BA-a under nitrogen atmosphere was shown in Fig. 1.5. The onset of thermal degradation of BA-a is approximately 220 °C. In their report, the authors suggested that the degradation of phenolic linkages and the Mannich bridges occurred simultaneously. The maximum weight loss was observed at 388 °C with the rate of 4 %/min. The authors further investigated and noticed that aniline was a major degrading component which is a consequence of Mannich bridge cleavage.

Moreover, the thermal oxidation of BA-a was also investigated, as exhibited in Fig. 1.6. The derivative curve of BA-a polymer showed a small and broad peak between 250 °C and 500 °C, followed by a major peak at approximately 600 °C. It is well recognized that the char of organic polymer occurred during heating to the temperature of 600 °C and the char started to degrade at temperature over 600 °C. The authors found that the BA-a polybenzoxazine completely degraded under air atmosphere at about 700 °C.

Coefficient of thermal expansion (CTE) is the tendency of matter to change in volume or dimension in response to a change in temperature. Upon a matter is heated, the molecules begin moving and become active; thus, the energy stored in the intermolecular bonds between atom changes. The length of the molecular bonds is greater. Solids typically expand in response to heating and contract on cooling. The changes in dimension with response to the changes in temperature of BA-a were examined by Rimdusit et al. [9]. The CTE value of BA-a polymer was reported to be about 57.7 ppm/ °C which is comparable with bisphenol-A epoxy [41].

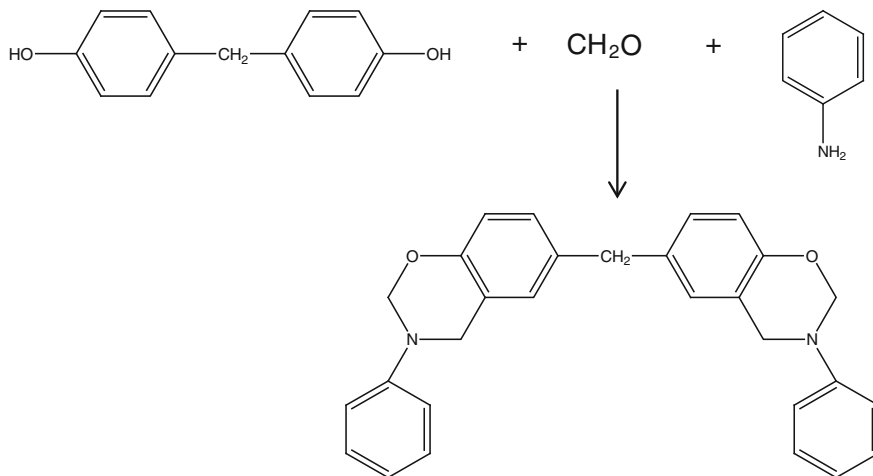
In terms of potential engineering applications of BA-a resin, the crucial advantage of low melt viscosity of BA-a provides ease of wetting on particle-filled and fiber-reinforced polybenzoxazine composite preparation. Consequently, the highly filled systems of various types of particles with BA-a benzoxazine resin matrix are achieved [12]. Various highly filled systems of benzoxazine resins are discussed in detail in [Chap. 4](#) of this book. The ability of BA-a benzoxazine resin to be alloyed with other polymers and resins is also one useful aspect of this resin. For examples, BA-a resin can be copolymerized with polyurethane and was reported to exhibit the synergism in glass transition temperature of the resulting copolymers [19, 37, 42]. The similar synergistic behavior is also observed in the system of benzoxazine–epoxy copolymers [43]. Furthermore, a combination of BA-a and cashew nutshell liquid oil has been reported to help lower the curing temperature and activation energy of the blend [44]. Additionally, BA-a benzoxazine resin modified with dianhydrides was reported to provide a remarkable increase in T_g as high as 263 °C which was much higher than that of the unmodified BA-a polymer. The resulting BA-a benzoxazine modified with dianhydride polymers also displays relatively high T_d up to 364 °C and substantial enhancement in char content with a value of up to 61 % by weight [45]. The polymer alloys' aspect of polybenzoxazine is discussed more comprehensively [Chap. 2](#) of this book.

1.2.2 Bisphenol-F- and Aniline-Based Benzoxazine Resin

Bisphenol-F and aniline-based benzoxazine monomer or bis(3,4-dihydro-2H-3-phenyl-1,3-benzoxazinyl)methane (BF-a) can be synthesized by the reaction of bisphenol-F, formaldehyde, and aniline according to solvent-less technology [36]. [Scheme 1.3](#) shows the reaction pathway of BF-a preparation. The physical appearance at room temperature of this resin is yellow powder similar to BA-a.

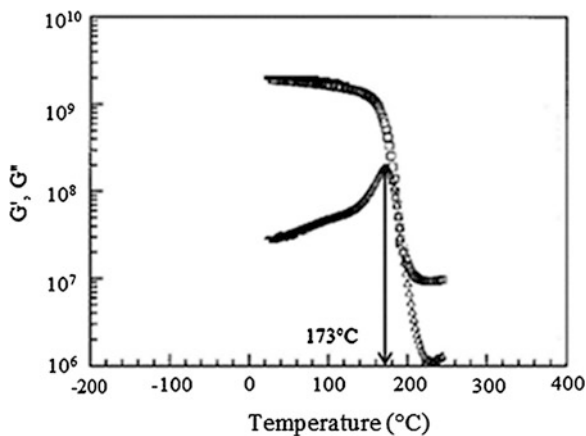
The DMA analysis of BF-a cured at 190 °C for 3 h was investigated by Kim et al. [30]. As noticed in [Fig. 1.7](#), the T_g observed from maxima peak of loss modulus curve of BF-a was exhibited at 173 °C which is close to that of BA-a benzoxazine resin.

The thermal degradation behavior of BF-a in nitrogen atmosphere was studied by Lin et al. [46]. The rate of weight loss of BF-a was found to be higher than that of BA-a by reaching 5 % of weight loss at 306 °C, whereas that of BA-a is reported at 325 °C. On the other hand, BF-a exhibited char content of 46 % which is higher than that of BA-a (29 %) [9], suggesting greater fire-resistant behavior of BF-a compared to BA-a.



Scheme 1.3 Reaction pathway of BF-a synthesis

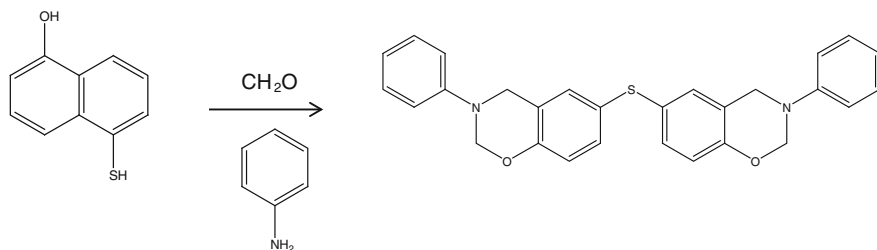
Fig. 1.7 DMA spectra of BF-a (adapted from Kim et al. (1999) [30])



1.2.3 Thiobiphenol- and Aniline-Based Benzoxazine Resin

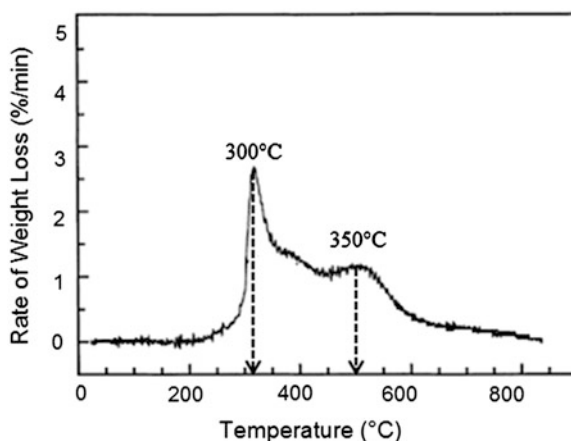
The synthesis of thiobiphenol-based benzoxazine resin (TD-a) can be carried out by three reactants, i.e., 4,4'-thiobiphenol, formaldehyde, and aniline in solvent-less synthesis [36] as shown in Scheme 1.4.

The outstanding characteristic of this type of benzoxazine resin is its high-temperature stability. Low et al. in 1999 [31] investigated the thermal behavior of thermal degradation of TD-a. The derivative curves of TD-a are illustrated in Fig. 1.8. A sharp peak of weight loss around 300 °C followed by a broad tail at about 350 °C was observed, indicating the wide degradation linkage of thiobiphenol. Moreover, the rate of degradation of TD-a was lower, compared with BA-a



Scheme 1.4 Synthesis of TD-a

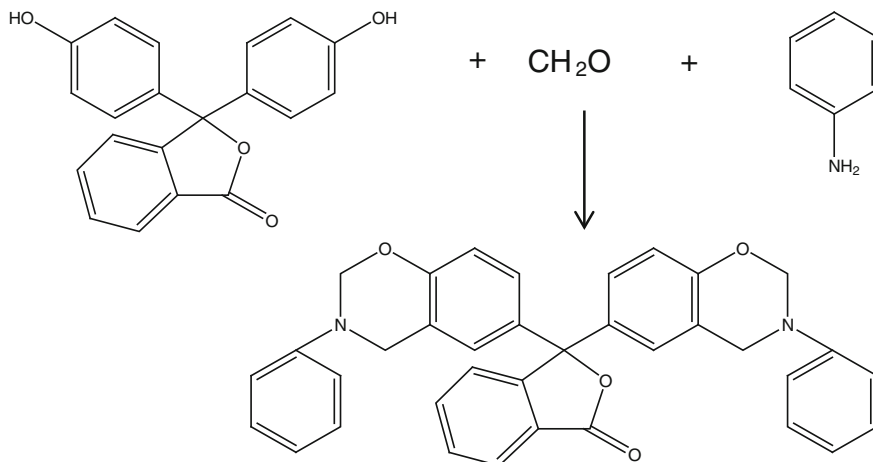
Fig. 1.8 Derivative of residual weight of TD-a under nitrogen degradation (adapted from Low et al. (1999) [31])



and showed the maximum rate of about 3 %/min at 300 °C, thus resulting in potentially high fire-resistant behavior. In comparison, the rate of weight loss of TD-a was slower than BA-a, which was reported to be 4 %/min at 388 °C. It might attribute to the stability in chemical structure, i.e., 4,4'-thiobiphenol, which is more thermally stable than bisphenol-A structure. Char yield of the TD-a polybenzoxazine has been reported to be 57 % compared to the value of 29 % for BA-a polybenzoxazine. The thiobiphenol-based benzoxazine monomer is thus potentially useful in applications such as fire-resistant material.

1.2.4 Phenolphthalein- and Aniline-Based Benzoxazine Resins

N-phenyl phenolphthalein-based benzoxazine resin (Boz-BP) was successfully synthesized using conventional method in mixed solvents of toluene and ethanol by Yang et al. [32]. The reaction of phenolphthalein, paraformaldehyde, and aniline can be carried out at 80 °C for 24 h to produce Boz-BP benzoxazine resin.



Scheme 1.5 Synthesis of N-phenyl phenolphthalein-based benzoxazine resin

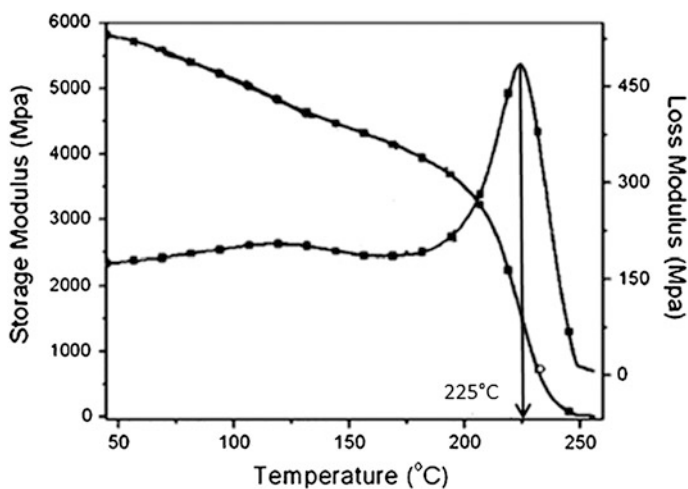


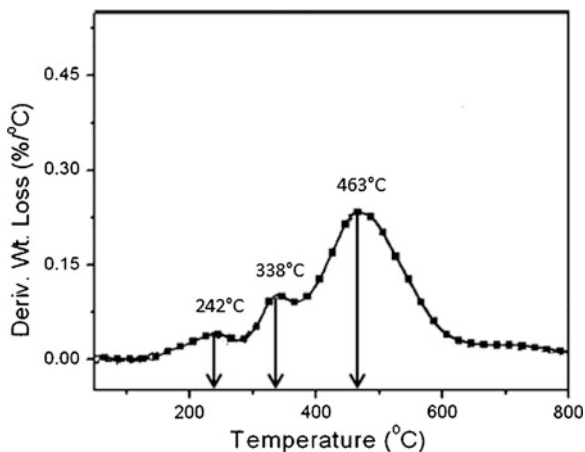
Fig. 1.9 Dynamic mechanic analysis thermogram of Boz-BP (adapted from Yang et al. (2011) [32])

The obtained benzoxazine resin is white powder with 78 % yield. The synthesis pathway is displayed in Scheme 1.5.

The DMA thermograms of Boz-BP were observed by Yang et al. as demonstrated in Fig. 1.9. The T_g of Boz-BP noticed from the maximum peak of loss modulus was 225 °C which was significantly higher than that of BA-a.

In terms of thermal degradation properties, the derivative curves of the TGA thermogram of Boz-BP are presented in Fig. 1.10. A three-stage weight loss

Fig. 1.10 Derivative TGA curve of Boz-BP (adapted from Yang et al. (2011) [32])

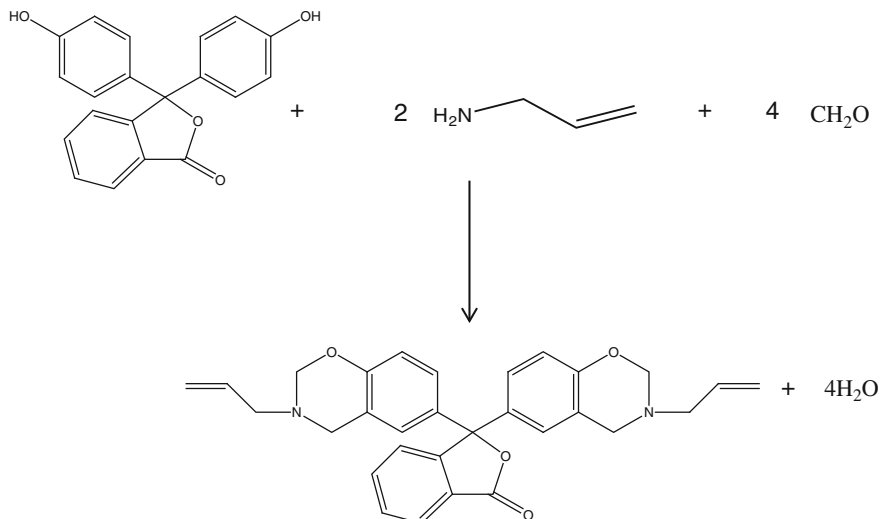


process was observed, centered around at 242, 338, and 463 °C, respectively. In comparison with BA-a, the first weight loss is shown at 199 °C. The first weight loss of BA-a and Boz-BP is attributed to the evaporation of amine cleavage. Thus, the enhancement in thermal stability of Boz-BP can be attributed to the well-protected amine part due to the reaction at para site of aniline. The T_d at 5 % weight loss and char content at 800 °C are determined to be 305 °C and 51 %, which is substantially higher than those of BA-a [32]. From the flammability of UL 94 test, Boz-BP is graded as V-0 criterion.

The CTE of Boz-BP is 47 ppm/ °C [32] which was lower than that of BA-a with CTE values of 57.7–62 ppm/ °C [16, 32]. The authors discussed that the improvement in CTE of Boz-BP is attributed to the para position substitution of aniline, incorporation of bulky phthalide structure into the crosslinked network of benzoxazine, and the formation of additional hydrogen bonding between carbonyl and hydroxyl groups.

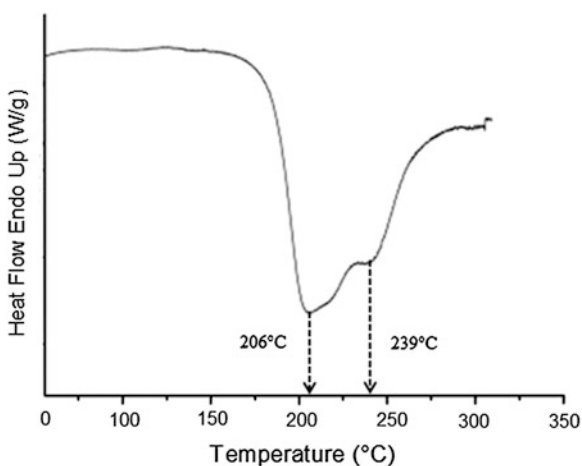
Furthermore, phenolphthalein is a well-known chemical used as a color change indicator [47], a component in temperature-resistant polymer [48] or optoelectronic photosensors and so on. Color change indicator ability of phenolphthalein-based benzoxazine resin was demonstrated by Cao et al. by the reaction of phenolphthalein (3,3-bis(4-hydroxyphenyl)-1(3H)-isobenzofuranone), allylamine, and paraformaldehyde at a stoichiometric ratio of 1:2:4 [47]. According to the reported procedure, phenolphthalein-based benzoxazine resin (3,3-bis(3-allyl-3,4-dihydro-2H-1,3-benzoxazine)-1(3H)-isobenzofuranone) (B-adi) was synthesized with a yield of about 80 %. The obtained benzoxazine resin is a transparent yellow viscous liquid at room temperature. The synthesis reaction is shown in Scheme 1.6.

The curing behavior of the phenolphthalein- and allylamine-based benzoxazine resin was elucidated in the literature using DSC as exhibited in Fig. 1.11. The two exotherms were apparently observed, in contrast to BA-a or BF-a benzoxazine resin types which show only one dominant exothermic peak [37]. The two



Scheme 1.6 Synthesis scheme of B-adi benzoxazine resin

Fig. 1.11 DSC thermogram of B-adi (adapted from Cao et al. (2006) [49])



exothermic peaks of B-adi were determined to be 206 and 239 °C, respectively. The two overlapped exotherms were vividly noticed, indicating that the two reactive functional groups of N-allyl and benzoxazine ring may react simultaneously at about the same temperature. Cao et al. further investigated the thermal polymerization of B-adi in order to identify each type of chemical reaction to each signal. It was concluded that the first exotherm attributed to N-allyl functional group and the second one attributed to the benzoxazine ring as it is known that thermal polymerization of N-allyl could occur at low temperature.

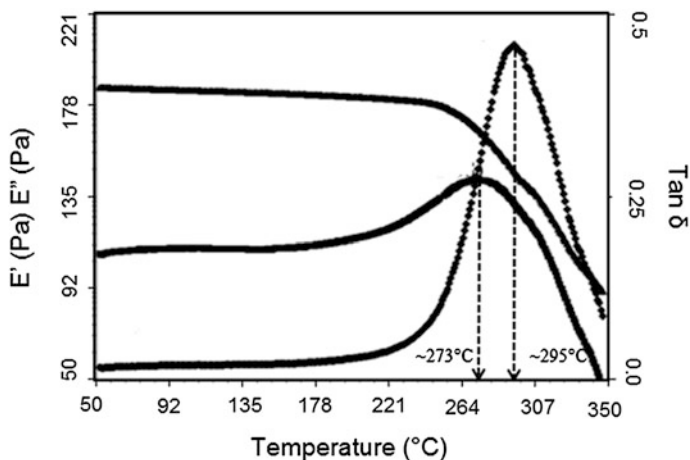


Fig. 1.12 DMA spectra of B-adi (adapted from Cao et al. (2006) [49])

The thermomechanical behavior of phenolphthalein- and allylamine-based benzoxazine resin was also investigated by Cao et al. [49]. As seen in Fig. 1.12, T_g of the polymer observed from the maximum of $\tan \delta$ and loss modulus is 295 and 273 °C, respectively. The T_g of phenolphthalein- and allylamine-based benzoxazine resin is much higher than BA-a or BF-a polybenzoxazines. In the DMA thermograms, the storage modulus of B-adi was constant up to 236 °C; thereafter, storage modulus decreased rapidly, and the rate of storage modulus decrease was maximal at 272 °C [49]. Similar to the T_g behavior of B-adi, the storage modulus of B-adi was constant up to an elevated temperature compared to that of BA-a in which storage modulus started to decrease at about 150 °C.

The thermal stability of B-adi was also carried out by TGA as shown in Fig. 1.13. The degradation temperature of B-adi polybenzoxazine at 5 % weight loss was found to be 336 °C, and its char yield at 800 °C was 40 %. The rate of weight loss reached a maximum at 405.5 °C. It was concluded that phenolphthalein-based benzoxazine resin containing three benzene rings in its structure provides substantial improvement in thermal behavior of the obtained polybenzoxazine. The authors also stated that the presence of the allyl group resulted in an increase in rigidity of the polymer by an increase in crosslink density. As a consequence, the polymer exhibits high T_g value and high char yield and possesses an excellent thermal stability. From DMA and TGA profile, the B-adi benzoxazine resin could be classified as high thermal stability and heat resistance materials, thus widen its applications over temperature range.

Phenolphthalein chemical is colorless when $\text{pH} < 8.2$ in medium, and it transforms into red when $\text{pH} > 8.2$. Thus, phenolphthalein is a proper color indicator at pH of about 8.2. The behavior of B-adi in alkaline medium is also observed by Cao et al. It was found that at the beginning, B-adi is red pink in color and transforms to amaranth in the strong alkaline medium, for example, in NaOH

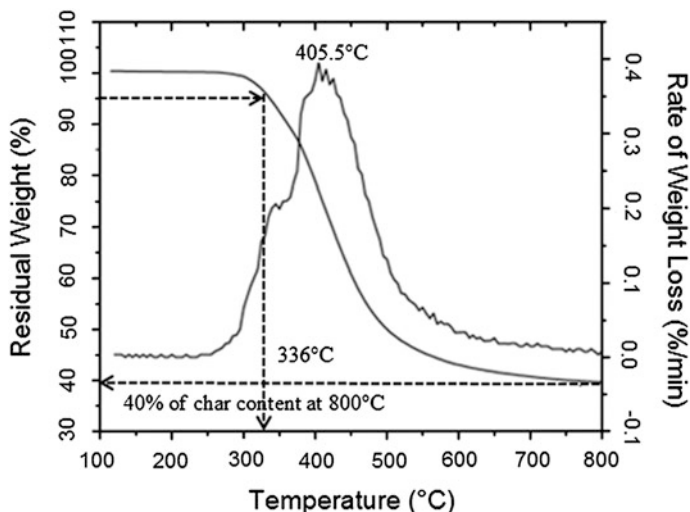


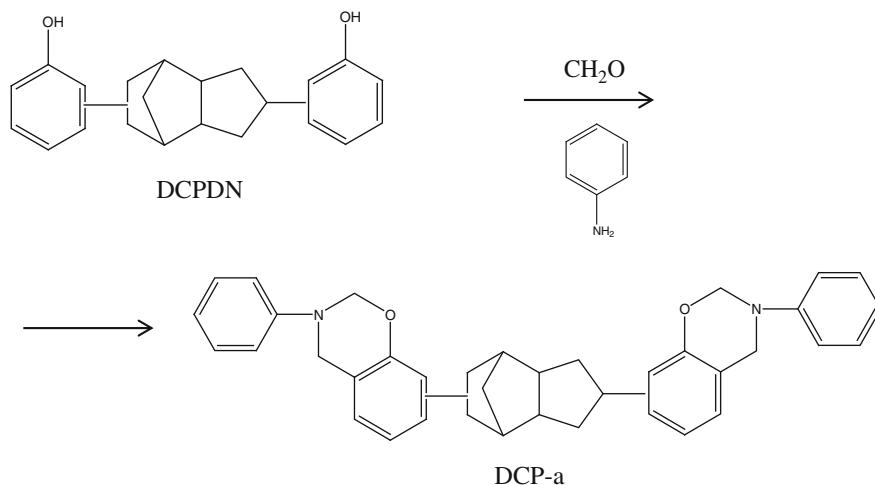
Fig. 1.13 TGA thermogram of B-adi and its rate of weight loss (adapted from Cao et al. (2006) [49])

solution. However, after titration with HCl, the amaranth solution transforms to colorless at pH of 10, indicating that phenolphthalein-based benzoxazine resin, B-adi, is a proper color indicator at pH of about 10 [49], which is slightly higher pH than phenolphthalein. The applications of this benzoxazine resin were thus widened by using phenolphthalein structure as a color indicator.

1.2.5 Dicyclopentadiene- and Aniline-Based Benzoxazine Resins

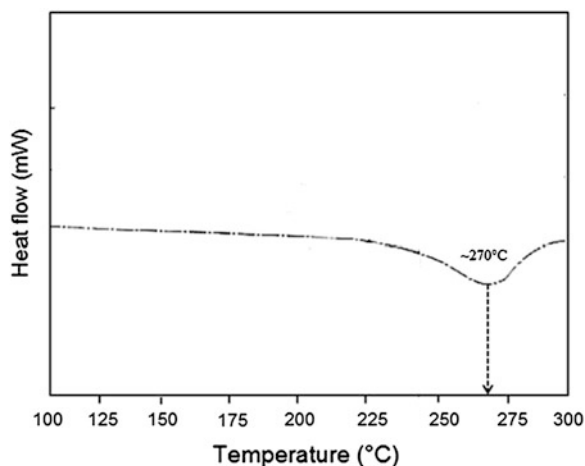
DCPNO is a by-product in oil refineries, with low cost and high reactivity. As seen in its molecular structure, DCPNO possesses highly hydrophobicity by linking each phenolic with nonpolar bridging group, thus contributes to excellent moisture resistance and to a dramatic reduction in the dielectric constant. The polybenzoxazine with DCPNO in its structure was expected to provide good thermal and mechanical properties in addition to low dielectric constant and low moisture absorption.

DCPNO-type polyhydrobenzoxazine could be prepared by the reaction of DCPNO phenol novolac, formaldehyde, and aniline in 1,4-dioxane solvent. The mixture was heated to reflux at 145 °C for 5 h to complete the reaction. The brown solid of DCP-a benzoxazine resin was obtained with a reported yield of 86 %. The synthesis of DCP-a was described by Shieh et al. [33]. The synthesis of DCP-a is shown in Scheme 1.7.



Scheme 1.7 Synthesis reaction of DCP-a

Fig. 1.14 DSC thermogram DCP-a benzoxazine resin (adapted from Shieh et al. (2006) [33])



In comparison with BA-a, the polymerization temperature of DCP-a benzoxazine resin is clearly higher. As seen in Fig. 1.14, the curing temperature of DCP-a was examined to be about 270 $^{\circ}\text{C}$.

The T_g observed from $\tan\delta$ of DCP-a was reported by Shieh and coworkers to be 183 $^{\circ}\text{C}$ and was observed to show a value similar to T_g of BA-a determined using the same technique.

The same authors also investigated the moisture absorptions of the fully cured DCP-a polybenzoxazine as shown in Table 1.2. In comparison with BA-a, DCP-a possessed much lower moisture absorption among the others with the report value of 0.21 %, whereas BA-a showed higher moisture absorption of 0.33 % after

Table 1.2 Moisture absorption and dielectric properties of cured polybenzoxazine (adapted from Shieh et al. (2006) [33])

Polybenzoxazine	Moisture absorption	Dielectric constant at 1 MHz	Dissipation factor
BA-a	0.33	3.31	0.0145
DCP-a	0.21	2.95	0.0095

immersed in 100 °C water for 24 h. Moisture absorption of DCP-a is an outstanding characteristic of this polybenzoxazine. The moisture absorption was attributed to hydrophobicity of materials as DCP-a showed cycloaliphatic in its structure which known to be hydrophobic in nature [33]. The absorbed moisture can act as plasticizer, which reduces the mechanical and thermal properties of cured resins. Moisture uptakes also reduce T_g of a laminate material as well.

Moreover, dielectric properties of DCP-a were also elucidated by Shieh et al. It was clearly seen from Table 1.2 that DCP-a possessed much lower dielectric constant (2.96) and dissipation factor (0.0095) than that of BA-a. Additionally, the dielectric constant of polymer from DCP-a was significantly lower than traditional phenolic resin (3.9–4.0). The lower dielectric constant of DCP-a is attributed to the greater free volume of molecule and hydrophobicity as seen in its molecular structure [50]. This low dielectric constant characteristic is desirable in an application such as electronic packaging materials.

Finally, for an application as an integrated circuit package or composite, the matrix material with low moisture absorption is required because water uptake may ionize ionic impurities and corrode the circuit. Furthermore, moisture absorption will increase the dielectric constant of laminate board. Consequently, lower moisture uptake is necessary, especially for laminate materials; thus, DCP-a is an excellent candidate for an integrated circuit packaging material or matrix resin for composite laminate, etc.

1.3 Major Producers of Benzoxazine Resins and Related Products

1.3.1 Huntsman Advanced Materials

Huntsman Advanced Materials is one of the major companies which have continuously developed benzoxazine resins as engineering materials for various potential applications. The benzoxazine resin products from Huntsman Advanced Materials have first been launched since 1994. Nowadays, Huntsman Advanced Materials provides five standard benzoxazine monomers for both industrial use and academic use with the trade names of ARALDITE® MT [51]. The trade names of benzoxazine resins commercialized by Huntsman Advanced Materials are listed

Table 1.3 Benzoxazine products commercialized by Huntsman Advanced Materials [57]

Benzoxazine monomer	Trade name
Bisphenol-A-based benzoxazine resin	ARALDITE [®] MT 35600
Bisphenol-F-based benzoxazine resin	ARALDITE [®] MT 35700
Thiodiphenol-based benzoxazine resin	ARALDITE [®] MT 35900
Phenolphthalein-based benzoxazine resin	ARALDITE [®] MT 35800
Dicyclopentadiene-based benzoxazine resin	ARALDITE [®] MT 36000

Table 1.4 Major properties of benzoxazine resin products commercialized by Huntsman Advanced Materials [57]

Materials based on benzoxazine resin	Typical properties		Thermal properties		Flammability UL-94 (sec)
	Viscosity at 120 °C (cP)	Reactivity at 190 °C (min)	T_g , DSC (°C)	T_g , DMA (°C)	
Bisphenol-A	<1,000	~ 15	~ 170	~ 180	>250
Bisphenol-F	<1,000	~ 20	~ 150	160–170	75–100
Thiodiphenol-	2,000–2,500	1–2.5	160–170	170–180	100–125
Phenolphthalein	3,000–3,500	5–10	190–200	230–240	<50
Dicyclopentadiene	3,500–4,000	10–15	~ 140	~ 140	>250

in Table 1.3. Moreover, major properties of these benzoxazine resin materials are shown in Table 1.4.

Additionally, Huntsman Advanced Materials also presented benzoxazine resins in liquid form. For example, Developmental LMB 6659 is bisphenol-F-based benzoxazine resin in 75 % of MEK solution and Developmental LMB 10640 is cardanol-based benzoxazine resin with the viscosity of 50–150 mPa s at 25 °C. Furthermore, mono-functional benzoxazine resins are one of the interesting products traded by Huntsman Advanced Materials, i.e., RD 2007-027, which is phenol-based benzoxazine resin with molecular weight of 211 and RD 2009-008 having molecular weight of 419.

Besides the five commercialized benzoxazine resins, Huntsman Advanced Materials also provides benzoxazine resin accelerators to be used as a catalyst for benzoxazine resin homopolymer and benzoxazine/epoxy combination. The benzoxazine accelerators are commercialized by the trade name of “Accelerator DT 300” and “Accelerator DT 310” with the melting point of 154–156 °C and 127–134 °C, respectively. These two accelerators could increase reactivity (i.e., gel time reduced by half), whereas Accelerator DT 310 possesses additional function of reducing curing temperature down to 160 °C [52]. Experimentally, DT300 which is known to be 4,4'-thiodiphenol has been proved to be a good accelerator by markedly reducing the gel time and activation energy of benzoxazine resin and benzoxazine/epoxy formulations [53].

1.3.2 Henkel Corporation

The commercial benzoxazine resin products have also been developed by Henkel Co., for aerospace applications. Henkel benzoxazine resins under the trade name of “Epsilon” have been commercialized with the service temperature of about 150 °C [54]. Major characteristics of Epsilon benzoxazine resin are summarized below.

Henkel’s Epsilon 99110 is designed for a broad range of applications with a high-temperature performance. Epsilon 99120 is claimed by Henkel to be a toughened benzoxazine resin, and Epsilon 99900 is a binder which is compatible with the Epsilon resins. The binder functions as an additional toughening, preforming, and compaction agent for the reinforcements. The viscosity of Epsilon 99110 and Epsilon 99120 was investigated by using temperature sweep mode under rheometry. It is known that for resin infusion, the viscosity below 10 poise is required. At the viscosity of 7 poise, the temperatures of Epsilon 99110 and Epsilon 99120 are 78 and 93 °C, respectively. The minimum achievable viscosity of those two resins is 0.6 and 1 poise. Both resins can also be processed over the full temperature range of 100–160 °C. Moreover, the viscosity of the benzoxazine resin products under storage at ambient temperature for 6 months and at 110 °C for 2 h exhibits only a small change which is acceptable for infusion characteristics. This behavior of benzoxazine resins is of great advantage for longtime shipping and storage.

The thermal properties of Epsilon 99110 and Epsilon 99120 are also investigated and reported by the company. The T_g of the fully cured polymers of the two resins observed according to ASTM E 1640 is 191 and 180 °C, which meet aerospace service temperature requirements.

For prepregs applications, 40 % volume fraction of Epsilon is reinforced with carbon fabric composites and the properties are reported in Table 1.5.

According to Epsilon’s high-performance materials, Henkel Co. has partnered with Airtech International to offer tooling carbon fiber prepregs for the manufacture of composite tools. The tools are claimed to be suitable for repeated cures at 180 °C while maintaining good dimensional stability and vacuum integrity. With the combination of being stable at ambient temperature and having a lower exotherm during the curing process, Henkel’s benzoxazine enables shorter cure cycles to be used for manufacture of thick tools without special precautions. Henkel and Airtech Materials Group have been awarded a JEC Paris Innovation Award Finalist from this product development.

Moreover, Henkel and Toho Tenax have developed the new benzoxazine resin-based prepregs with modern carbon fiber reinforcements for interior aircraft

Table 1.5 Mechanical properties of Epsilon 99110/carbon fabric produced by Henkel [58]

Property	Lay-up	Modulus	Strength
Tension	0/90	72.1/71.8	1,028/973
Compression	0/90	63.7/68.3	934/1,009
In plane shear	± 45	5.91	99.0
Interlaminar shear	0/90	–	66.7

applications. Additionally, the product offers many potential applications outside aerospace such as oil and gas extraction. In 2010, the product has also been awarded the JEC Paris Innovation Award Finalist with the development of Henkel's benzoxazine prepreg resin and film adhesive for Airbus A 380. In this specific application, the materials need to withstand high-temperature exposure, meet aircraft secondary structural design requirements, and flammability, smoke, and toxicity (FST) requirements to eliminate possibility of any smoke or toxic gases entering the passenger compartment. The use of Henkel's benzoxazine resin can replace bismaleimide with the significant cost reduction in processing and improved toughness while still meeting the high-temperature requirements, fluid resistance, and flammability.

Finally, "Epsilon 99110" benzoxazine resin has also been used as a solid precursor polymeric materials for preparing polybenzoxazine foam using azodi-carbonamide as a chemical blowing agent [55]. The resulting polybenzoxazine foam has been reported to possess good mechanical properties suitable for structural application with a substantial reduction in weight.

1.3.3 Gurit

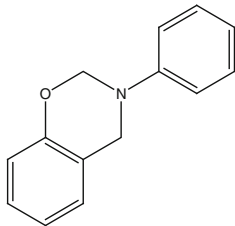
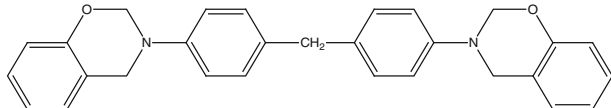
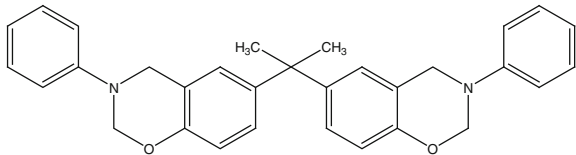
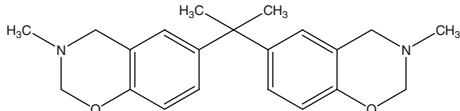
Gurit is a leading prepreg supplier for aircraft interiors and an innovative aviation industry since 1985. PB1000 is presented by Gurit as the next generation of aircraft interior prepreps (monolithic or sandwich structures, sidewalls, galleys, and seating) passenger floor and cargo floor. The company claims the benzoxazine resin to be free from phenol and formaldehyde, which satisfies the environment standards like AIRBUS AP2091. The benzoxazine resin used by the company can be cured under mild condition of 140 °C for 45 min and 160 °C for 15 min with nonvolatile release and generated a perfect void and porous free surface. Moreover, Gurit's novel PB1000 is claimed to fully comply with demanding international JAR/FAR fire protection regulations regarding commonly used fast curing process. With the unique material performance, PB1000 is claimed to be an effective choice for aircraft interior applications. As comparing the mechanical properties of PB1000 to phenolic resin, PB1000 possesses various excellent properties as seen in Table 1.6 [56]. The company suggests that PB1000 is clearly capable of replacing phenolic systems.

Additionally, the benzoxazine resin reinforced with E-glass prepreps is commercialized under the trade name of "PB1000-68-40" by Gurit. The prepreps consists of E-glass fabric impregnated with the benzoxazine PB1000. The material has been developed for the realization of extremely lightweight composite structures with high specific mechanical properties and high FST (flammability, smoke, toxicity) requirements. The composite structure is claimed to be utilized in the temperature range of -55 up to 80 °C. The obtained E-glass fiber-reinforced polybenzoxazine can be applied in aviation and aerospace industries as well as in rail industries.

Table 1.6 Comparison of typical mechanical values of benzoxazine resin and phenolic commercialized by Gurit (US7781 fabric/40 % resin)

Properties values	Standard	PB1000	Aerospace phenolic
Flexural strength (MPa)	ISO 178	550	320
Flexural modulus (GPa)	ISO 178	22	16
Interlaminar shear strength (MPa)	AITM 1.0019	28	18
Flammability (cm/s/s)	AITM 2.0002A	6/0/0	6/0/0
Smoke density (Dm)	AITM 2.0007A	19	5
Heat release (HRR/HR)	AITM 2.0006	50/25	30/25

Table 1.7 Commercialized benzoxazine resins provided by Shikoku Chemical Co.

Benzoxazine monomer structure	Abbreviation
	P-a
	P-d
	BA-a
	BA-m

1.3.4 Shikoku Chemical Corporation

Shikoku Chemical Co., is one of the leading companies to commercialize benzoxazine monomers. The company not only commercializes bifunctional benzoxazine resins, but also trades mono-functional benzoxazine resins as well including P-a (3-phenyl-3,4-dihydro-2H-1,3-benzoxazine), P-d (bis(4-(2H-benzol[e][1,3]-oxazine-3[4H]-yl)phenyl)methane), and bifunctional BA-m benzoxazine resin (2,2-bis(3,4 -dihydro-3-methyl-2H-1,3-benzoxazine)propane), besides the most

Table 1.8 List of published literatures that use the industrial benzoxazine monomers

Type of benzoxazine resins	Supplier	Published year	Reference
BA-a	Shikoku Chemical Co.	2000	[59]
BA-a	Shikoku Chemical Co.	2000	[42]
BA-a, P-a	Shikoku Chemical Co.	2002	[60]
P-a	Shikoku Chemical Co.	2003	[16]
BA-a	Shikoku Chemical Co.	2004	[61]
BA-a	Shikoku Chemical Co.	2005	[62]
BA-a	Shikoku Chemical Co.	2005	[11]
BA-a	Shikoku Chemical Co.	2006	[63]
BF-a	Shikoku Chemical Co.	2006	[64]
BA-a	Shikoku Chemical Co.	2007	[65]
BF-a	Shikoku Chemical Co.	2008	[66]
BA-m	Shikoku Chemical Co.	2008	[67]
BA-a, P-a	Shikoku Chemical Co.	2008	[68]
BA-a	Shikoku Chemical Co.	2009	[69]
BA-a	Huntsman Advanced Materials	2008	[70]
P-d	Shikoku Chemical Co.	2012	[71]
BA-a	Huntsman Advanced Materials	2012	[53]
BA-a	Huntsman Advanced Materials	2012	[72]
DCP-a	Huntsman Advanced Materials	2012	[73]
BA-a	Huntsman Advanced Materials	2012	[74]

widely used BA-a (bis(3,4-dihydro-2H-3-phenyl-1,3-benzoxazinyl)isopropane). Their chemical structures are listed in Table 1.7.

The list of some published literatures using benzoxazine monomers from the above-commercialized sources is tabulated in Table 1.8.

1.4 Conclusion

Nowadays, benzoxazine monomers have been commercialized by many leading manufacturers, for instance, Huntsman Advanced Materials, Henkel Corporation, Gurit, and Shikoku Corporation for utilizations in aerospace, electronics or civil engineering. With the tremendous flexibility in benzoxazine molecular design and with corresponding outstanding properties, five different types of benzoxazine resins have been commercialized with some unique characteristics to suit various applications. Bisphenol-A-based benzoxazine resin is a most common and most interesting type of benzoxazine resin, providing relatively mild condition for polymerization, very low melt viscosity, broad processing window, high reactivity, and good overall thermal properties. Bisphenol-F- and thiobiphenol-based benzoxazine resins provide higher thermal stability in terms of degradation temperature and char yield than BA-a. DCPNO-based benzoxazine resin, even though, possessed high curing temperature, but as the presence of greater benzene ring in

its structure, it behaves the much lower water absorption and excellent dielectric properties. The color indicator, also with superior thermal stability and glass transition temperature of phenolphthalein-based benzoxazine resin, has unique characteristics of this type of benzoxazine resin. All of these benzoxazine resins possess the same thermally curability of the oxazine ring structure of ease of handling. Consequently, these five types of benzoxazine resins have recently been manufactured and commercialized by several companies. Some related composite products have also been launched such as by Henkel.

References

1. Jubsilp C, Takeichi T, Rimdusit S (2010) Curing kinetics of benzoxazine-epoxy copolymer investigated by non-isothermal differential scanning calorimetry. *Polym Degrad Stabil* 95:918
2. Rimdusit S, Kunopast P, Dueramae I (2011) Thermomechanical properties of arylamine-based benzoxazine resins alloyed with epoxy resin. *Polym Eng Sci* 51:1797–1807
3. Rimdusit S, Ishida H (2000) Synergism and multiple mechanical relaxation observed in ternary systems based on benzoxazine epoxy and phenolic resins. *J Polym Sci Pol Phys* 38:1687–1698
4. Lui YL, Yu JM, Chou CI (2004) Preparation and properties of novel benzoxazine and polybenzoxazine with maleimide groups. *J Polym Sci Pol Chem* 42:5954–5963
5. Ishida H, Lee YH (2000) Infrared and thermal analyses of polybenzoxazine and polycarbonate blends. *J Appl Polym Sci* 81:1021–1034
6. Ishida H, Lee YH (2002) Study of exchange reaction in polycarbonate-modified polybenzoxazine via model compound. *J Appl Polym Sci* 83:1848–1855
7. Ishida H, Lee YH (2001) Synergism observed in polybenzoxazine and polycaprolactone blends by dynamics mechanical and thermogravimetric analysis. *Polymer* 42:6971–6979
8. Huang JM, Yang SJ (2005) Studying the miscibility and thermal behavior of polybenzoxazine/poly(ϵ -caprolactone) blends using DSC, DMA and solid state ^{13}C NMR spectroscopy. *Polymer* 46:8068–8078
9. Rimdusit S, Bangsen W, Kasemsiri P (2011) Chemorheology and thermomechanical characteristics of benzoxazine-urethane copolymer. *J Appl Polym Sci* 121:3669–3678
10. Jamshidi S, Yeganeh H, Mehdipour-Ataei S (2011) Poly(urethane-co-benzoxazine)s via reaction of phenol terminated urethane prepolymers and benzoxazine monomer and investigation of their properties. *Polym Advan Technol* 22:1502–1512
11. Takeichi T, Guo Y, Rimdusit S (2005) Performance improvement of polybenzoxazine by alloying with polyimide: effect of preparation method on the properties. *Polymer* 46:4909–4916
12. Rimdusit S, Kampangsaree N, Tanthapanichakoom W, Takeichi T, Suppakarn N (2007) Development of wood-substituted composites from highly filled polybenzoxazine-phenolic novolac alloys. *Polym Eng Sci* 47:140–149
13. Rimdusit S, Jiraprawatthagook V, Tiptipakorn S, Covavisaruch S, Kitano T (2006) Characterization of SiC whisker-filled polybenzoxazine cured by microwave radiation and heat. *Int J Polym Anal Ch* 11:441–453
14. Ishida H, Rimdusit S (1998) Very high thermal conductivity obtained by boron nitride-filled polybenzoxazine. *Thermochim Acta* 320:177–186
15. Agag T, Takeichi T (2011) Synthesis and characterization of benzoxazine resin-SiO₂ hybrids by sol-gel process: The role of benzoxazine-functional silane coupling agent. *Polymer* 52:2757–2763

16. Takeichi T, Guo Y (2011) Synthesis and characterization of poly(urethane-benzoxazine)/clay hybrid nanocomposites. *J Appl Polym Sci* 90:4075–4083
17. Rimdusit S, Pathomsap S, Kasemsiri P, Jubsilp C, Tiptipakorn S (2011) KevlarTM fiber-reinforced polybenzoxazine alloys for ballistic impact application. *Eng J* 15:23–40
18. Rimdusit S, Jongvisuttisun P, Jubsilp C, Tanthapanichakoon W (2009) Highly processable ternary systems based on benzoxazine, epoxy, and phenolic resins for carbon fiber composite processing. *J Appl Polym Sci* 111:1225–1234
19. Rimdusit S, Leingvachiranon C, Tiptipakorn S, Jubsilp C (2009) Thermomechanical characteristics of benzoxazine-urethane copolymers and their carbon fiber-reinforced composites. *J Appl Polym Sci* 113:3823–3830
20. Ishida H, Low HY (1998) Synthesis of benzoxazine functional silane and adhesion properties of glass-fiber-reinforced polybenzoxazine composites. *J Appl Polym Sci* 69:2559–2567
21. Kiskan B, Yaggi Y, Sahmetlioglu E, Toppare L (2007) Preparation of conductive polybenzoxazines by oxidative polymerization. *J Polym Sci Polym Chem* 45:999–1006
22. Wang YH, Chang CM, Liu YL (2012) Benzoxazine-functionalized multi-walled carbon nanotubes for preparation of electrically-conductive polybenzoxazines. *Polymer* 53:106–112
23. Kim SK, Kim KH, Park JO, Kim K, Ko T, Choi SW, Pak C, Chang H, Lee JC (2013) Highly durable polymer electrolyte membranes at elevated temperature: cross-linked copolymer structure consisting of poly(benzoxazine) and poly(benzimidazole). *J Power Sources* 226:346–353
24. Ye YS, Yen YC, Cheng CC, Chen WY, Wsai LT, Chang FC (2009) Sulfonated poly(ether ether ketone) membranes crosslinked with sulfonic acid containing benzoxazine monomer as proton exchange membranes. *Polymer* 50:3196–3203
25. Tasdelen CY, Erciyes AT (2013) Preparation of oil-modified polycaprolactone and its further modification with benzoxazine for coating purposes. *Prog Org Coat* 76:137–146
26. Rimdusit S, Ishida H (2000) Development of new class electronic packaging materials based ternary systems of benzoxazine, epoxy, and phenolic resins. *Polymer* 41:7941–7949
27. Li WH, Lehmann S, Mckillen J, Wong A, Wong R, Leach D (2010) Benzoxazine matrix resins for structural composite applications. SAMPE, Europe
28. Wu Y, Zeng M, Xu Q, Hou S, Jin H, Fan L (2012) Effects of glass to rubber transition of thermosetting resin matrix on the friction and wear properties of friction materials. *Tribol Int* 54:51–57
29. Ning X, Ishida H (1994) Phenolic materials via ring-opening polymerization of benzoxazines: effect of molecular structure on mechanical and dynamic mechanical properties. *J Polym Sci Phys* 32:921–927
30. Kim HJ, Brunovska Z, Ishida H (1999) Dynamic mechanical analysis on highly thermally stable polybenzoxazine with an acetylene functional group. *J Appl Polym Sci* 73:862–875
31. Low HY, Ishida H (1999) Structural effects of phenols on the thermal and thermo-oxidative degradation of polybenzoxazines. *Polymer* 40:4365–4376
32. Yang P, Gu Y (2011) Synthesis and curing behavior of a benzoxazine based on phenolphthalein and its high performance polymer. *J Polym Res* 18:1725–1733
33. Shieh JY, Lin CY, Huang CL, Wang CS (2006) Synthesis and characterization of novel dihydrobenzoxazine resins. *J Appl Polym Sci* 101:342–347
34. Xiang H, Ling H, Wang J, Song L, Gu Y (2005) A novel high performance RTM resin based on benzoxazine. *Polym Compos* 26:563–571
35. Brunovska Z, Ishida H (1999) Thermal study on the copolymers of phthalonitrile and phenylnitrile-functional benzoxazines. *J Appl Polym Sci* 73:2937–2949
36. Ishida H (1996) Process of preparation of benzoxazine compounds in solventless systems. US patent 5,543,516, 6 Aug 1996
37. Rimdusit S, Mongkhonsi T, Kamonchivanich P, Sujirote K, Thiptipakorn S (2008) Effects of polyol molecular weight on properties of benzoxazine-urethane polymer alloys. *Polym Eng Sci* 48:2238–2246
38. Harper CA (2004) Handbook of building materials for fire protection 2004. McGraw Hill, New York

39. Jubsilp C, Ramsiri B, Rimdusit S (2012) Effects of aromatic carboxylic dianhydrides on thermomechanical properties of polybenzoxazine-dianhydride copolymers. *Polym Eng Sci* 52:1640–1648
40. Rimdusit S, Thamprasom N, Suppakarn N, Jubsilp C, Takeichi T (2013) Effect of triphenylphosphate flame retardant on properties of arylamine-based benzoxazine. *Eng J* (in press)
41. Yasmin A, Daniel IM (2004) Mechanical and thermal properties of graphite platelet/epoxy composites. *Polymer* 38:4165–4176
42. Takeichi T, Guo Y, Aga T (2000) Synthesis and characterization of poly(urethane-benzoxazine) films as novel type of polyurethane/phenolic resin composites. *J Polym Sci A* 38:4165–4176
43. Rao BS, Reddy KR, Pathak SK, Pasala AR (2005) Benzoxazine-epoxy copolymers: effect of molecular weight and crosslinking on thermal and viscoelastic properties. *Polym Int* 54:1371–1376
44. Kasemsiri P, Hiziroglu S, Rimdusit S (2011) Effect of cashew nut shell liquid on gelation, cure kinetics, and thermomechanical properties of benzoxazine resin. *Thermochim Acta* 520:84–92
45. Jupsilp C, Takeich T, Rimdusit S (2011) Property enhancement of polybenzoxazine modified with dianhydride. *Polym Degrad Stabil* 96:1047–1053
46. Lin CH, Cai SX, Leu TS, Hwang TY, Lee HH (2006) Synthesis and properties of flame-retardant benzoxazines by three approaches. *J Polym Sci* 44:3454–3468
47. William E, Brenzovich J, Misty Do, Joana PS, Christopher JA (2003) Structure and properties of some cresolphthalein derivatives. *Dyes Pigm* 59:251–261
48. Mi Y, Zheng S, Chan CM, Guo Q (1998) Blends of phenolphthalein poly(ether ether ketone) and a thermotropic liquid crystalline copolyester. *J Appl Polym Sci* 69:1923–1931
49. Cao HW, Xu RW, Liu H, Yu DS (2006) Mannich reaction of phenolphthalein and synthesis of a novel polybenzoxazine. *Des Monomers Polym* 9:369–382
50. Hougham G, Tesoro G, Shaw J (1994) Synthesis and properties of highly fluorinated polyimides. *Macromolecules* 27:3642–3649
51. Tietze R (2007) The 5th triennial international aircraft fire and cabin safety research
52. AdMat specialty components selector guide 03.12_EN_EU (2012) Huntsman corporation
53. Chow WS, Grishchuk S, Burkhart T, Kocsis JK (2012) Gelling and curing behaviors of benzoxazine/epoxy formulations containing 4,4'-thiodiphenol accelerator. *Thermochim Acta* 543:172–177
54. Aerospace product selector guide (2012) Henkel corporation
55. Ardanuy M, Perez MA, Saja J, Velasco JI (2011) Foaming behavior, cellular structure and physical properties of polybenzoxazine foams. *Polym Adv Tech* 23:841–849
56. Gurit <http://www.gurit.com>. Accessed 10 Jan 2013
57. Araldite benzoxazine thermoset resins selector guide (2009) Huntsman corporation
58. Li W, Wong A, Leach D (2010) Advances in benzoxazine resins for aerospace applications. SAMPE Europe
59. Agag T, Takeichi T (2000) Polybenzoxazine-montmorillonite hybrid nanocomposites synthesis and characterization. *Polymer* 41:7083–7090
60. Takeichi T, Zeidam R, Agag T (2002) Polybenzoxazine/clay hybrid nanocomposites: Influence of preparation method on the curing behavior and properties of polybenzoxazine. *Polymer* 43:45–53
61. Agag T, Tsuchiya H, Takeichi T (2004) Novel organic-inorganic hybrids prepared from polybenzoxazine and titania using sol-gel process. *Polymer* 45:7903–7910
62. Lee YJ, Huang JM, Kuo SW, Chen JK, Chang FC (2005) Synthesis and characterizations of a vinyl-terminated benzoxazine monomer and its blending with polyhedral oligomeric silsesquioxane (POSS). *Polymer* 46:2320–2330
63. Yei DR, Fu HK, Chen WY, Chang FC (2005) Synthesis of a novel benzoxazine monomer-intercalated montmorillonite and the curing kinetics of polybenzoxazine/clay hybrid nanocomposites. *J Polym Sci B poly mer physi* 44:347–358

64. Gietl T, Lengsfeld h, Altstadt V (2006) The efficiency of various toughening agents in novel phenolic type thermoset resin systems. *J Mater Sci* 41:8226–8243
65. Agag T, Taepaisitphongse V, Takeichi T (2007) Reinforcement of polybenzoxazine matrix with organically modified mica. *Polym Composite* 28:680–687
66. Lin CH, Chang SL, Hsieh CW, Lee HH (2008) Aromatic diamine-based benzoxazines and their high performance thermosets. *Polymer* 49:1220–1229
67. Lu CH, Su YC, Wang CH, Haung CF, Sheen YC (2008) Thermal properties and surface energy characteristics of interpenetrating polyacrylate and polybenzoxazine networks. *Polymer* 49:4852–4860
68. Takeichi T, Saito Y, Agag T, Muto H, Kawauchi T (2008) High-performance polymer alloys of polybenzoxazine and bismaleimide. *Polymer* 49:1173–1179
69. Sponton M, Ronda C, Glia M, Cadiz V (2009) Development of flame retardant phosphorus- and silicon-containing polybenzoxazines. *Polym Degrad Stabil* 94:145–150
70. Yang L, Zhang C, Pilla S, Gong S (2008) Polybenzoxazine-core shell rubber–carbon nanotube nanocomposites. *Compos Part A: Appl S* 39:1653–1659
71. Chang HC, Lin CH, Lin HT, Dai SA (2011) Deprotection-free preparation of propargyl ether-containing phosphinated benzoxazine and the structure-property relationship of the resulting thermosets. *J Polym Sci* 50:1008–1017
72. Narayanan J, Jungman MJ, Patton DL (2012) Hybrid dual-cure polymer networks via sequential thiol–ene photopolymerization and thermal ring-opening polymerization of benzoxazines. *React Funct Polym* 72:799–806
73. Celina MC, Giron NH, Rojo MR (2012) An overview of high temperature micro-ATR IR spectroscopy to monitor polymer reactions. *Polymer* 53:4461–4471
74. Kaleemullah M, Khan SU, Kim JK (2012) Effect of surfactant treatment on thermal stability and mechanical properties of CNT/polybenzoxazine nanocomposites. *Compos Sci Technol* 72:1968–1976

Chapter 2

Polybenzoxazine Alloys

Abstract Polybenzoxazine is a class of high-performance materials possesses many intriguing characteristics. The ability of alloying with other minor components is one of the crucial properties for this novel kind of thermosetting, i.e., the properties of the rendered alloys and blends could be tailor-made to meet the requirements of any application. In this chapter, the reviews of the polybenzoxazine alloys in the aspects of some important characteristics (such as thermal and mechanical properties) were dedicated.

Keywords Polybenzoxazine · Alloys · Blends · Tailor-made properties

2.1 Introduction

Polybenzoxazine (PBZ), a novel class of high-performance phenolic resin, have attracted great attention as versatile materials for structural and engineering applications because they possess good flame retardance, and thermal properties of phenolic resins, including their high mechanical properties, with good sound and noise absorbance. This class of thermosetting polymer could be synthesized from phenol (or substituted phenols), aldehyde (such as formaldehyde, acid aldehyde, or pyromucic aldehyde), and amine groups. Even though these resin types were firstly produced in 1940s by Holly and Cope [1], the capability of polybenzoxazine has become well known recently in 1990s [2]. The novel polymers can be synthesized via either solvent or solventless technology. Additionally, the curing of the resins involves ring-opening polymerization with no need of any catalyst or curing agent for producing, and there is no by-product during curing, which leads to no void in the products. In addition, polybenzoxazines render near-zero volumetric shrinkage or expansion upon cure, high processability due to low melt viscosity before polymerization, low water uptake, high char yield, and low coefficient of thermal

expansion. Moreover, the polymers render low dielectric constant and dissipation loss, high mechanical performance and great molecular design flexibility [3–15]. Interestingly, the polymers possess a crucial property, i.e., the ability to be alloyed with many chemicals such as epoxy, polyurethane. This interesting property leads to the modification of mechanical and thermal properties of the rendered alloys. That means the drawback of the polybenzoxazine, i.e., its brittleness, could be managed by alloying with other polymers [3–15]. In this chapter, this review article is dedicated to the polybenzoxazine alloys and blends.

2.2 Benzoxazine/Epoxy Copolymers

Although polybenzoxazines (PBZ) possess high glass-transition temperature and modulus, it is reported that the crosslink density of PBZ is rather lower than that of other thermosetting polymers with the same properties. The reason is attributed to the fact that hydrogen bonding could be sufficient to hinder the chain mobility and induce the rigidity as observed in the glassy state [12]. Ishida and Allen studied the copolymerization between PBZ and diglycidyl ether of bisphenol-A (DGEBA), the most commonly used epoxy resin in the copolymer, could lead to higher crosslink network [13]. That also has an effect on the higher glass-transition temperature (T_g) than the parent polymers as reported by Rimdusit et al. [16, 17]. The authors proposed that the reaction between benzoxazine and epoxy were composed of two reactions, i.e., the first reaction is the polymerization reaction between the monomers of benzoxazine, and the second one is the reaction between epoxide group on the epoxy and the phenyl group on polybenzoxazine. Furthermore, it was reported that the reaction between epoxide group and phenyl group was expected to proceed after ring-opening polymerization of phenolic hydroxyl group in benzoxazine monomers occurred [11, 17, 18]; the proposed reaction is presented in Fig. 2.1 [9].

Additionally, the DMA results reveal the synergistic behavior of glass-transition temperature as shown in Fig. 2.2. It could be noticed that the copolymer at the epoxy content beyond 45 wt% presents the significant decrease of T_g with the system containing equal amount of both two components. This could be attributed to the fact that the stoichiometric ratio of components was approached; the excess small molecular weight epoxy could not be unreacted and remain in the network formed. This could hinder network formation and act as a plasticizer in the fully polymerized network as discussed by Rimdusit et al. [17].

2.3 Benzoxazine/Epoxy/Phenolic Ternary System

The ternary system of benzoxazine, epoxy, and phenolic resins was developed by Rimdusit and Ishida [19]. It was reported that the properties of the mixtures depends on the mass ratios of the starting materials. Interestingly, the synergistic

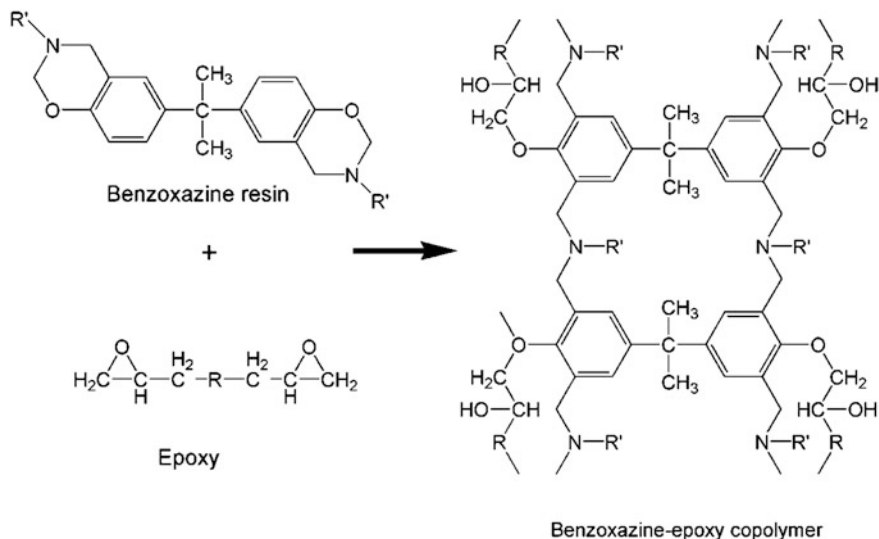
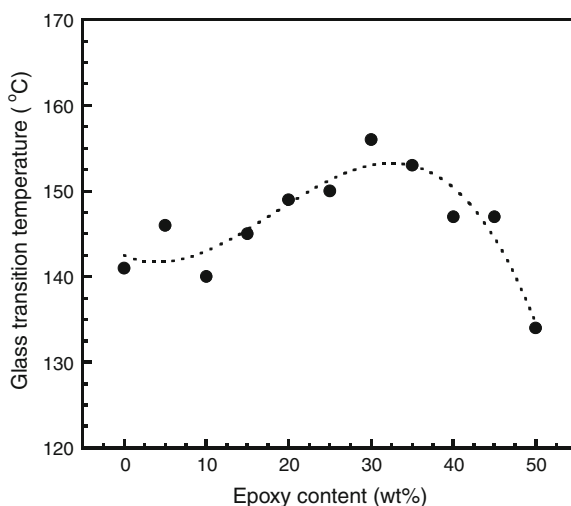


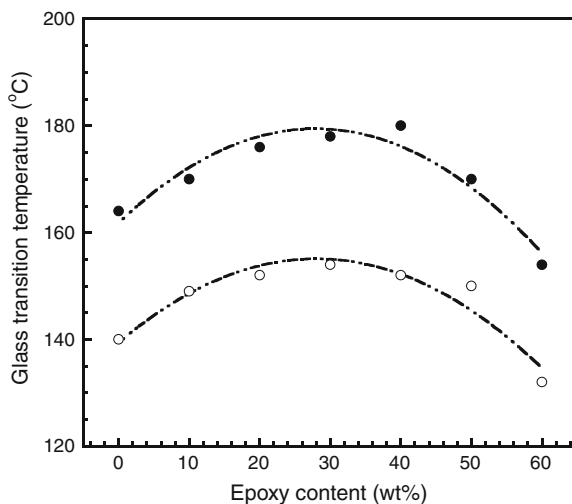
Fig. 2.1 Proposed reaction between benzoxazine monomer and epoxy

Fig. 2.2 Relationships between epoxy content and glass-transition temperature in benzoxazine-epoxy binary system



behavior of glass-transition temperature (T_g) is obtained. The relationships between the epoxy content and glass-transition temperature of the mixture with six blending ratios of benzoxazine/epoxy/phenolic resin (3/6/1; 4/5/1; 5/4/1; 6/3/1, 7/2/1, and 8/1/1) from DSC and DMA are exhibited in Fig. 2.3. It could be noticed that the highest glass-transition temperature observed from DMA is 180 °C, when the weight ratio of is 5/4/1 [13, 18]. The authors noted that the epoxy acted as diluents in the ternary system and increase the crosslink density and flexibility

Fig. 2.3 Relationships between the epoxy content and glass-transition temperature in the ternary system: (black circle) DMA values, (white circle) DSC values



compared with parent materials. Additionally, it was reported that the small amount of added phenolic resin could improve the crosslink density and the glass-transition temperature of benzoxazine/epoxy copolymer. The amount of phenolic resin in the range of 6–10 wt% was needed to obtain the highest T_g . Moreover, the synergistic behavior of glass-transition temperature was contributed to the rigidity from benzoxazine molecules and the increase of crosslink density from epoxy. It was reported that the small amount of phenolic resin leads to the decrease in the curing temperature of the ternary system in comparison with curing reaction of only benzoxazine/epoxy binary system.

2.4 Poly(Benzoxazine-Urethane) Alloys

The poly(benzoxazine-urethane) alloys were synthesized from urethane prepolymer and monofunctional or bifunctional benzoxazine resins. For example, the synthesis of the alloy using 3-phenyl-3,4-dihydro-2H-1,3-benzoxazine (Cm-type monofunctional benzoxazine resin) and urethane prepolymer (derived from polyethylene adipate polyol with molecular weight of 1000 Da and 2,4-tolylene diisocyanate at molar ratio of 1:2) are shown in Fig. 2.4 [20]. It was reported that during polymerization, there could be intermolecular reaction between hydroxyl groups (OH-) of benzoxazine monomer and isocyanate groups (NCO-) of urethane prepolymer. The cured poly(benzoxazine-urethane) alloys films were transparent, indicating good compatibility between two components. This is confirmed by the only one glass-transition temperature, suggesting no phase separation in the alloys. Furthermore, the authors reported that the decomposition temperature of the alloys were higher than that of pure polyurethane. That means even small amount of

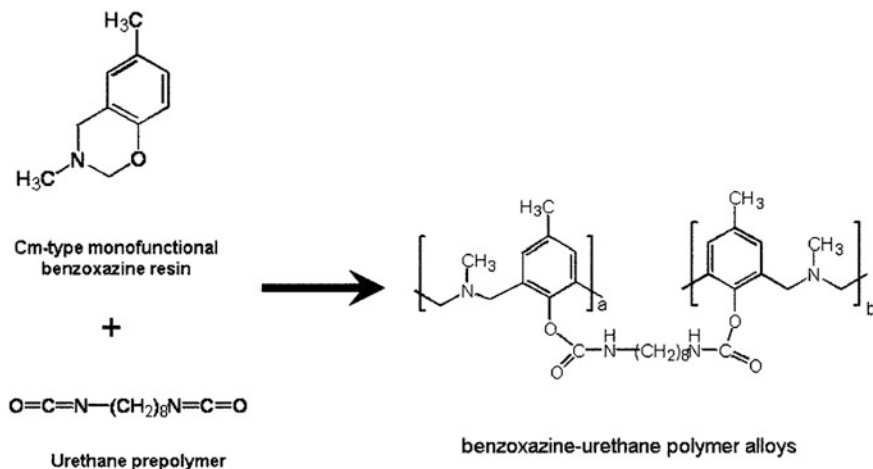


Fig. 2.4 Proposed reaction of Cm-type benzoxazine resin and urethane prepolymer

benzoxazine added in the polyurethane could increase the thermal stability of the polyurethane.

The alloys between BA-a (bifunctional benzoxazine) resin and urethane prepolymer (prepared from isophorone diisocyanate and polyether polyol with molecular weight of 2000 Da at the molar ratio of 2:1) was studied by Rimdusit et al. [21]. The authors reported that the enhancement of the glass-transition temperature (T_g) of the alloys also observed as seen in Fig. 2.5. It could be noticed that one glass-transition temperature is observed for the alloy synthesized from urethane prepolymer and either monofunctional or bifunctional benzoxazine resins. That exhibits high miscibility between the starting polymeric components because of the copolymer reaction [19, 21, 22].

The T_g of the alloys are noticeably higher than those of the parent resins, e.g., the alloy at 30 wt% of PU renders the glass-transition temperature of approximately 220 °C, while those of pure PU and PBZ are reported to be about -70 and 165 °C, respectively [11, 16–18, 23]. The effects of polyol molecular weight on the properties of poly(benzoxazine-urethane) alloys were investigated using various molecular weights, e.g., 1,000, 2,000, 3,000, and 5,000 [24]. The flexural strength values of the poly(benzoxazine-urethane) at different molecular weights of polyol are presented in Fig. 2.6. It could be seen that the strength of the binary systems did not reveal a linear relationship with the PU content but exhibited the synergistic behavior with the maximum values at the BA-a:PU ratio of 90:10. It was reported that there was no significant effect of polyol molecular weight on the glass-transition temperature (T_g) of the alloys. The synergy of T_g of polybenzoxazine has been reported in various alloy systems as the polybenzoxazine renders relatively low crosslink density in comparison with epoxy of the same type of bisphenol as starting material. The research related to the model of benzoxazine dimer and trimer structures has revealed the intermolecular and intramolecular

Fig. 2.5 DSC thermograms of the poly(benzoxazine-urethane) alloys at various BA-a:PU ratios: (black circle) 100:0, (white circle) 90:10, (black square) 80:20, (white square) 70:30

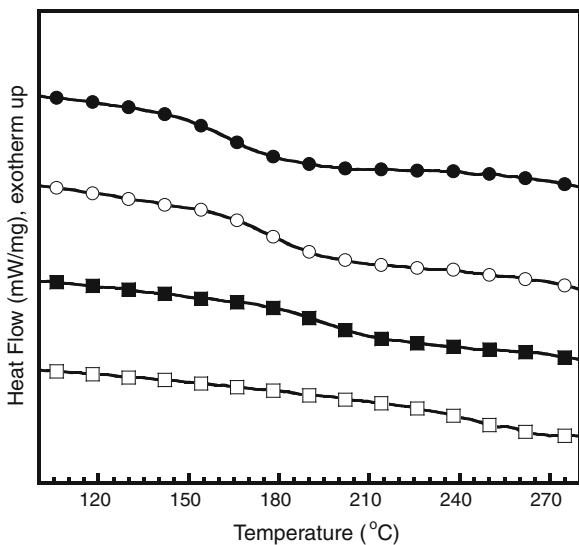
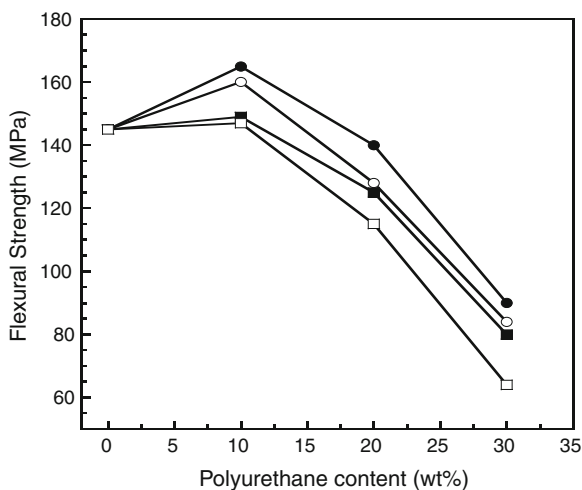
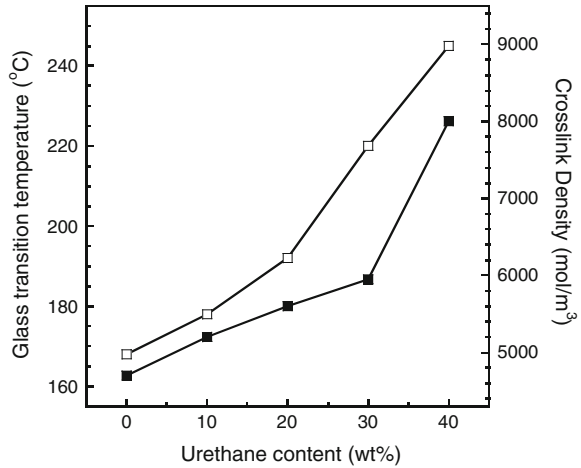


Fig. 2.6 Relationship between average values of flexural strength and urethane content at different polyol molecular weights: (black circle) 1000, (white circle) 2000, (black square) 3000, (white square) 5000



hydrogen bonding, hindering the network formation to obtain high crosslink density [12]. The addition of second polymer to form the alloy could increase the crosslink density of poly(BA-a) alloyed with PU elastomer. Figure 2.7 presents the effects of polyurethane contents on the glass-transition temperature and the crosslink density of the alloys of benzoxazine and polyurethane synthesized from the polyol at a molecular weight of 2000 with toluene diisocyanate (TDI) [16]. In the figure, the crosslink density of the copolymer networks, ρ_x , can be approximately calculated from the equilibrium value of shear storage modulus in the rubbery region (G_e') which equal to $E_e'/3$ as presented in Eq. (2.1)

Fig. 2.7 Relationships of urethane content on glass-transition temperature and crosslink density of poly(benzoxazine-urethane) alloy: (white square) glass-transition temperature, (black square) crosslink density



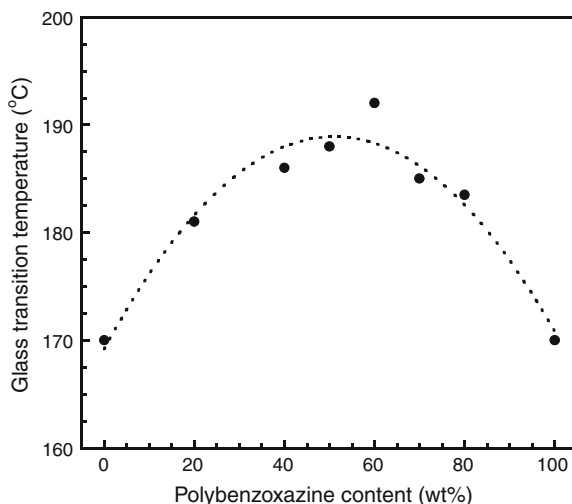
$$\log \left[\frac{E'_e}{3} \right] = 7.0 + 293(\rho_x) \quad (2.1)$$

where E'_e is an equilibrium value of tensile storage modulus at rubbery plateau in the unit of dyne/cm^2 . ρ_x is a value of crosslink density, being the amount of mole of network chains per unit volume of the polymers.

2.5 Polybenzoxazine/Poly(N-Vinyl-2-Pyrrolidone) Alloy

Su et al. [25] prepared the alloys between BA-a-type polybenzoxazine (PBZ) and poly(N-vinyl-2-pyrrolidone) (PVP); the thermal properties and hydrogen bonding of the alloys were determined. The authors reported that only one glass-transition temperature (T_g) was observed for all PVP contents, exhibiting complete miscibility in the PBZ/PVP alloy. The synergism of glass-transition temperature was reported as shown in Fig. 2.8. The highest value of glass-transition temperature could be found at the weight ratio of 50:50. Furthermore, the researchers reveal that the hydrogen bonding in polybenzoxazine/poly(N-vinyl-2-pyrrolidone) alloy could occur due to the interaction between the carbonyl group of poly(N-vinyl-2-pyrrolidone) and hydroxyl group of polybenzoxazine. This interaction could be sufficient to induce rigidity and impede the molecular mobility in the alloys, leading to the T_g synergism.

Fig. 2.8 Synergism of glass-transition temperature in the PBZ/PVP alloy

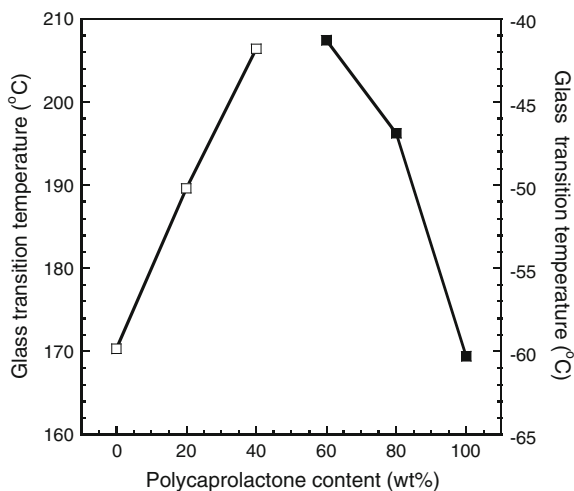


2.6 Polybenzoxazine/Poly(ϵ -Caprolactone) Blends

As a nature of phenolic materials, polybenzoxazines tend to be brittle. This characteristic limits the applications of this material. Thus, the flexural and impact properties of the polymers are expected to enhance when incorporating a component rendering a low glass transition (T_g). Huang and Yang [26] prepared the blends between bisphenol-A/methylamine-based benzoxazine resin (BA-m) and poly(ϵ -caprolactone) (PCL) via solution blending method. The miscibility and thermal behaviors of the blends were studied. They reported that the synergistic behavior of glass-transition temperature (T_g) was found in low content of PCL. As presented in Fig. 2.9, the T_g value of the blends is as high as ca. 206 °C, while those of poly(BA-m) and PCL are ca. 170 and -60 °C, respectively. This could be attributed to the fact that higher polymerization conversion occurred when PCL was presented as observed in the Fourier transform infrared spectroscopy (FTIR) results. The FTIR spectra revealed intermolecular hydrogen bonding between the hydroxyl groups of PBZ and the carbonyl groups of PCL during polymerization. This could lead to the improvement of T_g and the miscibility of poly(BA-m) and PCL. This can be implied that the addition of poly(ϵ -caprolactone) into polybenzoxazine could enhance the properties of the polybenzoxazine at high temperature. The enhancement of flexural properties of the polybenzoxazine/poly(ϵ -caprolactone) blends was reported by Ishida and Lee [27], while the phase separation was discussed by Zheng et al. [28].

Despite many outstanding characteristics of polybenzoxazine as previously mentioned, pure polybenzoxazine is not suitable for coating such as its brittleness. There has been an attempt to modify the properties of polybenzoxazine, i.e., the preparation of benzoxazine monomer with additional functional group, the synthesis of benzoxazine-based composites and alloys, and incorporation of

Fig. 2.9 Glass-transition temperature of polybenzoxazine/poly(ϵ -caprolactone) blends at various PCL contents: (*white square*) low content, (*black square*) high content



benzoxazine in polymer chain. Recently, there has been a study on the system of sunflower oil-modified polyester (SOMP) prepared via the ring-opening polymerization of ϵ -caprolactone [29]. Stannous octoate and partial glycerides were used as catalyst and initiator, respectively. The mole ratio of monomer by initiator was various to control the chain length of polycaprolactone and shorten the reaction time. The hydroxyl functional benzoxazine monomer was prepared by combining with SOMP. The FTIR results revealed the urethane linkage between the hydroxyl functional benzoxazine monomer (HFBA) and SOMP. The rendered alloys possess low brittleness. The thermal properties of the cured alloys and pure polymers are presented as shown in Table 2.1.

From Table 2.1, it reveals that the degradation temperature of cured HFBA was lower than cured SOMP-HFBA because of the highly cleavable Mannich bridges of HFBA. However, it could be noticed that after removing the volatile portion, the remained char yield is rather high.

Table 2.1 Thermal characteristics of the cured alloys and pure polymers (adapted from Taşdelen-Yücedağ et al. [29])

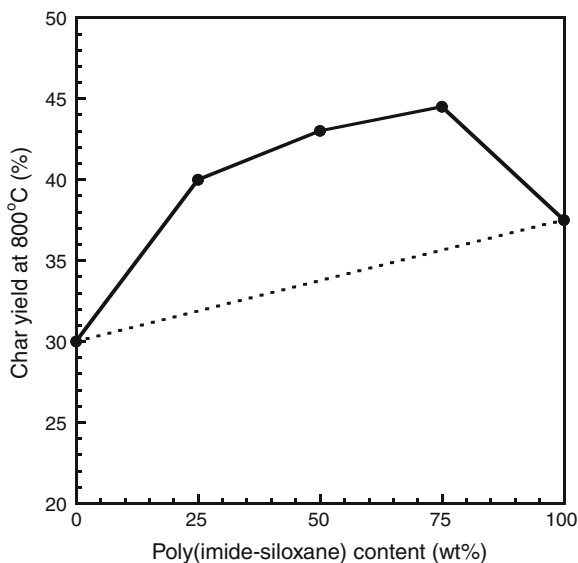
Sample	Degradation temperature at 5% weight loss (°C)	Char yield at 538 °C (%)
Pure SOMP-HFBA	304	1.1
SOMP-HFBA/HFBA (1/8 mol ratio)	291	26.6
SOMP-HFBA/HFBA (1/10 mol ratio)	274	26.4
Pure HFBA	270	28.8

2.7 Polybenzoxazine/Poly(Imide-Siloxane) Alloys

Ardhyananta et al. [30] reported the improvement of thermal stability, mechanical property, flame resistance, and flexibility of bisphenol-A/aniline-based polybenzoxazine (poly(BA-a)) by alloying with polydimethylsiloxane (PDMS) since PDMS is one of the most important silicones that have inorganic main chain, showing both high flexibility and many intriguing properties, e.g., good oxidative stability, low surface energy, high hydrophobicity, high gas permeability, and good biocompatibility [31]. The alloys at 7 and 13 wt% of PDMS revealed higher thermal stability, i.e., the degradation temperatures at 10 %weight loss are 352 and 368 °C, respectively. These values are greater than that of pure polybenzoxazine (326 °C). It was reported that the glass-transition temperature determined from E'' peak of DMA results presented two values. The higher T_g was in the range of 176–185 °C, while the lower T_g was in the range of 63–72 °C. These T_g values correspond to those of poly(BA-a) and PDMS components, respectively. This behavior revealed the phase separation of the alloy in microscale. In addition, the char yield at 850 °C of the alloys increased with increasing PDMS content. The values of residual weight were in the range of 40–46 %, presenting the enhancement of the flame retardancy. In addition, they reported that the obtained alloy film render higher tensile strength and elongation at break than neat poly(BA-a) due to the toughening effect of PDMS. Recently, the effect of pendant groups of polysiloxane, e.g., PDMS, PMPS, and PDPS on thermal properties have been reported by Ardhyanant et al. [31]. The phenyl group of polysiloxanes as PMPS and PDPS improved their compatibility with poly(BA-a). The alloying could enhance the glass-transition temperature because of high crosslink density by plasticizing effect of polysiloxanes. Moreover, poly(BA-a)/PDMS alloy exhibited the optimum improvement of decomposition temperature, while poly(BA-a)/PDPS presented the most effectiveness of flame retardancy. That means the thermal properties of the polybenzoxazine/poly(imide-siloxane) alloys depends on the types of polysiloxanes.

In order to enhance the miscibility of the alloy between poly(BA-a) and polysiloxanes, the polybenzoxazine alloying with PDMS-containing polyimide as poly(imide-siloxane) with hydroxyl functional group (PI-Si(OH)) was developed by Takeichi et al. [32]. The researcher reported that only one glass-transition temperature was observed at ca. 300 °C because crosslinked polymer networks were formed. It is worthy to note that in case of poly(BA-a) alloyed with poly(imide-siloxane) without hydroxyl functional group (PISi), the synergy of char yield was reported at certain content of PISi as presented in Fig. 2.10 [33]. The phenomenon could be due to a large amount of aromatic ring in the blends with some chemical interaction between poly(BA-a) and PISi.

Fig. 2.10 Char yield of the polybenzoxazine/poly(imide-siloxane) alloys



2.8 Polybenzoxazine/Polyimide Blends

Takeichi et al. [34] prepared the polymeric blends using a bifunctional benzoxazine resin, 6,6'-(1-methylethylidene)bis(3,4-dihydro-3-2H-1,3-benzoxazine) (BA-a) and a polyamic acid (PAA, intermediate compound to synthesize polyimide) or soluble polyimide (PI) derived from bisphenol-A di(phthalic anhydride) ether (BPADA) and oxydianiline (ODA). The results of loss modulus (E'') and loss tangent ($\tan\delta$) exhibited only one glass-transition temperature (T_g) in both systems of poly(BA-a)/PAA and poly(BA-a)/PI. That means these blending systems were miscible. The T_g s was shifted to higher temperature when increasing the content of imide. In comparison at the same ratio, the T_g s of poly(BA-a)/PAA alloys were slightly higher than that of poly(BA-a)/PI alloys. For example, at 30 wt% of poly(BA-a), the T_g of poly(BA-a)/PI alloys is 205 °C, while that of poly(BA-a)/PAA is higher than 215 °C. That indicates the formation of crosslinked structure in the alloys of poly(BA-a)/PAA. In aspect of thermal stability of poly(BA-a)/PI alloys and poly(BA-a)/PAA alloys, the value of decomposition temperature increased with the increase of imide content. In addition, the synergism of char yield was observed as shown in Fig. 2.11. It was presented that an interpenetrating polymer network (IPN) structure occurred in the systems. The PAA was imidized in situ with the polymerization of BA-a. This leads to the formation of aromatic ester group (AR-COOR). The proposed reaction between PAA and BA-a is presented in Fig. 2.12. The researchers explained that the combination of poly(BA-a) and PAA contains IPN structure, while that of poly(BA-a) and PI are supposed to be pure semi-IPN structures.

Fig. 2.11 Synergism of char yield in the polybenzoxazine/polyimide blends

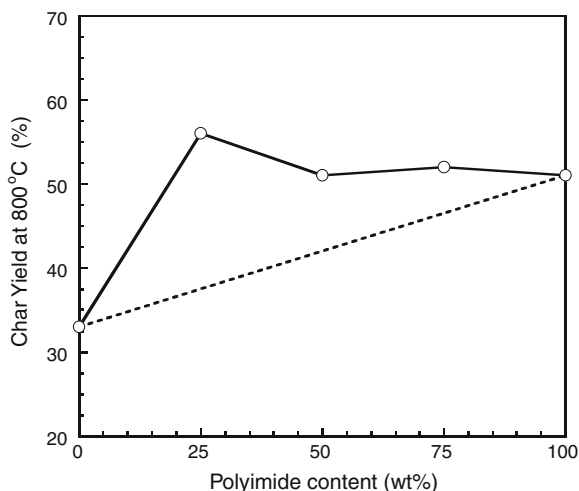
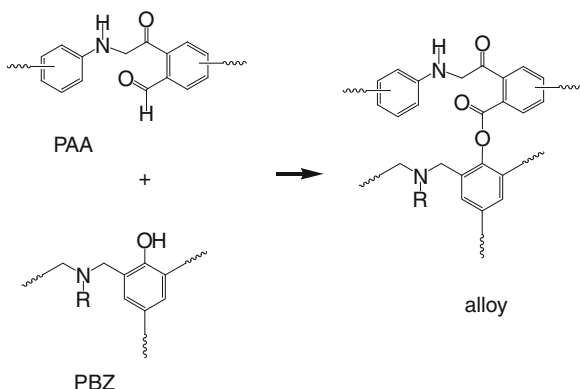


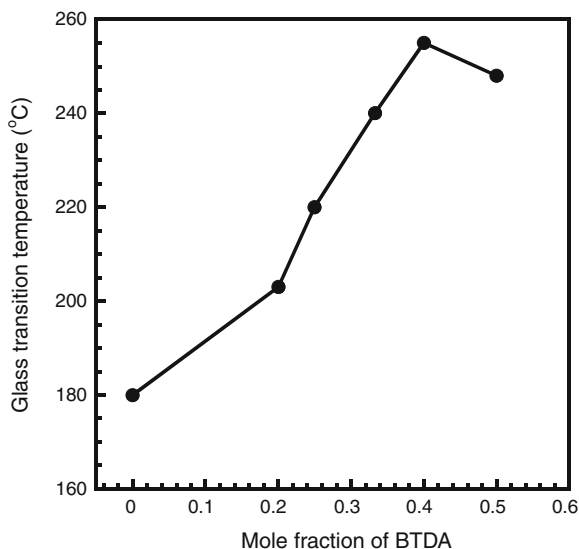
Fig. 2.12 Proposed reaction between PAA and PBZ



2.9 Polybenzoxazine/Dianhydride Copolymer

As previously mentioned in the section of the polybenzoxazine/polyimide blends, Takeichi et al. [34] reported that the chemical bonding between carboxylic acid of poly(amic acid) to generate aromatic ester group (Ar-COOR). Thus, the chemical bonding could be expected in the system of poly(BA-a) copolymerized with dianhydride (BTDA). In general, BTDA is applied as comonomer for high tensile strength polyimide fiber, films, and foams to render outstanding mechanical and electrical performances including excellent heat insulation and fire retardancy. Recently, the copolymers prepared from bisphenol-A/aniline-type benzoxazine resin (BA-a) and BTDA in N-methyl pyrrolidone (NMP) solvent were studied by Rimdusit and Jubsilp [35] and Jubsilp et al. [36]. From their works, the results from FTIR spectra showed that the chemical interaction between hydroxyl groups

Fig. 2.13 Glass-transition temperature of the polybenzoxazine–dianhydride copolymer at various BTDA mole fractions

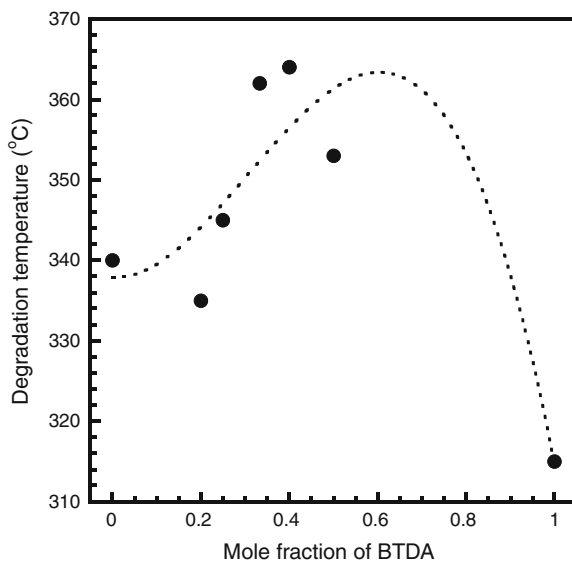


of poly(BA-a) and anhydride groups of dianhydride occur to generate ester linkages at the spectrum of 1730 cm^{-1} , similar to the peak found in the benzoxazine containing polyester studied by Tuzun et al. [37].

When the poly(BA-a) was incorporated with dianhydride, the ester linkages (the functional group with structural flexibility) were formed. That is able to make the rigid poly(BA-a) flexible. Furthermore, the transparency of copolymer indicates that there is no phase separation in the binary system. This physical appearance of fully cured copolymer is in agreement with the DSC results, which presents the single glass-transition temperature (T_g). It is worthy to note that the synergism of (T_g) was observed in the poly(BA-a) modified with BDTA, i.e., the T_g value of the BA-a:BDTA copolymer at the weight ratio of 60:40 (mole fraction of BDTA = 0.4) was reported to be $255\text{ }^\circ\text{C}$. This value is significantly higher than that of unmodified poly(BA-a), i.e., $173\text{ }^\circ\text{C}$ as presented in Fig. 2.13. The T_g improvement of poly(BA-a) is attributed to the increase in crosslink density of the copolymers determined by dynamic mechanical analysis (DMA). Additionally, the degradation temperatures of the copolymer were remarkably higher than those of the parent components as exhibited in Fig. 2.14. The residual weight or char yield of the copolymer at $800\text{ }^\circ\text{C}$ was as high as ca. 61 %, much higher than that of pure poly(PBA-a). Thus, the obtained copolymer possesses high mechanical properties with excellent fire retardancy.

Recently, there was an investigation on the effects of aromatic tetracarboxylic dianhydrides on the thermomechanical properties of poly(BA-a)-dianhydride copolymer [38]. Three different tetracarboxylic dianhydrides were determined, i.e., pyromellitic dianhydride (PMDA), 3,3',4,4' biphenyltetracarboxylic dianhydride (s-BPDA), or 3,3',4,4' benzophenonetetracarboxylic BTDA. The authors discussed that the rendered copolymer of poly(BA-a) and three types of dianhydride

Fig. 2.14 Degradation temperature of the polybenzoxazine–dianhydride copolymer at various BTDA mole fractions



could be potential candidates for high-performance materials with excellent mechanical integrity for high temperature applications. The glass-transition temperatures (T_g) of the copolymers were reported to be in the order of poly(BA-a):PMDA > poly(BA-a):s-BPDA > poly(BA-a):BTDA. The difference of the glass transition is relevant to the rigidity of dianhydride components. All types of dianhydride render significantly higher T_g than that of neat poly(BA-a) due to the improved crosslink density. Moreover, the decomposition temperature at 10 % weight loss of neat poly(BA-a) was 361 °C, while those of the copolymers increased in the order of poly(BA-a):PMDA (426 °C) > poly(BA-a):s-BPDA (422 °C) > poly(BA-a):BTDA (410 °C). This thermal stability could be related to the aromatic skeleton of the acid dianhydride component, i.e., phenylene unit > biphenyl unit > benzophenone unit [37].

2.10 Polybenzoxazine/Lignin Alloys

The curing and thermal behaviors of polybenzoxazine alloyed with lignin were investigated by Noru-Eddine et al. [39]. Two types of polybenzoxazines were determined, i.e., phenol-based benzoxazine (Pa) and bisphenol-A-based benzoxazine (Ba). The DSC results reveal the initial temperature (T_i), final temperature (T_f), peak curing temperature (T_p), heat of enthalpy of curing (ΔH), and glass-transition temperature (T_g) of the alloys as shown in Table 2.2. The results revealed that the maximum curing temperatures of the mixtures were less than that of neat benzoxazine monomer. The heat of polymerization of the mixture between

Table 2.2 DSC results of the polybenzoxazine/lignin alloys at various lignin contents (adapted from Noru-Eddine et al. [39])

Mpiass ratio of benzoxazine and lignin	T_i (°C)	T_p (°C)	T_f (°C)	ΔH (J/g)	T_g (°C)
Pa-type polybenzoxazine	228	254	277	298	210
Pa:lignin = 95:5	182	226	274	440	214
Pa:lignin = 90:10	196	221	268	188	216
Pa:lignin = 85:15	162	207	266	319	218
Pa:lignin = 80:20	161	207	282	227	218
Pa:lignin = 75:25	150	207	277	224	223
Pa:lignin = 70:30	133	203	264	202	237
Ba-type polybenzoxazine	215	261	313	277	240
Ba:lignin = 95:5	111	229	301	330	304
Ba:lignin = 90:10	127	226	309	395	309
Ba:lignin = 85:15	143	256	297	284	310
Ba:lignin = 80:20	142	219	299	300	310
Ba:lignin = 75:25	136	215	299	339	310
Ba:lignin = 70:30	152	212	285	303	311

benzoxazine monomer and lignin had no relationship with the mass content. The increase in the lignin content leads to the increase in T_g . This could be attributed to the increase in crosslink density. In general, the value of T_g is related to the mobility of the polymer backbone and the crosslink density. Therefore, the lignin polymer could make network structure denser and the mobility of the backbone lower than the neat polybenzoxazine. Recently, Emranul Haque et al. [40] prepared and studied the polymer alloys of bisphenol-A-based polybenzoxazine and lignin by mixing two components and following with thermal curing. It was revealed that lignin accelerates the polymerization of benzoxazine. At the lignin content up to 2 wt%, the alloy is transparent. In case of higher content, the phase separation was observed. In aspect of thermal stability at lignin content of 10 wt%, the highest onset of decomposition temperature was observed. Moreover, it was reported that the char yield of the alloy film was increased with increased the lignin content. That indicates the higher flame retardancy of the alloy film than the neat polybenzoxazine.

2.11 Potential Applications of Polybenzoxazine Blends and Alloys

The wide applications of polybenzoxazine blends and alloys are in many areas, i.e. for fabricating molded and casted stuffs, as bonding particles, for ion exchange uses, for lamination and impregnation process, in manufacturing composites including electrical components, etc., because of the ability to be alloys with various kinds of resins or polymers. The property is able to broaden the range of applications of the polymer [8, 41, 42]. At present, the benzoxazine resins are

commercially produced as the component in prepreg composites due to their excellent toughness and stability at high temperature, significantly low shrinkage enhancing equipment surface quality, and drastically long out-life. In addition, liquid form of benzoxazine resin can be applied in the process of vacuum-assisted resin transfer molding (VARTM) and resin transfer molding (RTM) because of their excellent characteristics, e.g., easiness to process in VARTM and RTM, wide processing window, long storage time in room temperature. Another application of this resin is as film adhesive for composite bonding and high temperature composites. Moreover, benzoxazine resins are a good chemical to substitute phenolic resins attributed to nontoxicity before and upon cure and great fire resistant characteristics, high glass-transition temperature. Therefore, the familiar uses of the polybenzoxazine are such as the prepreg for aircraft interior parts that must meet the fire, smoke, and toxicity (FST) regulations. Recently, benzoxazine has been developed and favorably introduced for the applications in the halogen-free printed circuit board (PCB) manufacturing due to their many outstanding characteristics [43].

Furthermore, recently, the polybenzoxazine alloyed with poly(benzimidazole) has been developed for the purpose of highly durable polymer electrolyte membranes at high temperature (over 100 °C) [44]. The casting method is applied to the solution of a poly[2,2'-(*m*-phenylene)-5-5'-bibenzimidazole] and di-functional benzoxazine monomer, HFa benzoxazine, in *N,N*-dimethylacetamide before stepwise heating. The rendered films are potential to be produced in large scale by roll-to-roll coating. The products provide the thermal and mechanical stability.

References

1. Holly FW, Cope AC (1944) Condensation products of aldehydes and ketones with *o*-Aminobenzyl alcohol and *o*-Hydroxybenzylamine. *J Am Chem Soc* 66:1875–1879
2. Liu J, Ishida H (1996) A new class of phenolic resins with ring-opening polymerization. The polymeric materials encyclopedia. In: Salamone JC (ed), CRC Press, Florida, pp 484–494
3. Nair CPN (2004) Advances in addition-cure phenolic resins. *Prog Polym Sci* 29:401–498
4. Ghosh NN, Kiskan B, Yagci Y (2007) New high performance thermosetting resins: synthesis and properties. *Prog Polym Sci* 32:1344–1391
5. Yagci Y, Kiskan B, Ghosh NN (2009) Recent advancement on polybenzoxazine—a newly developed high performance thermoset. *J Polym Sci Part A: Polym Chem* 47:5565–5576
6. Endo T, Sudo A (2009) Development and application of novel ring-opening polymerizations to functional networked polymers. *J Polym Sci: Part A: Polym Chem* 47:4847–4858
7. Kumar KSS, Nair CPR (2010) Polybenzoxazines: chemistry and properties, iSmithers Rapra Publishing, England
8. Ishida H (1996) Process for preparation of benzoxazine compounds in solventless systems. US Patent 5,543,516
9. Ning X, Ishida H (1994) Phenolic materials via ring-opening polymerization: synthesis and characterization of bisphenol-A based benzoxazines and their polymers. *J Polym Sci Part B: Polym Phys* 32:921–927
10. Shen SB, Ishida H (1996) Development and characterization of high-performance polybenzoxazine composites. *Polym Compos* 17:710–719

11. Shen SB, Ishida H (1999) Dynamic mechanical and thermal characterization of high-performance polybenzoxazines. *J Polym Sci Part B: Polym Phys* 37:3257–3268
12. Ishida H, Allen DJ (1996) Physical and mechanical characterization of near-zero shrinkage polybenzoxazines. *J Polym Sci Part B: Polym Phys* 34:1019–1030
13. Ishida H, Low HY (1997) A study on the volumetric expansion of benzoxazine-based phenolic resin. *Macromolecules* 30:1099–1106
14. Wang YX, Ishida H (2002) Development of low-viscosity benzoxazine resins and their polymers. *J Appl Polym Sci* 86:2953–2966
15. Ishida H, Rodriquez Y (1995) Curing kinetics of a new benzoxazine-based phenolic resin by differential scanning calorimetry. *Polymer* 36:3151–3158
16. Rimdusit S, Bangsen W, Kasemsiri P (2011) Chemorheology and thermomechanical characteristics of benzoxazine-urethane copolymers. *J Appl Polym Sci* 132:3669–3678
17. Rimdusit S, Kunopast P, Dueramae I (2011) Thermomechanical properties of arylamine-based benzoxazine resins alloyed with epoxy resin. *Polym Eng Sci* 51:1797–1807
18. Kumar KSS, Nair CPR, Ninan KN (2009) Investigations on the cure chemistry and polymer properties of benzoxazine–cyanate ester blends. *Eur Polym J* 45:494–502
19. Rimdusit S, Ishida H (2000) Development of new class of electronic packaging materials based on ternary systems of benzoxazine, epoxy, and phenolic resins. *Polymer* 41:7941–7949
20. Takeichi T, Guo Y, Agag T (2000) Synthesis and characterization of poly(urethane-benzoxazine) films as novel type of polyurethane/phenolic resin composites. *J Polym Sci-A* 38:4165–4176
21. Rimdusit S, Pirstpindvong S, Tanthapanichakoon W, Damrongsakkul S (2005) Toughening of polybenzoxazine by alloying with urethane prepolymer and flexible epoxy: a comparative study. *Polym Eng Sci* 45(3):288–296
22. Takeichi T, Guo Y (2001) Preparation and properties of poly(urethane-benzoxazine)s based on monofunctional benzoxazine monomer. *Polymer J* 33(5):437–443
23. Rimdusit S, Ishida H (2000) Synergism and multiple mechanical relaxations observed in ternary systems based on benzoxazine, epoxy, and phenolic resins. *J Polym Sci Pol Phys* 38:1687–1698
24. Rimdusit S, Mongkhonsi T, Kamonchaivanich P, Sujitrot K, Tiptipakorn S (2008) Effects of polyol molecular weight on properties of benzoxazine-urethane polymer alloys. *Polym Eng Sci* 48:2238–2246
25. Su YC, Kuo SW, Yei DR, Xu H, Chang FC (2003) Thermal properties and hydrogen bonding in polymer blend of polybenzoxazine/poly(N-vinyl-2-pyrrolidone). *Polymer* 44:2187–2191
26. Huang JM, Yang SJ (2005) Studying the miscibility and thermal behavior of polybenzoxazine/poly(3-caprolactone) blends using DSC, DMA, and solid state ¹³C NMR spectroscopy. *Polymer* 46:8068–8078
27. Ishida H, Lee YH (2001) Synergism observed in polybenzoxazine and poly(ϵ -caprolactone) blends by dynamic mechanical and thermogravimetric analysis. *Polymer* 42(16):6971–6979
28. Zheng S, Lu H, Guo Q (2004) Thermosetting blends of polybenzoxazine and poly(ϵ -caprolactone): phase behavior and intermolecular specific interactions. *Macromol Chem Phys* 205(11):1547–1558
29. Taşdelen-Yücedağ Ç, Erciyas AT (2013) Preparation of oil-modified polycaprolactone and its further modification with benzoxazine for coating purposes. *Prog Org Coat* 76:137–146
30. Ardhyananta H, Wahid MH, Sasak M, Agag T, Kawauchi T, Ismail H, Takeichi T (2008) Performance enhancement of polybenzoxazine by hybridization with polysiloxane. *Polymer* 49:4585–4591
31. Ardhyananta H, Kawauchi T, Ismail H, Takeichi T (2009) Effect of pendant group of polysiloxanes on the thermal and mechanical properties of polybenzoxazine hybrids. *Polymer* 50:5959–5969
32. Takeichi T, Agag T, Zeidam R (2001) Preparation and properties of polybenzoxazine/poly(imide-siloxane) alloys: In situ ring-opening polymerization of benzoxazine in the presence of soluble poly(imide-siloxane). *J Polym Sci Pol Chem* 39:2633–2641

33. Tiptipakorn S, Damrongsakkul S, Ando S, Hemvichian K, Rimdusit S (2007) Thermal degradation behaviors of polybenzoxazine and silicon-containing polyimide blends. *Polym Degrad Stabil* 92(7):1265–1278
34. Takeichi T, Guo Y, Rimdusit S (2005) Performance improvement of polybenzoxazine by alloying with polyimide: effect of preparation method on the properties. *Polymer* 46:4909–4916
35. Rimdusit S, Jubsilp C (2007) Polymer from anhydride modified polybenzoxazine. Thailand Patent pending. Issue Number 5543516
36. Jubsilp C, Takeichi T, Rimdusit S (2010) Property enhancement of polybenzoxazine modified with dianhydride. *Polym Degrad Stabil* 96(6):1047–1053
37. Tuzun A, Kiskan B, Alemdar N, Erciyes AT, Yagci Y (2010) Benzoxazine containing polyester thermosets with improved adhesion and flexibility. *J Polym Sci Polym Chem* 48:4279–4284
38. Jubsilp C, Ramsiri B, Rimdusit S (2012) Effects of aromatic carboxylic dianhydrides on thermomechanical properties of polybenzoxazine-dianhydride copolymers. *Polym Eng Sci* 52(8):1640–1648
39. Nour-Eddine EM, Yuan Q, Huang F (2012) Investigation of curing and thermal behavior of benzoxazine and lignin mixtures. *J Appl Polym Sci* 125:1773–1781
40. Emranul Haque HM, Islam Z, Kawauchi T, Takeichi T (2012) Preparation and properties of polybenzoxazine/lignin alloy. *Adv Mater Process Technol* 217–219:571–577
41. Ishida H (1999) Composition for forming high thermal conductivity polybenzoxazine-based material and method. US Patent 5900447
42. Ishida H, Rimdusit S (2001) Ternary systems of benzoxazine, epoxy, and phenolic resins. US Patent 6207786
43. Chen LC (2010) Halogen-free varnish and prepreg thereof. US patent 7842401
44. Kim SK, Kim KH, Park JO, Kim K, Ko T, Choi SW, Pak C, Chang H, Lee JC (2013) Highly durable polymer electrolyte membranes at elevated temperature: Cross-linked copolymer structure consisting of poly(benzoxazine) and poly(benzimidazole). *J Power Sour* 226:346–353

Chapter 3

Highly Filled Systems of Polybenzoxazine Composites

Abstract One outstanding property of benzoxazine resins is their very low A-stage viscosity, and therefore, it provides good filler wetting characteristic and allows large amount of filler or reinforcement to be incorporated in the matrix resin during composite fabrication. The relatively broad processing window with suitable chemorheological properties also renders the resins their ability to fabricate special composite systems of a highly filled kind. In this book chapter, we discuss the above high processability of benzoxazine resins to form various types of highly filled systems. These special kinds of composite materials are of crucial practice and a key success in such applications as dental composites, orthopedic composites, wood-substituted composites, thermally conductive composites, or friction and wear composites.

Keywords Highly filled composite • A-stage viscosity • Particle packing

3.1 Introduction

Highly filled composite materials have been developed and investigated for various applications such as in the area of dental and orthopedic medicine, structural plastic materials, paper coatings, automotive products, wood composite, electronic packaging, bipolar plate in fuel cell, erosion resistance, and friction wear. [1–12]. The highly filled composites are defined as the dispersion of filler particles in polymer matrix close to the maximum packing density of the particles, which identified experimentally by its maximum observed density that is equal to its theoretical density [10]. In principle, characteristics of the particles, i.e., their shape, size, and size distribution, have significant effect on the packing characteristics of the particulate composite materials [13], in particular the highly filled ones.

Moreover, in the composite fabrication process, the resin viscosity, which is related to the resin flow-out and wetting characteristics, is an important factor,

which influences the quantity of the particulate filler to be incorporated. Benzoxazine resin, a new class of phenolic resins, possesses various characteristics that make it suitable for use as a matrix of high-performance composites, such as its self-polymerizability upon heating, no release of by-products during curing, very low A-stage viscosity, near-zero shrinkage, low water absorption, and high thermal stability with relatively high char formation, as well as good mechanical performance [14–16].

A very low A-stage viscosity, one of the most useful properties of benzoxazine resins, results in an ability of the resins to accommodate relatively large quantity of filler while still maintaining their good processability when compared with traditional phenolic resins. For example, Ishida and Rimdusit reported that the use of a low melt viscosity benzoxazine resin filled with boron nitride (BN) ceramics could provide a composite material with a maximum BN content of up to 78.5 % by volume or 88 % by weight resulting in a very high improvement on the composite thermal conductivity with the value as high as 32.5 W/mK [10]. In the system of polybenzoxazine–wood composite, substantial amount of woodflour filler (i.e., up to 70.5 % by volume or 75 % by weight) was reported to be incorporated in a polybenzoxazine matrix with a significant enhancement in the resulting thermal and mechanical properties of the obtained wood composites [8]. Moreover, the successful use of polybenzoxazine as a matrix for highly filled composites has been reported in the various other types of fillers or reinforcing agents such as graphite [12], alumina [17], and nanosilica [18].

Though typical bifunctional benzoxazine resins are solid at room temperature, they provide relatively low values of their molten stage or A-stage viscosity. As mentioned previously, a lower viscosity of a resin can enhance an ability of the resin to accommodate greater amount of filler and increase filler wettability of the resin during the preparation of the molding compound. Some previous studies have been done to utilize reactive diluents to lower liquefying temperature as well as to further reduce melt viscosity of the benzoxazine resins such as by adding a liquid epoxy [19] as well as a liquid monofunctional benzoxazine resins [20–22]. Although a significant reduction in viscosity and liquefying point was obtained using the liquid epoxy, the resulting alloy mixtures were reported to render higher curing temperature than that of the neat benzoxazine resin. Recently, Jubsilp et al. reported that a monofunctional phenol–aniline type benzoxazine resin (Ph-a) as a reactive diluent for bifunctional benzoxazine resin showed possible effect on curing behaviors of the monomer mixtures in contrast to the effect observed using epoxy diluent. The curing peak temperature observed in the BA-a/Ph-a mixtures is systematically shifted to a slightly lower temperature with increasing the Ph-a diluent [22]. Consequently, highly filled and high-performance polymer composites from benzoxazine-based polymers have been successfully developed and reported [8, 10, 12, 17, 18].

3.2 High Processability Characteristics of Benzoxazine Resins

One outstanding characteristic of benzoxazine resins in terms of their processability is their ease of monomer synthesis from an invention of the solventless technology by Ishida and Agag [15]. In addition, the as-synthesized monomers from the solventless synthesis have been shown to yield monomers of relatively high purity with low content of oligomers or other high molecular weight species. Consequently, even the as-synthesized monomers can provide a highly desirable low A-stage viscosity value. Solid-state $^1\text{H-NMR}$ spectroscopy is very useful for the study of the benzoxazine chemical structure and the purity of benzoxazine monomer simultaneously. For example, the structure of as-synthesized bisphenol-A—*o*-aniline type benzoxazine monomer (BA-a) was investigated by Kasemsiri et al. [23] using $^1\text{H-NMR}$ spectrum as shown in Figs. 3.1, 3.2. The methyl proton of bisphenol-A showed the signal at 1.58 ppm (a). The characteristic peaks assignable to methylene ($\text{Ar-CH}_2\text{-N}$) of oxazine ring and methylene ($\text{O-CH}_2\text{-N}$) were observed at 4.53 (b) and 5.24 ppm (c), respectively. The group of signals at 6.87–7.83 ppm (d) exhibits aromatic proton. Moreover, the disappearance of signal at 3.6 ppm suggested that the obtained monomers exhibited negligible quantity of methylene proton of either opening ring dimers or oligomers [24, 25]. Therefore, the spectra suggested that the as-synthesized benzoxazine resin is highly pure.

Figure 3.3 exhibits the processing window of the BA-a-based benzoxazine, which is solid at room temperature. The viscosity of the resin initially decreases due to heating past its liquefying or softening point to reach its minimum value. At the point of minimum viscosity, the resin can conveniently be processed or transferred into the mold. In the highly filled composite manufacturing process, the low melt viscosity resins are required in typical formulations to achieve easier handling and to increase filler loading. The softening temperature of the BA-a monomers was determined to be 76 °C at the viscosity of 500 Pa.s. In Fig. 3.3, the incorporation of the liquid Ph-a in the solid BA-a resin also yielded a softer solid at room temperature, ranging from BP91 to BP64. Lowering the resin liquefying

Fig. 3.1 Structure of bifunctional BA-a benzoxazine monomer

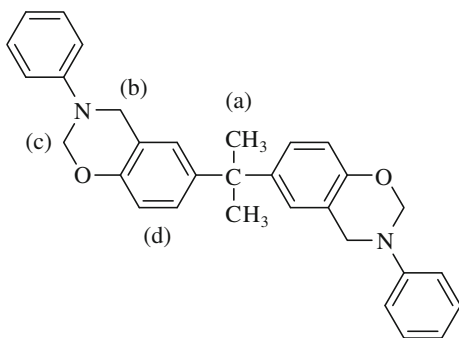


Fig. 3.2 ¹H-NMR of the benzoxazine monomer

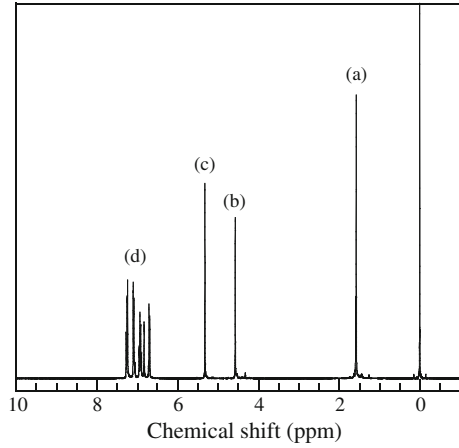
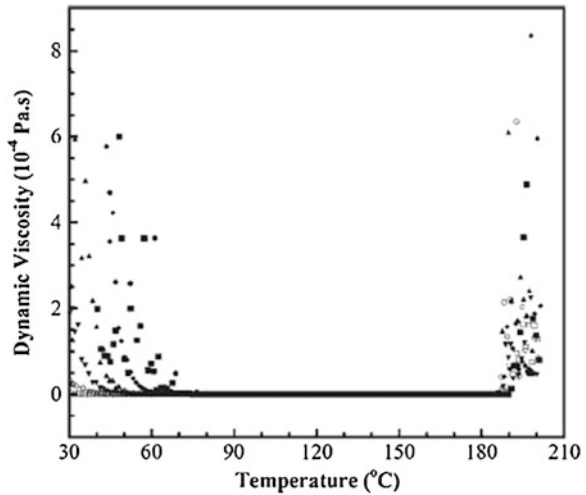


Fig. 3.3 Processing window of BA-a (B)/Ph-a (P) resin mixtures at various Ph-a resin using a heating rate 2 °C/min: (circle) BA-a resin, (square) BP91, (diamond) BP82, (triangle) BP73, (inverted triangle) BP64, (left pointing triangle) BP55, (right pointing triangle) Ph-a resin

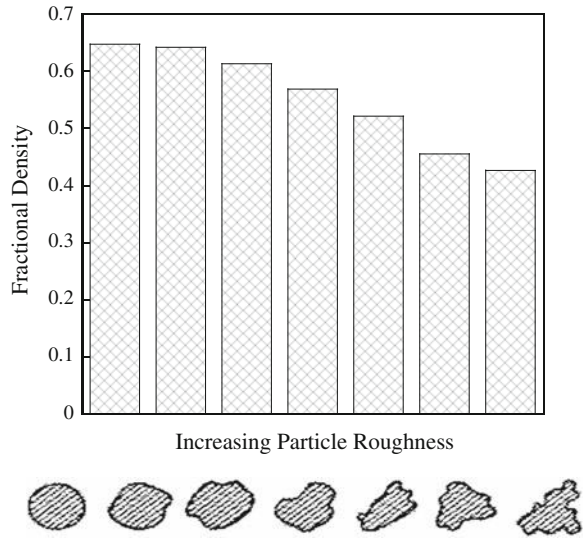


temperature enables the use of lower processing temperatures for a compounding process, which is also highly desirable in most composite applications [22].

3.3 Fundamentals of Particle Packing Characteristics [26]

In order to achieve maximum filler packing in the composites, characteristics of the particulate filler are known to play a crucial role in this purpose. This section summarizes major features of the particulate filler to provide maximum packing density value in composite materials. The detail discussion on particle packing characteristics can be further studied in an excellent monograph by German [26].

Fig. 3.4 Fractional density for monosized powders versus roughness as expressed by a typical particle profile



For monosized spheres, the fractional packing density is between 0.60 and 0.64 [26]. In the case of the actual density, the value depends on the filler characteristics, namely the size and shape, and factors including the adsorbed moisture. The packing density ranges from 30 to 65 % of theoretical value; the lower value is representative of irregular and sponge filler.

Figure 3.4 gives the fractional packing density for various monosized irregular particle shapes. The figure reveals that interparticle friction depends on particle surface irregularities. The greater the surface roughness or the more irregular the particle shape, the lower the packing density as the shape departs from equiaxed (spherical). As the particle shapes become more rounded (spherical), the packing density increases.

Furthermore, the packing of fibers provides an illustration of a decreasing packing density as the particles have a larger length-to-diameter or the aspect ratio (L/D). Figure 3.5 plots the fractional packing density versus the length-to-diameter ratio for fibers. Obviously, fractional packing density improves as the particles approach a smooth, equiaxed shape.

To overcome the packing limits of particulate filler, we can tailor the particle size distribution for greater packing density. Bimodal particle size mixtures can pack to higher densities than monosized particles. The key to improve packing then rests with the particle size ratio. In principle, small particles are selected to fit the interstices between large particles without forcing the large particles apart. In addition, even smaller particles can be chosen to fit into the remaining pores, giving a corresponding enhancement in the particle packing density or the reduction in the void volume between the particles. The basis for the phenomenon is illustrated in Fig. 3.6. In the figure, the fractional density is shown as a function of composition for a mixture of large and small particulate spheres. At the maximum packing composition, there is a greater volume of large particles than small

Fig. 3.5 A change in packing density with the length-to-diameter ratio (L/D) for fibers (i.e., best packing occurs with equiaxed particles)

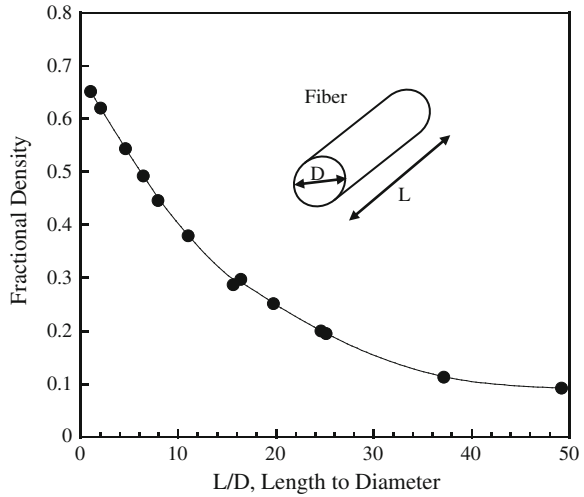
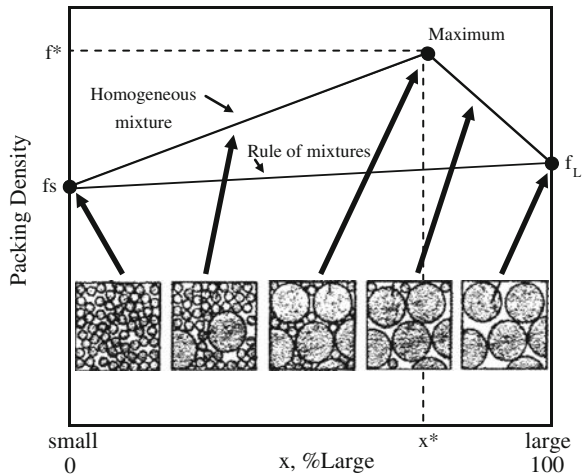


Fig. 3.6 Plot of fractional packing density versus composition for bimodal mixtures of large and small spheres



particles. The relative improvement in packing density depends primarily on the particle size ratio of the large and small particles. Within a limited range, the greater the size ratio shows the higher the maximum packing density [26].

Starting with the large particles, the packing density initially increases as small particles are incorporated to fill the voids between the large particles, which corresponds to the right hand side of Fig. 3.6. Eventually, the quantity of small particles fills all of the spaces between the large particles. On the other hand, beginning with the small particles, clusters of small particles and their associated voids can be eliminated and replaced with a full density region everywhere when a large particle is added. The packing benefit of replacing small particles with the large particle continues until a concentration where the large particles contact one

another. Figure 3.6 shows this process on the left hand side of the curve. The point of maximum packing density corresponds to the intersection of those two curves. At this point, the large particles are in point contact with one another and all of the interstitial voids are filled with the small particles. The optimal composition in terms of the weight fraction of large particle X^* depends on the amount of void spaces between large particles, which equals $(1 - f_L)$, where f_L is the fractional packing density of the large particles [30],

$$X^* = f_L / f^* \tag{3.1}$$

With the packing density at the optimal composition f^* given as,

$$f^* = f_L + f_S(1 - f_L) \tag{3.2}$$

And the fraction packing density for the small particle is f_S .

The ideal fractional density of each of spherical particle, i.e., large and small particle sizes, can pack to obtain the maximum packing density is 0.637. To obtain the maximum packing density value higher than 0.637, if the corresponding mass fraction of large particle for maximum packing is 0.734, while the mass fraction of the small particle sizes is of 0.266, the expected fractional packing density would be 0.86 [26].

Figure 3.7 illustrates how the packing density increases with the particle size ratio (large diameter divided by small diameter). Note the dramatic change in behavior at the particle size ratio corresponding to one particle filling the triangular pores between the large particles at roughly a 7:1 size ratio. In principle, increasing the packing density will increase with the homogeneity of the mixture. In practice, randomly mixed systems will have property range between unmixed and fully mixed and typically exhibit some in homogeneities that deviate actual packing from the ideal.

Fig. 3.7 Effect of particle size ratio on the packing density for mixtures consisting of 70 % large particles and 30 % small particles

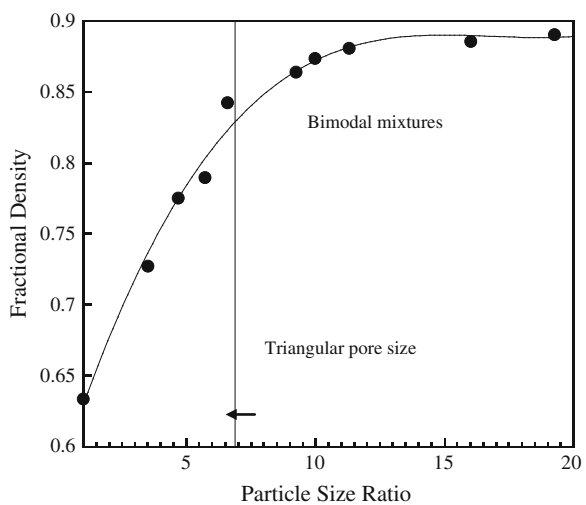


Table 3.1 Effect of particle size distribution on packing density showing relation between particle size ratio and maximum packing density

Number of component	Size ratio	Weight percent	Packing fraction
1	–	100	0.64
2	7:1	73:27	0.86
3	49:7:1	75:14:11	0.95
4	343:49:7:1	73:14:10:3	0.98

Table 3.2 Effect of BN particle size on packing densities of polybenzoxazine composites [10]

Boron nitride (grade)	Average particle size (μm)	Type	ϕ_m (wt %)
HCPH	9	Flake	60
HCJ325	45	Aggregate	75
TS1890	75	Aggregate	85
HCJ48	225	Aggregate	88

Similar to the behavior of spheres, a density increase is associated with blending different particle sizes of similar shapes. However, a major difference between spherical and nonspherical particles is that the initial packing is typically higher for spheres. In summary, the greater the surface roughness, shape irregularity, or particle aspect ratio will lead to the lower the inherent packing density of the particles.

Though the relative density gain is similar for spherical and nonspherical particles, the starting density for nonspherical particles is lower. Accordingly, at all compositions, the nonspherical mixture will provide lower in density. In addition, the idea developed for bimodal mixtures for packing density enhancement can be extended to multimodal systems, as seen in Table 3.1.

Ishida and Rimdusit [10] studied the dependence of the different BN powder characteristics on the maximum packing densities of the obtained polybenzoxazine composites as exhibited in Table 3.2. From their result, the larger the average particle size of BN with bimodal size distribution, the higher the maximum packing density of the composite, which is in agreement with the theory of particle packing discussed above [26].

3.4 Highly Filled Polybenzoxazine Microcomposite

3.4.1 Highly Filled Wood-Substituted Composites from Polybenzoxazine

Wood–polymer composites’ (WPC) popularity and expansion into residential markets and construction industries including siding, exterior decking and railing material are due to the product’s perceived low maintenance and environmental

performance (life span and absence of toxic chemicals) relative to chemically treated solid wood [27]. The focus in wood–polymer composite research has been on enhancement of mechanical integrity of the wood composite and the improvement in the interfacial adhesion between the hydrophilic wood and hydrophobic polymer matrix. Studies have concentrated especially on various coupling agents and chemical treatments to improve adhesion between these two components [27–31].

In our previous reports, good interfacial adhesion between the woodflour filler and the matrix was observed in the polybenzoxazine–wood composites without any additional treatment on the woodflour filler [8]. This is because a phenolic hydroxyl group–based polybenzoxazine (PBA-a) structure formed by ring opening reaction of BA-a upon thermal treatment might be from chemical bonds with the woodflour filler. In addition, the low melt viscosity of BA-a type polybenzoxazine allows substantial amount of woodflour to be easily incorporated into the composites up to 70.5vol %. As a result, substantial improvement in the storage modulus at room temperature as well as in the rubbery plateau modulus of the polybenzoxazine–wood composites over the neat polymer was observed as shown in Fig. 3.8.

Figure 3.9 is a plot of the loss moduli of the unfilled and woodflour-filled polybenzoxazines as a function of temperature. The peak positions of the loss moduli were used to indicate the glass transition temperature (T_g) of the specimens. The outstanding compatibility between the woodflour and the polybenzoxazine matrix is evidently seen from the large improvement in the composite's T_g with the value as high as 220 °C at 70.5vol % of the filler comparing with the T_g value of 160 °C of the neat polybenzoxazine. This T_g enhancement of up to 60 °C is hardly found in other filled polymeric systems [32].

Fig. 3.8 Storage modulus of woodflour-filled polybenzoxazine composites at different filler contents: (square) neat resin, (diamond) 34.6vol %, (triangle) 44.3vol %, (inverted triangle) 54.4vol %, (left pointing triangle) 65.0vol %, (right pointing triangle) 70.5vol %

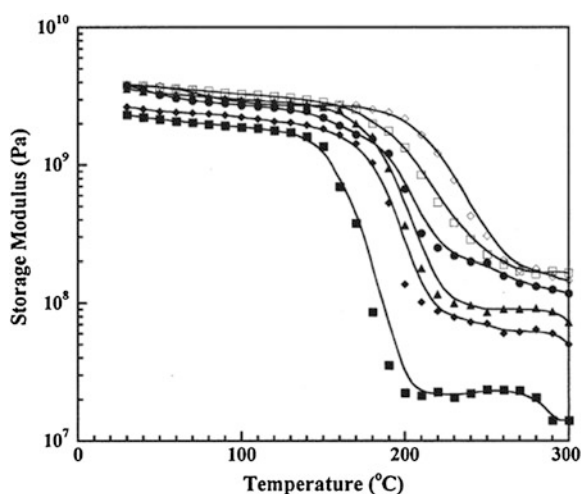
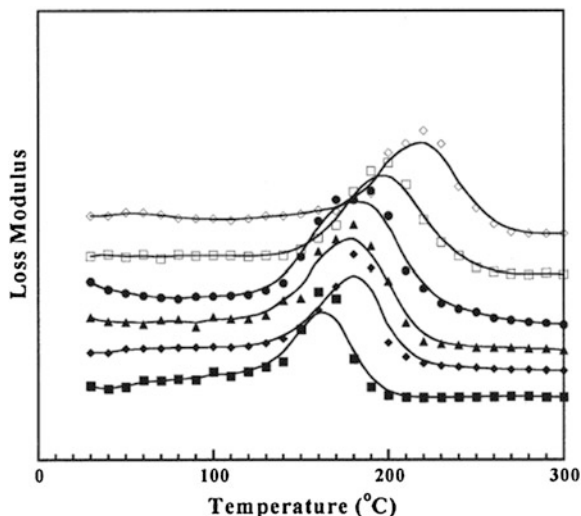
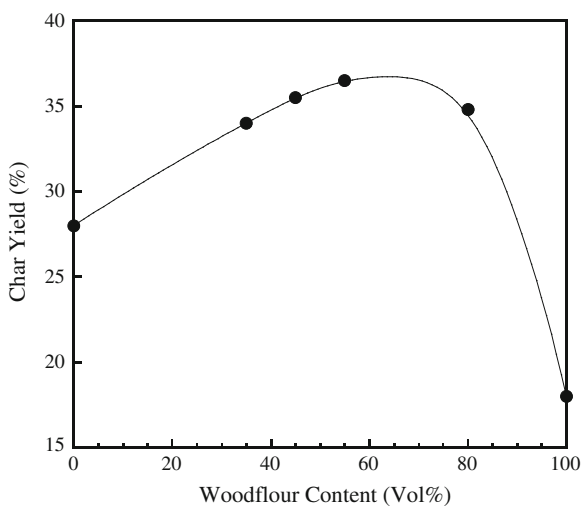


Fig. 3.9 Loss modulus of the polybenzoxazine composites at different filler contents: (square) neat resin, (diamond) 34.6vol %, (triangle) 44.3vol %, (inverted triangle) 54.4vol %, (left pointing triangle) 65.0vol %, (right pointing triangle) 70.5vol %



Interestingly, Fig. 3.10 showed the synergistic behavior of char yields in the highly filled systems. The observed synergistic behavior in the char formation of this polybenzoxazine composite system may be attributed to the substantial chemical bonding between the woodflour filler and the polybenzoxazine matrix because of their similar phenolic nature and their relatively high availability of the free OH group. In some other wood-substituted composites, char formation as a function of woodflour contents tends to provide a behavior following a rule of mixture or even showed negative deviation phenomenon [27–31, 33].

Fig. 3.10 Effect of woodflour content on the char yield of the woodflour-filled polybenzoxazine composite reported at 800 °C under nitrogen atmosphere



3.4.2 Boron Nitride-Filled Polybenzoxazine for Electronic Packaging Application

In 1998, Ishida and Rimdusit have been reported very high thermal conductivity of 32.5 W/mK obtained by BN-filled polybenzoxazine at its maximum filler loading of 78.5 % by volume (88 % by weight). Up to present, this composite system still provides the highest reported thermal conductivity value among polymer composites [34–36]. In terms of mechanical properties, the moduli of the highly filled polybenzoxazine–BN composites were found to greatly increase with increasing amount of the BN as shown in Fig. 3.11. This observed behavior corresponds to the high thermal conductivity value of the specimen because, in theory, heat particle or phonon conducts better in a stiffer material, i.e., higher acoustic velocity. The modulus at room temperature of 85 % by weight BN filler is very high, exceeding 10 GPa, which is a value comparable to continuous fiber glass–reinforced phenolics. The detail discussion of this composite is presented in Chap. 4.

3.4.3 Highly Filled Systems of Alumina and Polybenzoxazine

Alumina is one of the major mechanical reinforcement in plastics. The dynamic mechanical property of the alumina-filled polybenzoxazine and epoxy was investigated and compared in Fig. 3.12. At room temperature, the storage modulus (E') of the polymer composites steadily increased with increasing alumina content. From the figure, the polybenzoxazine–alumina composite showed higher storage modulus at each filler content compared with the epoxy composites. At the

Fig. 3.11 Storage modulus of boron nitride-filled polybenzoxazine as a function of the filler content

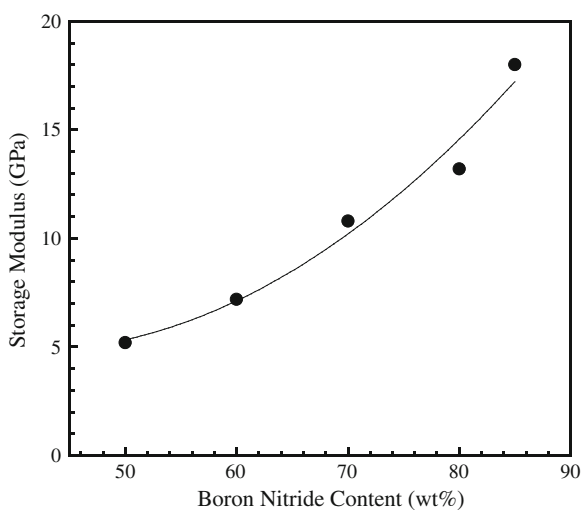
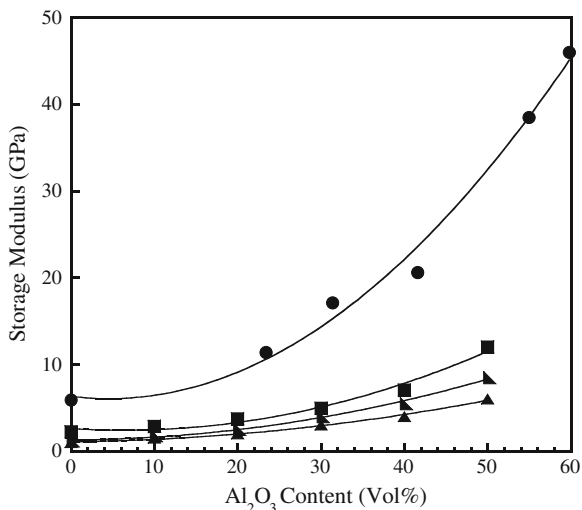


Fig. 3.12 Storage modulus of Al_2O_3 composites as a function of alumina content (circle) polybenzoxazine [17] (square) epoxy [1], (left pointing triangle) DGEBA/D230 [37], and (right pointing triangle) DGEBA/D400 [37]



maximum alumina content of 83 wt% (60vol %), the storage modulus as high as 46 GPa was obtained. This high reinforcing effect from an addition of rigid particulate filler into the polymer matrix is attributed to the strong interfacial interaction between the alumina and the polybenzoxazine.

The glass transition temperature of the neat polybenzoxazine was determined to be 176 °C, whereas the glass transition temperature of the highly filled composites was increased systematically with the alumina content up to about 188 °C as shown in Table 3.3. An increase in the T_g with an addition of the alumina confirms the good interfacial adhesion between the alumina filler and polybenzoxazine matrix resulting in a high restriction of the mobility of the polymer chains; thus, the higher T_g observed.

Surface hardness is generally investigated as one of the most important factors that are related to the wear resistance of materials. Table 3.3 reveals the Vickers microhardness (HV) values of the neat polybenzoxazine and alumina-filled polybenzoxazine composite at different alumina contents. The surface hardness of the alumina composites increased substantially with increasing alumina content. The HV value of the alumina-filled polybenzoxazine composites with the alumina

Table 3.3 Glass transition temperature and hardness of highly filled PBA-a/ Al_2O_3 composites [17]

Al_2O_3 content (wt %)	Glass transition temperature (°C)	Hardness (MPa)
0	176	388
50	178	515
60	180	609
70	182	766
80	188	1038
83	185	1124

contents ranging from 0 to 83 % by weight was 388–1,123 MPa. The HV value of alumina-filled composite at 83wt % was found to be 189 % higher than that of the neat polybenzoxazine. Consequently, the resulting composites should be highly useful as wear-resistant materials.

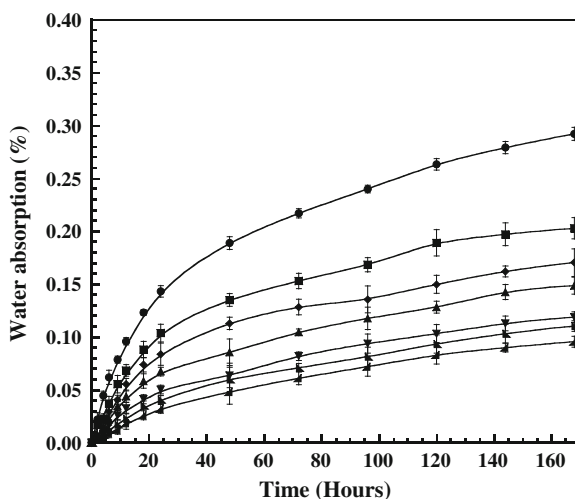
3.4.4 Graphite-Filled Polybenzoxazine Composites

Graphite is the most commonly used material for a bipolar plate [38–40]. It has a good electrical conductivity and excellent corrosion resistance with a relatively low density of about 2.2 g/cm^{-3} . However, it lacks mechanical strength and has poor ductility. Flexible graphite-based composite bipolar plates made from polymer/graphite mixture are considered as an attractive option for polymer exchange membrane fuel cell (PEMFC). They offer the advantage of lower cost, rapid processing, and higher flexibility, and they show reduced weight in comparison with metal bipolar plates and pure graphite.

Jin-Chul Yun et al. [40] observed a moisture absorption, which occurred in composites, resulting on the reduction of the mechanical and electrical properties. They showed that the absorbed moisture introduces small cracks in the polymer resin. In addition, they assessed that the imperfect bonding as defect or voids between polymer and graphite are likely susceptible areas for moisture absorption. Therefore, considering this factor is important. The Department of Energy (DOE) proposed a technical target of bipolar plates for the year 2010 in which the main water uptake has values of much less than 0.3 %, which is the value desired in the industrial standard of typical composites for bipolar plate [41].

Figure 3.13 reveals the plot of the water absorption percentage against time of highly filled composites between graphite and polybenzoxazine. The water

Fig. 3.13 Water absorption of graphite-filled polybenzoxazine composites: (circle) polybenzoxazine (square) 40wt %, (diamond) 50wt %, (triangle) 60wt %, (inverted triangle) 70wt %, (left pointing triangle) 75wt %, (right pointing triangle) 80wt %



adsorption values of all graphite–polybenzoxazine composites at different filler contents ranging from 40 to 80 % by weight were recorded up to 168 h of the immersion. All composite samples at different graphite contents exhibited a similar behavior, that is, the specimens absorbed water more rapidly during first stages (0–24 h) and at a slower rate beyond that up to their saturation points. The water uptake of all compositions at 24 h is <0.11 % and only ca. 0.03 % at a filler content of 80 % by weight. Furthermore, the water uptake up to 168 h is only 0.2 % at graphite content of 40 % by weight and steadily lower at higher graphite contents. The decrease in water absorption with increasing graphite content is attributed to the presence of the more hydrophobic nature of the graphite filler in the polymer composites. At the polymer composite contained with 50wt % graphite content, these values were also significantly lower than water absorption values of other composite systems such as those of graphite filled with epoxy [42]. For example, Du and Jana reported a 24-h water uptake of about 1.8 % for graphite–epoxy composite, whereas only about 0.1 % for graphite–benzoxazine composite was observed comparing at a fixed graphite content of 50 % by weight as exhibited in Fig. 3.14.

The electrical conductivity is one of the most important characteristics among those requirements for a bipolar plate application. The property is largely influenced by the total filler loading and an ability to form a conductive network of the conductive filler used [12, 43–46]. As per the recent benchmark given by DOE, USA, the recommended value of electrical conductivity for bipolar plate is $>100 \text{ S.cm}^{-1}$ [41]. Table 3.4 depicts electrical conductivity of the graphite-filled polymer composites at different weight fractions of graphite. It is evident that the conductivity of the composite increased with an increase in graphite content. Our highly filled graphite–polybenzoxazine composites at 70–80 % by weight of

Fig. 3.14 Water absorption of graphite-filled polymer composites at 50wt % graphite content with different polymer matrices: (circle) polybenzoxazine, (square) epoxy [42]

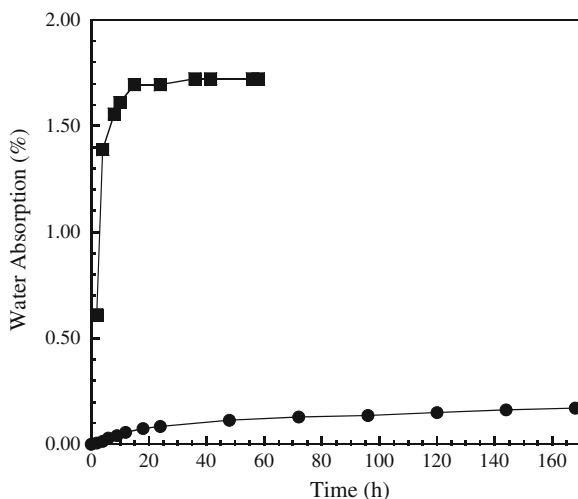


Table 3.4 Electrical conductivity (Scm^{-1}) of graphite composites

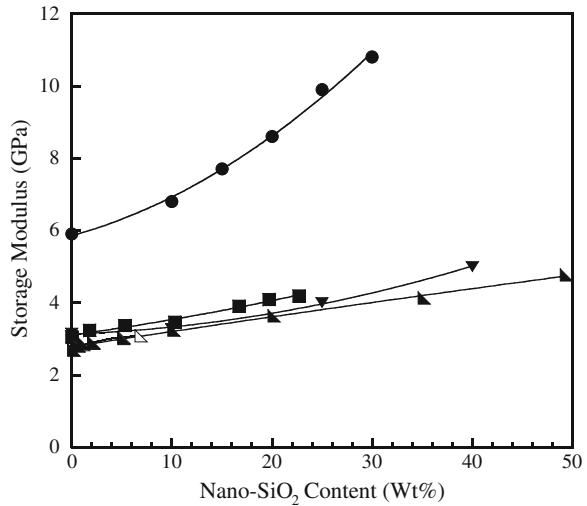
Graphite content (wt %)	PBA-a [12]	Novolac epoxy [43]	Phenol formaldehyde [44]	Epoxy [45, 46]
40	0.39	–	–	–
45	–	–	–	–
50	2.55	–	–	1.25
55	–	–	–	2.5
60	8.4	–	–	5
65	–	–	–	15
70	104	53	24.8	32.5
75	215	78	66.1	71.25
80	245	100	64.8	117.5
85	–	125	83	–
90	–	133	95.2	–

graphite content were found to be a promising candidate for bipolar plate for the fuel cell application as they showed relatively high electrical conductivity of $104\text{--}245 \text{ S.cm}^{-1}$, which evidently meet that of DOE requirements. Moreover, our polybenzoxazine composites showed greater enhancement in electrical conductivity than those in other graphite/polymer systems such as novolac epoxy [43], phenol formaldehyde [44], and epoxy [45, 46] comparing at the same graphite loading [43–46], i.e., in the case of resole-type phenol formaldehyde resin, the electrical conductivity value was reported to be 125 S.cm^{-1} for the 65vol % graphite, whereas at the graphite content of 85vol %, the highest electrical conductivity value was reported to be 235 S.cm^{-1} [12].

3.5 Highly Filled Polybenzoxazine Nanocomposites

There are different types of commercially available nanoparticles that can be incorporated into the polymer matrix to form polymer nanocomposites. Depending on the application, the researcher must determine the type of nanoparticle needed to provide the desired effect. The most commonly used nanoparticles in the literature are as follows: montmorillonite organoclays (MMT), carbon nanofibers (CNFs), polyhedral oligomeric silsesquioxane (POSS[®]), carbon nanotubes (MWNTs, SWNTs), nanosilica, aluminum oxide, titanium oxide, and others. The highly filled nanocomposites were always found in the dispersion of the nanosilica into the different polymers [18, 47–50]. The storage modulus of polymer nanocomposites, containing nanosilica as filler, is shown in Fig. 3.15. The storage modulus of all nanocomposite systems was increased with increasing nanosilica content. The polybenzoxazine nanocomposite in our investigation showed higher storage modulus than the other nanocomposite systems at the same amount of nanosilica. The value of storage modulus indicates the material's ability to store

Fig. 3.15 Storage modulus of silica nanocomposites as a function of nanosilica content of the different polymer matrices: (circle) polybenzoxazine [18], (square) epoxy [48], (inverted triangle) polyurethane [49], (left pointing triangle) cyanate ester with 40 nm of nanofiller [50], (left pointing triangle) cyanate ester with 12 nm of nanofiller [50]



the energy of external forces without permanent strain deformation. Therefore, higher storage modulus is associated with a higher elastic property of materials. Furthermore, the greater enhancement of the storage modulus observed in nano-SiO₂-filled PBA-a than in epoxy and cyanate ester composite systems as compared in Fig. 3.16 implies the greater interaction between the nano-SiO₂ and the polybenzoxazine matrix than that in epoxy and cyanate ester resins. These results imply that BA-a resin is a highly effective adhesive for the nano-SiO₂ filler.

Microhardness values and percentage of improvement in the polymer nanocomposites as a function of the nano-SiO₂ content are depicted in Fig. 3.17,

Fig. 3.16 Percentage of storage modulus improvement in silica nanocomposites as a function of nanosilica content of the different polymer matrices: (circle) polybenzoxazine [18], (square) epoxy [48], (inverted triangle) polyurethane [49], (left pointing triangle) cyanate ester with 40 nm of nanofiller [50], (left pointing triangle) cyanate ester with 12 nm of nanofiller [50]

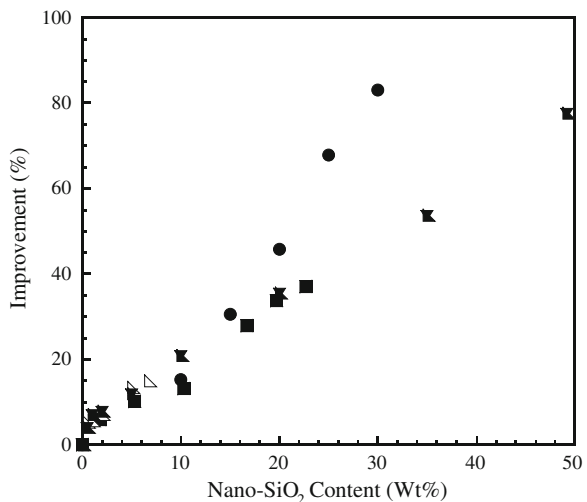
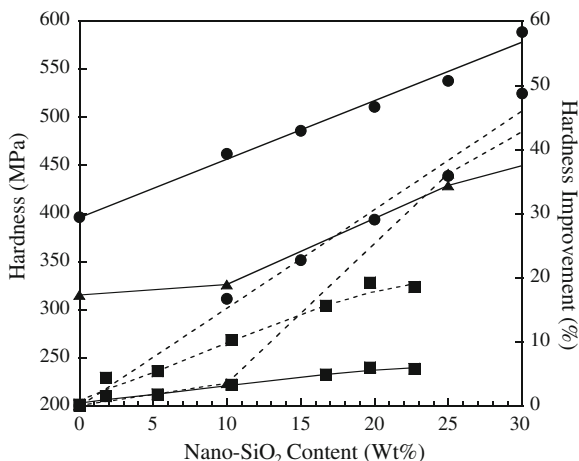


Fig. 3.17 Microhardness of silica nanocomposites as a function of nanosilica content of the different polymer matrices: (circle) polybenzoxazine, (square) epoxy [47], (triangle) polyurethane [48], (Hyphen) polyurethane [48], (dashed-line) hardness, percentage improvement



revealing a linear relationship between the hardness values and the amount of the nano-SiO₂. The hardness of the nanocomposites was found to increase with the nanosilica contents. Interestingly, our polybenzoxazine nanocomposites showed greater enhancement in hardness than those in epoxy/nano-SiO₂ comparing at the same filler content [48, 49]. The large increase in microhardness is attributed to a much higher hardness of the nano-SiO₂ (1,103–1,120 MPa) [51] compared with the neat polybenzoxazine. Moreover, the relatively small standard deviation in hardness values with strong hardening effect is attributed to the homogeneous dispersion of the nanofiller in the polybenzoxazine matrix and to the strong filler–polymer interactions with decreasing interparticle distance when the amount of the filler increases. As a result, polybenzoxazine/nano-SiO₂ molding compounds show a hardness characteristic suitable for high-performance coating material compared with the traditional epoxy coating system.

References

1. Venkatesulu B, Thomas MJ (2010) Erosion resistance of alumina-filled silicone rubber nanocomposites. *IEEE T Dielects Elect Insul* 17(2):615–624
2. Fasihi M, Garmabi H (2011) Evaluation and optimization of the mechanical properties of highly filled PVC/(wood flour) composites by using experimental design. *J Vinyl Addit Techn* 17(2):112–119
3. Kaully T, Siegmann A, Shacham D (2008) Mechanical behavior of highly filled natural CaCO₃ composites: effect of particle size distribution and interface interactions. *Polym Composite* 29(4):396–408
4. Hauser RA, King JA, Pagel RM, Keith JM (2008) Effects of carbon fillers on the thermal conductivity of highly filled liquid-crystal polymer based resins. *J Appl Polym Sci* 109(4):2145–2155
5. Du L, Jana SC (2007) Highly conductive epoxy/graphite composites for bipolar plates in proton exchange membrane fuel cells. *J Power Sources* 172(2):734–741

6. Pick B, Pelka M, Belli R, Braga RR, Lohbauer U (2011) Tailoring of physical properties in highly filled experimental nanohybrid resin composites. *Dent Mater* 27:664
7. Li Z, Gao H, Wang Q (2012) Preparation of highly filled wood flour/recycled high density polyethylene composites by in situ reactive extrusion. *J Appl Polym Sci* 124(6):5247–5253
8. Rimdusit S, Tanthapanichakoon W, Jubsilp C (2006) High performance wood composites from highly filled polybenzoxazine. *J Appl Polym Sci* 99(3):1240–1253
9. Bengtsson M, Baillif ML, Oksman K (2007) Extrusion and mechanical properties of highly filled cellulose fiber–polypropylene composites. *Compos A* 38(8):1922–1931
10. Ishida H, Rimdusit S (1998) Very high thermal conductivity obtained by boron nitride-filled polybenzoxazine. *Thermochim Acta* 320(1–2):177–186
11. Abenojar J, Martinez MA, Velasco F, Pascual-Sanchez V, Martin-Martinez JM (2009) Effect of boron carbide filler on the curing and mechanical properties of an epoxy resin. *J Adhesion* 85(4–5):216–238
12. Pengdam A (2012) Graphite based benzoxazine composites for an application as bipolar plates in fuel cell. Master's degree. Department of Chemical Engineering, Faculty of Engineering, Chulalongkorn University, Bangkok
13. Fu SY, Feng XQ, Lauke B, Mai YW (2008) Effects of particle size, particle/matrix interface adhesion and particle loading on mechanical properties of particulate–polymer composites. *Compos B* 39(6):933–961
14. Kumar KSS, Nair CPR (2010) Polybenzoxazines: chemistry and properties. iSmithers Rapra Publishing, England
15. Ishida H, Agag T (2012) Handbook of benzoxazine resin. Elsevier Press, Oxford
16. Rimdusit S, Tiptipakorn S, Jubsilp C, Takeichi T (2013) Polybenzoxazine alloys and blends: some unique properties and applications. *React Funct Polym* 73(2):369–380
17. Kajohnchaiyagual J (2013) Thermal and mechanical properties of highly-filled alumina-polybenzoxazine composites. Master's degree. Department of Chemical Engineering, Faculty of Engineering, Chulalongkorn University, Bangkok
18. Dueramae I, Jubsilp C, Takeichi T, Rimdusit S (2013) High thermal and mechanical properties enhancement obtained in highly filled nanocomposites of polybenzoxazine and fumed silica. (in submitted: Composites Part B)
19. Ishida H, Allen DJ (1996) Mechanical characterization of copolymers based on benzoxazine and epoxy. *Polymer* 37(20):4487–4495
20. Huang MT, Ishida H (1999) Dynamic mechanical analysis of reactive diluent modified benzoxazine-based phenolic resin. *Polym Polym Compos* 7(4):233–247
21. Wang YX, Ishida H (2002) Development of low-viscosity benzoxazine resins and their polymers. *J Appl Polym Sci* 86(12):2953–2966
22. Jubsilp C, Takeichi T, Rimdusit S (2007) Effect of novel benzoxazine reactive diluent on processability and thermomechanical characteristics of bi-functional polybenzoxazine. *J Appl Polym Sci* 104(5):2928–2938
23. Kasemsiri P (2012) Development of light weight ballistic armor from fibers-reinforced with benzoxazine alloys. Doctoral's degree. Department of Chemical Engineering, Faculty of Engineering, Chulalongkorn University, Bangkok
24. Takeichi T, Kano T, Agag T (2005) Synthesis and thermal cure of high molecular weight polybenzoxazine precursors and the properties of the thermosets. *Polymer* 46(26):12172–12180
25. Ishida H, Low HY (1998) Synthesis of benzoxazine functional silane and adhesion properties of glass-fiber-reinforced polybenzoxazine composites. *J Appl Polym Sci* 69(13):2559–2567
26. German RM (1989) Particle packing characteristics. *Metal Powder*, New Jersey
27. Smith PM, Wolcott MP (2005) Wood-plastic composites emerging products and markets. In: Abstracts of the 8th international conference of wood fiber plastic composites, Madison, May
28. Dalvg H, Klason C, Strmvall HE (1985) The efficiency of cellulosic fillers in common thermoplastics II: filling with processing aids and coupling agents. *Int J Polym Mater* 11(1):9–38
29. Maldas D, Kokta BV, Daneault C (1989) Influence of coupling agents and treatments on the mechanical properties of cellulose fiber–polystyrene composites. *J Appl Polym Sci* 37(3):751–775

30. Raj RG, Kokta BV, Daneault C (1989) Use of wood fibers in thermoplastics. VII. The effect of coupling agents in polyethylene–wood fiber composites. *J Appl Polym Sci* 37(4):1089–103
31. Felix JM, Gatenholm P (1991) The nature of adhesion in composites of modified cellulose fibers and polypropylene. *J Appl Polym Sci* 42(3):609–620
32. Kiziltas A, Gardner DJ, Han Y, Yang HS (2011) Dynamic mechanical behavior and thermal properties of microcrystalline cellulose (MCC)-filled nylon 6 composites. *Thermochim Acta* 519(1–2):38–43
33. Ichazo MN, Albano C, Gonzalez J, Perera R, Candal MV (2001) Polypropylene/wood flour composites: treatments and properties. *Compos Struct* 54(2–3):207–214
34. Honga JP, Yoona SW, Hwanga T, Oha JS, Honga SC (2012) High thermal conductivity epoxy composites with bimodal distribution of aluminum nitride and boron nitride fillers. *Thermochim Acta* 537:70–75
35. Tenga CC, Maa CCM, Chiou KC, Leeb TM, Shihe YF (2011) Synergetic effect of hybrid boron nitride and multi-walled carbon nanotubes on the thermal conductivity of epoxy composites. *Mater Chem Phys* 126(3):722–728
36. Drova G, Feller LJ, Salagnac P, Glouannec P (2006) Thermal conductivity enhancement of electrically insulating syndiotactic poly (styrene) matrix for diphasic conductive polymer composites. *Polym Adv Technol* 17(9–10):732–745
37. McGrath LM, Parnas RS, King S, Schroeder JL, Fischer DA, Lenhart JL (2008) Investigation of the thermal, mechanical, and fracture properties of alumina-epoxy composites. *Polymer* 49(4):999–1014
38. Kong Y, Li X, Yao C, Wei J, Chen Z (2012) Chiral recognition of tryptophan enantiomers based on a polypyrrole-flake graphite composite electrode column. *J Appl Polym Sci* 126(1):226–231
39. Zhang P, Xue WT, Zhao Y, Liu P (2012) Positive temperature coefficient effect and interaction based on low-density polyethylene/graphite powder composites. *J Appl Polym Sci* 123(4):2338–2343
40. Yun JC et al (2007) Degradation of graphite reinforced polymer composites for PEMFC bipolar plate after hydrothermal ageing. In: Abstract of the 16th International conference on composite materials, Advanced Composites Center, Tokyo, 8–13 July 2007
41. Department of Energy (2013) Technical plane fuel cells. http://www1.eere.energy.gov/hydrogenandfuelcells/mypp/pdfs/fuel_cells.pdf. Accessed Jan 2013
42. Du L, Jana SC (2007) Highly conductive epoxy/graphite composites for bipolar plates in proton exchange membrane fuel cells. *J Power Sources* 172(2):734–741
43. Kakati BK, Sathiyamoorthy D, Verma A (2011) Semi-empirical modeling of electrical conductivity for composite bipolar plate with multiple reinforcements. *Int J Hydrogen Energy* 36(22):14851–14857
44. Kakati BK, Yamsani VK, Dhathathreyan KS, Sathiyamoorthy D, Verma A (2009) The electrical conductivity of a composite bipolar plate for fuel cell applications. *Carbon* 47(10):2413–2418
45. Suherman H, Sulong AB, Sahari J (2013) Effect of the compression molding parameters on the in-plane and through-plane conductivity of carbon nanotubes/graphite/epoxy nanocomposites as bipolar plate material for a polymer electrolyte membrane fuel cell. *Ceram Int* 39(2):1277–1284
46. Hui C, Hong L, Li Y, Yue H (2011) Effects of resin type on properties of graphite/polymer composite bipolar plate for proton exchange membrane fuel cell. *J Mater Res* 26(23):2974–2979
47. Zhang H, Zhang Z, Friedrich K, Eger C (2006) Property improvements of in situ epoxy nanocomposites with reduced interparticle distance at high nanosilica content. *Acta Mater* 54(7):1833–1842
48. Zhang H, Tang L, Zhang Z, Gub L, Xu Y, Eger C (2010) Wear-resistant and transparent acrylate-based coating with highly filled nanosilica particles. *Tribol Int* 43(1–2):83–91
49. Goertzen WK, Kessler MR (2008) Dynamic mechanical analysis of fumed silica/cyanate ester nanocomposites. *Compos A* 39(5):761–768
50. Harry SK (1987) Handbook of fillers. Chem Tec Publishing, New York

Chapter 4

High Thermal Conductivity of BN-Filled Polybenzoxazines

Abstract This chapter discusses one engineering application of polybenzoxazines as a highly thermally conductive electronic packaging encapsulant. The combination of various useful properties of benzoxazine resins and their resulting polymers has been demonstrated to render a very high thermally conductive polymer composite. Thermal conductivity value as high as 32.5 W/mK in hexagonal boron nitride-filled polybenzoxazine, up to present, remains the highest reported thermal conductivity value in the literature. Other outstanding properties of the resulting composites as an electronic packaging encapsulant are also discussed in this chapter.

Keywords Thermally conductive composite • Highly filled composites • Polybenzoxazine • H-boron nitride • Electronic packaging encapsulant

4.1 Introduction

One of the major material properties involves its thermal behavior. Thermal conductivity, thermal diffusivity, specific heat capacity, and thermal expansion coefficient are four major thermal properties of materials [1, 2]. Table 4.1 exhibits the thermal conductivity values of various materials. Polymers are considered to be good heat insulating materials, while many ceramic materials are good thermally conductive materials. From the table, we can see that perfect crystalline nonmetallic materials, such as diamond or cubic boron nitride, have thermal conductivity values much higher than those of metallic materials. This is due to the fact that the flow of heat energy for nonmetallic materials occurs only by means of phonon propagation, which is much more effective than the flow of heat energy by electron movement, which is the major mechanism of heat transfer in metallic materials.

Table 4.1 Thermal conductivity at 20 °C of materials [2, 3]

Materials	Thermal conductivity (W/mK)
Diamond	2,000
Graphite	2,000
C-boron nitride	1,300
Silver	427
H-boron nitride	20–400
Aluminum nitride	195
Iron	80
Aluminum oxide	22
Silicon dioxide (crystalline)	14
Silicon dioxide (amorphous)	1.3
Glass	0.8
Water	0.66
HDPE	0.52
LDPE	0.33
Epoxy	0.14
Air	0.026

The importance of thermal conductivity in polymer and polymer composites has significantly intensified in recent years particularly in the electronic industry as more compact and low loss design for power apparatus and electronic packaging have been of urgent concern for present development. Polymers are commonly used as a binder in molding compounds for electronic packaging encapsulants and in fiber-reinforced substrate for electronic wiring boards. The major requirements for such applications include good adhesion of the polymer binder to the constituents that are to be coated or protected. Typical curing processes require short cure duration with a maximum cure temperature of 150 °C. The molding compounds should have at least 1 h pot life and at least six-month shelf life. No volatile and toxic components should be produced or released during the curing and service stages. In terms of reliability of the electronic packages, the material used should possess a high glass-transition temperature of at least 150 °C and exhibit less than 1 % linear shrinkage during curing with low residual stress after curing of less than 5 MPa. It is important that the material causes no stress-related failures of the assembly during temperature cycling, i.e., should provide high thermal conductivity value as well as low thermal expansion coefficient mismatch between its molding compounds and the protected electronic parts. Sufficient mechanical protection is one key function of the polymer encapsulants. Finally, the material should be cost competitive [4–6].

The possibility to solve these stringent material requirements has been demonstrated by the use of relatively novel family of polymeric systems, namely polybenzoxazine. Benzoxazine resins have been reported to provide many outstanding characteristics including relatively high thermal stability, high glass-transition temperature, and high char yield. Molecular design flexibility of the resins is tremendous and therefore creates a large family of these polymers. They

are one of the few groups of thermosetting resins which, in the pure form, possess very low melt viscosity which greatly facilitates filler wetting and mixing. The resins also provide high-performance cured specimens [7, 8]. Composite materials obtained from these resins show high potential use in various applications such as electronic packages [9–11], bipolar [12], electrolyte membrane for fuel cell [13], or binder resin for frictional material [14].

As mentioned earlier, one major property of polymeric molding compound for electronic packaging application is an ability of the material to dissipate heat with sufficient rate typically by incorporating with high thermal conductive fillers. The incorporation of highly thermally conductive ceramic materials in polymers in order to improve the thermal conductivity of encapsulant or substrate has long been studied [5]. The composite should exhibit balanced properties of high thermal conductivity and thermal stability of the ceramic component while retaining ease of processing and low dielectric constant of the polymer matrix.

In a recent review by Tanaka and coworkers [15], inorganic ceramic fillers such as SiO_2 , Al_2O_3 , AlN , and BN with micrometer in size are generally selected to achieve highly thermally conductive polymer composite packages with electrical insulation capability. In their report, the key features of the polymer composites with high thermal conductivity characteristics consist of (1) the use of micrometer size filler dramatically enhanced thermal conductivity of the material compared to the nanometer size filler. (2) The larger the microfiller size, the higher the thermal conductivity of the composite. (3) Nanofiller can also improve thermal conductivity but providing the value of within 1 W/mK. (4) Fillers with higher inherent thermal conductivity values are better for the enhancement of thermal conductivity of the composites. (5) Polymer matrices with higher thermal conductivity are better than the lower conductivity ones. (6) Filler orientation is one critical factor to enhance thermal conductivity of the materials. (7) A thermal conductivity value of 20 W/mK was achieved by orientation of polymers by magnetic field. (8) Coupling agents are important to raise thermal conductivity of the specimens. (9) Coupling agent shows a more pronounced effect on thermal conductivity enhancement of the composites based on nanofillers than microfillers. (10) Maximum thermal conductivity value of 5 W/mK was obtained in Al_2O_3 -filled composites. (11) Thermal conductivity value of 9.1 W/mK was obtained in polyimide filled with AlN/BN hybrid fillers. (12) Mesogen epoxy loaded with 55 % by volume of alumina (size = 10 μm) provides a thermal conductivity value up to 10 W/mK. (13) Thermal conductivity value of 11 W/mK was achieved in epoxy filled with AlN having a particle size of 7 μm and at a loading of 60 % by volume. (14) Thermal conductivity value of 19 W/mK is the maximum for ordinary epoxy using a multimodal particle size mixing of hexagonal BN (0.6 μm) and cubic BN (1 μm). (15) The maximum thermal conductivity value in polymer composite so far is 32.5 W/mK using hexagonal BN with average particle size of 225 μm and the matrix materials is polybenzoxazine. Table 4.2 lists the examples of polymer composite systems with relatively high thermal conductivity values (≥ 4 W/mK) reported so far [15].

Table 4.2 Polymer composite systems with thermal conductivity value greater than 4 W/mK (adapted from Tanaka et al. [15])

Polymer matrix	Fillers	Filler size (μm)	Content (%)	k (W/mK)
Polybenzoxazine	BN	225	78.5 vol.	32.5
Epoxy	BN	0.6 (h), 1 (c)	27 vol.	19
Epoxy	AlN	7	60 vol.	11
Epoxy	BN (silane)	5–11	57 vol.	10.3
Polyimide	AlN/BN	79/xx	70 vol.	9.3
PVDF	AlN	12 (whisker)	60 vol.	7.4
Polyimide	BN	8	60 wt.	7
Epoxy	BN	5–11	57 vol.	5.3
Epoxy	BN	Conglomerated	64.9 wt.	5.13
Epoxy	Al ₂ O ₃	10	55 vol.	5
Epoxy	AlN	0.5 (whisker)	47 vol.	4.2
Epoxy	Diamond	<10	70 vol.	4.1

This chapter discusses the composite system based on the boron nitride-filled polybenzoxazine which, up to present, provides the highest thermal conductivity value among those reported in the literatures and has been issued the US patent in 1999 [8]. The principle behinds the successful thermal conductivity enhancement of this highly filled polybenzoxazine composite is discussed below.

4.2 High Thermal Conductivity Electronic Packaging Materials Obtained by Boron Nitride-Filled Polybenzoxazine (Reproduced from [5] with permission)

The concept of effective thermal management by maximizing the formation of conductive networks while minimizing the heat resistance along the heat-flow path is well recognized. Berman [16] explained the transport of heat in nonmetals by the flow of phonons or lattice vibrational energy. The thermal resistance is caused by various types of phonon scattering processes, e.g., phonon–phonon scattering, boundary scattering, and defect or impurity scattering. Therefore, in order to maximize the thermal conductivity in materials, these phonon scattering processes must be suppressed. Phonons travel in matter with the speed of sound. In theory, the scattering of phonons in composite materials is mainly due to the existence of an interfacial thermal barrier from acoustic mismatch, or the damage of the surface layer between the filler and the matrix [17, 18]. These interfacial phonon scattering phenomena are similar to the scattering of light due to differences in refractive indices of the media.

Consequently, we generated the idea of maximizing the formation of highly thermally conductive networks and minimizing the thermal resistance along the

conductive paths by first choosing the filler which should be able to form many heat-flow paths. The maximum packing of the filler in the matrix is one way to assure the formation of near-perfect conductive networks. To achieve high packing density composites, the use of large size particles with multimodal particle size distribution and low aspect ratio with smooth surface texture as a second phase were suggested [19]. Secondly, the thermal resistance would be reduced by the combination of various techniques. The selection of particles which have perfect lattice or crystal structure as much as possible to suppress the scattering of phonons by lattice defects is essential. This kind of filler is normally found in highly thermally conductive ceramics, such as boron nitride or aluminum nitride. The large particle size, i.e., low particle surface area, is desired to minimize the scattering of phonons due to the interfacial thermal barrier. Moreover, the use of large particle size tends to form fewer thermally resistant junctions of the polymer layers than the small particle size at the same filler content. Finally, the layer of the matrix resin between the particles must be as thin as possible, to such a degree that its mechanical properties are still high enough for the application, to reduce the thermal resistance due to the resin itself. This can be achieved by using a resin which has low melt viscosity. Furthermore, the low viscosity resin generally aids in filler mixing during the molding compound preparation. These hypotheses are based on one important assumption that the adhesion between the filler and the matrix resin is good; otherwise, the third phase, an air gap, may occur and will also have a high contribution to the overall conductivity of the composites. Therefore, the choice of resin which possesses low melt viscosity and excellent adhesion with the selected filler is preferred.

In the report by Ishida and Rimdusit, the authors used bisphenol-A/methylamine-type benzoxazine resin (BA-m) to form a highly filled molding compound and composite with hexagonal boron nitride. The resin was used as-synthesized without further purification. The monomer is solid at room temperature. It was ground into fine powder and stored in a refrigerator for future use. Table 4.3 lists major properties of the BA-m benzoxazine resin used by Ref. 5.

Table 4.3 Properties of bisphenol-A/methylamine-type polybenzoxazine (BA-m)

Properties	Values
Density	
Monomer ($\times 10^{-3}$ kg/m ³)	1.159
Polymer ($\times 10^{-3}$ kg/m ³)	1.122
Thermal expansion coefficient ($\times 10^6$ m/m °C)	69
Glass-transition temperature (8 °C)	180
Heat capacity (J/kg °C)	1,415
Water absorption at room temperature (wt%)	
24 h	0.17
120 days	1.15
G'_{RT} (GPa)	1.8
Melt viscosity at 100 °C (Pa S)	1.2

The filler used was hexagonal boron nitride (grade HCJ48) supplied by Advanced Ceramics. The powder consists of large aggregates of flake-like boron nitride crystals fabricated by hot-pressing technology. The powder has bimodal size distribution with mean particle size of ca. 225 μm . The monomer powder was dry mixed well with boron nitride at a desired volume fraction. The mixture was then heated up to ca. 80 $^{\circ}\text{C}$ in a mixer and was mixed by hand for ca. 10 min. The compound in the form of paste was then compression molded into various dimensions depending upon the types of experiments. All the specimens were thermally cured at 200 $^{\circ}\text{C}$ with pressure of 0.1 MPa for 2 h. The specimens were left to cool down at room temperature in the open mold for ca. two hours before using.

Figure 4.1 shows the density of boron nitride-filled polybenzoxazine as a function of filler content. The theoretical densities of the composites were calculated based on the density of boron nitride of 2.25 g/cm^3 and the density of polybenzoxazine, BA-m, of 1.122 g/cm^3 [20].

In Fig. 4.2, the compositions of the composites were confirmed again by using TGA. Most observed composite densities especially at higher filler contents showed good agreement with the values calculated from the compositions analyzed by TGA, suggesting negligible amount of voids. The reason that the densities of specimens at low range of filler contents are somewhat higher than those of the original molding compound is due to the greater loss of resin by overflowing out of the mold than that in case of higher filler contents. In this study, we defined the maximum packing density of each type of filler by its maximum observed density that is equal to the theoretical density. Using boron nitride grade HCJ48, we were able to make a specimen with maximum packing density up to 78.5 % by volume (88 % by weight) as shown in Fig. 4.1. The attempt to add boron nitride

Fig. 4.1 Maximum packing density of boron nitride-filled polybenzoxazine using boron nitride grade HCJ48. (black square) theoretical density, (black circle) experimental density

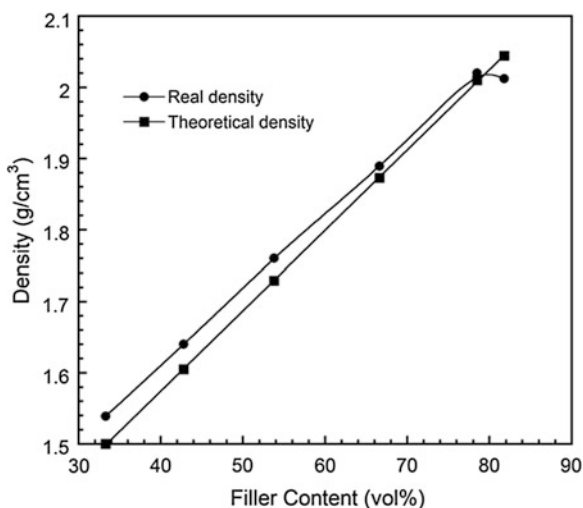
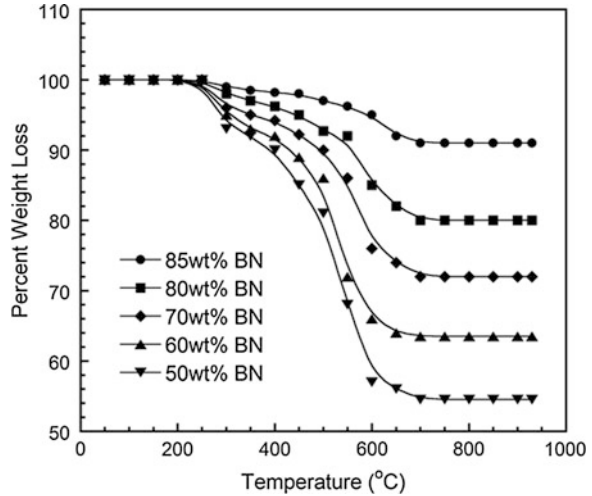


Fig. 4.2 TGA experiment for composition determination of composite samples. (filled triangle) 50 wt% BN, (filled inverted triangle) 60 wt% BN, (black diamonds) 70 wt% BN, (black square) 80 wt% BN, (black circle) 85 wt% BN



beyond 78.5 % by volume tended to decrease the observed composite packing density to a value lower than the theoretical value due to void formation.

The maximum packing densities of four grades of BN are summarized in Table 4.4. From the result, we can see that the larger the average particle size of boron nitride, the higher the maximum packing density of the composite, which is in good agreement with the theory of particle packing [19]. One of our reasons to choose a large average particle size of boron nitride filler is to be able to obtain the maximum packing density in the specimen as thermal conductivity seems to have characteristics of both a path-dependent property, i.e., the conductivity values increase rapidly beyond the percolation threshold, and a bulk property, i.e., the conductivity values are strongly dependent on filler loading. The use of maximum packing density of filler in the composite can, at the same time, render a large number of conductive networks in the composite which fulfills both path-dependent and bulk properties.

The maximum achievable boron nitride loading in our system, 78.5 % by volume, surpassed the maximum boron nitride loading reported by Bujard, 31 % by volume [21]. This is due to the fact that our boron nitride powder has a large average particle size (225 μm) and has low effective aspect ratio as it is an aggregate of fake-like crystals. Moreover, the filler also has bimodal particle size distribution. The effect of particle size on a packing density was investigated by

Table 4.4 The effect of particle size on composite packing densities

Boron nitride (grade)	Average particle size (μm)	Type	ϕ_m (wt%)
HCPH	9	Flake	60
HCJ325	45	Aggregate	75
TS1890	75	Aggregate	85
HCJ48	225	Aggregate	88

Ruschau et al. [22, 23]. Their observation was consistent with the theory of particle packing [19] which states that, in an unimodal particle size distribution, the packing density decreases with smaller particle size due to an increase in particle surface area, lower particle mass, and a greater importance of weak short-range forces including electrostatic fields and surface adsorption of moisture and other wetting liquids that can lead to agglomeration. The high aspect ratio particles, such as flake or fiber, greatly exhibit the bridging phenomenon in compacts. Though the bridging assists in the formation of the conductive network by lowering the percolation threshold, it lowers the packing density. The multimodal distribution of the particles also plays a significant role in enhancing the packing density. Although packing density is higher in multimodal particle mixtures, German [19] observed that there is less benefit to make the mixtures beyond the bimodal system to a trimodal or more complex system which are more difficult to obtain and handle. As a consequence, the use of boron nitride grade HCJ48 having a bimodal particle size distribution with large average particle size should be sufficient in obtaining high particle packing.

The effect of particle size on thermal conductivity was studied using an apparatus for steady-state thermal conductivity measurement based on the Colora thermoconductometer or Schroder technique [24]. All specimens used were the composites of 30 % by weight of polybenzoxazine and 70 % by weight of boron nitride, which is the composition beyond the typical percolation threshold of bond percolation. The boron nitride used was a mixture of large particle size grade (HCJ48 with 225 nm average particle size) and a smaller particle size grade (TS1890 with 75 nm average particle size). Increasing the composition of the large particle size grade of boron nitride resulted in higher thermal conductivities as shown in Fig. 4.3. This is due to the fact that the network formation of the large particle filler has less heat resistant junctions than that of the smaller size filler. As a result, the thermal conductivity of the specimens beyond the percolation threshold increases with increasing the fractional composition of the large particle size grade of boron nitride filler.

Figure 4.4 shows the thermal diffusivities of boron nitride-filled polybenzoxazine as a function of filler content. These values can be converted into thermal conductivity by multiplying thermal diffusivity value with the sample's heat capacity and density. In order to determine the thermal conductivities of the composites, densities and heat capacities of the composites are needed. The heat capacity of each specimen was determined by MDSC. Table 4.5 shows the thermal diffusivities, heat capacities, and composite densities of specimens at different compositions and the corresponding values of thermal conductivities.

From Fig. 4.5, we can see that, once the conductive networks of the large particle size are formed, the thermal conductivity of the composites will exceed that of the smaller particles as the formation of the conductive paths of the large particles renders less thermal resistance along the paths [25]. The phenomenon is more pronounced at the filler content exceeding the maximum packing of smaller particles since the maximum packing of smaller particle size is less than the

Fig. 4.3 Effect of particle size on the composite thermal conductivity

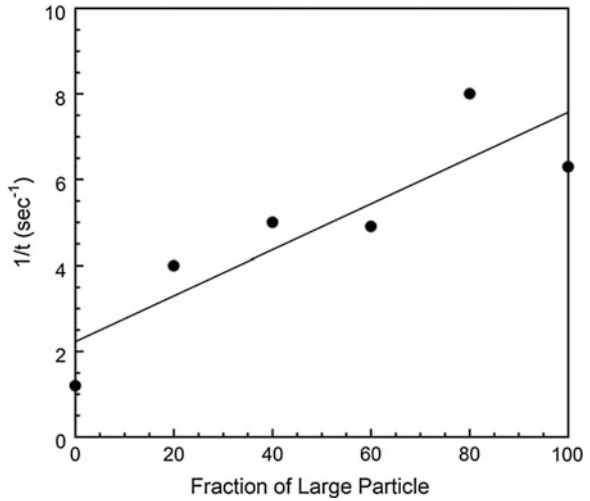
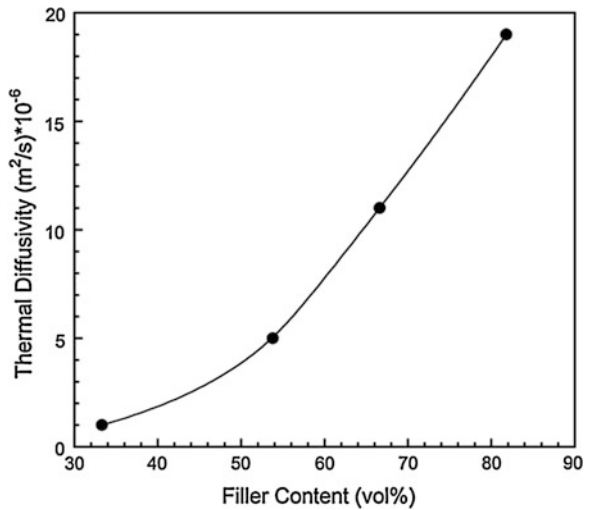


Fig. 4.4 Thermal diffusivity of boron nitride-filled polybenzoxazine as a function of filler contents

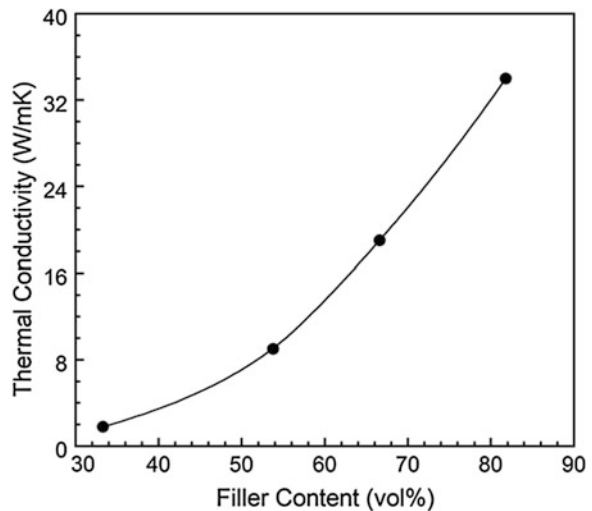


maximum packing of the larger particles [22, 23]. Our experimental results are in good agreement with the above statement.

We have produced a composite with a remarkably high value of thermal conductivity of 32.5 W/mK at 78.5 % by volume of boron nitride filler. The value was averaged from the value of 30.8 W/mK at the center of the sample and 34.2 W/mK at the edge of the sample. This value is ca. 15 times higher than the maximum achieved thermal conductivity value found in epoxy filled with small flake-like boron nitride [21] and about eight times greater than the state-of-the-art value found in alumina-filled epoxy [26].

Table 4.5 Thermal conductivity of boron nitride-filled polybenzoxazine

Filler content	$\alpha \times 10^6$ (m ² /s)	C _p (J/kg K)	ρ ($\times 10^{-3}$ kg/m ³)	k (W/mK)
33	0.91	1,069	1.593	1.50
54	5.22	933	1.758	8.56
66	10.8	897	1.889	18.3
78.5	19.2	841	2.012	32.5

Fig. 4.5 Thermal conductivity of boron nitride-filled polybenzoxazine as a function of filler contents

An anisotropic behavior of this composite was also observed. By measuring linear coefficient of thermal expansion, LCTE, of 80 % by weight of boron nitride-filled polybenzoxazine, we obtain the LCTE value of the sample measured along the z direction to be 44.2×10 m/m °C, while the LCTE value measured in the x and y directions is 7.17×10 m/m °C. The result reveals an anisotropic behavior of this composite material. This is due to the fact that boron nitride powder has anisotropic property and possesses high aspect ratio from its fake structure which can strongly contribute to the anisotropic LCTE of this composite. Although the boron nitride powders used are the aggregates of the fake crystals which have low effective aspect ratio, the anisotropic LCTE obtained implies the anisotropic orientation of the fakes in the aggregates.

Bond percolation is used to explain formation of conductive networks by the filler in the composite materials. This theory can normally explain the insulator–conductor transition well in path-dependent properties of materials such as electrically conductive composites as a point at which the first conductive path is formed. The filler content, ϕ , at this transition point is called the percolation threshold, ϕ_c . However, thermal conductivity seems to be an intermediate property between a path-dependent property and a bulk property. Hence, the thermal conductivity value in the composite material depends on both the formation of the

filler network and the filler loading. Generally, the percolation threshold of thermally conductive composite is difficult to define. Agari et al. [27, 28] demonstrated an indirect technique used to identify the percolation threshold of the composite by using filler which can affect both electrical and thermal properties of the composites, such as carbon black. In our system, we use a percolation threshold of 0.198 which is the currently accepted percolation threshold for a three dimensional network [29]. In their analysis, the authors obtained the critical exponent having the value of 2.02 which is in good agreement with the value of 2 in bond percolation for a three dimensional system [29].

Figure 4.6 shows the storage shear moduli of the composites with filler loadings ranging from 50 to 85 % by weight. The moduli of the composites expectedly increase with increasing amount of boron nitride. This corresponds to the high conductivity value of specimen as heat conducts better in a stiffer material, i.e., higher acoustic velocity. The modulus at room temperature of 85 % by weight filler is very high, exceeding 10 GPa which is a value comparable to continuous fiberglass-reinforced phenolic. Thus, the formation of a network from low aspect ratio filler produces a similar composite strength as that from a high aspect ratio reinforcement, such as glass fiber. Moreover, the storage modulus of the composite at all compositions exhibited fairly stable values up to ca. 200 °C due to the high-performance property of the polybenzoxazine matrix. From Fig. 4.6, the moduli of these composites increase rapidly nonlinearly with increasing filler contents.

The glass-transition temperatures of the filled systems were obtained from the maximum value of G as shown in Fig. 4.7. We observe a large increase of ca. 40–45 °C in the glass-transition temperatures of the composites relative to the glass-transition temperature of the homopolymer made from BA-m resin, i.e., 180 °C [20]. The implication of this phenomenon is possibly due to the contribution of the good interfacial adhesion between the boron nitride filler and

Fig. 4.6 Storage modulus of boron nitride-filled polybenzoxazine as a function of temperature at different filler loadings. (filled inverted triangle) 50 wt% BN, (filled triangle) 60 wt% BN, (black diamonds) 70 wt% BN, (black square) 80 wt% BN, (black circle) 85 wt% BN

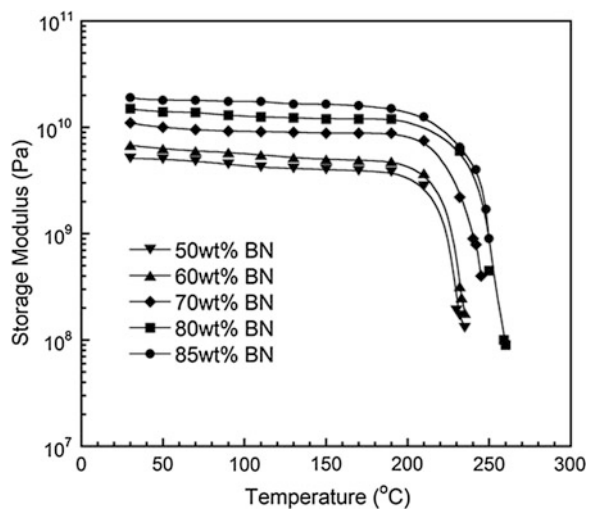


Fig. 4.7 Loss modulus loss modulus of boron nitride-filled polybenzoxazine as a function of temperature at different filler loadings. (*filled inverted triangle*) 50 wt% BN, (*filled triangle*) 60 wt% BN, (*black diamonds*) 70 wt% BN, (*black square*) 80 wt% BN, (*black circle*) 85 wt% BN

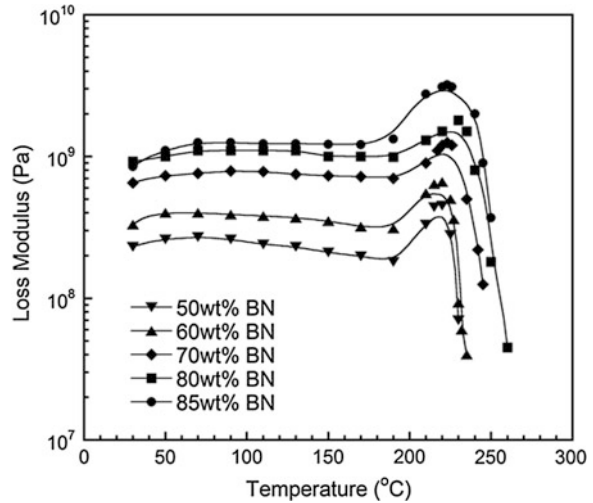
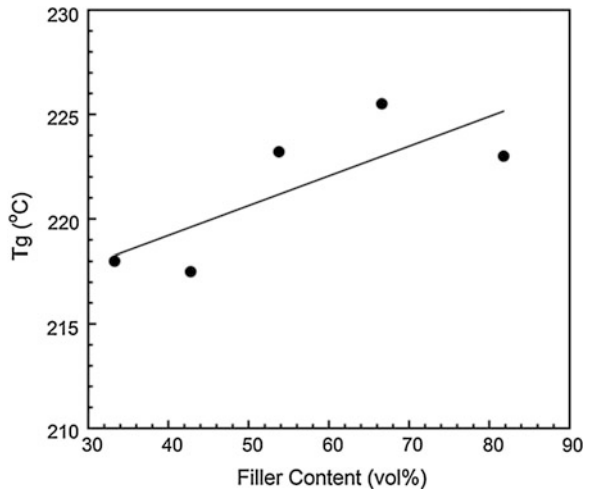


Fig. 4.8 The effect of filler loading on glass-transition temperature of boron nitride-filled polybenzoxazine



polybenzoxazine matrix. The stiff boron nitride filler can highly restrict the mobility of the polymer matrix which adheres on the filler surface and could lead to the large increase in the glass-transition temperatures of their composites. It is also possible that the boron nitride surface acted as a catalyst and the molecular architecture of the crosslinked polybenzoxazine was affected. Figure 4.8 shows the plot between the glass-transition temperatures as a function of filler contents. From the plot, we observed an increasing tendency of the glass-transition temperature as filler contents increased.

The electron micrograph of the fracture surface of the composite is shown in Fig. 4.9. The picture shows smooth interfaces between the filler and the resin

Fig. 4.9 SEM micrograph showing fracture surface of BN-filled polybenzoxazine

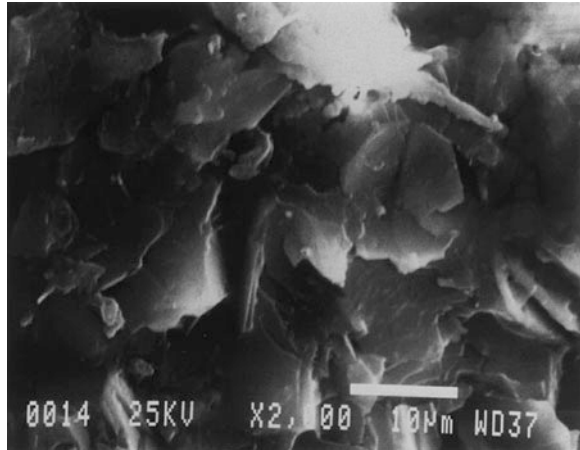
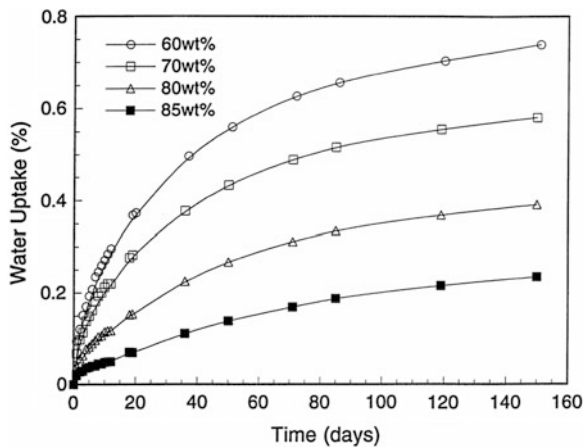


Fig. 4.10 Water uptake of boron nitride-filled polybenzoxazine up to 150 days at different filler contents. (circle) 60 wt%BN, (square) 70 wt% BN, (triangle) 80 wt% BN, (black square) 85 wt% BN



which signifies good interfacial adhesion of the boron nitride filler and polybenzoxazine matrix. The good adhesion of boron nitride and polybenzoxazine is one of the significant contributions to the high thermal conductivity values of their composites as poor interfacial adhesion can lead to strong scattering of heat energy at the filler–matrix interfaces.

Figure 4.10 shows the water absorption of the composites at different filler contents ranging from 60 to 85 % by weight up to 150 days. As the filler content increases, the water uptake decreases. These composites show very low room temperature water uptake having values much <0.2 % which is the value desired in the industrial standard of typical composites for electronic packaging. As seen in the following Fig. 4.11, the water uptake of all compositions at 24 h is <0.1 % and only ca. 0.02 % at a filler content of 85 % by weight. From the curves, the water uptake up to 150 days is <0.8 % at a filler content of 60 % by weight and

Fig. 4.11 Water uptake of boron nitride-filled polybenzoxazine up to 24 h at different filler contents

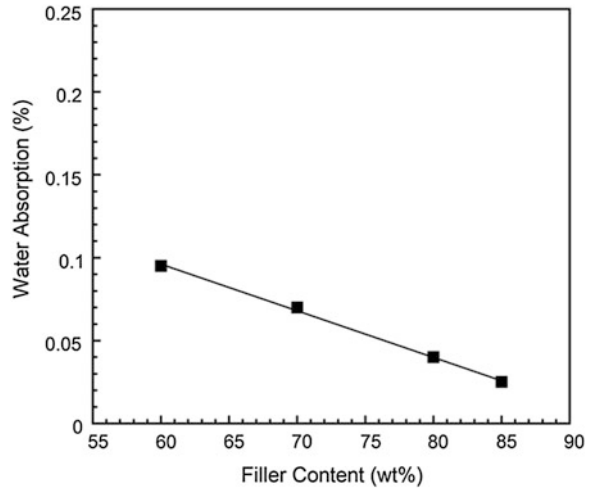
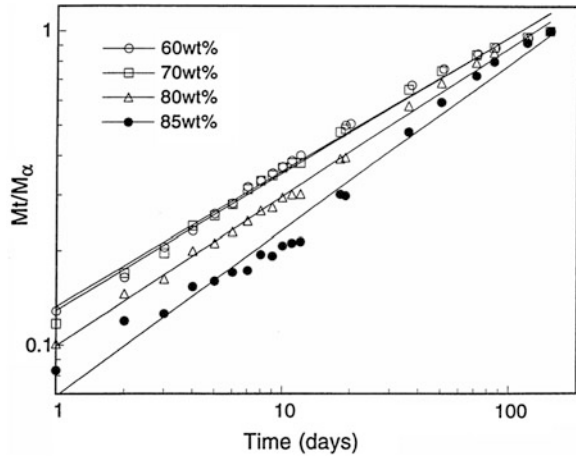


Fig. 4.12 Plots between $\log M_t/M_\infty$ and time to determine the diffusion exponents in Eq. (1). (circle) 60 wt%BN, (square) 70 wt%BN, (triangle) 80 wt%BN, (black circle) 85 wt%BN



lower at higher filler contents, which is considered to be very low. The generalized equation to explain the diffusion in the materials can be expressed as

$$M_t/M_\infty = k_n t^n \tag{1}$$

where M_t is the mass of sample at time t and M_∞ the mass of sample at saturation or infinite time.

The diffusion behaviors can be classified as follows: supercase II ($n > 1$), case II ($n = 1$), anomalous ($1/2 < n < 1$), classical/Fickian ($n = 1/2$), or pseudo-Fickian ($n < 1/2$) [30].

Figure 4.12 illustrates $\log M_t/M_\infty$ versus $\log t$ plots which show the slopes ranging from 0.43 to 0.53. Thus, we can conclude that our composite material exhibited a behavior close to Fickian-type diffusion.

4.3 Conclusions

The thermal conductivity of boron nitride-filled polybenzoxazine exhibited a very high conductivity value. The remarkably high value was obtained using the well-recognized concept of thermal management in composite materials by maximizing the formation of conductive networks while minimizing the thermal barrier resistance along the heat-flow path. The concept was accomplished by using highly thermally conductive filler with a matrix resin which has low melt viscosity and good adhesion to the filler. In addition, a large particle size with multimodal particle size distribution was used. Boron nitride and polybenzoxazine have properties that meet all these requirements and thus exhibit a very high thermal conductivity value. This molding compound also exhibits high and stable mechanical strength up to 200 °C with a high T_g value of ca. 220 °C. Water absorption at room temperature for 24 h of this composite is very low. Boron nitride-filled polybenzoxazine has many outstanding properties which makes it suitable for an application as a molding compound for the electronic packaging industry and other applications with high thermal conductivity.

References

1. Kroschwitz JJ, editor-in-chief (1985) Encyclopedia of polymer science and engineering. Wiley Interscience, New York
2. Godovsky YK (1992) Thermophysical properties of polymers. Verlag, New York
3. Werdecker W, Aldinger F, Heraeus WC (1984) IEEE 1984 electronic components conference. New Orleans, 14–16 May 1984, pp 402
4. Lau JH, Wong CP, Price JL, Nakayama W (1998) Electronic packaging: design, materials process, and reliability. McGraw-Hill, New York
5. Ishida H, Rimdusit S (1998) Very high thermal conductivity obtained by boron nitride-filled polybenzoxazine. *Thermochim Acta* 320:177–186
6. Rimdusit S (2000) Development of high reliability and high processability thermosets for electronic packaging applications based on ternary systems of benzoxazine, epoxy, and phenolic resins. Doctoral Dissertation, Case Western Reserve University, Ohio
7. Ishida H, Agag T (2011) Handbook of benzoxazine resins. Elsevier, New York
8. Kumar KSS, Nair CPR (2010) Polybenzoxazine: chemistry and properties. iSmith Rapra Publishing, UK
9. Ishida H (1999) US Patent 5,900,447
10. Ishida H, Rimdusit S (2001) US Patent 6,207,786
11. Song-Hua S, Lejun W, Tian-An C (2007) US Patent 7,179,684
12. Hyoung-Juhn K, Yeong-Chan E, Sung-Yong C, Ho-Jin K, Jin-Kyoung M, Dong-Hun L, Ju-Yong K, Seong-Jin A (2009) US Patent 7,510,678

13. Seong-Woo C, Jung-Ock P (2012) US Patent 8,323,849
14. Kuihara S, Idei H, Aoyagi Y, Kuroe M (2012) US Patent 8,227,390
15. Tanaka T, Kuzako M, Okamoto K (2012) Toward high thermal conductivity nano micro epoxy composites with sufficient endurance voltage. *J Intern Counc Elect Eng* 2:90–98
16. Berman R (1973) Heat conductivity of non-metallic crystals. *Contemporary Physics*, vol 14, pp 101
17. Ruth R, Donaldson KY, Hasselman DPH (1992) Thermal conductivity of boron carbide–boron nitride composites. *J Am Ceram Soc* 75:2887
18. Pettersson S, Mahan GD (1990) Theory of the thermal boundary resistance between dissimilar lattices. *Phys Rev B* 42:7386
19. German RM (1989) Particle packing characteristics. Metal powders industries federation. Princeton, New Jersey
20. Ishida H, Allen DJ (1996) Gelation behavior of near-zero shrinkage polybenzoxazines. *J Polym Sci Phys Ed* 34:1019
21. Bujard P (1988) Thermal conductivity of boron nitride filled epoxy resins: temperature dependence and influence of sample preparation. In: thermal phenomena in the fabrication and operation of electronic components. Proceedings of I-THERM, May 1988, IEEE, Los Angeles, p 41
22. Ruschau GR, Newnham RE (1992) Critical volume fractions in conductive composites. *J Compos Mater* 26:2727
23. Ruschau GR, Yoshikawa S, Newnham RE (1992) Percolation constraints in the use of conductor-filled polymers for interconnects. In: 42nd electronic components and technology conference, proceedings IEEE, May 1992, IEEE, Piscataway, p 481
24. Schroder J (1963) Apparatus for determining the thermal conductivity of solids in the temperature range from 20 to 200 °C. *Rev Sci Instrum* 34:615
25. Padilla A, Sanchez-Solis A, Manero O (1988) A note on the thermal conductivity of filled polymers. *J Compos Mater* 22:616
26. Bujard P, Kuhnlein G, Ino S, Shiobara T (1994) Thermal conductivity of molding compounds for plastic packaging. *IEEE Trans Compn Packg Manu Tech Part A* 17:527
27. Agari Y, Uno T (1985) Thermal conductivity of polymer filled with carbon materials: effect of conductive particle chains on thermal conductivity. *J Appl Polym Sci* 30:2225
28. Agari Y, Ueda A, Nagai S (1994) Electrical and thermal conductivities of polyethylene composites filled with biaxial oriented short-cut carbon fibers. *J Appl Polym Sci* 52:1223
29. Sahimi M (1994) Applications of percolation theory. Taylor and Francis, London
30. Neogi P (ed) (1996) Diffusion in polymers. Marcel Dekker, New York

Chapter 5

Newly High-Performance Wood-Substituted Composites Based on Polybenzoxazines

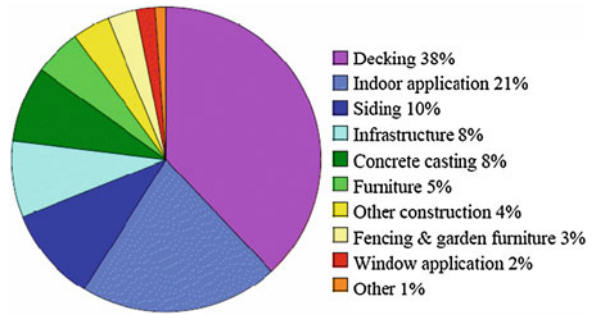
Abstract Wood-substituted composites of natural woodflour-filled polybenzoxazine and their polybenzoxazine alloys with high mechanical properties, good thermal stability, and reduced water uptake have been developed. The outstanding compatibility between the woodflour and the polybenzoxazine-based polymer matrix is evidently seen from the large improvement in the composite's mechanical properties, glass-transition temperature (T_g), and char yield as also evidently seen in the fracture surface of the wood polymer composites based on polybenzoxazine. At the optimal woodflour content of 70 % by weight in polybenzoxazine results in the composite's T_g as high as 200 °C or about 40 °C greater than that of the neat polybenzoxazine and the modulus in a range of 6.4–6.8 GPa compared to that of natural *Hevea brasiliensis* wood, i.e., 9.7 GPa. Polybenzoxazine is thus proved to be useful as an effective binder for lignocellulosic materials such as woodflour.

Keywords Wood-substituted composite · Polybenzoxazine · Phenolic · Epoxy · Cashew nut shell liquid · Woodflour

5.1 Introduction

Wood is an important raw material, which has been used by human beings since early years. The reason for its diverse and great utilization is related to its good physical strength, esthetically pleasing characters, and low processing cost. However, nowadays, the forest area in the world particularly hardwood forest is seriously decreasing while the quantity of using natural wood as a major materials in various applications is still high. Over the 20-year period ending in 1994, the world population increased by 40 %. In that same period, global consumption of wood increased to 37 %. This per capita demand varied slightly between 0.66 and 0.67 m³. If the demand for wood continues at this rate, it will be necessary to

Fig. 5.1 Wood polymer composite applications in Europe, 2004 [5]



increase the production of wood products for the next 4–6 decades by 0.3–0.7 billion m^3 per decade. Since the current total annual wood harvest globally is approximately 3.5 billion m^3 , the anticipated increase in the demand is significant. In addition, during the 1980s, there was a decrease of 2 % in the world's forest due to deforestation excluding the forest that was logged and left to regenerate. Therefore, over last decade, the new materials with the natural's wood properties to use for substituting natural wood were studied to find their way into the market as wood-substituted materials. The new wood replacement is wood polymer composites which are a form-shaped composite material made of cellulosic fillers, i.e., woodflour/fiber, and thermosetting/thermoplastic polymers with acceptable relative strength and stiffness, high durability, low maintenance cost, fewer prices relative to other competing materials, extended lifetime compared with many wood products, and the fact that it is a natural resource [1, 2] wood polymer composite applications as shown in Fig. 5.1 are regarded.

Wood polymer composites have firmly established themselves on the American, European, and Asian markets due to their sustainability and manifold characteristics, i.e., 100 % recycle and up to 80 % renewable resources. Market share and applications of wood polymer composites in the past five years have been growing rapidly by reporting of wood–plastic composite information center of Washington State University, especially for applications such as decking and railing. Wolcott and Smith [3] have been recorded that the sales of wood polymer composites in 2005 exceed \$1.0 billion. Two-thirds of the produced composites are comprised of decking and railing products, accounting for \$0.7 billion, while window and door frame products are projected to be valued at approximately \$0.27 billion. In addition, the growth market of wood polymer composites in north American has been reported approximately 13 % per year from 1998 to 2008 and was valued at US\$220 million [4] while, in Europe, and the market share of the wood polymer composites in total wood product consumption in 2006 was estimated at far less than 1 %, while annual growth rates in the wood-based polymer composite consumption are estimated at over 10 %. Interestingly, in 2007, wood polymer composite production in Europe was estimated at approximately 100,000 tons. The leading countries are Germany, Austria, Belgium, the Netherlands, and Scandinavia. In addition, in this area, a strong trend toward the solid deck execution has been observed since 2010.

Hackwell Group also reported that European production of wood polymer composites has both diversified in its applications and grown rapidly over the last five years to reach 193,000 tonnes by 2010. In addition, a new report forecasts continuing growth to almost 360,000 tonnes by 2015, which represents an average annual growth of 13 %, but nevertheless a slowing in growth compared with the 2005–2010 period, as a result of the continuing difficulties in European economies. However, growth rates in the wood polymer composite market vary: while the American market is fairly saturated, the European Union shows growth rates of up to 25 % per year, while the highest growth rates are today found in Asia, and especially in Japan, where it holds a 60 % market share in architectural landscaping in the public and private construction sectors.

In case of composite products based on polymer and wood filler, the polymeric matrices used can generally separate to thermosetting polymers, i.e., epoxy and phenolic resins that are majority of binder up to 70 % of wood polymer composites such as particleboard materials. The other polymeric matrix is thermoplastic polymer. Recently, this polymeric matrix has been developed to increase more and more for using to be a binder of wood polymer composite, i.e., polyethylene, polypropylene, poly(vinylchloride), and acrylonitrile–butadiene–styrene (ABS). Interestingly, the wood polymer composites can effectively solve high flammability, high water absorption due to be hydrophilic material as well as termite irresistibility of the natural wood. The potential applications for the wood polymer composites include siding, roofing, residential fencing, picnic tables, benches, landscape timber, patios, gazebos and walkways, road furniture, and playground equipment. However, a major problem encountered in using thermoplastic matrices is its rather poor interfacial adhesion between the untreated polar wood fillers and the strongly hydrophobic characteristics of the polymeric matrix. Therefore, mechanical performance of the wood-substituted composites based on thermoplastic polymer is relatively poor that results in limiting thermoplastic-based wood polymer composites present use to common nonstructural end-uses. Another significant shortcoming of this type of matrix is the relatively low filler content, typically less than 50–60 % by weight, that can be added into the matrix. To achieve greater filler content, modification of the interface between the wood fillers and the matrix either by physical or chemical treatment is required. However, surface treatment of filler particles normally increases the steps and the cost of processing.

In recent years, the trend is shifting slightly toward a greater number of wood polymer composite's applications in the automobile industry. Structural components may also have the potential to become a future focus of production in addition to the current major area of car body parts. The natural filler-reinforced polymer composites have been interested in interior and exterior parts for car manufactures because the composites can serves a twofold objective: to lower the overall weight of the vehicle thus increasing fuel efficiency and to increase the sustainability of their manufacturing process. Many companies such as Mercedes Benz, Toyota, and DaimlerChrysler have already accomplished and they are looking to expand the uses of natural fiber composites. In addition, Hackwell

Group has been reported that BASF in North America is introducing a new resin developed for natural fiber thermosetting composites. Acrodur thermosetting acrylic copolymer is already being used in a door panel substrate for the BMW 7 Series sedan molded by Dräxlmaier Group in Germany. It is used to impregnate a mat made of wood fibers, i.e., sisal and jute, or other natural materials to produce a 70 % fiber composite. On curing process, Acrodur resin has been crosslinked by heating during compression molding to become thermosetting.

Therefore, the highly filled composites based on polybenzoxazine, newly thermosetting polymer, for applications required good mechanical strength, high thermal stability, and fire resistance as well as eco-friendly materials, are developed. Para-woodflour was selected as a reinforcing filler because of its availability as a low-cost waste wood material in Southeast Asia, i.e., Thailand and Malaysia.

5.2 High-Performance of Para-Woodflour-Filled Polybenzoxazine Composites

Since January 1989, Thailand has banned all commercial logging in its hardwood forests. Therefore, softwood has been accepted to use for substituting hardwood. However, the conventional hardwood, i.e., rubber wood or *Hevea brasiliensis* (Table 5.1) which is also called para-rubber wood in Thailand is one of the more durable lumbers nowadays used in furniture industry because it is considered the most eco-friendly lumber, as it is only harvested after the rubber wood tree has completed its lifetime growing cycle which is generally 26–30 years. Therefore, the para-rubber wood is one of the alternative eco-friendly, simply using up a waste product of the latex production industry unlike other woods such as mahogany, teak, oak, and birch that are cut down for the sole purpose of producing furniture. In consequence, woodflour or sawdust of rubber wood tree which is abundant and a major waste of the furniture or sawmill industry in Thailand.

As aforementioned, wood polymer composites are highly attractive as a product to replace natural wood since their properties can be formulated to imitate wood materials with some characteristics even being superior to the natural wood. Recently, Rimdusit et al. [6] have studied bisphenol-A/aniline-based benzoxazine

Table 5.1 Properties of para-rubber wood

Properties	
Density at 16 % moisture content (g/cm ³)	0.56–0.64
Static bending at 12 % moisture content (N/mm ²)	66
Modulus of elasticity at 12 % moisture content (N/mm ²)	9,700
Hardness (N)	4,350
Tangential shrinkage coefficient (%)	1.2
Radical shrinkage coefficient (%)	0.8

Source Sarkar Plywood Rubber Wood-Sarkar Plywood Pvt. Ltd.

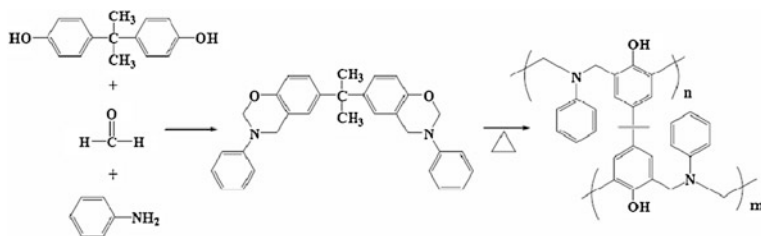
Table 5.2 Mechanical properties of natural fibers [7]

Fiber	Specific gravity	Modulus (GPa)	Specific modulus (GPa)	Tensile strength (MPa)
Jute	1.30	55	38	393
Sunhemp	1.07	35	32	398
Pineapple	1.56	62	40	170
Glass fiber-E	2.50	72	28	3,400

resin (as abbreviated BA-a) filled with para-rubber woodflour which can be obtained in a relatively cheap price. In addition, generally, natural filler inherently possesses low density, high specific strength, and high specific modulus as evidently shown in Table 5.2. From this table, though natural fibers show lower absolute modulus than inorganic fiber such as the fiberglass, their specific properties clearly render much greater values. These characteristics are essential in the application that strength and weight of the composite products are of major concern such as in automobile part.

Thermosetting polymer that was selected as a matrix of wood-substituted composites as reported by Rimdusit et al. [6] is polybenzoxazine. The benzoxazine resin has many attractive and useful properties including no curing agent required, near-zero shrinkage upon crosslinking, no by-product released during cure. In addition, its polymer shows good mechanical properties, high thermal stability, low water absorption, low flammability, and low A-stage viscosity as stated by Ishida and Tareg [8]. A significant ability of the bisphenol-A/aniline-based benzoxazine resin (BA-a), synthesized using the patented solventless method [9] to yield bifunctional monomers shown in Fig. 5.2, is low A-stage viscosity that helps in filler wetting with substantial amount of the para-rubber woodflour filler can be incorporated into the polybenzoxazine matrix.

Interestingly, the relatively low A-stage viscosity of the BA-a resin enabled the incorporation of a large amount of untreated para-rubber woodflour with particle size less than 149 μm up to 75 % by weight (70.5 % by volume) which is its maximum packing of highly filled polybenzoxazine system, i.e., 1.380 g/cm^3 calculated based on the density of para-rubber woodflour of 1.490 g/cm^3 and the density of poly(BA-a), of 1.185 g/cm^3 . The results show the significant properties, i.e., thermal, mechanical, and some physical properties, of the polybenzoxazine

**Fig. 5.2** Bisphenol-A/aniline-based polybenzoxazine [Poly(BA-a)]

filled with para-rubber woodflour particularly high glass-transition temperature, i.e., from 160 °C for the unfilled system to 220 °C for 75 % by weight of para-rubber woodflour filler. On the other hand, degradation temperature at 5 % weight loss ($T_{d,5}$) was expectedly observed to decrease with the para-rubber woodflour content and the char yield at 800 °C of the polybenzoxazine wood showed synergistic characteristics with the value of 36 %, compared with 28 % of the neat polybenzoxazine matrix and 18 % of the para-rubber woodflour as shown in Table 5.3.

In addition, the superior mechanical properties, i.e., modulus of elasticity under flexure mode or flexural modulus (E_f) of the para-rubber woodflour-filled polybenzoxazine composites than that of polybenzoxazine matrix, were observed. Flexural modulus is measure of how a material will deform and strain when weight or force is applied on fixed materials. Therefore, the flexural modulus value is used as an indication of a material's stiffness under flexure mode. From the table, the E_f measured at room temperature (25 °C) of the para-rubber woodflour-filled polybenzoxazine composite with 20–75 % para-rubber woodflour contents which show the relatively high the E_f to be 6.8–7.3 GPa compared to that of the E_f of the natural para-rubber wood is recorded as 8.0–9.7 GPa [10]. Therefore, the E_f of wood-substituted polybenzoxazine composites is in the vicinity of the natural para-rubber wood. Moreover, modulus of rupture under flexure test or flexural strength (ρ_f) that is defined as a material's ability to resist deformation under the action of flexure force as high as 60–70 MPa was achieved in these highly filled system which are significantly close to that of natural para-rubber wood, i.e., 74 MPa [10].

The interfacial adhesion between woodflour and polymer matrix plays an important role in determining the performance, i.e., thermal and mechanical properties of the wood-substituted polymer composites. Generally, theories of adhesion can be attributed to five main mechanisms, i.e., adsorption and wetting, mechanical interlocking, electrostatic interactions, chemical bonding and diffusion, which can occur at the interface either in isolation or in combination to produce the bond. In the polybenzoxazine filled with para-rubber woodflour filler without surface modification, the enhanced physical–mechanical properties, i.e., modulus and glass-transition temperature composites, were observed as we

Table 5.3 Properties of para-rubber woodflour-filled polybenzoxazine composites

Para-rubber woodflour (wt %)	T_g (°C)	T_d (°C)	Char yield (%)	E_f (GPa)	ρ_f (MPa)	Water absorption at 24 h (%)
0	160	323	28	4.7	76	0.11
40	180	298	34	5.6	–	0.97
50	185	283	35	5.8	61	2.32
60	190	280	36	5.9	60	2.37
70	200	–	–	6.5	60	3.79
75	220	–	–	6.8	61	5.88
80	–	276	35	6.6	61	8.11
100	240	275	18	9.7	66	–

expected due to strong para-rubber woodflour-polybenzoxazine bonding via chemical bonding and mechanical interlocking adhesions. The hydrogen bonding formations are possible in this composite system as shown in Fig. 5.3.

Scanning electron microscopy (SEM) technique was employed to observe the morphology at the para-rubber woodflour/polybenzoxazine interface as shown in Fig. 5.4. Typically, the SEM technique revealed the appearance of three types of interfacial adhesion, i.e., woodflour/fibers, woodflour/fibers breakage, and fibrillation. The woodflour/fibers pull-out morphology corresponds to weak adhesion of the two phases. On the other side, the breakage and fibrillation of woodflour/fibers were observed on the fractured surface, which implies the existence of substantial degree of adhesion between the two components.

From Fig. 5.4, the interfacial adhesion characterization of wood-substituted polybenzoxazine composites shows good bonding because the para-rubber woodflour breakage and fibrillation were observed. This indicated the significant compatibility between the polybenzoxazine matrix and polar-hydrophilic wood materials, i.e., cellulose and hemicelluloses which have a strong polar hydroxyl groups in their structures. This makes the woodflour highly compatible with polar acidic or basic polymers such as the polybenzoxazine. Therefore, the good interfacial adhesion is essential to transfer a stress from the polybenzoxazine matrix to the para-rubber woodflour filler and thus improve the mechanical strength and the thermal stability of this wood-substituted polymer composite. In addition, the physical penetration of the benzoxazine resin with low α -stage viscosity into the microstructure of para-woodflour also causes mechanical interlocking of the polybenzoxazine into irregularities of para-woodflour.

Meanwhile, some wood-substituted polymer composites such as polyethylene and polypropylene wood composites show no good compatibility due to the poor interfacial adhesion between polar-hydrophilic woodflour/fibers in nature (high surface tension) and nonpolar-hydrophobic thermoplastic polymers (low surface

Fig. 5.3 The possible hydrogen bonding in the lignocellulosic filler–polybenzoxazine composite system

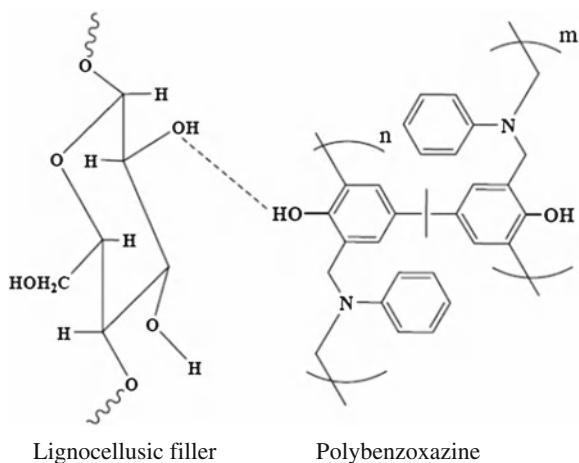
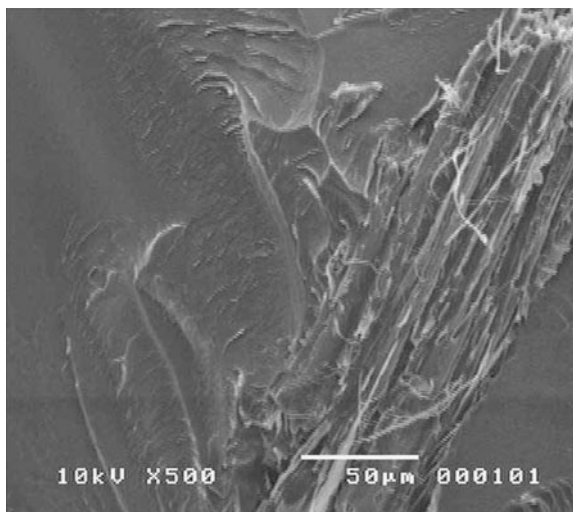


Fig. 5.4 Fracture surface of polybenzoxazine filled with para-rubber woodflour



tension). This characteristic leads to wood-substituted polymer composites with poor dispersions of woodflour/fibers in the polymer matrices due to strong woodflour/fiber-woodflour/fiber interactions resulting from hydrogen bonding [11], and poor mechanical properties of the composites, particularly tensile, impact strengths and elongation at break. Therefore, many researchers have reported surface modification of the woodflour/fiber to overcome these problems [12]. Ashori and Nourbakhsh [13] have studied some physical and mechanical properties of polypropylene reinforced with MAPP-treated-oak or MAPP-treated-pine woodflour fillers with 250- μm particle size. The authors have reported that the flexural modulus and strength of the polypropylene-filled with oak woodflour at 40 % by weight was 1.92 and 26.0 MPa, respectively, while those of the polypropylene-filled with pine woodflour at the same content were 2.06 and 30 MPa, respectively. Therefore, when compared with those values of the polypropylene composites, the relatively higher flexural modulus (5.00 GPa) and flexural strength (54.0 MPa) of polybenzoxazine reinforced with untreated para-woodflour in the range of 250–297- μm particle size at 40 % by weight was observed [6]. For wood-based composites and panel products, an optimal flexural strength is required [14] i.e., 3.0–23.5 MPa for particleboard-grade requirements, 11.0–19.5 MPa for particleboard-flooring product-grade requirements, and 14.0–34.5 MPa for medium-density fiberboard (MDF). Interestingly, for polybenzoxazine wood composites show flexural strength up to 60.0–70.0 MPa which is more than sufficient for high strength wood-substituted products. In addition, comparison of mechanical properties of our polybenzoxazine wood composites with the other system at the same wood filler content was also listed in Table 5.4.

Furthermore, one of the important properties, the water absorption content when exposed to humid environment, has seriously considered of wood-substituted polymer composite industries since absorbed significant amounts of

Table 5.4 Comparison of mechanical properties of polybenzoxazine wood [6] with related wood polymer composites [15]

Composites properties	Flexural	
	Modulus, GPa	Strength, MPa
PBA-a + 40 % para-rubber woodflour	5.59	58.7
PP + 40 % woodflour	3.03	44.2
PP + 40 % woodflour + MAPP	3.08	53.1
PP + 40 % wood fiber	3.25	47.9
PP + 40 % wood fiber + MAPP	3.22	72.4

water adversely affect most physico-mechanical properties, i.e., decrease of mechanical moduli, decrease of yield strength, change of yield/deformation mechanisms; hygrothermal degradation, i.e., microcracks, aging, chain scission through hydrolysis, degradation of fiber/matrix interface in composites; swelling stresses. Typically, in wood-reinforced polymer composite industries, the tempered hardboard with thickness ranging from 2.1 to 9.5 mm defines the water content of less than 10–30 % by weight, or the standard hardboard in the same range thickness requires the water absorbed in the sample of less than 15–40 % by weight. According to experimental results of the para-woodflour-substituted polybenzoxazine composites with a thickness of 3.2 mm carried out according to ASTM D570-98 standards, the water absorption content calculated using the following Eq. (5.1) of the polybenzoxazine composites filled with 40–80 % by weight (34.6–76.1 % by volume) of para-woodflour is in the range of 5–25 % by weight as listed in Table 5.3 which meets the above industrial requirements and the water absorption content of the polybenzoxazine wood composites were significantly less than that of natural wood, i.e., 20–300 % [16].

$$WA(t) = \frac{W(t) - W_0}{W_0} \times 100 \quad (5.1)$$

where $WA(t)$ is the water absorption at time t , W_0 is the dried weight, and $W(t)$ is the weight of sample at a given immersion time t .

Interestingly, the significantly decreased water absorption content of natural wood was observed as expected because the hydroxyl group ($-OH$) of polybenzoxazine chemically bonded with the $-OH$ groups in the lignocellulosic filler, and this limits the water absorption content for polybenzoxazine wood composites, as shown in Fig. 5.5.

Moreover, the para-woodflour-filled polybenzoxazine composites are compared with related wood polymer composites. It was found that, at the same absorption time (24 h) and filler content (50 % by weight), our para-woodflour-filled polybenzoxazine wood composite can absorb water significantly less than those of untreated natural wood–fiber polymer composites, i.e., novolac resin filled with banana, hemp, and agave fibers. The para-rubber woodflour-reinforced polybenzoxazine composite has a water absorption value of 2.37 % by weight, while

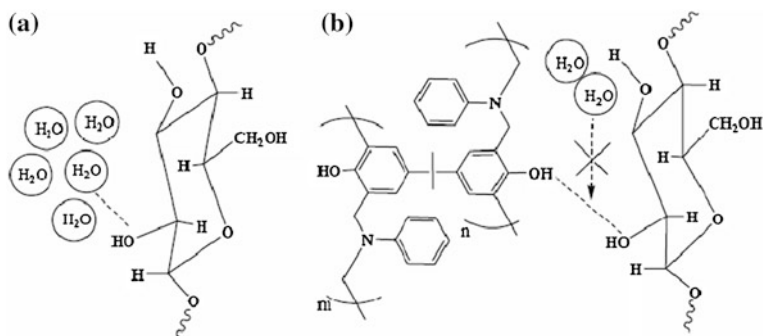


Fig. 5.5 Water absorption behavior of natural wood filler (a) and polybenzoxazine wood composites (b)

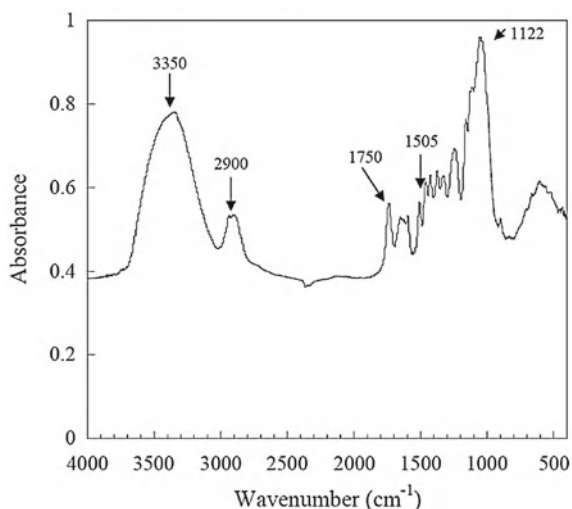
the untreated agave-fiber composite, the best result among those three natural wood-fiber novolac composites, has a rather higher water absorption value approximately 10 % by weight [17].

In general, woodflour/fiber, lignocellulosic materials, composes of a polar-hydrophilic natural polymeric material possessing many hydroxyl groups ($-OH$), which is able to combine with water molecules. Therefore, the wood-substituted polymer composites absorb water when they containing lignocellulosic material, i.e., cellulose and hemicelluloses which in the presence of hydroxyl and carboxylic groups, are used in moist areas. However, it is believed that no significant change occurs in the microstructure of the wood-substituted polymer composites, because the reinforcing filler is encapsulated in the nonpolar-hydrophobic matrix polymer. The molecular structures of para-woodflour filler was performed by Fourier transform infrared spectroscopy (FT-IR) technique which is well known to be suitable for the quick characterizations of very low amounts of nonsoluble materials. The obtained FT-IR spectra given in Fig. 5.6 show the basic structures of para-woodflour filler.

A strong broad hydroxyl ($-OH$) group stretching vibrations are observed from $3,300$ to $3,600\text{ cm}^{-1}$ and the bands associated with the aromatic and aliphatic $C-H$ stretching are presented at $3,000-2,800\text{ cm}^{-1}$. The bands centered near $1,750-1,725\text{ cm}^{-1}$ associated with the carbonyl ($C=O$) stretching in the carboxylic ($-COOH$) and ester ($COO-$) groups, and another at $1,122\text{ cm}^{-1}$ is likely due to $C-O$ and $C-C$ stretching of cellulose components. Most of these bands have contributions from both carbohydrates (cellulose and hemicelluloses; 70–80 %) and lignin (20–30 %). In addition, the intensity of the band of aromatic skeletal vibrations $1,505\text{ cm}^{-1}$ is observed for lignin contents [18].

Moreover, the FT-IR spectra of woodflour after thermal treatment were presented. The spectra considerably changed from that of untreated woodflour/fiber. The aromatic and aliphatic $C-H$ stretching peak at $3,000-2,800\text{ cm}^{-1}$ decreases after thermal treatment when compared to untreated woodflour/fiber. This result indicates the loss of some hydrocarbon compounds as volatile while broad

Fig. 5.6 IR spectra of para-rubber woodflour



absorption peaks of a strong broad hydroxyl (-OH) group were still detected at $3,600\text{--}3,300\text{ cm}^{-1}$. In addition, the carbonyl peak at $1,750\text{--}1,725\text{ cm}^{-1}$ was reduced in comparison to both the $3,600\text{--}3,300\text{ cm}^{-1}$ and $1,505\text{ cm}^{-1}$, indicating that these functional groups lost from the surface due to the decomposition of lignin [19].

As above mentioned, the polymers and their corresponding composites are typically sensitive to changes in their environment and their mechanical properties may vary widely with conditions. Therefore, in recent years, to predict the mechanisms of water transport in polymer composite materials, many researchers have investigated. Moisture absorption in polymeric composites has shown to be governed by several different mechanisms. The first involves diffusion of water molecules inside the micro gaps between polymer chains. The second involves capillary transport into the gaps and flaws at the interfaces between fiber and the matrix. This is a result of poor wetting and impregnation during the initial manufacturing stage. Typically, based on these mechanisms, there are three known mechanisms of water transport in polymer composites classified according to the relative mobility of the water and of the polymer segments, which are Fickian diffusion, relaxation-controlled, and nonFickian or anomalous [20]. In the case of wood-substituted polymer composites, the dominant mechanism depends on factors such as woodflour/fiber content, chemical structure of the polymer, dimensions and morphology of the woodflour/fiber filler, polymer-woodflour/fiber filler interfacial adhesion, humidity, and temperature. Hygroscopic and hydrophilic materials of wood polymer composites results in moisture absorption. Moisture transfer in wood or wood polymer composites has been quoted by Skaar and Adhikare [21] that moisture movement is mainly controlled by diffusion when the moisture content of the wood is below the fiber saturation point (FSP) indicated that the moisture diffusion was a combination of two movements: the vapor diffusion through the void structure and the bound water diffusion through the cell

wall. Therefore, a diffusion model based on Fick's second law has been developed to describe this mass transfer process which is unsteady-state system, the concentration changes with time. For the case of thin plane with uniform initial distribution and equal initial surface concentrations under unsteady-state, the generalized equation for the diffusion behavior can be expressed by

$$\frac{M_t}{M_\infty} = 1 - \sum_{n=0}^{\infty} \frac{8}{(2n+1)^2 \pi^2} \exp\left[\left(-D(2n+1)^2 \pi^2 t / (4l^2)\right)\right] \quad (5.2)$$

where M_t denotes the total amount of diffusion substance entering the sheet at time t , M_∞ denotes the corresponding quantity after infinite time, D is the diffusion coefficient, and l denotes the half thickness of sheet.

At initial absorption stage, moisture absorption (M_t) shows linear increase with t . Therefore, Eq. (5.2) is simplified to the following equation:

$$M_t = \frac{2M_\infty \sqrt{D}}{\sqrt{\pi}} \frac{\sqrt{t}}{l} \quad (5.3)$$

$$D = \frac{\pi}{4} M_\infty^{-2} l^2 \theta^2 \quad (5.4)$$

where θ is the slope of the plot between M_t and $t^{1/2}$

However, the composite materials result in different behavior of moisture absorption with Fick's law. The generalized equation for explaining the diffusion behavior in composite materials can be expressed in Eq. (5.5).

$$\frac{M_t}{M_\infty} = k_n t^n \quad (5.5)$$

where M_t = the water absorption at time t , M_∞ = the water absorption at saturation point or infinite time k_n and n = constants

The diffusion behaviors can be classified as supercase II ($n > 1$), case II ($n = 1$), anomalous ($1/2 < n < 1$), classical/Fickian ($n = 1/2$), or pseudo-Fickian ($n < 1/2$) [ref].

The classical diffusion theory or Fickian ($n = 1/2$) was used to explain the behavior of moisture absorption for woodflour/fiber polymer composites. Figures 5.7 and 5.8 illustrate M_t/M_∞ versus $t^{1/2}$ plots of para-rubber woodflour-reinforced polybenzoxazine composites at various para-rubber woodflour filler contents.

From the plots in Fig. 5.7, we can see that the polybenzoxazine wood composites filled with para-rubber woodflour about 40 and 50 % by weight show classical diffusion behavior while the diffusion behavior of the polybenzoxazine wood composites filled with para-woodflour about 60–80 % by weight was observed to be two-step. Therefore, increasing para-woodflour contents show significant effect on the diffusion behavior of the polybenzoxazine wood composites. One mechanism is that of coupled mass and momentum transport or

Fig. 5.7 Plots of M_t/M_∞ and \sqrt{t} of polybenzoxazine wood composites at various para-rubber woodflour contents: (filled circle) 40 wt%, (filled square) 50 wt%

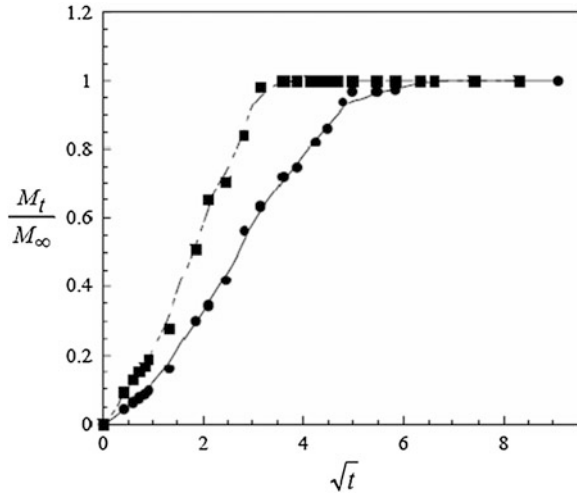
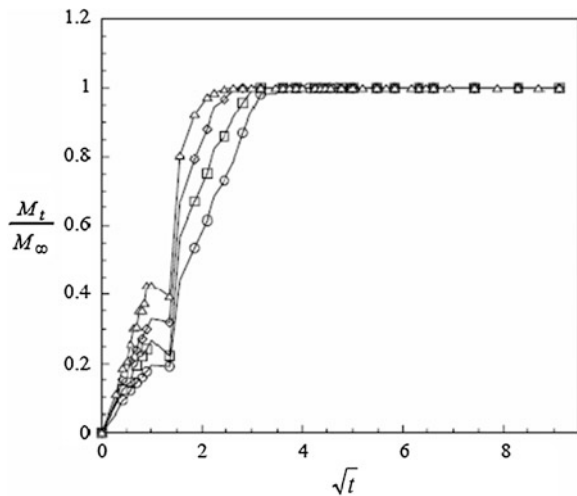


Fig. 5.8 Plots of M_t/M_∞ and \sqrt{t} of polybenzoxazine wood composites at various para-rubber woodflour contents: (circle) 60 wt%, (square) 70 wt%, (diamond) 75 wt%, (triangle) 80 wt%



coupled through swelling as well as glassy inhomogeneous network of polybenzoxazine in nature.

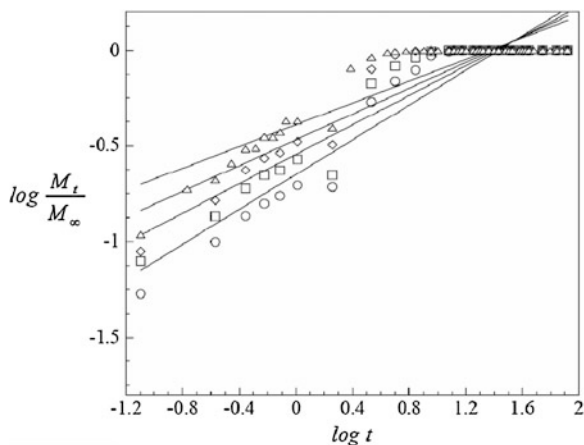
Figure 5.8 illustrates $\log M_t/M_\infty$ versus $\log t$ plots of the polybenzoxazine wood composites filled with 60, 70, 75, and 80 % by weight which showed the slopes which are n value approximately 0.45, 0.39, 0.34, and 0.28, respectively. Thus, we can conclude that our composite materials filled with para-rubber woodflour about 40–50 % by weight exhibited behavior close to Fickian-type diffusion ($n = 0.5$) while that filled with para-woodflour more than 60 % by weight displayed a pseudo-Fickian. Furthermore, the larger constant value (k) informed the affinity between the material and the water molecules refers to the

stronger the interactions with the water molecules. As expected, the k value of polybenzoxazine wood composites increased with increasing para-rubber woodflour contents, i.e., 0.22, 0.29, 0.34, and 0.41 for 60, 70, 75, and 80 % by weight woodflour content, respectively (Fig. 5.9).

5.3 Fire-Retardant Para-Woodflour-Filled Polybenzoxazine Alloy Composites

In spite of the merits mentioned above, the natural wood still has many weak points such as high water absorption (30–200 %) due to be hydrophilic material in nature that lead to splinter, warp or twist, termite irresistibility, and high flammability (LOI = 21) indicated relatively high burning potential which limits its use in some applications. Therefore, wood-substituted composites from waste wood materials, i.e., sawdust or woodflour and resin binder, play a key role to solve these problems by combining those complementary properties of the filler and the polymer matrix. In recent years, low flammability, one of the most important properties of wood-substituted polymer product used in constructions, is required. White and Dietenberger [22] have quoted that “statutory requirements pertaining to fire safety are specified in the building codes or fire codes. These requirements fall into two broad categories: material requirements and building requirements. Material requirements include such things as combustibility, flame spread, and fire endurance. Building requirements include area and height limitations, fire stops and draft stops, doors and other exits, automatic sprinklers, and fire detectors.” Building codes related with fire rating for construction materials have provided definitions for some terms commonly used to describe how a given material or assembly will perform in a fire. Terms those have been defined including of combustible, noncombustible, fire resistance, and ignition resistant.

Fig. 5.9 Plots of $\log M_t/M_\infty$ versus $\log t$ of the polybenzoxazine wood composites at various para-rubber woodflour contents: (circle) 60 wt%, (square) 70 wt%, (diamond) 75 wt%, (triangle) 80 wt%



Combustible and noncombustible refer to the performance of a material such as wood, cement, and steel while fire resistance and ignition resistant can refer to a material or an assembly, i.e., all the components in a wall-siding, insulation, and sheathing products. Generally, many common construction materials such as wood, wood-substituted polymer composites, and plastic products which are commonly used for decking and siding have been considered to be the combustible materials that readily ignite and burn [23].

Lately, poly(vinyl chloride), PVC, is one of the most utilized thermoplastics as a matrix polymer for fire-resistant wood composites due to its inherently low flammability (LOI = 50) [24]; however, during its combustion, the polymer can release hydrochloric (HCl) gas which is both corrosive and toxic. Furthermore, some systems of wood polymer composites are incorporated with flame retardants for improving their fire-resistant ability. Basically, flame retardants function under heat to yield products that would be more difficult to ignite than pure polymers, or that do not propagate flame readily. Although an addition of flame retardant, i.e., antimony trioxide (Sb_2O_3), decabromodiphenyl oxide (DBDPO), and alumina trihydrate (ATH), reduces flammability of materials, the mechanical properties are usually sacrificed and the use of flame retardant also obviously increases the material cost. [25]. Moreover, mechanical properties of thermoplastic wood composites have been investigated by several workers [26, 27]. The flexural strength of PVC wood composites was reported to be approximately 46 MPa [26] compared to the value of 66 MPa of para-rubber wood whereas flexural characteristics of woodflour-reinforced polyethylene were investigated by Farid et al. [27]. The properties of the polyethylene wood composite with 50 % by weight of woodflour content showed a relatively low flexural modulus value of 1.05 GPa and low flexural strength value of merely 19 MPa. Furthermore, thermosetting wood composites have been investigated in mechanical properties. Ayrilmis et al. [28] have studied the mechanical properties, modulus, and strength under flexure mode of particle boards based on phenol–paraformaldehyde and woodflour/rice husk particle mixtures (89–92 % by weight). The flexural modulus and strength of particle board have been reported from 2.3 to 2.6 GPa and from 12.8 to 14.0 MPa, respectively. These results suggest that thermoplastics wood composites may not effectively be used for high load-bearing applications.

Recently, high-performance wood polybenzoxazine alloy composites with relatively high flame-retardant characteristics and good mechanical properties have been investigated by Rimdusit et al. [29]. As above mentioned, one intriguing characteristic of the benzoxazine resin is its ability to be alloyed with other resin such as phenolic novolac [30]. Phenolic novolac resins containing aromatic phenol units linked predominantly by methylene bridges were synthesized from phenol (carboxylic acid) with less than equimolar proportions of formaldehyde under acidic conditions. In addition, the raw material, i.e., phenols, can be replaced using cresols or bisphenol. The general chemical structure of the phenolic novolac is shown in Fig. 5.10.

Phenolic resins are found in a myriad of industrial products. They are applied as adhesives or matrix binders in engineered woods (plywood), brake linings, clutch

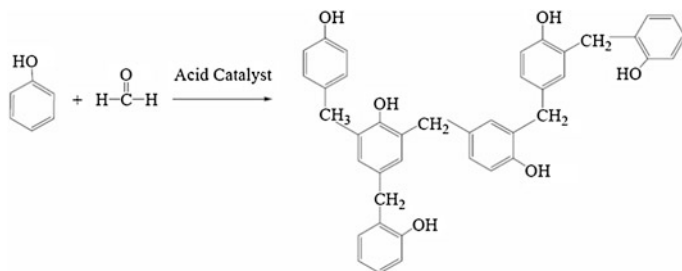
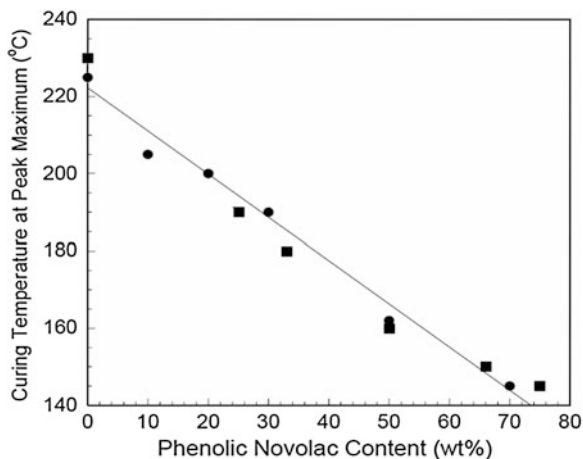


Fig. 5.10 Preparation and molecular structure of phenolic novolac resin

plates, circuit boards, coatings, and adhesives. In addition, the resins are of particular interest in structural applications due to their inherent fire-resistant properties yielding limiting oxygen index (LOI) values about 25–33 although smoke generation of phenolic networks occurred upon burning, chemical resistance, electrical insulation, dimension stability, and low cost. Phenolics have a broad range of applications varying from construction to electronics and aerospace. In the case of phenolic, composites have many desirable performance qualities including high-temperature resistance, creep resistance, excellent thermal insulation and sound damping properties, corrosion resistance, and excellent fire/smoke toxicity properties. However, they possess two significant disadvantages that are low toughness and generated water after curing reaction which can be remain trapped within the composite's sample that lead to damage the structure of the composite materials. Therefore, current commercial novolacs are limited to applications where high strength is not a requirement. However, for wood-substituted polymer materials, the advantages of using phenolic novolac resin as wood binder are their known high compatibility with wood, high char yield, no toxic by-products from burning, and its low cost. The addition of phenolic resin can sometimes significantly enhance fire-resistant properties of the base polymers it is with incorporated.

Rimdsut et al. [29] have studied the effect of phenolic novolac resin contents on curing temperature, flame resistance, thermal stability, and mechanical properties of wood polymer composites prepared from bisphenol-A/aniline-based benzoxazine resin (BA-a)-phenolic novolac alloys as a wood composite matrix filled with 50 wt% para-woodflour having particle size in the range 50–150 μm . In this work, the authors have presented the curing exotherms of the mixtures between benzoxazine monomer and phenolic novolac resin that the curing acceleration is observed from the shift of the curing exotherm peaks to lower temperature when the amount of phenolic novolac resin in the mixture increases, i.e., the curing exotherm of the benzoxazine monomer with a peak maximum of about 225 $^{\circ}\text{C}$ while that of the mixtures between benzoxazine monomer and phenolic novolac resins with a peak maximum in ranging of 145–205 $^{\circ}\text{C}$ as plotted in Fig. 5.11. The relationship between the exotherm peaks and the amount of

Fig. 5.11 The relationship between the curing temperature at peak maximum and phenolic novolac content in the benzoxazine/phenolic novolac mixtures: (filled circle) Data from Rimdusit et al. [29] at 0, 10, 20, 30, 50, and 70 wt% (filled square) Data from Rimdusit et al. [30] at 0, 25, 33, 50, 66, and 75 wt%



phenolic resin in the binary mixture suggests that phenolic novolac resin acts as an initiator for benzoxazine monomer as previously observed by Rimdusit et al. [30].

Aforementioned, fire safety is an important concern in all types of construction. Fire prevention basically means the elimination or suppression of an ignition of combustible materials by controlling either the source of heat or combustible materials. Due to its hydrocarbon nature of its molecular constituents, wood and wood-substituted polymer materials will burn when exposed to heat (high enough temperature) and air (oxygen). Thermal degradation of the materials occurs in stages. The degradation process and the exact products of thermal degradation depend upon the heating rate as well as temperatures. The sequence of events for combustion is quoted by White and Dietenberger [22] as follows: (5.1) wood, responding to heating, decomposes or pyrolyzes into volatiles. They become much more pronounced above 300 °C (5.2) volatiles, some of which are flammable, can be ignited if the volatile–air mixture is of the right composition in a temperature range of about 400–500 °C. This gas-phase combustion appears as flame (5.3) with air ventilation, and the char oxidation becomes significant around 200 °C. This char oxidation is seen as glowing or smoldering combustion until only ash residue remains. This solid phase combustion will not proceed if flaming combustion prevents a supply of fresh air to the char surfaces. Several characteristics are used to quantify the burning behaviors of wood polymer composites including LOI, burning rate, heat of combustion (HOC), smoke generation, and heat release rate (HRR).

In this work, flammability properties of the polybenzoxazine–phenolic novolac wood composites via LOI and rate of burning were listed in the Table 5.5. The LOI is the minimum concentration of oxygen, expressed as a percentage that will support combustion of a material. It is measured by passing a mixture of oxygen and nitrogen over a burning specimen and reducing the oxygen level until a critical level is reached [31]. Materials with high LOI values are recommended for high fire risk applications, principally for internal structures and components, since the

Table 5.5 Limiting oxygen index (LOI) of rubber woodflour-filled polybenzoxazine composites compared with that of other polymers and composites

Samples	LOI (%)	Burning rate (mm/min)
<i>Polymers</i>		
Polybenzoxazine based on bisphenol-A/aniline	30 [29]	–
Poly(BA-a)/phenolic alloys	31 [29]	–
Phenolic resin	25, 33 [29, 33]	–
Epoxy resin	24 [34]	–
Polyimide	36 [35]	–
Polypropylene (PP)	17 [29]	40–75 [36]
Poly(vinyl chloride)	50 [29]	–
<i>Composites</i>		
Poly(BA-a) + 50 wt % para-RW ^a	25 [29]	17
BP70/30 (50 wt %) + 50 wt % para-RW	26.2	No burning rate
BP50/50 (50 wt %) + 50 wt % para-RW	27.1	No burning rate
BP30/70 (50 wt %) + 50 wt % para-RW	28.1	–
BP30/70 (40 wt %) + 60 wt % para-RW	26.2	–
PP + 50 wt % sawdust	–	31 [37]

Note ^a para-RW is para-rubber woodflour

materials offer the potential to self-extinguish when the fire becomes deprived of oxygen [32], while the rate of burning is a general term used to describe the linear combustion rate at which a given material is consumed by fire. It is measured in length over time at given temperature. From the Table 5.5, the LOIs of all benzoxazine (B)-phenolic novolac (P)wood composites at various phenolic novolac contents in ranging of 30, 50, and 70 % by weight were above the self-extinguishable limit, i.e., LOI > 26. Furthermore, burning rate of 50 wt% para-rubber woodflour-reinforced polybenzoxazine–phenolic novolac alloy composites was also displayed in Table 5.5. We can see that the burning rate of the benzoxazine–phenolic wood composites decreased when the amount of phenolic novolac resin increased. The burning rate was 17 mm/min in the polybenzoxazine wood, while that of 50 wt% para-rubber woodflour-reinforced BP73 and BP55 composites does not burn.

In addition, effect of para-rubber woodflour contents (50 and 70 % by weight) on mechanical bending properties and thermal stability, i.e., degradation temperature at 10 % weight (T_{d10}) and char yield at 850 °C of the para-rubber woodflour-reinforced polybenzoxazine–phenolic novolac alloy composites at various phenolic novolac contents, was also investigated as listed in Table 5.6.

From the table, the mechanical bending properties, i.e., flexural modulus and strength, provide an excellent measure of the degree of reinforcement provided by the para-rubber woodflour to the polybenzoxazine–phenolic novolac wood composites. From the table, the flexural modulus increases with para-rubber woodflour content, while flexural strength slightly decreases with the woodflour content. However, at the same woodflour content, increasing of phenolic novolac resin results in improvement in flexural strength, suggesting that there is stress transfer

Table 5.6 Mechanical and thermal properties of polybenzoxazine–phenolic novolac alloy composites filled with para-rubber woodflour with 50 and 70 % by weight

BP alloy matrix (wt%)	E_f (GPa)		ρ_f (MPa)		T_{d10} (°C)		Char yield (%)		T_g (°C)
	50 wt%	70 wt%	50 wt%	70 wt%	50 wt%	70 wt%	50 wt%	70 wt%	
Poly(BA-a)	5.8	6.1	60	59	305	290	36	32	198
BP90/10	5.7	6.1	61	59	311	295	37	35	218
BP80/20	6.4	6.4	65	58	313	296	40	35	202
BP70/30	5.3	6.0	66	62	313	298	40	36	–
BP50/50	5.5	6.1	65	69	313	299	40	36	–
BP30/70	–	–	–	–	313	294	38	34	–

from the matrix to the woodflour filler respective of the amount of the phenolic novolac resin present. Furthermore, thermal stabilities, i.e., T_{d10} and char yield at 800 °C, of each of woodflour compositions were found to enhance with increasing of the phenolic novolac content. Therefore, the presence of the phenolic novolac resin helps to retard the flammability of the polybenzoxazine–phenolic novolac wood composites. Interestingly, addition of the phenolic novolac resin increases the glass-transition temperature of the composites, particularly in BP91 wood composite. This characteristic was ascribed to stronger bonding between the polybenzoxazine–phenolic novolac matrix and the woodflour filler than that between the polybenzoxazine matrix and the woodflour filler.

5.4 Ternary System Based on Benzoxazine, Epoxy, and Phenolic Resins Filled with Para-Rubber Woodflour

Epoxy resins are of interest due to their wide use as structural components. They are easily manufactured and commonly used as matrix materials in structural composites, as adhesives, or as coatings. This resin has long been used in an electronic part assembly, electronic circuit board, and electronic encapsulation because their well-characterized properties include high strength as well as good thermal and chemical stability. In addition, epoxy resin has wide range of curing temperature, low shrinkage, outstanding corrosion resistance, and relatively low water absorption; however, they are rather flammable materials and possess rather low thermal stability compared to phenolic resin.

Generally, the epoxy resin used most widely is made by condensing epichlorohydrin with bisphenol-A, diphenylol propane. An excess of epichlorohydrin is used to leave epoxy groups on each end of the low molecular weight polymer. Depending on molecular weight, the epoxy resin is a viscous liquid or a brittle high-melting solid. Figure 5.12 shows the formation of the crude diglycidyl ether of bisphenol-A (DGEBA). From the reaction, DGEBA is obtained by reacting

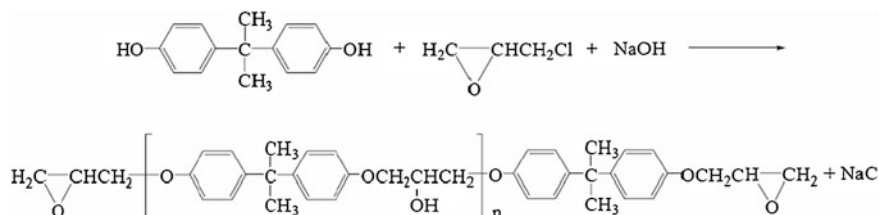


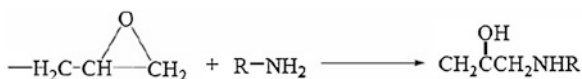
Fig. 5.12 Epoxy prepolymer based on bisphenol-A and epichlorohydrin

epichlorohydrin with bisphenol-A in the presence of sodium hydroxide. The reaction takes place in two steps; they are the formation of a chlorohydrin intermediate and the dehydrohalogenation of the intermediate to the diglycidyl ether, respectively. Each molecule of the diglycidyl ether will react with that of the bisphenol-A at the epoxide group, forming eventually the higher molecular weight DGEBA epoxy resin.

Epoxide groups may homopolymerize or react with active hydrogen atoms in other molecules, usually termed hardeners or co-reactants, to produce copolymers. Cure of an epoxy resin may involve either or both of these reactions and can be very complex, since reaction of an epoxide with one functional group can produce new functional groups for additional reaction with epoxide, and so on. The epoxy resins are cured by many types of materials, i.e., polyamines, polyamides, polysulfides, urea- and phenol-formaldehyde, and acids or acid anhydrides, through coupling or condensation reactions [38]. The reaction with amines involves opening the epoxide ring to give a β -hydroxyamino linkage as shown in Fig. 5.13.

Acids and acid anhydrides react through esterification of the secondary hydroxyl groups on the epoxy resin as well as with the epoxide groups. The phenolic and amino resins may react in several ways, including condensation of methylol groups with the secondary hydroxyls of the epoxy, and reaction of the epoxide groups with phenolic hydroxyls and amino groups. Epoxy resin can also be cured by cationic polymerization, using Lewis acid catalysts such as BF_3 and its complexes, which form polyethers from the epoxide groups. However, these curing agents have their own advantages and disadvantages. The amine groups used with room temperature to cure epoxy resins are volatile, smelly, and rather toxic to the user, while the polyamide groups can adversely affect the processability of epoxy resin due to its rather high viscosity of the high molecular weight polyamide, although high-performance-cured system can be obtained. In case of the acid anhydrides and Lewis acid group, they may cause corrosion to the processing apparatus. As a result, many researchers have proposed to utilize a novel class of epoxy crosslinkers based on self-polymerizable benzoxazine resins to solve the problems of the currently used curing agents [39, 40].

Fig. 5.13 Epoxy prepolymer based on bisphenol-A and epichlorohydrin



Recently, low-viscosity ternary mixtures of benzoxazine, epoxy, and phenolic resins have been developed by Rimdusit and Ishida [8]; benzoxazine resin imparts thermally curable, low water uptake, high char yield, and mechanical strength to the material, while epoxy is used mainly to reduce the viscosity of the mixture for special application such as highly filled composite's matrix, underfilling in the electronic packaging encapsulation. The effect of epoxy resin on the viscosity of benzoxazine–epoxy resin mixtures is listed in Table 5.7. Furthermore, an epoxy resin also gives higher crosslink density material with improved thermal stability as well as lowers the ambient temperature modulus of the ternary systems. In addition, the mixture of benzoxazine (B), epoxy (E), and phenolic novolac (P) resins to form the BEP ternary systems can provide a large variety of resin properties suitable for wide applications, particularly in the highly filled systems.

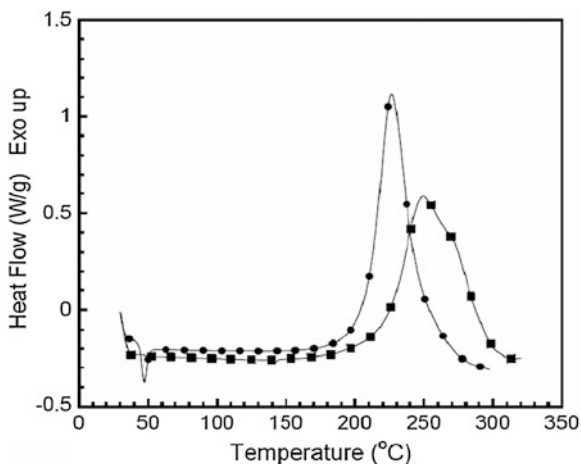
Moreover, several authors have reported the reaction between an epoxy resin and a benzoxazine resin. The ring opening of benzoxazine and epoxy took place simultaneously with no catalyst for both monomers. The oxirane ring opens when it reacts with the hydroxyl group, which results from the benzoxazine ring opening to afford a network structure. Recently, curing kinetics of benzoxazine–epoxy copolymer investigated by nonisothermal differential scanning calorimetry was studied by Jubsilp et al. [40] to understand the nature of curing process of the benzoxazine–epoxy resins. The authors have reported that the curing of benzoxazine–epoxy resin mixture was consisted of two dominant reactions (reaction 5.1 and reaction 5.2), as evidenced by the presence of a double peak on the DSC thermograms as depicted in Fig. 5.14.

The activation energy value via isoconversional method, i.e., Flynn–Wall–Ozawa of the reaction 5.1 of the benzoxazine–epoxy curing (81 kJ/min), is similar to that of the neat benzoxazine resin curing (81 kJ/min from Kissinger method) [42]. Therefore, reaction 5.1 was confirmed to be the reaction among the benzoxazine monomers while the activation energy value of reaction 5.2 is substantially higher than that of reaction 5.1 and is closer to that of epoxy curing, i.e., 118 kJ/min which is in excellent agreement with those reported for etherification by Cole et al. (101.4 kJ/mol) [43] and for homopolymerization by Sbirrazzuoli et al. (104, 170 kJ/mol) [44]. Then, reaction 5.2 is attributed to side reactions such

Table 5.7 Viscosity of benzoxazine–epoxy resin mixtures at various epoxy resin contents

BEP compositions (weight ratios)	Viscosity at 100 °C (Pa·s)	
	Data from Rimdusit et al. [30]	Data from Rimdusit et al. [41]
BEP 111	7.0	–
BEP 121	0.3	–
BEP 131	0.3	–
BET 811	–	917.3
BEP 721	–	616.3
BEP 631	–	235.6
BEP 541	–	80.9
BEP 451	–	43.0

Fig. 5.14 DSC thermograms of benzoxazine–epoxy resin mixture recorded at heating rate of 10 °C/min: (filled circle) Benzoxazine resin, (filled square) Benzoxazine (50 wt%)-epoxy (50 wt%) mixture



as etherification reaction of the glycidyl ether by a hydroxyl group of polymerized benzoxazine resin or homopolymerization. Furthermore, the autocatalytic models proposed were found to adequately describe the curing kinetics of both reactions of the benzoxazine–epoxy resins. Consequently, a mathematical model for autocatalytic kinetics of benzoxazine–epoxy system (reaction 5.1) can be obtained.

$$\frac{d\alpha}{dt} = 14.43 \exp(81/RT)(1 - \alpha)^{1.6} \alpha^{0.9} \quad (5.6)$$

Similarly, mathematical model for autocatalytic kinetics of benzoxazine–epoxy system (reaction 5.2) is presented in Eq. (5.7).

$$\frac{d\alpha}{dt} = 21.85 \exp(118/RT)(1 - \alpha)^{1.5} \alpha^{0.7} \quad (5.7)$$

Moreover, Jubsilp et al. [45] have been investigated gelation kinetic parameter, i.e., activation energy, of benzoxazine–epoxy–phenolic resin. Gelation has been quoted by Prime that “Gelation is the incipient formation of a cross-linked network, and it is the most distinguishing characteristic of a thermoset, then, a thermoset loses its ability to flow and is no longer processable above the gel point, and therefore gelation defines the upper limit of the work life.” In addition, gel point, the transition point from a polymer solution to gel, is a function of the extent of reaction or the fraction of functional groups reacted, and gel time is the time interval from the start of a network forming process to the gel point by heating, addition of catalyst into a liquid system. Therefore, the gelation reaction can be represented by a generalized kinetic equation:

$$\ln(t_{\text{gel}}) = \ln \left(\int_0^{x_c} \frac{dx}{dt} \right) - \ln(A) + \frac{E_a}{RT} \quad (5.8)$$

where t_{gel} is the gel time, A is the preexponential factor, E_a is the activation energy, and T is temperature in Kelvin.

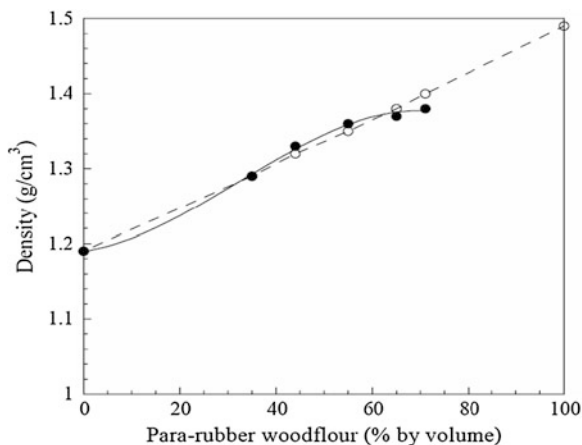
Thus, the overall activation energies for gel formation of BEP resin mixtures, determined from the temperature 130–150 °C, can be examined from the slope of the plots between $\ln(t_{\text{gel}})$ against $1/T$ as is summarized in Table 5.8. From the table, the overall activation energy values for BEP network formation ranged from 35 to 40 kJ/mol, depending on the BEP composition. The maximum of overall activation energy of the BEP541 implied the formation of the most dense gel structure of the sample BEP541. This characteristic agrees with previous work reported by Rimdusit et al. [41] that the moduli of the BEP ternary systems in the rubbery plateau increase with increasing amount of epoxy in the BEP mixtures. The greater plateau moduli of the specimens which have higher amount of epoxy diluents are attributed to higher crosslink density in the materials.

Therefore, in recent years, the effect of epoxy resin in the ternary system on mechanical, thermal performance of BEP composites filled with 70 % by weight of para-rubber woodflour which is about the maximum packing of the filler used. The observed densities of all BEP wood composites remained equal to their theoretical densities, for example, the density values of BEP811 wood composites as a function of para-rubber woodflour content are illustrated in Fig. 5.15. These highly filled composite systems can be produced due to the relatively low melt viscosity of the BEP resin systems used.

Table 5.8 Activation energy of gelation of BEP resin mixtures based on rheological data

BEP composition (weight ratios)	Activation energy (kJ/mol)
BEP 721	35
BEP 631	36
BEP 541	40

Fig. 5.15 The maximum packing density of para-rubber woodflour-filled BEP composites: (circle) Theoretical density, (filled circle) Experimental density



As we know that dynamic mechanical analysis (DMA) is a powerful technique to determine thermomechanical properties of polymer materials. DMA permits calculation of the viscoelastic properties of wood-substituted polymer composites and provides valuable insights into the relationship among structure, morphology, and properties of wood-substituted polymer composites. Figure 5.16 presents DMA that measures the mechanical properties, i.e., storage and loss modulus under flexure mode as a function temperature of BEP composites filled with 70 % by weight of para-rubber woodflour.

From the figure, we can observe an improvement in the storage modulus values of the 70 wt% para-rubber woodflour BEP composites when benzoxazine resin content increased, i.e., 7.6 GPa for BEP541, 8.3 GPa for BEP721, and 9.7 GPa for BEP811 since the effect of the more rigid molecular structure of the polybenzoxazine compared with that of the epoxy used. In addition, the reinforcing effect of para-rubber woodflour filler on the BEP alloys implying substantial interfacial bonding between the BEP matrix (dark areas) and the para-rubber (white areas) woodflour as observed SEM photograph in Fig. 5.17. The woodflour/fiber breakage was observed. The property represents one of the significant load transfers, which contribute to the high modulus values of the wood composite materials.

In addition, a clear transition is seen at temperature approximately 130, 140, and 150 °C for BEP541, BEP721, and BEP811 composites, respectively. This is glass transition, which is the major transition in the composites. Below glass-transition temperature, the storage modulus values drop as the temperature increases. In the vicinity of glass-transition temperature, a very considerable drop is observed, which indicates that the composite is going through a glass/rubber transition. It is also important to keep in mind that glass transition determined from storage modulus spectrum generally differs from what is determined from loss modulus spectrum, because they actually show two different stages in transition. In the former, the onset of the transition is observed, while in the latter, the peak point is considered.

Fig. 5.16 Storage moduli spectra of 70 wt% para-rubber woodflour-reinforced BEP composites at various epoxy contents: (filled circle) BEP811, (filled square) BEP721, (filled diamond) BEP541

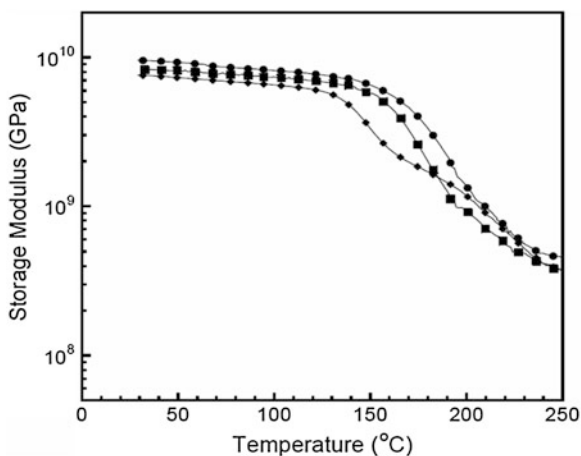
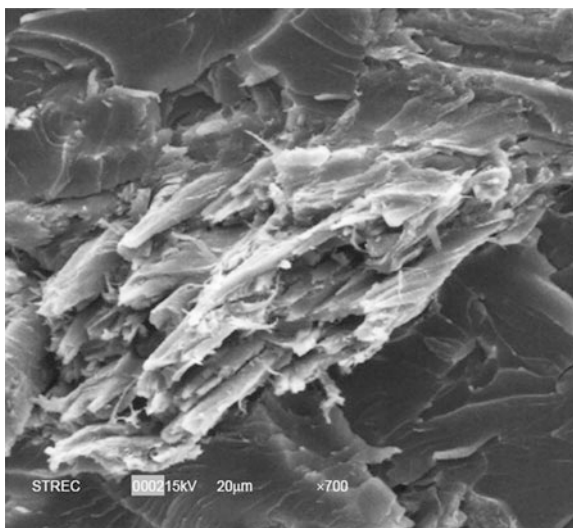
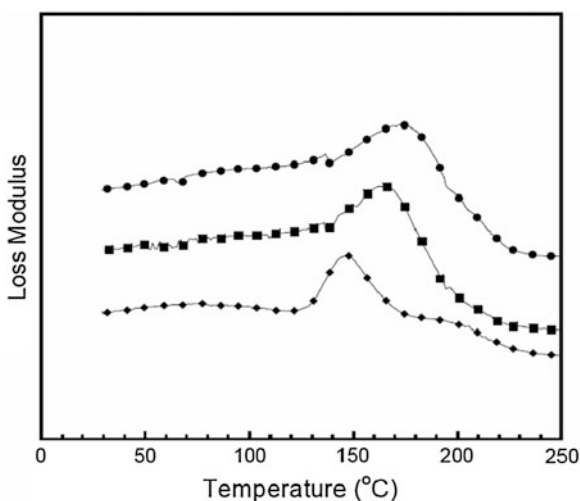


Fig. 5.17 SEM micrographs of fracture surface of BEP matrix filled with para-rubber woodflour filler



The loss moduli spectra of BEP composites filled with 70 % by weight of para-rubber woodflour were plotted in Fig. 5.18. All BEP wood composite formulations exhibited a major transition, i.e., the glass transition that is easily seen. This transition which is observed around 172, 164, and 146 °C for the wood composites based on BEP811, BEP721, and BEP541 matrices, respectively. As mentioned above, the glass-transition temperature observed in loss modulus curve was higher than what was determined from storage modulus curve. Again, glass-transition temperature was significantly shifted to higher temperatures when benzoxazine resin in BEP matrix mixtures increased. This is due to outstanding compatibility

Fig. 5.18 Loss moduli spectra of 70 wt% para-woodflour-reinforced BEP composites at various epoxy contents: (filled circle) BEP811, (filled square) BEP721, (filled diamond) BEP541



between the para-rubber woodflour and the polybenzoxazine fraction as above discussed. This makes benzoxazine alloys highly attractive as a binder or matrix for the production of high-performance wood composites with highly filled capability.

Thermal stability, degradation temperature, and char yield, through measurement using thermogravimetric analysis (TGA) at 20 °C/min under nitrogen atmosphere of 70 wt% para-rubber woodflour-reinforced BEP composites at various epoxy contents, i.e., BEP811, BEP721 and BEP541, are listed in Table 5.9. From the table, the degradation temperature at 10 % weight loss (T_{d10}) of the BEP wood composites was found to be approximately 297 °C which is lower than that of BEP matrices, i.e., ~380 °C. This is indicated that the present of the para-rubber woodflour lowered the thermal stability of the BEP matrices. However, the degradation temperature of the para-rubber woodflour increased about 22 °C in comparison to the neat para-rubber woodflour, i.e., $T_{d10} = 300$ °C [6] which might derive from the BEP matrix coating around the para-rubber woodflour. The char yield, the percent residue at 800 °C, of the BEP composites filled with para-rubber woodflour filler is also listed in Table 5.9. It can be seen in this table that the char yield of the BEP wood composites clearly increased as the benzoxazine content increased. Char yields of the BEP wood composite prepared from BEP811 was 37 % whereas that prepared from BEP541 decreased to about 32 %, as compared to that of the para-rubber woodflour having approximate value of 18 % [6].

5.5 Novel Cardanol-Benzoxazine-Based Wood Composites

In recent years, the preparation of fine chemicals from renewable materials has become a significant attention with recycling the large amount of agro-industrial wastes to produce, through environmentally sustainable processes, fine chemicals which can be used for different purposes. One of the new materials from renewable bio-sources is cardanol and its derivatives which are used to form new compound such as cashew nut shell liquid (CNSL), a versatile by-product of the cashew industry. Cardolite Coporation Inc. has reported that natural (i.e., cold, solvent extracted) CNSL contains approximately 70 % anacardic acid, 18 % cardol, and 5 % cardanol, with the remainder being made up of other phenols and less polar substances. As can be seen in Fig. 5.19, anacardic acid, cardanol, and cardol consist

Table 5.9 Thermal stability of 70 wt % para-rubber woodflour-reinforced BEP composites at various epoxy contents

BEP composition (weight ratios)	T_{d10} (°C)	Char yield (%)
BEP 811	296 (376) ^a	37 (33) ^b
BEP 721	297 (379)	35 (33)
BEP 541	297 (383)	32 (30)

Note ^a, ^b T_{d10} and char yield at 800 °C of BEP matrix

of mixtures of components having various degrees of unsaturation in the alkyl side chain. In technical (i.e., heat extracted) CNSL, the heating process leads to decarboxylation of the anacardic acid to form cardanol. Typically, the composition of technical CNSL is approximately 52 % cardanol, 10 % cardol, 30 % polymeric material, with the remainder being made up of other substances. However, each component of CNSL depends on the purification–distillation. Commercially, cardanol is the main component approximately 84 % of CNSL and is itself a mixture of 3-*n*-pentadecylphenol, 3-(*n*-pentadeca-8-enyl)phenol, 3-(pentadeca-8,11-dienyl)phenol, and 3-(pentadeca-8,11,14-trienyl)phenol [46].

Recently, Kasemsiri et al. [47] have been investigated properties of experimentally manufactured wood polymer composites based on bisphenol-A/aniline-type benzoxazine (BA-a)-CNSL copolymer and eastern redcedar woodflour which also provided an economic incentive to convert a costly land management problem into the value-added products of wood composite panels. The author found that an eastern redcedar woodflour (WF)/BA-a/CNSL compound shows the lower curing temperature than that of BA-a/CNSL matrix. Moreover, eastern redcedar woodflour content also results in curing temperature that decreased with increasing eastern redcedar woodflour content as shown in Table 5.10.

This is due to anacardic acid in CNSL might act as a curing accelerator, which caused a shift of the exotherm of the ring-opening reaction of the benzoxazine resin to lower temperature. The possible reaction between polybenzoxazine and CNSL is shown in Fig. 5.20.

Furthermore, from the table, the activation energies of curing reaction of BA-a/CNSL filled with eastern redcedar woodflour was reported to be 72–77 kJ/min which are lower than that of benzoxazine resin, i.e., around 84–87 kJ/mol. This observation is good evidence that eastern redcedar particles not only decreased curing temperatures but also reduced the activation energy of the benzoxazine matrices. This would be possibly due to the catalytic effect of eastern redcedar woodflours as mentioned above. The decrease in curing temperature and activation energy of wood composites has a positive effect on the wood composite

Fig. 5.19 Constituents of cashew nut shell liquid

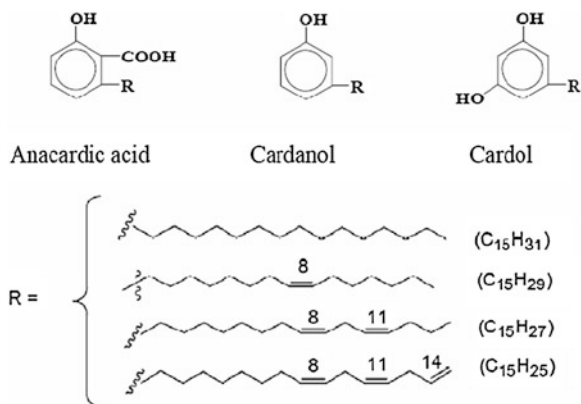
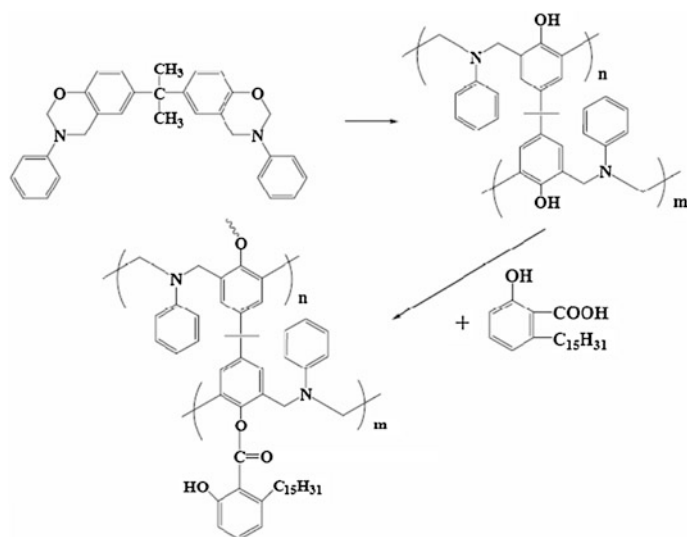


Table 5.10 Curing behavior of benzoxazine–CNSL filled with eastern redcedar woodflour composites

Sample	Curing temperature T_{cure} ($^{\circ}\text{C}$)	Activation energy (kJ/min)
BA-a	225	84 [41]
BA-a/CNSL (85/15)	214	–
BA-a/75 wt % WF	–	77
BA-a/CNSL (85/15) with 50 wt% WF	211	–
BA-a/CNSL (85/15) with 70 wt% WF	203	–
BA-a/CNSL (85/15) with 75 wt% WF	200	72

**Fig. 5.20** A possible reaction between polybenzoxazine and cashew nut shell liquid [47]

manufacturing, i.e., a relatively lower manufacturing temperature or lower energy consumption can be used.

The thermal and mechanical properties of the obtained wood composites based on benzoxazine–CNSL were also studied as listed in Table 5.11.

The dynamic mechanical characteristics of BA-a/CNSL matrix and their composites are related to the properties of the components, the morphology of the materials, and the nature of the interfacial adhesion between the wood filler and polymer matrix. From the table, the storage modulus (E') of the BA-a/CNSL wood composites is higher than that of neat BA-a/CNSL matrix, while Young's modulus under static flexure mode of those materials, which is calculated from the slope of the initial part of a stress–strain curve, is similar conceptually to the storage modulus, shows the similar trend to storage modulus values. Furthermore, the BA-

Table 5.11 Thermal and mechanical properties of benzoxazine–CNSL filled with eastern redcedar woodflour composite

WF content (wt %) in BA-a/CNSL (85/15)	E' (GPa)	E_f (GPa)	σ_f (MPa)	T_g from E'' ($^{\circ}$ C)
0	3.24	4.27	62	147
50	4.25	5.80	34	162
70	4.42	6.83	44	180
75	4.48	7.09	47	188

a/CNSL exhibits more thermal stability than the neat BA-a/CNSL matrix as the T_g of the BA-a/CNSL wood composites is higher than that of the neat BA-a/CNSL matrix. This behavior can be attributed to the effect of restriction of segmental motion of matrix possibly due to the substantial interfacial bonding from the presence of the phenolic structure in lignin fraction of eastern redcedar particles and the abundance of hydroxyl moieties in the filler.

Furthermore, as aforementioned, water seems to be an environmental factor that affects practically all materials exposed to exterior conditions. It is expected that water may also affect performance and properties of wood-substituted polymer composites including mechanical properties, dimensional stability, warping, and intensification of biological activity. As listed in Table 5.12, it was observed that water absorption of the polybenzoxazine–CNSL filled with eastern redcedar woodflour composites increases with the increasing of eastern redcedar woodflour content. This behavior was expected since the water absorption of these composites is mainly due to the presence of woodflour that contains numerous hydroxyl groups (–OH), which are available for interaction with water molecules by hydrogen bonding. However, wood interacts with water not only on the surface, but also in the bulk. Generally, there are three main regions in the composite where the adsorbed water can reside: the lumen, the cell wall, and the gaps between woodflour and polymer matrix in the case of weak interface adhesion are found. However, for these composites, the found low water absorption values compared with moisture absorption at 24 h of two commercial wood polymer composites decking products, i.e., Trex[®] (12 %) and Strandex[®] (6 %). This indicates that the eastern redcedar woodflour was satisfactorily encapsulated in the BA-a/CNSL matrix, suggesting that no significant change occurs in the microstructure of the composites as the authors have been reported that the absorption of water in the

Table 5.12 Water absorption and surface roughness of benzoxazine–CNSL filled with eastern redcedar woodflour composites

WF content (wt %) in BA-a/CNSL (85/15)	Water absorption at 24 h (%)	Average roughness, R_a (μ m)
0	0.11 [48]	–
50	1.3	4.21
70	5.0	4.00
75	5.2	2.32

eastern redcedar woodflours-filled BA-a/CNSL approached toward the Fickian diffusion case, as the value of n constant values ranges from 0.46 to 0.55.

Moreover, the degree of surface roughness of the eastern redcedar woodflour-filled polybenzoxazine/CNSL composites plays an important role since any surface irregularities will affect the final quality of the product. Typically, surface roughness is a function of raw material characteristics, species, particle size and distribution and manufacturing variables, press parameters, resin content, face layer densification, and sanding process of the panels. In addition, differences in the average surface roughness of the produced wood polymer composite materials were most likely due to the amount of the wood filler. In this work, the surface roughness measurement using stylus technique (a fine stylus profilometer Hommel T-500 unit equipped with a TK-300 skidless-type pick-up) based on average roughness (R_a) was considered to evaluate the surface characteristics of the eastern red cedar woodflour-filled polybenzoxazine/CNSL composites. From the Table 5.12, the average roughness was found for the polybenzoxazine/CNSL wood composites having a R_a in the range of 2.32–4.21 μm which are lower than that of polypropylene reinforced with woodflour at 50 and 70 % by weight, i.e., 3.6 and 6.8 μm , respectively [49].

5.6 Conclusions

Polybenzoxazine and its alloy were found to be high-performance wood composite binders with high mechanical properties and reduced water uptake that may be summarized as follows:

The mechanical properties of the para-rubber woodflour-filled polybenzoxazine composites from DMA and flexural test at para-rubber woodflour content below the optimum filler packing, i.e., 75 % by weight, show approximately linear relationship with filler loading. The outstanding compatibility between the woodflour and the polybenzoxazine matrix is evidently seen from the large improvement in the composite's T_g and char yield. Water absorption of the composites is greatly reduced with increasing the amount of polybenzoxazine due to the inherent low water absorption of the matrix.

Polymer alloys of benzoxazine resin and phenolic novolac resin were found to be the binders of the highly filled wood composite systems. The addition of phenolic novolac resin in the benzoxazine resin effectively reduced the curing temperature of the alloys whereas the benzoxazine resin helped improve the mechanical and thermal integrity of the alloy matrices. These useful properties of the alloys were obtained when the amount of the phenolic novolac was maintained at <20 % by weight. The benzoxazine/phenolic mixture at weight ratios 80:20 was evaluated to provide optimal performance among the others. High woodflour content at 70 wt% can be incorporated into the alloy to yield good processing ability and high-performance wood composite systems with relatively high flame-retardant characteristics.

High-performance wood composites from highly filled ternary systems of benzoxazine (B), epoxy (E), and phenolic (P) resins, i.e., BEP resins, were achieved. The woodflour content of 70 % by weight can be incorporated into the ternary systems due to the relatively low melt viscosity of the ternary mixtures. The experimental results indicated that the increasing amount of epoxy fraction in the ternary systems enhanced the alloys' flexural strength and toughness. The resulting BEP wood composites showed relatively high flexural modulus value up to 8.3 GPa and flexural strength up to 70 MPa in BEP811-filled system. The increase in polybenzoxazine fraction in the BEP ternary systems was found to effectively enhance the mechanical and thermal characteristics such as the flexural modulus and the glass-transition temperature of the resulting wood composites.

Interestingly, benzoxazine resin alloyed with CNSL was observed to be a good binder for natural fiber. The addition of CNSL and eastern redcedar particles effectively reduced the curing temperature and activation energy of benzoxazine resin. The effects of the eastern redcedar particles content on the thermal and mechanical increased with optimum amount of the eastern redcedar filler to benzoxazine–CNSL matrix at 75:25 by weight that attributed to good compatibility between the filler and the matrix. The wood composites at various contents of particles also showed relatively low percentages of water absorption. The obtained wood composites based on eastern redcedar particles also provided an economic incentive to convert a costly land management problem into the value-added products of wood composite panels.

References

1. Deka M, Saikia CN (2000) Chemical modification of wood with thermosetting resin: effect on dimensional stability and strength property. *Bioresour Technol* 43:179–181
2. Chen X, Gu Q, Mi Y (1998) Bamboo fiber-reinforced polypropylene composites: a study of the mechanical properties. *J Appl Polym Sci* 69:1891–1899
3. Smith PM, Wolcott MP (2005) Woodfiber-plastic composite markets and applications. In: 39th international wood composites symposium and technical workshop, Washington State University, Pullman, Washington USA
4. Johnson DA, Urich JL, Krainbill M (1999) Overview of new industrial market for agricultural materials-wheat straw plastics. In: *Proceedings of the 1999 Ag Fiber. Technology Showcase*. Ag Fiber Communications, TN
5. Brooks D, Wahl A (2008) Modified wood and wood-plastic composites are substituting for traditional wood products. In: Wahl A (ed) *Wood market trends in Europe, FPInnovations™*, Canada, pp 24–28
6. Rimdusit S, Tanthapanichakoon W, Jubsilp C (2006) High performance wood composites form highly filled polybenzoxazine. *J Appl Polym Sci* 99:1240–1253
7. Saheb DN, Jog JP (1999) Natural fiber polymer composites: a review. *Adv Polym Technol* 8:351–363
8. Ishida H, Agag T (2011) *Handbook of benzoxazine resins*. Elsevier, New York
9. Ishida H (1996) U.S. Pat. 5,543,516
10. Ministry of Commerce and Industry: Government of India (2003) Available at: <http://rubberboard.org.in/RubberWood.asp>. Accessed 1 March 2013

11. Woodhams RT, Thomas G, Rogers DK (1984) Wood fibers as reinforcing fillers for polyolefins. *Polym Eng Sci* 24:1166–1171
12. Pérez E, Famá L, Pardo SG, Abad MJ, Bernal C (2012) Tensile and fracture behaviour of PP/wood flour composites. *Compos Part B Eng* 43:2795–2800
13. Shori A, Nourbakhsh A (2011) Preparation and characterization of polypropylene/wood flour/nanoclay composites. *Eur J Wood Wood Prod* 69:663–666
14. Youngquist JA (1999) Wood-based composites and panel products, In: *Wood Handbook*, U.S. Department of Agriculture, Government Printing Office, Madison, WI, Chapter 10
15. Stark NM, Rowlands RE (2003) Effects of wood fiber characteristics on mechanical properties of wood polypropylene composites. *Wood Fiber Sci* 35:167–174
16. Simonsen J, Jacobsen R, Rowell R (1998) Wood-fiber reinforcement of styrene-maleic anhydride copolymers. *J Appl Polym Sci* 68:1567–1573
17. Mishra S, Naik JB (1998) Absorption of steam and water at ambient temperature in wood polymer composites prepared from agro-waste and novolac. *J Appl Polym Sci* 68:1417–1421
18. Li Q, Matuana LM (2003) Study of the surface of cellulosic materials modified with functionalized polyethylene coupling agents. *J Appl Polym Sci* 88:278–286
19. Hon DNS, Xing LM (1992) Viscoelasticity of biomaterials. ACS symposium series 489. American Chemical Society, Washington, D.C
20. Wang W, Sain M, Cooper PA (2006) Study of moisture absorption in natural fiber plastic composites. *Compos Sci Technol* 66:379–386
21. Sarkar S, Adhikare B (2001) Jute felt composite from lignin modified phenolic resin. *Polym Compos* 22:518–527
22. White RH, Dietenberger MA (1999) Fire safety. In: *Encyclopedia of wood*, U.S. Department of Agriculture, US
23. Quarles SL (2013) Fire ratings for construction materials. Senior Scientist, Insurance Institute for Business and Home Safety, Richburg, SC
24. Harper CA (2004) *Handbook of building materials for fire protection*. McGraw-Hill, New York
25. Lyons JW (1991) Flame retardants. In *Encyclopedia of chemical technology*. 10:348
26. Chetanachan W, Sookkho D, Sutthitavil W, Chantasatramamy N, Sinsermsuksakul R (2001) PVC wood: a new look in construction. *J Vinyl Additive Technol* 7:134–137
27. Farid SI, Kortschot MT, Spelt JK (2002) Wood-flour-reinforced polyethylene: viscoelastic behavior and threaded fasteners. *Polym Eng Sci* 42:2336–2350
28. Ayrlimis N, Kwon JH, Han TH (2012) Effect of resin type and content on properties of composite particleboard made of a mixture of wood and rice husk. *Int J Adhes Adhes* 38:79–83
29. Rimdusit S, Kampangsaeree N, Tanthapanichkoon W, Takeichi T (2007) Development of wood-substituted composites from highly filled polybenzoxazine–phenolic novolac alloys. *Polym Eng Sci* 47:140–149
30. Rimdusit S, Ishida H (2000) Development of new class of electronic packaging materials based on ternary systems of benzoxazine, epoxy, and phenolic resins. *Polymer* 41:7941–7949
31. McCrum NG, Buckley CP, Bucknall CB (1997) *Principles of polymer engineering*, 2nd edn. Oxford University Press, USA
32. Mouritz AP, Gibson AG (2006) *Fire properties of polymer composites materials*. Springer, Berlin, pp 4–5
33. Chang CL, Ma CCM, Wu DL, Kuan HC (2003) Preparation, characterization, and properties of novolac-type phenolic/SiO₂ hybrid organic–inorganic nanocomposite materials by sol–gel method. *J Appl Polym Sci* 41:905–913
34. Chiang CL, Ma CCM (2002) Synthesis, characterization and thermal properties of novel epoxy containing silicon and phosphorus nanocomposites by sol–gel method. *Eur Polym J* 38:2219–2224
35. Liu J, Gao Y, Wang F, Wu M (2000) Preparation and characteristics of nonflammable polyimide materials. *J Appl Polym Sci* 75:384–389

36. Karain HG (2003) Handbook of polypropylene and polypropylene composites, 2nd edn. Taylor & Francis, New York, p 87
37. Sain M, Park SH, Suhara F, Law S (2004) Flame retardant and mechanical properties of natural fibre-PP composites containing magnesium hydroxide. *Polym Degrad Stabil* 83:363-367
38. Lee SM (1990) International encyclopedia of composites, 2nd edn. VCH Publishers, New York
39. Ishida H, Allen DJ (1996) Mechanical characterization of copolymers based on benzoxazine and epoxy. *Polymer* 37:4487-4495
40. Jubsilp C, Punson K, Takeichi T, Rimdusit S (2010) Curing kinetics of benzoxazine-epoxy copolymer investigated by non-isothermal differential scanning calorimetry. *Polym Degrad Stabil* 95:918-924
41. Ishida H, Rimdusit S (2000) Synergism and multiple mechanical relaxations observed in ternary systems based on benzoxazine, epoxy, and phenolic resins. *J Polym Sci Polym Phys* 38:1687-1698
42. Jubsilp C, Damrongsakkul S, Takeichi T, Rimdusit S (2006) Curing kinetics of arylamine-based polyfunctional benzoxazine resins by dynamic differential scanning calorimetry. *Thermochim Acta* 447:131-140
43. Hsieh TH, Su AC (1990) Cure kinetics of an epoxy-novolac molding compound. *J Appl Polym Sci* 41:1271-1289
44. Kim WG, Lee JY, Park KY (1993) Curing reaction of *o*-cresol novolac epoxy resin according to hardener change. *J Polym Sci Polym Chem* 31:633-639
45. Jubsilp C, Takeichi T, Hiziroglu S, Rimdusit S (2008) High performance wood composites based on benzoxazine-epoxy alloys. *Bioresource Technol* 99:8880-8886
46. Vasapollo G, Mele G, Sole RD (2011) Cardanol-based materials as natural precursors for olefin metathesis. *Molecules* 16:6871-6882
47. Kasemsiri P, Hiziroglu S, Rimdusit S (2011) Properties of wood polymer composites from eastern redcedar particles reinforced with benzoxazine resin/cashew nut shell liquid copolymer. *Compos A* 42:1454-1462
48. Kasemsiri P, Hiziroglu S, Rimdusit S (2011) Effect of cashew nut shell liquid on gelation, cure kinetics, and thermomechanical properties of benzoxazine resin. *Thermochim Acta* 520:84-92
49. Ayrilmis N (2011) Effect of fire retardants on surface roughness and wettability of wood plastic composite panels. *BioResource* 6:3178-3187

Chapter 6

Polybenzoxazine Composites for Ballistic Impact Applications

Abstract This chapter discusses the utilization of polybenzoxazine/urethane alloys with fine-tuning properties for ballistic impact composite application. The ballistic impact study of KevlarTM fiber-reinforced polybenzoxazine alloys under the test weapon with standard 124 grains round lead projectile and a copper outer coating (Full Metal Jacket) typically used in the 9-mm handgun at an impact velocity of 426–431 m/s is reported. The polybenzoxazine/urethane alloy matrices at various urethane prepolymer contents were prepared to evaluate the effect of different urethane contents on the thermal, mechanical as well as ballistic resistant properties. Experimental results reveal a synergy in glass transition temperature and some mechanical properties of the alloys at the composition range of 10–30 % by weight of urethane fraction the thus provide a fascinating group of high temperature polymers with improved flexibility and enhanced a ballistic resistant characteristic.

Keywords Polybenzoxazine · Urethane · Ballistic properties · KevlarTM fiber · NIJ standard

6.1 Introduction

The development of composite technology represents one of the most significant advances in material science since the 1940s. In the United States, the current market status for advanced protective gear and armor, including data from 2004, estimates for 2015 an examination of personal protective industry regulations and standards technological issues crucial to the industry to climb more than 20 % over the period 2010–2015, reaching as much as \$3 billion by 2015 [1]. Fiber-reinforced composites are made from high-strength fibers embedded in metallic, ceramic, or polymeric matrices. Especially, polymeric matrices have been the most widely used for composites reinforced by synthetic fibers. In recent years, composites based on

polymer matrix are increasingly being used in the armor structure due to high strength and stiffness to weight ratios that results in polymer matrix composites having quite popular as lightweight armor when compared with armor made from hard and rigid materials such as bronze, brass, and steel. Furthermore, the hard and rigid materials alone cannot provide effective energy dissipation such as material deformation and breakage although they have the ability to resist penetration. Therefore, the invention of synthetic fiber is the great improvement in armor design which can improve the weight, flexibility, and breathe characteristics [2].

There are two types of armor that are prepared from woven fabrics. They are the soft body armor and the soft armor structure. Soft body armor is used as the protective garment for military and law enforcement personnel against ballistic injuries. There are presently two types of ballistic threats: the penetration of handgun bullets and the piercing of fragmented shells. The soft body armor is prepared in the form of a vest to protect the torso of a human body. Another type of armor is composite armor systems, i.e., nonstructural and structural composite armors. In case of nonstructure, composite armor is often regarded as a parasitic armor element because it is added to an existing structure to provide ballistic protection. The existing structure may be a car, truck, ship, engine case, or shelter. The latter type is structural armors or load-bearing, providing ballistic resistance. They are used on armored vehicles, military vessels and vehicles, shelters, shields, etc. They are prepared from multiple layers of fabrics combined with a resin binder. The resin content is carefully controlled to achieve a balance of structural and ballistic properties.

In recent years, the high strength of fibers has been developed rapidly for armor structure. Fibers conventionally used include aramids (KevlarTM or TwaronTM), high-performance polyethylene (HPPE) fibers, i.e., SpectraTM or DyneemaTM, nylon fiber, glass fiber, PBO (Zylon), and the like [3] which are listed in Table 6.1. The selection of fibers for application depends heavily on its mechanical property, and such a fiber should possess a high tensile and compressive modulus, high tensile and compressive strength, high damage tolerance, low specific weight, good adhesion to matrix materials (for structural composites), and a good temperature resistance. Moreover, another factors must be considered, i.e., sonic velocity and energy absorption of the specimens. Fibers provide excellent impact resistance in that the fibers have high sonic velocity (V_s) and high specific energy absorption (E_{sp}) because of its distribution of kinetic energy upon ballistic impact. Both of them depend on some physical parameters with the relationship shown in Eqs. (6.1) and (6.2).

$$E_{sp} = \frac{1}{2} \left[\frac{\sigma_{rupt} \times \epsilon_{rupt}}{\rho} \right] \quad (6.1)$$

$$V_s = \sqrt{\frac{E}{\rho}} \quad (6.2)$$

Table 6.1 Comparison of industrial filament yarns

Fiber	E_t (GPa)	σ_t (GPa)	E_b (%)	ρ (g/cm ³)	Moisture regain (%)	LOI	Heat resistance (°C)
Aramid	60–115	2.8–3.2	1.5–4.5	1.38–1.45	4.5	29	400–550
HS-PE	90–140	2.8–4.0	2.9–3.8	0.97	0	16.5	150
Polyester	13.8–15	1.12	14.5–25	1.38	0.4	17	260
PBI	5.6	–	30	1.40	15	41	550
PBO	280	5.5	2.5	–	–	–	–
Nylon	5.5	1.0	18.3	1.14	–	–	–
S-Glass	85–87	4.65	5.3	2.48	0.1	100	300
E-Glass	69	2.41	3.5	2.55	–	–	–
Steel	200	1.72	1.4–2.0	7.8–7.86	0	–	–

Note HS-PE is high-strength polyethylene, PBI is polybenzimidazole, and PBO (Zylon) is poly (p-phenylenebenzobisoxazole)

where σ_{rupt} , ϵ_{rupt} , ρ , and E are fiber stress at rupture, elongation at rupture, its density, and fiber's elastic modulus, respectively.

For the complete understanding of ballistic impact of composites, different damage and energy absorption mechanisms should be understood. The possible energy absorption mechanisms of a composite are deformation of primary and secondary yarns, delamination, and matrix deformation as shown in Fig. 6.1. For the different composite systems, the different mechanisms can be dominant. In addition, properties of polymer matrix and reinforced fiber also affect the energy absorption mechanisms of the composite. In composite fabrication, the addition of matrix resin to a woven fabric provides the composite to be strong enough to serve in normal applications, whereas the longitudinal wave velocity of the composite with a resin matrix is slowed by its rigid crossover points. At these points, the longitudinal wave velocity will be extensively reflected, which results in a high strain gradient in the reinforced fiber and restricts transverse deflections of the composite. However, the bonded layers permit load transfer to secondary yarns through the continuum of a matrix and allow impact energy propagates in the thickness direction and spreads over a large area on back layers of the composite. This is an important mechanism for an armor design to stop very high velocity projectile. In order to minimize the effect of the rigid crossover points, which inhibits longitudinal wave propagation, some delamination between fiber and resin should be achieved. Moreover, some flexibility in transverse deflection of the composite is also necessary to get the maximum efficiency in armor applications.

Jacobs and Dingenen [3] suggested high-performance fibers used in ballistic products as being characterized by their low density, high strength, high energy absorption, and high sonic velocity because of its distribution of kinetic energy upon ballistic impact. In ballistic products, the major fibers used include glass fibers, aramid (KevlarTM), high-performance polyethylene (UHMPE) fibers. The relationship between specific energy absorption and sonic velocity of each fiber

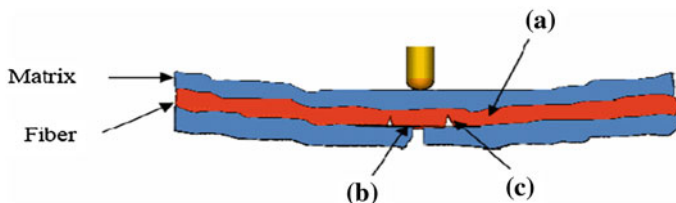


Fig. 6.1 Three principal damage mechanisms for low-velocity impact **a** matrix deformation, **b** delamination (macroscopic)/depending (microscopic), **c** fiber failure

has been presented in Fig. 6.2, and the types of fiber used as reinforcing materials for ballistic resistance have been summarized in Table 6.2.

In addition, from the Table 6.2, the types of binders such as thermoplastic polymers, thermosetting resins, and alloys between thermoplastics and thermosets have been used as matrices for ballistic resistance. The resin function is to hold the fibers firmly in a three-dimensional array of crossing layers. The selection of a resin for the ballistic composite depends on its required characteristics. Some important factors should be considered including rigidity, environmental resistance, thermal stability, wear resistance, combustibility, processing ability, and shelf-life. The resin content is generally carefully controlled to achieve a balance of structure and ballistic properties. The amount of resin necessary to consolidate the fibers comprises 75–80 % by weight having been reported [5]. If the amount of resin substantially increases above the desired amount, the matrix will become a major part of the armor volume weakening the materials. However, if the resin is substantially less than that required to wet all fibers, this will result in the composite material wherein the fibers are not properly consolidated and held in the proper position so that upon impact, the fiber tends to separate relatively easily, allowing the projectile to pass through before the fiber absorbs impact forces [6].

Fig. 6.2 Primary ballistic figures of merit for various fibers (Modified from [3])

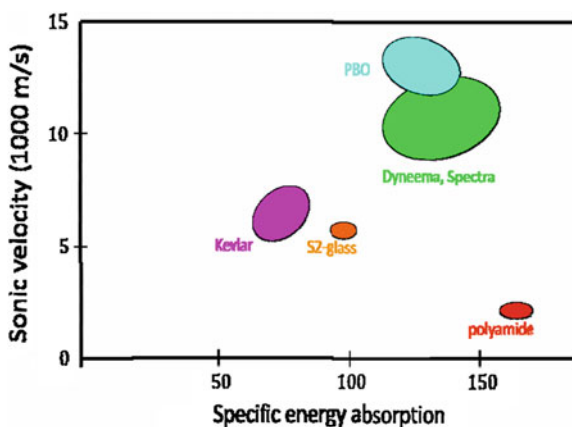


Table 6.2 Review on US patents of polymer composite ballistic armor [4]

Fiber	Matrix	Matrix properties	Reference	
1. Spectra™	Thermosetting	<ul style="list-style-type: none"> Elastomer Modulus 500,000 psi Strength 3,000 psi at high temperature Below the melting point of fiber 	Patent no. 4,748,064 Date: May 31, 1988	
			Patent no. 4,403,102 Date: Sep 6, 1983	
	Thermoplastic elastomer	<ul style="list-style-type: none"> Areal density 4.5 oz/yd. 	Patent no. 5,724,670 Date: Mar 10, 1998	
			Patent no. 5,534,343 Date: Jul 9, 1996	
	Urethanes	<ul style="list-style-type: none"> Low modulus Below the melting point of fiber 	Patent no. 4,403,102 Date: Sep 6, 1983	
			Patent no. 5,480,706 Date: Jan 2, 1996	
	Styrene-isoprene-styrene (SIS) dissolved in methylene chloride	<ul style="list-style-type: none"> $T_g = -55^\circ\text{C}$ Melt index = 9 g/min using Modulus 100 psi at 300 % elongation 	Patent no. 5,093,158 Date: Mar 3, 1992	
			Patent no. 4,748,064 Date: May 31, 1988	
	2. Kevlar™	Thermosetting	<ul style="list-style-type: none"> Impact strength 17 J/m, 32 mm thick $T_g = 170^\circ\text{C}$ 	Patent no. 5,190,802 Date: Mar 2, 1993
				Patent no. 4,748,064 Date: May 31, 1988
Phenolic resin		<ul style="list-style-type: none"> Below the melting point of fiber 	Patent no. 4,639,387 Date: Jan 27, 1987	
	Patent No. 4,550,044 Date: Oct 29, 1985			
Polyester	<ul style="list-style-type: none"> Modulus 500,000 psi Strength 3,000 psi at high temperature 	Patent no. 5,102,723 Date: Apr 7, 1992		
		Patent no. 3,956,447 Date: May 11, 1976		
Epoxy	<ul style="list-style-type: none"> Strength 3,000 psi at high temperature 	Patent no. 3,956,447 Date: May 11, 1976		
		Patent no. 3,956,447 Date: May 11, 1976		

(continued)

Table 6.2 (continued)

Fiber	Matrix	Matrix properties	Reference
3. Glass fiber	Thermosetting <ul style="list-style-type: none"> • Phenolic • Polyester 	Moldable MW. range 800–5,000 or more	Patent no. 5,215,813 Date: Jan 1, 1993 Patent no. 4,639,387 Date: Jan 27, 1987 Patent no. 4,550,044 Date: Oct 29, 1985
4. Mixed fibers <ul style="list-style-type: none"> • Aramid and carbon • Aramid and glass • Carbon and glass • Carbon, glass, and spectra 	Thermoplastic <ul style="list-style-type: none"> • Urethane • Styrene-isoprene-styrene (SIS) • Ethylene-acrylate, methacrylate copolymer, vinyl ester phenolic polyimide, polycarbonate or the like 	<ul style="list-style-type: none"> • Flexibility • Resistance to degradation • $T_g = -55^\circ\text{C}$ • Melt index = 9 g/min using • Modulus 100 psi at 300 % elongation • High modulus • Higher in impact resistance 	Patent no. 4,639,387 Date: Jan 27, 1987 Patent no. 4,822,439 Date: Apr 18, 1989 Patent no. 4,732,803 Date: Mar 22, 1988

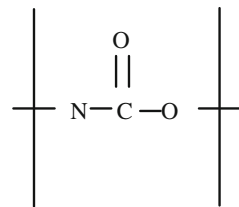
In general, the resins used as a binder in ballistic armor have an adhesive characteristic with respect to the fiber but with the tensile strength less than that of the fiber. That is, upon impact, the fiber will function predominantly to transmit impact force along its longitudinal axis. In principle, it is required that the resin should not hold the fiber much rigidly along the surface but allow some small amount of movement of the fiber surface longitudinally within the resin. Obviously, the composite structure resists and provides a limited fiber, spreading transversely to the fiber axis upon projectile impact. Phenolic resins provide one future class of resins suitable for a matrix of a composite armor. Phenolic resins are inexpensive, can be handled using conventional processing technology, and do not bond too firmly to ballistic fibers, especially KevlarTM. However, phenolics do require that moisture be driven from the resins during a curing stage which is one additional step in the composite fabrication process. Other binders which have been reported to be used for KevlarTM-reinforced composites consisted of epoxy resin, styrene–isoprene–styrene, and phenolic polymer alloys with poly(vinyl butyl ether), etc. [7–9].

Nowadays, polybenzoxazine alloys as a ballistic composite have been reported [10]. The property balance of the material renders the polybenzoxazine with good thermal, chemical, electrical, mechanical, and physical properties including very low A-stage viscosity, near-zero shrinkage, low water absorption, high thermal stability, good fire-resistant characteristics, and fast development of mechanical properties as a function of curing conversion [11]. Interestingly, enhancement in thermal and mechanical properties was observed in polybenzoxazine alloy systems, i.e., polymer alloys of BA-a/PU [12, 13]. This makes polybenzoxazine possible to fine-tune and enhance the properties of the ballistic armor composites.

6.2 Polybenzoxazine/Urethane Polymer Alloys

Urethane prepolymer is class of polymer which contains urethane group. The urethane functional group is formed by the chemical reaction between an alcohol and an isocyanate as shown in Fig. 6.3. The polymer is resulted from a reaction between alcohols having two or more reactive hydroxyl groups per molecule (diol or polyols) and isocyanates that have more than one reactive isocyanate group per molecule (a diisocyanate or polyisocyanate). Thus, diisocyanates and diols (and

Fig. 6.3 Urethane linkage



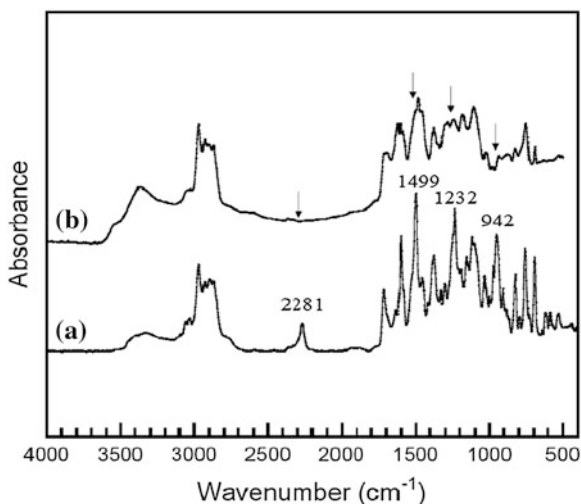
polyols) are the principal raw materials used in the manufacturing of polyurethanes.

The functionality of the hydroxyl-containing reactant or the isocyanate can be varied; therefore, a wide variety of linear, branched, and crosslinked structures can be formed. The hydroxyl-containing components cover a wide range of molecular weights and types, including polyester and polyether polyols. The polyfunctional isocyanates can be aromatic aliphatic, cycloaliphatic, or polycyclic in structure and can be used directly as produced or modified. This flexibility in the selection of urethane reactants leads to the wide range of the resulting properties. The excellent properties of polyurethane account for the facts that their use is economically feasible and that their range of applications is steadily increasing. In some instance, they are even irreplaceable. Among these properties are unique combination of a high elastic modulus, good flexibility, exceptional tear and abrasion resistance, resistance to mineral oils and lubricants, resistance to UV radiation, and finally providing fairly easy and efficient processing [14].

In 2005, Rimdusit et al. [12] have investigated an improvement in toughness of rigid polybenzoxazine by alloying with isophorone diisocyanate-/polyether polyol (IPDI)-based urethane prepolymers (PU) with molecular weight of 2,000. The authors have reported that the toughness of alloys of bisphenol-A-/aniline-based polybenzoxazine (PBA-a) and the PU systematically increases with the amount of PU tougheners due to the addition of more flexible molecular segments in the polymer alloys. Interestingly, glass transition temperature (T_g) curve of BA-a/PU polymer alloys was found to be higher than that of the parent resins, i.e., 165 °C for PBA-a [10, 11] and -70 °C for PU [13], while T_g from $\tan\delta$ of the BA-a/PU polymer alloys at 90/10 and 70/30 mass ratio was found to be 200 and 275 °C, respectively. The authors reported great enhancement in the flexibility and thermal properties of BA-a/PU polymer alloys since the reaction formation between the isocyanate group (NCO) of the urethane prepolymer and the phenolic hydroxyl group of polybenzoxazine which is observed in FTIR spectrum in Fig. 6.4. This reaction formation resulted in greater crosslinked structure as observed in FTIR technique. Figure 6.4a reveals the spectrum of the BA/PU prepolymer at a mass ratio of 70/30, which presented the mixed fingerprints of both the benzoxazine resin and the urethane prepolymer, i.e., peaks at 942 cm^{-1} (C–O–C stretching mode of benzoxazine ring), 1,232 cm^{-1} , 1,499 cm^{-1} (tri-substituted benzene ring in BA-a) from the benzoxazine resin and that of 2,281 cm^{-1} (NCO group). After being fully cured, the oxazine ring is known to be opened by the breakage of a C–O bond of the monomer, which further reacted with the NCO group of the PU. The mechanism was previously proposed by Takeichi et al. [15]. Figure 6.4b also exhibits the spectrum of BA-a/PU polymer alloys, indicating the absorbances at 1,232 cm^{-1} (C–O–C stretching mode in benzoxazine ring), 1,499 and 942 cm^{-1} (tri-substituted benzene ring in BA-a), and 2,281 cm^{-1} (NCO group) disappeared.

Therefore, from FTIR experimental, the model reaction showed that polybenzoxazines obtained by thermal ring-opening polymerization of their precursors contain phenolic hydroxyl group, which reacted further with NCO groups of urethane prepolymer as presented in Fig. 6.5.

Fig. 6.4 IR spectra of the compounds: **a** mixture of BA-a and PU and **b** BA-a/PU alloy



Moreover, an incorporation of PU into polybenzoxazine can enhance thermal stability of all BA-a/PU polymer alloys. The decomposition temperature at 5 % weight loss for these alloy systems was approximately 340 °C, while that for the PBA-a was 330 °C. As a result, the crosslinked density was improved, which marginally stabilizes against the thermal degradation of the polybenzoxazine. In addition, thermomechanical property via the linear coefficient of thermal expansion (CTE) of the BA-a/PU polymer alloys has also been reported by Rimdusit et al. [13]. As we know that, the CTE is the tendency of the material expansion in response to a change in temperature. In general, when a material is heated, its particles begin moving and become active, thus maintaining a greater average separation. Materials that contract with increasing temperature are rare; this effect is limited in size and only occurs within limited temperature ranges. The material's CTE is calculated from the degree of expansion divided by the change in temperature as shown in Eq. (6.3), and generally, the CTE varies with temperature.

$$\alpha = \frac{dl}{l \times dT} \quad (6.3)$$

where dl is the change in length of material in the direction being measured, l is overall length of material in the direction being measured, and dT is the change in temperature over which dl is measured.

In the BA-a/PU polymer alloys, the synergistic behavior in linear CTE of these polymer alloys was observed in the vicinity of 10–20 % by weight as reported in Table 6.3. The linear CTE values decrease with increasing levels of overall crosslink density. This characteristic is due to increasing numbers of covalent crosslinks in the polymer alloy network that serves to inhibit expansion in response to temperature increases, whereas the PU content beyond 20 wt% in the BA-a/PU polymer alloys resulted in increasing the linear CTE with increasing crosslink

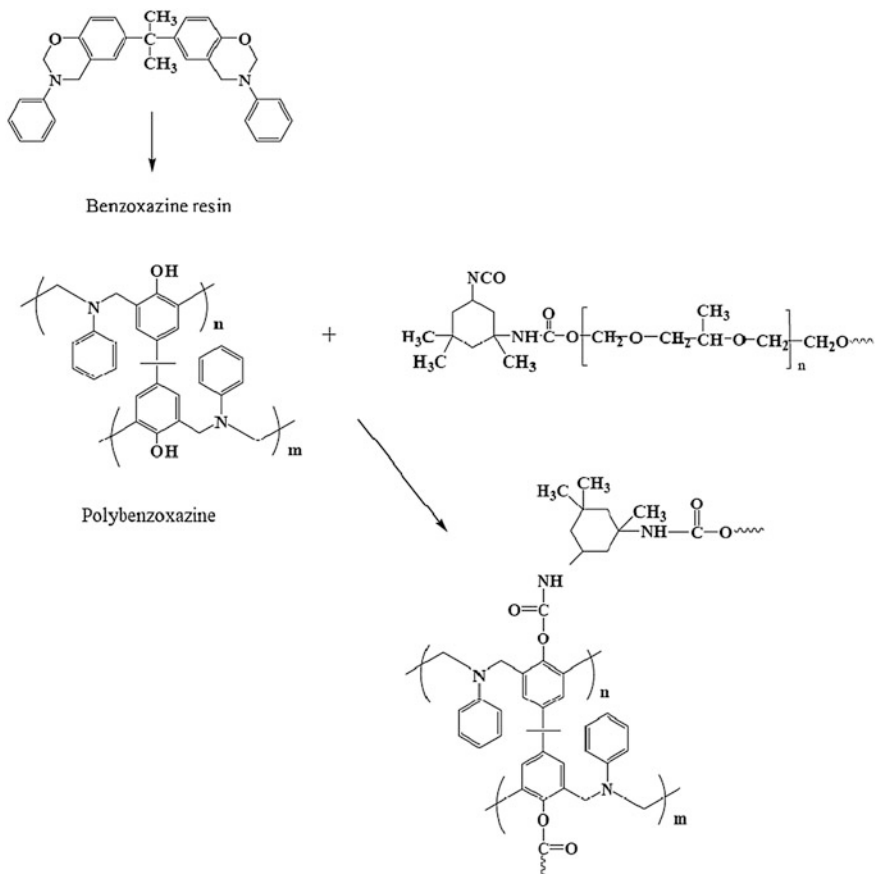


Fig. 6.5 Reaction scheme of polybenzoxazine-urethane prepolymer

Table 6.3 Linear coefficient of thermal expansion

PU content (wt%)	CTE (ppm/°C)	Crosslink density (mol/m ³)
0	57.7	4,338
10	44.7	4,829
20	53.0	5,227
30	82.8	5,443
40	90.2	7,779

density. This is expected to have different network structures [16]. Therefore, the effect of crosslink density enhancement in the alloy's CTE dominated the effect of the higher expansion of the PU, provided that the PU mass fraction was maintained below 20 % by weight.

6.3 Novel KevlarTM Fiber-Reinforced Polybenzoxazine/Urethane Composites

Recently, the work deals with the characterization, i.e., ballistic properties, thermomechanical behavior, and thermal stabilities of a lightweight ballistic composites from KevlarTM-reinforcing fiber having benzoxazine(BA-a)/urethane prepolymer (PU) polymer alloys as a matrix reported by Rimdusit et al. [10]. As we know that, one class of fibers useful for the ballistic armor application is polyamide fiber, e.g., KevlarTM because of its excellent thermal properties, highly crystalline, and highly oriented fine structure as well as high tensile properties. Its highly crystalline, highly oriented structure gives rise to high modulus which is required for enhancing sonic velocity than steel wire, glass fiber, nylon, and polyesters. The high tenacity (strength per linear density unit) and moderate elongation of KevlarTM fiber provide high toughness, and thus, high work is needed to break the transverse deformation. In addition, it has a relatively low density, which makes most KevlarTM-reinforced structure a lighter weight for a given strength and stiffness [17]. These characteristics attribute to the fairly effective absorption and distribution of the impact force along the longitudinal axis; therefore, useful for ballistic applications.

Kevlar is the registered trademark for a para-aramid synthetic fiber, related to other aramids such as Nomex and Technora. Kevlar was developed at DuPont in 1965 [18], this high-strength material was first commercially used in the early 1970s as a replacement for steel in racing tires. Typically, it is spun into ropes or fabric sheets that can be used as such or as an ingredient in composite material components (Table 6.4).

For DuPontTM Kevlar[®] fiber, the KevlarTM range covers a spectrum of strength and modulus values, from low modulus Kevlar[®]29 (K29), through high modulus Kevlar[®]49 (K49), to very high modulus Kevlar[®]149 and very high-strength Kevlar[®]129 as well as Kevlar KM2 as listed in Table 6.5. A variety of woven fabrics is also used in aircraft and helicopter parts, electrical wiring boards, coated

Table 6.4 Chemical and physical properties of Kevlar aramid fiber [17]

Properties	Value
High melt temperature	530 °C
Zero-strength temperature	640 °C
High glass transition temperature	375 °C
Low density versus glass (2.55) and steel (7.86)	1.44 g/cm ³
Thermal stability	Relatively high
Combustibility	Low
Conductivity	Nonconductive
Specific strength and modulus	High
Creep	Low
Environmental stability in sea water, oil, solvents	Good

Table 6.5 Yarn properties of various grades of KevlarTM fibers (determined on 10 inch twisted yarns: ASTM D-885)

Yarn property	Kevlar [®] 29	Kevlar [®] 49	Kevlar [®] 68	Kevlar [®] 119	Kevlar [®] 129	Kevlar [®] 149
Tensile strength (Kpsi)	420	420	420	440	485	340
Initial modulus (Mpsi)	10.3	17.4	14.4	8.0	14.0	21.0
Elongation (%)	3.6	2.8	3.0	4.4	3.3	1.5
Density (g/cm ³)	1.44	1.45	1.44	1.44	1.45	1.45
Moisture regain (%)*	6.0	4.3	4.3	–	–	1.50

Note * Moisture regain (%) at 25 °C, 65 % RH

fabrics, and also soft ballistic body armor. Woven fabrics of KevlarTM fiber are widely used in composites, armor, aircraft cargo liners, and marine applications.

Rimduisit et al. [10] have been investigated the effect of alloy compositions on the thermal, mechanical, and ballistic composite properties of 80 wt% KevlarTM-reinforced polybenzoxazine/PU composites. Table 6.6 shows that the glass transition temperatures (T_g s) of Kevlar-reinforced polybenzoxazine/PU alloy composites were significantly higher than those of KevlarTM-reinforced polybenzoxazine composite and the T_g s of the composites based on polybenzoxazine/PU alloys was also found to increase with the mass fraction of urethane. This enhancement in the T_g could be attributed to the increase in the crosslink density of the binary systems as previously reported by Rimduisit et al. [12]. Furthermore, this phenomenon could be due to the substantial interfacial adhesion between the fiber and the matrix. While the degradation temperatures at 10 % weight loss (T_{d10}) of 80 wt% KevlarTM-reinforced polybenzoxazine/PU alloy composites were found to increase systematically with increasing the mass fraction of the polybenzoxazine in the polymer alloys. The T_{d10} of the 80 wt% KevlarTM-reinforced polybenzoxazine/PU alloys composites with the polybenzoxazine compositions of 60–100 % by weight was in the range from 373 to 495 °C. The char yield values are related to the flammability of materials and are essential for some ballistic armor applications since when the armor is penetrated, the heat is generated. The material could first decompose by thermally initiated mechanisms or thermo-oxidative decomposition. It has been reported that char could decrease the diffusion rate of decomposed, flammable gases toward the flame front and decrease the burning of the material. From the Table 6.6, we can see that a remarkable

Table 6.6 Thermal and mechanical properties of 80 wt% KevlarTM-reinforced BA-a/PU composites at various PU contents

PU content (wt%)	T_g (°C) from E'' curve	T_{d10} (°C)	Char yield (%)	E_f (GPa)	ρ_f (MPa)
0	180	459	46	18.2 ± 0.4	163 ± 11
10	185	473	44	16.3 ± 0.6	135 ± 10
20	195	414	43	16.1 ± 2.8	109 ± 22
30	218	409	41	12.4 ± 2.1	80 ± 15
40	235	373	39	7.7 ± 1.6	52 ± 13

improvement in char yield, the percent residue at 800 °C, of the composites was clearly observed when the polybenzoxazine content increased. This could be attributed to the fact that urethane contained aliphatic structure, while polybenzoxazine contained benzene rings [19]. Therefore, the increase in polybenzoxazine content leads to the increase in benzene ring structure having more thermal stability and more char yield.

In addition, from the Table 6.6, the increase in the elastomeric PU content in the BA-a/PU polymer alloy resulted in samples with tougher characteristics; the flexural properties, i.e., modulus and strength of the KevlarTM-reinforced BA-a/PU composites increased with increasing the mass fraction of polybenzoxazine. The phenomenon was due to the fact that the addition of the rubbery urethane polymer into the rigid polybenzoxazine was able to lower either the strength or the stiffness of the resulting polybenzoxazine alloys.

6.4 Ballistic Properties of KevlarTM Fiber-Reinforced Benzoxazine/Urethane Composites

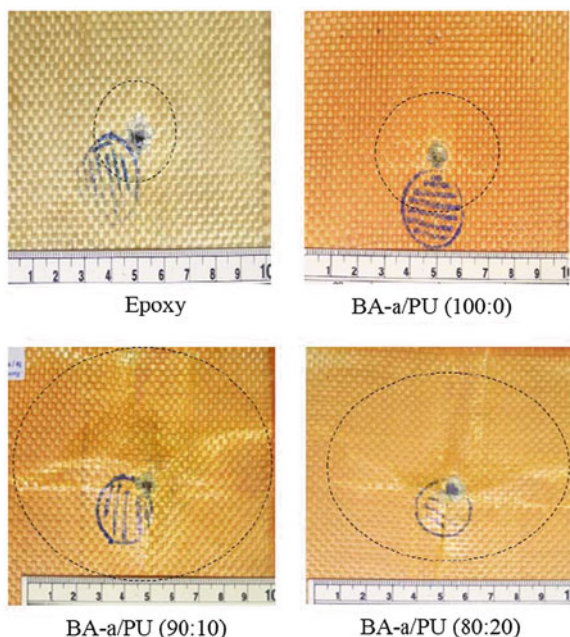
A low-level ballistic impact test was performed on the 20-ply laminates (10 piles/panel and 10/10 arrangement) with sample size of 25.4 × 25.4 × 1.8 mm of the 80 wt% KevlarTM-reinforced BA-a/PU polymer alloy composites using a 9-mm handgun with standard lead projectiles having lead outer coating, and it was found that the optimal composition of BA-a/PU polymer alloys for the composites should be approximately 20 wt% of PU because the firing results indicated that the mass ratio of the BA-a/PU = 90:10 and the BA-a/PU = 80:20 matrix alloys exhibited ballistic penetration resistance in comparison with the other matrix alloy compositions, i.e., BA-a/PU = 100:0 and the epoxy matrix as listed in Table 6.7.

In principal, one major component of the energy absorption mechanisms in ballistic impact is the delaminated area. From Fig. 6.6, the relatively larger delaminated area of the composites based on the BA-a/PU = 80:20 matrix alloys than

Table 6.7 Effect of BA/PU alloy compositions on ballistic impact resistance of the 80 wt% KevlarTM-reinforced BA-a/PU polymer alloy composites using standard lead projectiles with lead outer coating typically used in 9-mm hand gun

Matrix	Configurations Plate 1/Plate 2	Penetration resistance	
		Plate 1	Plate 2
BA-a/PU (60:40)	10/10	No	No
BA-a/PU (70:30)	10/10	No	No
BA-a/PU (80:20)	10/10	Yes	Yes
BA-a/PU (90:10)	10/10	Yes	Yes
Poly(BA-a)	10/10	No	No
Epoxy	10/10	No	No

Fig. 6.6 Pictures of the fire tested composites using different types of matrices



that of the composites based on BA-a/PU = 100:0, BA-a/PU = 90:10, and the epoxy matrix was observed.

As a result, a larger damaged area of the 80 wt% KevlarTM-reinforced BA-a/PU polymer alloy composites compared with the 80 wt% KevlarTM-reinforced polybenzoxazine and the 80 wt% KevlarTM-reinforced epoxy configuration composite was observed. The cross-sections of the front plate of the 80 wt% KevlarTM-reinforced BA-a/PU (90:10) polymer alloy and the 80 wt% KevlarTM-reinforced BA-a/PU (80:20) polymer alloy are also illustrated in Fig. 6.7a and b, respectively, revealing the macroscopic delamination of the Kevlar's cloth in the 10-ply-thick composites.

Furthermore, the visual appearance of the projectiles after a low-level ballistic impact test with the composites based on the BA-a/PU = 80:20 and BA-a/PU = 90:10 matrix alloys was illustrated in Fig. 6.8. We can observe that the standard lead projectile after a low-level ballistic impact test with the composite based on the BA-a/PU = 80:20 was more damaged than that with the composite based on the BA-a/PU = 90:10. Therefore, the variation in the BA-a/PU polymer alloy compositions could allow an optimal interaction between the alloy matrix and its reinforcing fiber, which leads to obtaining the outstanding ballistic performance.

Upon ballistic impact, polymer composites retard the projectile by reducing its kinetic energy. There are several mechanisms of absorption of kinetic energy for composite material, including tensile failure of fibers, elastic deformation of composite, interlayer delamination, shear between layers in the composite, and inertia effect. The absorption of kinetic energy may be attributed according to basic

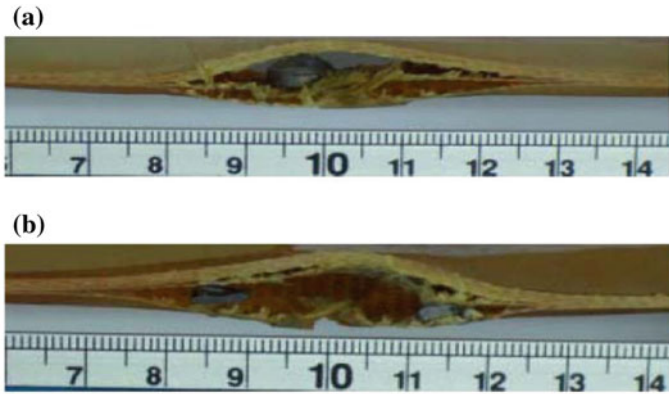


Fig. 6.7 Damaged panel cross-sections of specimen having arrangement of 10/10 that could stop standard lead projectiles with lead outer coating typically used in 9-mm hand gun: **a** first panel of 80 wt% Kevlar™-reinforced BA-a/PU (90:10) polymer alloy composite and **b** first panel of 80 wt% Kevlar™-reinforced BA-a/PU (80:20) polymer alloy composite

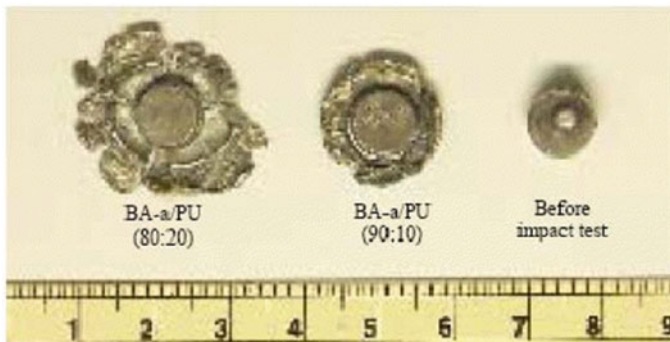


Fig. 6.8 Image of the standard lead projectiles used for 80 wt% Kevlar™-reinforced BA-a/PU polymer alloy composites at various PU contents

factors such as mechanical properties of the composite's constituent direction of fiber arrangement and interfacial strength. In general, the absorption of kinetic energy of the composite materials can qualitatively evaluate via fracture morphology. The composite laminates experience various types of fracture: delamination, intraply cracking, matrix cracking, fiber breakage, and fiber damage that depends on the interlayer materials [20]. The fracture surface morphology of the fracture produced at the first layer of the 80 wt% Kevlar™-reinforced BA-a/PU (80:20) polymer alloy composites after having been low-level ballistic impact tested was observed using scanning electron microscopy (SEM). From Fig. 6.9a, we can see that the Kevlar fiber fractures were multiple split break along fiber direction and skin off as similarly observed in carbon fiber/epoxy composite system

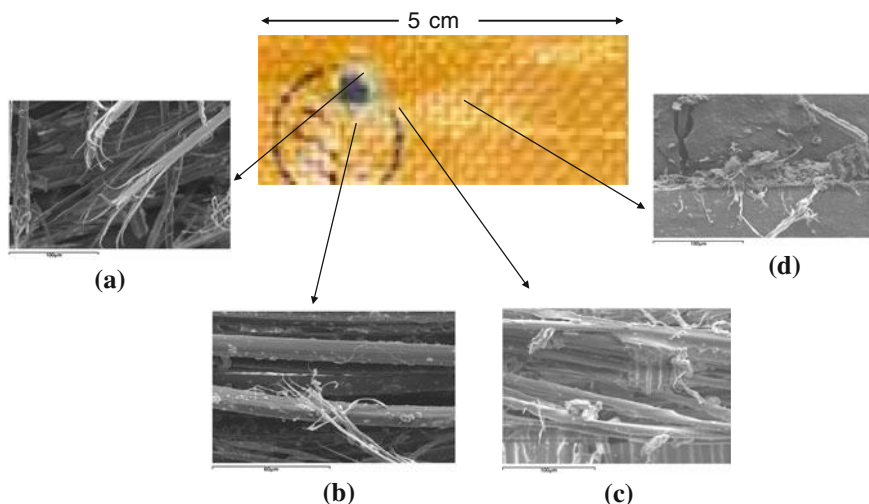


Fig. 6.9 SEM micrographs of fracture surface of the 80 wt% KevlarTM-reinforced BA-a/PU (80:20) polymer alloy composites: **a** fiber fracture, **b** interfacial failure, **c** matrix cracking, and **d** no failure area

[21] which indicated that Kevlar fiber significantly exhibited potential for resistance to ballistic impact. In addition, the results reveal that the fracture surfaces near the center of ballistic impact of the 20-ply laminates of 80 wt% KevlarTM-reinforced BA-a/PU (80:20) polymer alloy composites as shown in Fig. 6.9b exhibited substantial level of adhesive failure in which the fibers were largely stripped off the matrix materials with only small fragments of the matrix remained adhere to the fibers. Figure 6.9c shows the micrograph of the fracture surface of the composite. In this area, good bonding between fibers and the BA-a/PU polymer matrix was observed and no failure area was depicted in Fig. 6.9d.

Consequently, the selection of a suitable matrix resin that renders the most energy absorption characteristics with particular reinforcing fiber used is crucial to the successful ballistic performance of the composite armor. In this work, it therefore seemed likely that the BA-a resin shows a synergistic behavior in ballistic performance with the PU system used with BA-a/PU (80:20), rendering the most outstanding ballistic performance. The BA-a/PU (80:20) polymer alloy was, therefore, further used to fabricate the composite armors for higher protection level evaluation.

In general, personal body armors covered by ballistic impact standard, which is National Institute of Justice (NIJ), are classified into seven classes, by level of ballistic performance. The ballistic threat posed by a bullet depends, among other things, on its composition, shape, caliber, mass, angle of incidence, and impact velocity. As of the year 2000, ballistic resistant body armor suitable for full-time wear throughout an entire shift of duty is available in classification Types I, II-A, II, and III-A, which provide increasing levels of protection from handgun threats.

Table 6.8 NIJ standard of body armor showing type of caliber and bullet as well as the projectile velocity in each category

Protection level	Caliber	Bullet type, weight	Velocity (m/s)	Accepted hit/panel
I	0.38 special	Round nose lead, 158 grains (10.2 g)	259	5
	0.22 special	Long rifle high velocity lead, 40 grains (2.6 g)	320	5
II-A	9 mm	Full metal jacket, 124 grains (8.0 g)	332	5
	0.40 S&W	Full metal jacket, 180 grains (11.7 g)	322	5
II	9 mm	Full metal jacket, 124 grains (8.0 g)	358	5
	0.357	Magnum jacketed soft point, 158 grains (10.2 g)	425	5
III-A	9 mm	Full metal jacket, 124 grains (8.0 g)	426	5
	0.44	Magnum lead semi-wad cutter gas checked 240 grains (15.5 g)	426	5
III	7.62 × 51 mm (0.30 Winchester)	Full metal jacket, 150 grains (9.7 g)	838	5
VI	0.30 caliber	Armor piercing, 166 grains (10.8 g)	868	1

Source Thailand Ministry of Defense 2004

Type I body armor, which was first issued during the NIJ demonstration project in 1975, is the minimum level of protection that any officer should have. Officers seeking protection from lower velocity 9 mm and 0.40 S and W ammunition typically wear type II-A body armor. For protection against high velocity 0.357 Magnum and higher velocity 9 mm ammunition, officers traditionally select Type II body armor. Type III-A body armor provides the highest level of protection available in concealable body armor and provides protection from high velocity 9 mm and 0.44 Magnum ammunition. Type III-A armor is suitable for routine wear in many situations; however, departments located in hot, humid climates may need to carefully evaluate their use of Type III-A body armor for their officers. Types III and IV armors, which protect against high-powered rifle rounds, are clearly intended for use only in tactical situations when the threat warrants such protection. In December 1978, the National Bureau of Standards and National Institute of Law Enforcement and Criminal Justice (now NIJ) first classified the ballistic body armors into several categories according to projectile size and velocity in its NILE/CJ report. The current NIJ classification for police body armor as shown in Table 6.8.

Rimdusit et al. [10] have also been investigated the ballistic properties of the 80 wt% Kevlar™-reinforced BA-a/PU (80:20) polymer alloy composites to be the composite armors for higher protection level evaluation. The composites were prepared approximate thicknesses of 1.8, 3.5, and 5.0 mm for panel manufactured 10, 20, and 30 pile composites, respectively. The areal densities were 0.48 g/cm² for the 10 piles, 0.48 g/cm² for the 20 piles, and 0.70 g/cm² for the 30 piles panel composites. The effect of number of piles and panel arrangement of the 80 wt%

Table 6.9 Effect of number of piles and panel arrangement of the 80 wt% KevlarTM-reinforced BA-a/PU (80:20) polymer alloy composites after ballistic impact at projectile velocities required by NIJ standard level II-A and III-A [10]

Projection level	Configurations	Penetration resistance	Damaged dimensions of rare plate	
			Diameter (mm)	Depth (mm)
II-A	10/10/0	No	–	–
	20/0/0	No	–	–
	10/10/10	Yes	69.5	10.8
	20/10/0	Yes	44.5	7.8
	30/0/0	Yes	66.6	8.7
III-A	20/10/10/0	No	–	–
	30/20/0/0	Yes	93.3	13.6
	10/10/30/0	Yes	119.1	19.5
	30/20/10/0	Yes	90.3	11.0
	30/10/10/10	Yes	66.1	10.1

KevlarTM-reinforced BA-a/PU (80:20) polymer alloy composites on ballistic impact at projectile velocities required by NIJ standard level II-A and III-A is listed in Table 6.9.

From the table, we can see that the penetration resistance results of the composite after impact with projectile velocities for the NIJ level II-A ballistic test were observed for the 30-ply composite arrangements, while all composite laminates assembled to have a combined thickness of 20 plies of the KevlarTM did not pass this level of the NIJ standard for ballistic protection. From the delaminated area measurement, it is apparent that a sample with an arrangement of the 20-ply panel in front of the 10-ply panel (20/10 configuration) exhibited the best ballistic performance via the damaged dimension. The damaged area of this sample arrangement was significantly smaller than that of the other two arrangements, i.e., the 10/10/10 and 30/0/0 configurations. The damaged and delaminated areas of sample after impact with projectile velocities required by NIJ standard for level II-A with 10/10/10, 20/10/0, and 30/0/0 arrangements are also illustrated in Fig. 6.10a, b, and c, respectively, revealing the macroscopic damaged area of the KevlarTM's cloth in the 30-ply-thick composites with different arrangements.

Therefore, the arrangement of composite panel in the firing test was found to be one important factor on the ballistic performance of the composites. The front panel with at least 20 plies of KevlarTM cloth was thus necessary for the level II-A resistance of perforation and was supposed to possess sufficient properties to destroy or deform this type of projectile. Therefore, the 80 wt% KevlarTM-reinforced BA-a/PU (80:20) polymer alloy composites with the combined thickness of 40, 50, and 60 plies were subjected to a ballistic impact evaluation at a projectile velocity required by NIJ standard for level III-A. This level III-A test is currently reported maximum level of protection based on polymer composites. From the table, we can see that the test weapon with standard 124 grains, round lead projectile with a copper outer coating (Full Metal Jacket) typically used in the 9-mm

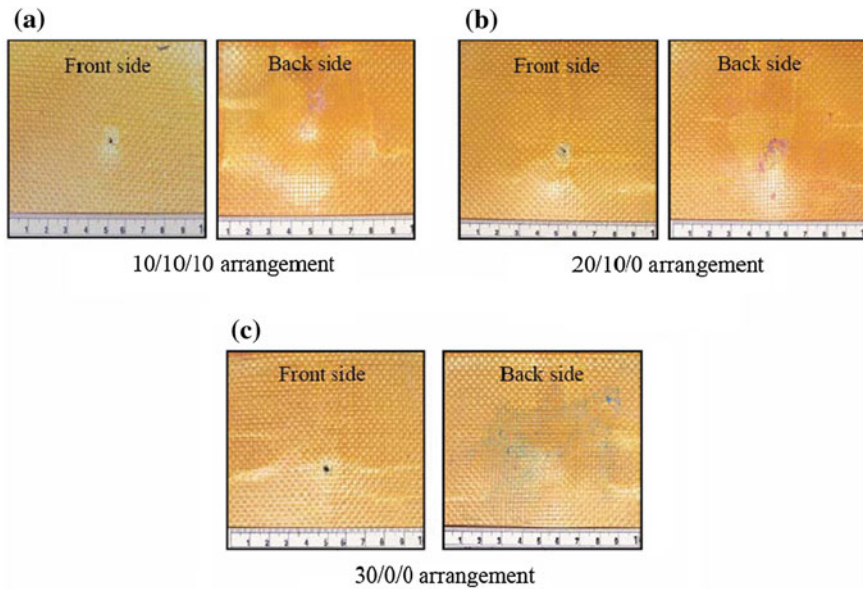


Fig. 6.10 Visual appearance of damaged and delaminated area of Kevlar™-reinforced BA-a/PU (80/20) composites after impact with projectile velocities required by NIJ standard for level II-A with the composite arrangement of: **a** 10/10/10, **b** 20/10/0, and **c** 30/0/0

handgun having a speed required by level III-A could be stopped with at least 50 plies of the composites by observation of the damage area evaluation confirmed that the arrangement of composite panels had an important effect on their ballistic protection. It can be seen that the composite with 30/20/0 arrangement rendered the damaged depths and diameters smaller than those of the composite with the 10/10/30 arrangement. This result implied that the composite arrangement for level III-A protection needed at least 30-ply composite panel as a front plate in the impact direction with observation of visual appearance of damaged and delaminated area of the composites after ballistic impact test at various panel arrangements as shown in Fig. 6.11. The sufficiently stiff panel seemed to play a crucial role as to deform the shape of the projectile as discussed previously.

Interestingly, in the combined 60-ply-thick composite panels, the two types of arrangements (30/20/10 and 30/10/10/10 configurations) were again found to lead to different damaged areas and deformed depths. The composite with 30/10/10/10 configuration rendered less damaged area than that of composite with 30/20/10 configuration. Since the number of the Kevlar™ plies combined was the same in each tested sample, the sample arrangement with the thicker panel of 30 plies for level III-A was to be on the front and was found to be essential in the successful ballistic impact resistance of the composites with lower degree of sample deformations.

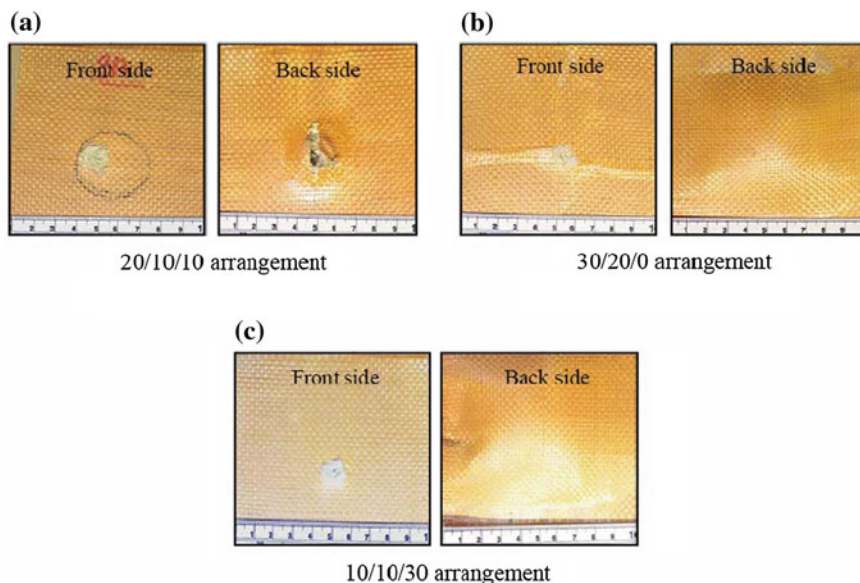


Fig. 6.11 Visual appearance of damaged and delaminated area of KevlarTM-reinforced BA-a/PU (80/20) composites after impact with projectiles required by NIJ standard for level III-A with the composite arrangement of: **a** 20/10/10, **b** 30/20/0, and **c** 10/10/30

6.5 Conclusions

The suitable matrix alloy based on benzoxazine and urethane resins for a light-weight ballistic composites from KevlarTM-reinforcing fiber having bisphenol-A-/aniline-based polybenzoxazine (BA-a)/urethane prepolymer (PU) alloys as a matrix was determined. The synergism in the glass transition temperature can be observed in KevlarTM-reinforced BA-a/PU polymer alloy composites. This phenomenon was due to the addition of urethane prepolymer which is attributed to improve crosslinked density of the matrix alloys. However, the increase in the PU fraction significantly lowered the stiffness and degradation behavior of the composites. The results of low-level ballistic impact measurement using a 9-mm handgun of the 20-ply KevlarTM-reinforced composites revealed that the composite from the BA-a/PU matrix at weight ratio 80:20 exhibited 100 % ballistic penetration resistance. The appropriate thickness of KevlarTM-reinforced BA-a/PU (80:20) composite panel was 30 plies and 50 plies to resist the penetration from the ballistic impact equivalent to levels II-A and III-A of NIJ standard. The arrangement of composite panels with the higher stiffness panel at the front side also showed the best efficiency ballistic penetration resistance.

References

1. Lane RA (2005) High performance fibers for personnel and vehicle armor systems AMPTIAC. Rome, NY, pp 1–10
2. Tyrone L, Turbak AF (1991) High-tech fibrous materials. American Chemical Society, Washington, DC
3. Jacobs MJN, Dingenen JLV (2001) Ballistic protection mechanisms in personal armor. *J Mater Sci* 36:3137–3142
4. Pathomsap S (2005) Development of ballistic armor from Kevlar fiber and polybenzoxazine alloys. Chulalongkorn University, Thailand
5. Park AD (2003) Lightweight soft body-armor product. U.S. Patent 6,651,543
6. Epel JN (1987) Fibrous armor material. U.S. Patent 4,369,387
7. Denommee DR (1976) Method of making deep draw laminate articles. U.S. Patent 3,956,447
8. John N (1992) Structural sandwich panel with energy-absorbing material. U.S. Patent 5,102,723
9. Li LH, Kwon YD, Prevorsek DC (1996) Fire resistance ballistic resistant composite armor. U.S. Patent 5,480,706
10. Rimdusit S, Pathomsap S, Kasemsiri P, Jusilp C, Tiptipakorn S (2011) KevlarTM fiber-reinforced polybenzoxazine alloys for ballistic impact applications. *Eng J* 15:23–39
11. Ishida H, Allen DJ (1996) Mechanical characterization of copolymers based on benzoxazine and epoxy. *Polymer* 37:4487–4495
12. Rimdusit S, Pristpindvong S, Tanthapanichakoon W, Damrongsakkul S (2005) Toughening of polybenzoxazine by alloying with urethane prepolymer and flexible epoxy: a comparative study. *Polym Eng Sci* 45:288–296
13. Rimdusit S, Bangsen W, Kasemsiri, (2011) Chemorheology and thermomechanical characteristics of benzoxazine-urethane copolymers. *J Appl Polym Sci* 121:3669–3678
14. Wirpsza Z (1993) Polyurethane chemistry, technology and application. Singapore, Ellis Horwood PTR. Prentice Hall, New York
15. Takeichi T, Guo Y, Rimdusit S (2005) Performance improvement of polybenzoxazine by alloying with polyimide: effect of preparation method on the properties. *Polymer* 46:4909–4916
16. Bandyopadhyay A, Odegard GM (2012) Molecular modeling of crosslink distribution in epoxy polymers. *Model Simul Mater Sci Eng* 20:1–22
17. Yang HH (1993) Kevlar aramid fiber. West Sussex, Wiley, New York
18. Kwolek S, Mera H, Takata T (2002) High-Performance fibers in Ullmann's encyclopedia of industrial chemistry 2002. Wiley-VCH, Weinheim
19. Ishida H, Agag T (2011) Handbook of benzoxazine resins. Elsevier, New York
20. Morye SS, Hine PJ, Duckett RA, Carr DJ, Ward IM (2000) Modeling of the energy absorption by polymer composites upon ballistic impact. *Compos Sci Technol* 60:2631–2642
21. Sohn MS, Hu XZ, Kim JK, Walker L (2000) Impact damage characterisation of carbon fibre/epoxy composites with multi-layer reinforcement. *Compos B* 31:681–691

Chapter 7

Electrical Conductivity of Filled Polybenzoxazines

Abstract As similar to other polymeric materials, polybenzoxazines (PBz) in nature exhibit the insulative characteristics. In order to extend the range of PBz to suit for various applications (such as electrostatic materials, conductive adhesives, etc.), the modification of the polymer has been made. The practical and low-cost method is compositing the polymer with electrically conductive filler. In this chapter, the composite systems of PBzs filled with conductive fillers (such as inherently conductive polymer, carbon-based filler, and metallic filler) were reviewed and compared with some composite systems (i.e., epoxy and phenolic resins). The theoretical concept of electrical conductivity, the inherently conductive polymer and the potential applications of the composites were also included.

Keywords Polybenzoxazine composites · Electrical conductivity · Conductive filler

7.1 Introduction

Electrical conductivity is one of the crucial properties being concerned for many applications of the materials. In electronic industry for many decades, there has been reported about large number of losses from electrostatic discharge (ESD) or the charge transfer to electrically sensitive devices. These problems could occur during production, assembling, storage, and transportation. In 2006, the losses associated with ESD were reported at between a half billion and five billion dollars annually [1]. Therefore, the use of suitable materials to match their applications is not dispensable.

As similar to general polymers, polybenzoxazines (PBz) typically perform as insulator based on their conductivity value. Kimura et al. [2] studied the volume resistivity of the bisphenol-A based benzoxazine with cyanate ester resin. In the study, the monomers of 2,2-bis(3,4-dihydro-3-phenyl-1,3-benzoxazine) propane benzoxazine (bifunctional benzoxazine, Ba) were blended with 2,2-bis(4-

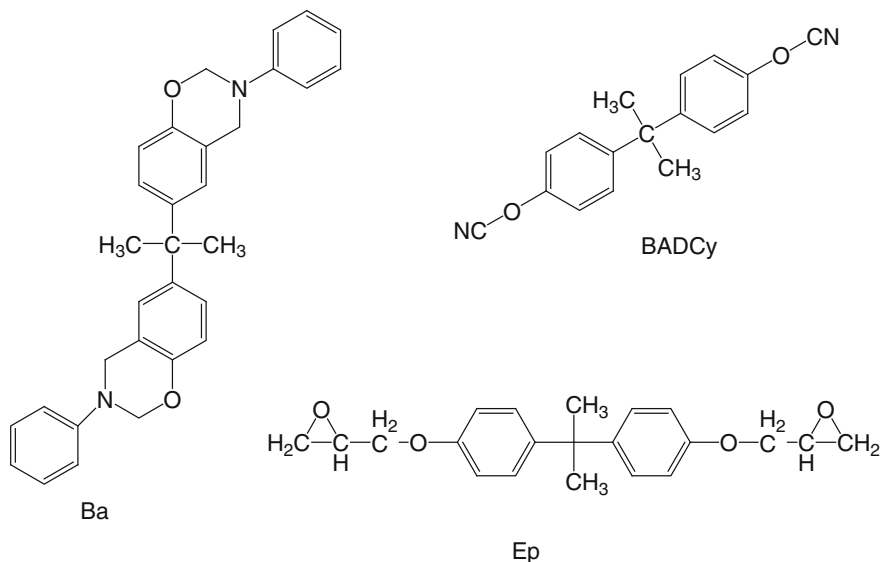


Fig. 7.1 Chemical structures of Ba, BADCy (bisphenol based cyanate ester), and Ep (monofunctional cyanate)

cyanatophenyl) propane (bisphenol-A based cyanate ester, BADCy) and 2-phenyl-2-(4-cyanatophenyl) propane (mono functional cyanate). Their chemical structures are presented as Fig. 7.1. The researchers reported that the volume resistivity of BA/BADCy and Ba/Ep was in the range of 10^{15} – 10^{16} Ω cm.

7.2 Types of Materials Classified Based on Electrical Resistivity

According to the electrostatic discharge association (ESDA), all materials can be classified into 4 main types, i.e., electrical insulator, antistatic materials, static dissipative materials, and electrical conductor. In case of electrically conductive materials, the electrical charges are able to go to ground or another object contacting or coming close to. In case of insulative materials, high electrical resistance and difficulty to ground were observed. That leads to the remains of static charges in the place on the insulative materials for a long period of time. The ranges of electrical resistivity for each type are shown in Table 7.1.

It has been reported that the major applications of electrically conductive polymers are ESD and electromagnetic interference EMI protection [4–8]. The application ranges of filled conductive polymer are related to the surface/volume resistivity. It is noted that a surface resistivity for EMI shielding applications typically is lower than 10 Ω /sq, while that for ESD applications is in the range of

Table 7.1 Types of materials classified based on electrical resistivity range [3]

Type of material	Surface resistivity (Ω/sq)	Volume resistivity ($\Omega \text{ cm}$)
Electrical insulator	At least 10^{12}	At least 10^{11}
Static dissipative material	10^5 – 10^{12}	10^4 – 10^{11}
Electrical conductor	Less than 10^5	Less than 10^4
Antistatic material	Not correlated	Not correlated

10^6 – $10^9 \Omega/\text{sq}$. The surface resistivity of plastic is not less than $10^{12} \Omega/\text{sq}$, whereas that of metal is in the range of 10^{-1} – $10^{-5} \Omega/\text{sq}$ [9].

In order to enhance the electrical conductivity of polymers, there are many methods such as the modification of polymer structure, and the addition of electrical conductive filler. The latter method is much easier and economical. Therefore, the conductive fillers and conductive polymeric composites are mainly discussed in this chapter.

7.3 Conductive Path and Percolation Threshold

Typically, polymeric materials perform as electrical insulator due to their high electrical resistivity. When the small amount of electrically conductive filler was added into the polymer, the resistivity of the filled polymer is still high. In case that the filler is further loaded to the system, the connection between each small unit of filler is formed. If the amount of conductive filler (in shape of powder, particles, flake, platelet, or fiber) is high enough to provide the conductive path (as exhibited in Fig. 7.2), the resistivity of the composite is drastically low. The relationship between the electrical resistivity and filler content is presented in Fig. 7.3. The region of the graph for the significant decrease is called percolation zone; the minimum content of the filler to obtain the low resistivity is also called percolation threshold.

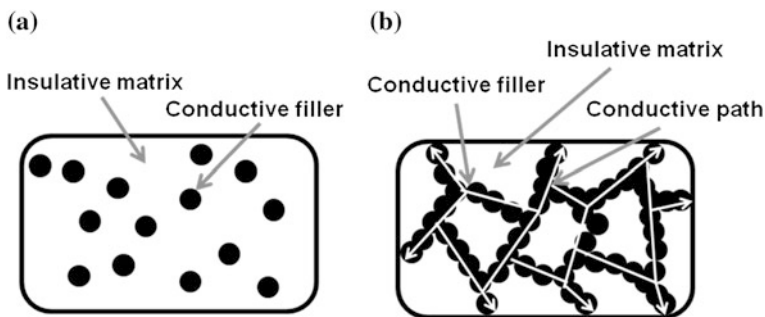
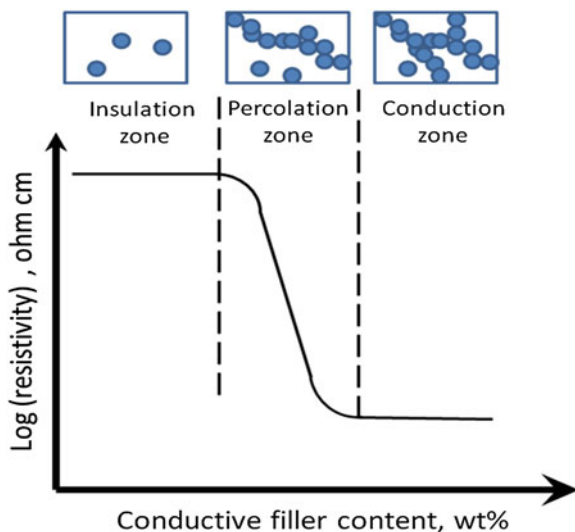


Fig. 7.2 Filler distribution in polymer composite: **a** at low content, **b** conductive path at high enough content [10]

Fig. 7.3 The relationship between electrical resistivity and filler content



From Fig. 7.3, electrical resistivity significantly decreased when the conductive filler content is greater than the percolation threshold. The relationship between conductivity (σ) and resistivity (ρ) is shown in Eq. 7.1. The change of conductivity beyond the percolation threshold can be expressed in Eq. 7.2, which was developed by Kirkpatrick [11] and Stauffer [12].

$$\rho = \frac{1}{\sigma} \quad (7.1)$$

$$\sigma = \sigma_0(P - P_c)^t \quad (7.2)$$

where P_c is the threshold probability of forming a conductive path, P is equivalent to the volume fraction of conducting phase beyond the threshold content, t is the conductivity exponent, and σ_0 is the pre-factor. Anyhow, it is worthy to note that this classical percolation theory can be applied to the system of polymers mixed with conductive filler with the following conditions: the filler must be spherical particles with monodispersion and have an isotropic conductivity.

Theoretically, there are many factors having effects on the value of percolation such as polymer polarity, polymer viscosity, degree of crystallization of polymer, conductive filler types [13]. Miyasaka et al. [14] determined the effects of polymer matrix types on the electrical conductivity of the composites. The researcher revealed that the polarity of the polymer possibly relates to the critical content at the percolation, i.e., the low polarity of the polymer matrix leads to the low percolation content. It also has been reported that the low surface tension of the polymer also results in the low percolation contents [15, 16]. The percolation content also depends on polymer viscosity [17], i.e., the high viscosity of the polymer matrix provides the high percolation content. It is attributed to the high

viscosity could cause the decrease in aspect ratio of the filler and obstruct the three-dimensional formation of conductive paths [18]. Types of conductive filler are the important factors related to percolation content due to the difference of the inherent nature [13].

7.4 Inherently Conductive Polymer Filler

Before determining the systems of polymer composites filled with inherently conductive polymer, the properties of this polymer should be discussed. The inherently conductive polymer has many interesting properties, such as light weight, high strength per weight, low consumption of processing energy. Furthermore, this type of polymer provides large change in the color when oxidized or reduced, the redox process is reversible. There is ability to tune the electrical conductivity by chemical manipulation of polymer backbone, dopants, and degree of doping. This kind of polymer could be used as filler in polymer composite systems.

In general, the conductive polymer composed of conjugated ladder-type structure and/or aromatic structure. The chemical structures of well-known inherently conductive polymers are presented as seen in Fig. 7.4. The main chains of some conductive polymers contain nitrogen or sulfur atoms. In this figure, the structure form of polyaniline (PANI) could be conductive only when m (the repeating unit) is equal to 0.5. It is worthy to be noted that the inherently conductive polymers without doping are insulative.

When the electrically conductive polymers are doped, there are two possible cases, i.e., p -type doping and n -type doping. For p -type doping, the lone pair

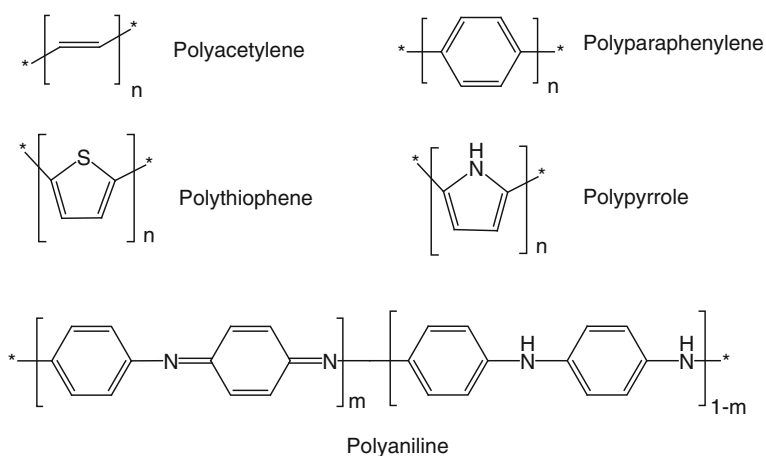
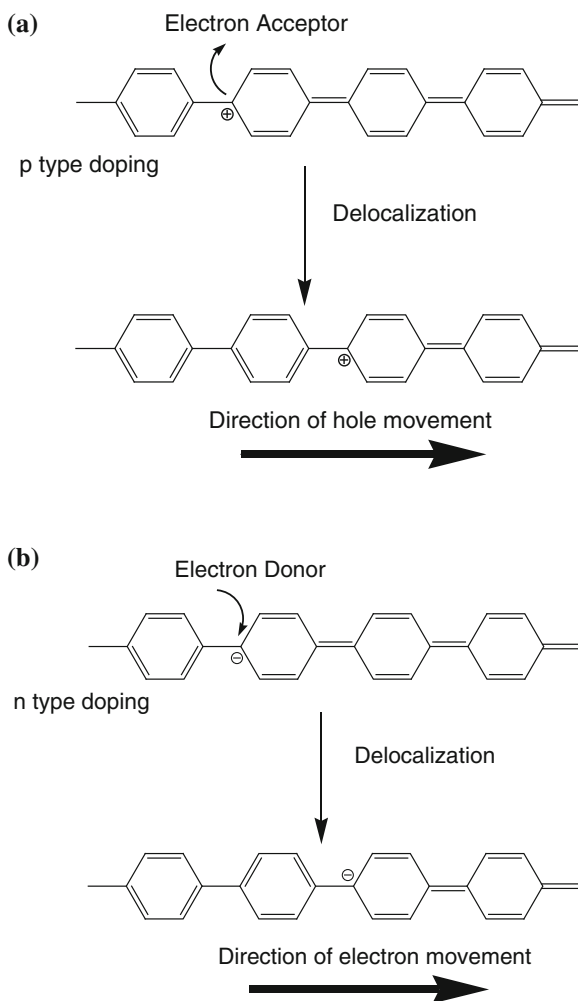


Fig. 7.4 Chemical structures of well-known inherently conductive polymers [19]

Fig. 7.5 Direction of electron and hole movement in polyparaphenylene: **a** *p*-type doping, **b** *n*-type doping [20]



electrons are removed from the main chain. Then, positive charge (hole) occurs. In case of *n*-type doping, the electrons are added into the main chain. Thus, the negative charge or excess electron occurs. Due to the delocalization of the π bonds available in the system, the electrons and holes in the main chain can move as shown in Fig. 7.5.

Typically, the conductive polymers could be either *n*-type or *p*-type doped. The types of polymers and their doping types are presented in Table 7.2. The well-known properties of the electrical conductive polymers are also shown in Table 7.3.

From Table 7.3, it could be noticed that few types of inherently conductive polymer have good stability to the environment with good processability.

Table 7.2 Inherently conductive polymers and their types of doping [20, 21]

Polymer	Type of doping
Polyacetylene	<i>n, p</i>
Polyparaphenylene	<i>n, p</i>
Polyparaphenylene sulfide	<i>p</i>
Polyparaphenylene vinylene	<i>p</i>
Polypyrrole	<i>p</i>
Polythiophene	<i>p</i>
Polyisothionaphthene	<i>p</i>
Polyaniline	<i>p</i>

Table 7.3 Properties of well-known conductive polymers [20]

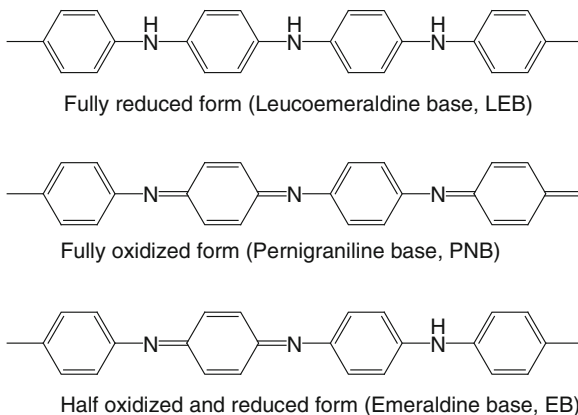
Polymer	Conductivity (S/cm)	Stability	Processability
Polyacetylene	10^3-10^5	Poor	Poor
Polyphenylene	10^3	Poor	Poor
Polyphenylene vinylene	10^3	Poor	Poor
Polyphenylene sulfide	10^2	Poor	Excellent
Polypyrrole	10^2	Good	Good
Polythiophene	10^2	Good	Excellent
Polyaniline	10	Good	Good

Therefore, not all the inherently conductive polymer is suitable and generally found in the filled polymer composites [21].

PANI is one of the well-known conductive polymers used as filler in the composite systems. Based on the oxidation state, there are three forms of PANI as presented in Fig. 7.6 [21], i.e., Leucoemeraldine base (LB) which is yellow in fully reduced form, Pernigraniline base (PB) which is violet in fully oxidized form, and emeraldine base (EB) which is blue or green in half-oxidized form. Both LB and PB forms are not conductive, while only EB form is able to be doped with protonic acid. After doping, EB color is changed from blue to green.

Four most crucial factors effecting on the electrical conductivity of PANI have been reported as follows [21–26]:

- (a) Oxidation level and molecular arrangement: As mentioned early, there is low electrical conductivity in case of no EB structure in PANI. Thus, the alternative arrangement of quinoid and benzenoid rings in PANI (half-oxidized and reduced form) is the most important factor to achieve a high value of conductivity [21, 22].
- (b) Molecular weight of the inherently conductive polymer: In case that the long chain of PANI molecule, the imperfection, e.g., distortion in chain symmetry effecting on the continuous charge delocalization process in chain. This results in a decrease in conductivity [21–27].

Fig. 7.6 Three oxidation states of polyaniline [21]

- (c) Percent crystallinity of and inter-chain separation: The electrical conductivity of the system increase with the increase in crystallinity. With the decrease in d -spacing, the conductivity trend to increase due to the probability of inter-chain hopping of charge [21–26].
- (d) Doping percentage and type of dopants: With different kinds of doping agents, methods of doping and conditions, the rendered doped PANI provides different doping percentages leading to different electrical conductivity as presented in Table 7.4.

Table 7.4 Conductivity and processability of some dopant types/doping conditions of polyaniline (PANI) [21]

Doping condition and type of dopant	Conductivity (S/cm)	Processability
HCl doped, in aqueous medium	10–12	Difficult
HCl doped, EB film cast from NMP then doped	24	Difficult
H ₂ SO ₄ doped	6.5	Difficult
Lauric acid doped, in aqueous medium	0.4	Difficult
Camphorsulfonic acid (CSA) doped, formed in solution	200–400	Solution processable
Aromatic phosphoric diester doped, in solution or mechanical mixing	1–10	Solution/melt processable
CSA doped, EB film from chloroform: <i>m</i> -cresol = 30:70 and CSA mixed as powder	70	Solution processable
Polyaniline synthesized in benzene sulfonic acid	2	Solution processable
<i>n</i> -dodecylbenzene sulfonate-doped polyaniline (PANI-DBSA) doped, thermal doping	1–10	Solution/melt
Diphenyl phosphate doped, in chlorobenzene	65	Melt processable
Polyaniline synthesized in sulfanilic acid	3.1	Melt processable

Table 7.5 Effect of PANI contents and EB dose on electrical conductivity of the composites [27]

PANI content + radiation dose	Volume conductivity (S/cm)
Pure PI without radiation	3.42×10^{-16}
0 phr + 200 kGy	1.86×10^{-4}
10 phr + 200 kGy	2.16×10^{-4}
20 phr + 100 kGy	1.86×10^{-4}
20 phr + 200 kGy	2.01×10^{-4}
20 phr + 300 kGy	2.32×10^{-4}

Table 7.6 Effect of PANI contents on the conductivity of composites doped with HCl [27]

PANI content (phr)	Volume conductivity (S/cm)
0	1.4×10^{-5}
10	7.0×10^{-5}
20	8.5×10^{-5}

Recently, the composites between polymers filled with PANI have been developed. Tiptipakorn et al. [28] studied the effects of electron beam (EB) on irradiated polyimide (PI)/PANI composites. The research developed the composites prepared from PI and PANI dissolved in N-methyl-2-pyrrolidone (NMP). The composites were radiated with EB at 0, 50, 150, 200, and 300 kGy. The electrical conductivity and thermal properties of the radiated composites were determined and compared with those of the composites doped with 6 M HCl. Table 7.5 reveals the relationship between PANI contents and EB dose on the conductivity of PI/PANI composites, while Table 7.6 exhibits the effects of PANI contents on the conductivity of composites doped with HCl. The results revealed that the conductivity was enhanced from 3.42×10^{-16} S/cm (untreated pure PI) to 6.97×10^{-5} S/cm (non-radiated PI filled with 10 phr of PANI and doped with HCl). The conductivity was increased to 2.16×10^{-4} S/cm in case of PI filled with 10 phr of PANI radiated at 200 kGy.

As presented in Figs. 7.7 and 7.8, it was reported that the glass transition temperature of the composite increased with increasing PANI content for either EB radiation method or HCl doping method. The electrical conductivity values of the radiated composites were higher than those of composites doped with HCl at the same PANI content.

It can be noticed that the glass transition temperatures were increased at low content of PANI. This could be attributed to the fact that the small amount of PANI particle (in nanoscale) could impede the mobility of the PBz molecules. At high content (more than 10 phr), the agglomeration of PANI could occur; this could lower the ability to hinder the polymer mobility. Therefore, the glass transition temperature was decreased.

The research of PBz filled with PANI was carried out by Tiptipakorn et al. [29]. The researchers studied thermal properties of this composite system and reported that the addition of PANI was able to increase the char yield and the decomposition temperatures at maximum weight loss (T_{dmax}) of the composites. The char yield increased from ca. 37 % (pure PBz) to ca.41 % (20 phr of PANI) and

Fig. 7.7 Effect of polyaniline content on the glass transition temperature at 0 kGy [27]

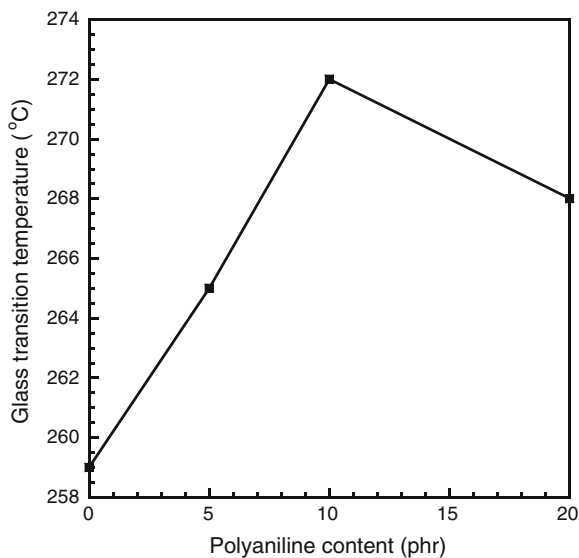
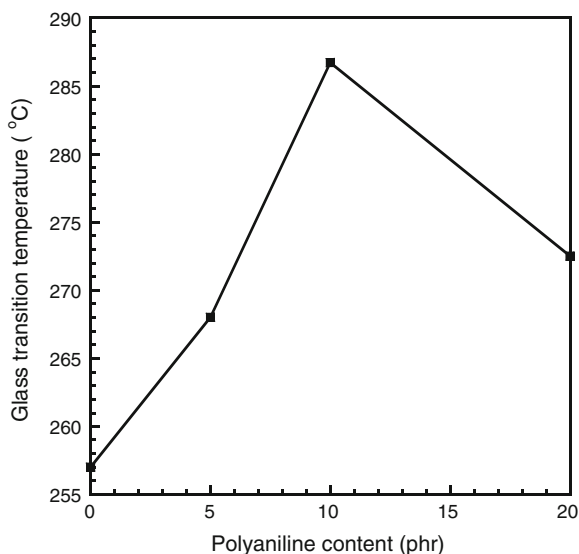
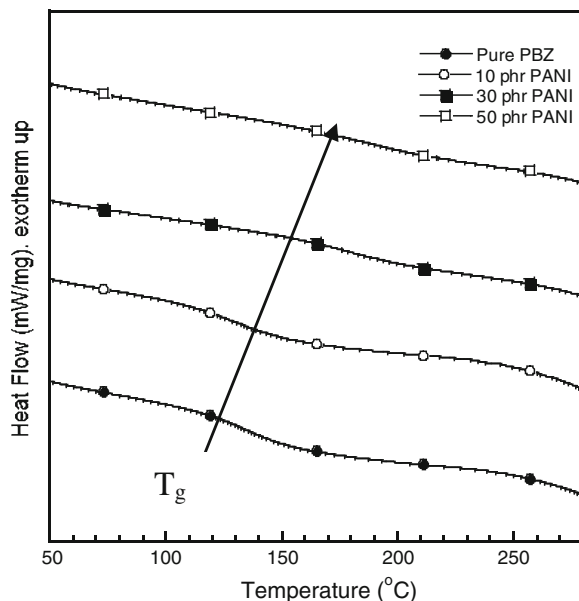


Fig. 7.8 Effect of polyaniline content on the glass transition temperature at 150 kGy [27]



ca.46 % (40 phr of PANI). This could be due to the amount of aromatic ring in the chemical structure of composites was higher than that of pure PBz [29]; therefore, the T_{dmax} was increased from ca. 396 °C (pure PBz) to ca. 414 °C (20 phr of PANI) and ca. 417 °C (40 phr of PANI). The researchers also reported that the glass transition temperature of the PBz/PANI nanocomposites was increased with the increase in PANI as presented in Fig. 7.9. This phenomenon is similar to that was found in the system of fumed-silica-filled PBz [30].

Fig. 7.9 DSC thermograms of the nanocomposites between PBZ and PANI [28]



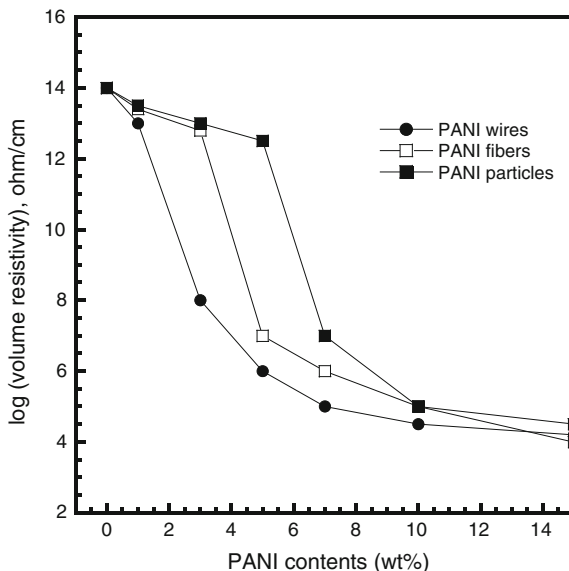
It is possibly attributed to the presence of the nano-particle that made the PBZ/PANI composite stiffer.

Nowadays, a few researches relevant to PBz filled with inherently conductive polymer have been conducted. However, some studies in the similar systems such as phenolic resin and epoxy have been reported [31–33]. Ho [31] studied the system of novolac phenolic resin blended with PANI doped with dodecyl benzenesulfonic acid (DBSA). The conductivity of the blends was determined at various doped polyaniline (PADB) as presented in Table 7.7. It could be noticed that the values of conductivity and glass transition temperature were increased with the increase in PADB. At the low content of PADB, the composites were heterogeneous.

Jia et al. [32] developed and characterized the epoxy-anhydride system containing PANI doped with DBSA. Two forms of PANI–DBSA were prepared at excess DBSA, i.e., powder and paste. The results exhibited that the paste form led to the dispersion improvement of PANI–DBSA in the resin and then the lower percolation content was shown. The excess amount of DBSA could impede the curing reaction of epoxy and hardener; however, this shortcoming could be remedied by the use of high concentration of accelerator. Recently, Jia et al. [33] prepared the composites composed of epoxy (EP) filled with hydrochloric acid-doped PANI with different shapes (particles, fibers, and wires). The electrical conductivity values of the composites were determined. The results indicated that the composites composed of PANI wires provided the lowest percolation threshold. The volume resistivity values of the composites at various PANI contents are presented in Fig. 7.10.

Table 7.7 The conductivity and glass transition temperature of the Novolac phenolic resin blended with PADB [31]

Novolac/ PADB	Optical microscope image	Apparent conductivity ($S\text{ cm}^{-1}$)	Normalized conductivity ($S\text{ cm}^{-1}$)	Glass transition temperature ($^{\circ}\text{C}$)
99/1	Heterogeneous	0.06	6.5	49
70/30	Homogeneous	2.18	7.3	58
50/50	Homogeneous	2.74	5.5	65
30/70	Homogeneous	3.47	5.0	66

Fig. 7.10 Resistivity of the EP/PANI composites with different PANI shapes [32]

7.5 Carbon-Based Electrically Conductive Fillers and Their Polymer Composites

Carbon-based materials (such as carbon nanotube, carbon fiber, graphene) have played an important role as electrically conductive filler. In the recent times, there have been many researches related to the composites filled with carbon-based filler [34, 35]. The comparison of the properties between carbon nanotube and graphite is exhibited in Table 7.8 [35].

7.5.1 Carbon Nanotube Filled Composites

In nature, carbon nanotube possesses many intriguing properties such as high flexibility, low density, and large aspect ratio (as high as over 1,000) [34]. Many

Table 7.8 Comparison of properties of carbon nanotube and graphite [35]

Property	Carbon Nanotube	Graphite
Density (g cm^{-3})	0.8 for SWCNT; 1.8 for MWCNT	2.26
Elastic Modulus (TPa)	ca. 1 for SWNT ca. 0.3–1 for MWNT	1
Strength (GPa)	50–500 for SWNT 10–60 for MWNT	130
Resistivity ($\mu\Omega \text{ cm}$)	ca. 5–50	50

publications have been focused on the electrical properties of the polymer filled with this kind of nano-filler. The electrical properties of some epoxy composites filled with both single-walled carbon nanotube (SWCNT) and multi-walled carbon nanotube (MWCNT) are summarized as presented in Table 7.9. It could be noticed that the processing method and types of the CNT have effects on the electrical conductivity and percolation content.

Recently, there has been a research on benzoxazine-functionalized multi-walled carbon nano-tubes using benzoxazine-containing compound (BPA-FBz) and polymer (PFBz). The results revealed that the cross-linked pellets of MWCNT-FBz and MWCNT-PFBz provided surface electrical conductivity of 0.05 S/cm.

Table 7.9 Some epoxy composites filled with carbon nanotube (CNT) and their electrical properties [34]

Type of carbon nanotube	Processing method	Matrix electrical conductivity (S/m)	Composite electrical conductivity (S/m)	Percolation content (wt%)	References
MWCNT	Solution mixing	ca. 4×10^{-9}	ca. 0.4	0.18	[36]
MWCNT	Bulk mixing	ca. 10^{-8}	ca. 0.2	0.5–1	[37]
Aligned MWCNT	Shear mixing	ca. 10^{-9}	ca. 2	0.0025	[38]
SWCNT	High frequency sonication method	–	ca. 1.25×10^{-3}	0.074	[39]
MWCNT	Solution mixing	ca. 10^{-7}	ca. 0.5	0.5	[40]
SWCNT	Solution mixing	ca. 2×10^{-11}	ca. 10	0.062	[41]
MWCNT	Calendering process	ca. 10^{-8}	ca. 0.01	Less than 0.1	[42]
MWCNT	Calendering process	ca. 10^{-15}	ca. 50	Less than 0.1	[43]
MWCNT	Solution mixing	1.2×10^{-14}	ca. 3×10^{-3}	0.6	[44]
SDS ^a Suspended MWCNT	Bulk mixing	5.1×10^{-12}	ca. 2.5×10^{-7}	0.5	[45]
MWCNT	Roll milling	ca. 10^{-15}	ca. 0.1	0.1	[46]

^a SDS = Sodium dodecyl sulfate

The composites between BPA-FBz and MWCNT-FBz rendered high electrical conductivities (ca. 7×10^{-5} S/cm) with good mechanical strength [47].

7.5.2 Graphene- and Graphene-Based Polymer Nanocomposites

Recently, graphene-/graphite-based polymer nanocomposites have attracted the attention of the researchers. The interesting point of view is that the enhancement of properties of the polymer could be obtained at very low content of loaded filler [48–50]. Table 7.10 presents the electrical properties of epoxy nanocomposites with different types of graphene-/graphite-based fillers.

Recently, Kimura et al. [51] developed benzoxazine resin composites filled with graphite for the bipolar plate in fuel cell. The researchers compared the electrical conductivity values of benzoxazine composites and phenolic composites filled with different types of graphite particles, i.e., synthetic graphite (SG), expanded graphite (EP), and natural graphite (NG). The resistivity values of the composite are shown in Table 7.11. It could be noticed that the electrical resistivity of the graphite filled composite based on benzoxazine resin was lower than that of the one based on phenolic resin. This is possibly attributed the fact that benzoxazine provide better flow ability and lower viscosity, leading to the smaller gap between the graphite particles.

Table 7.10 Electrical properties of graphene-/graphite-based epoxy nanocomposites [35]

Type of filler	Filler content	Process	Conductivity of matrix (S/m)	Conductivity of composite (S/m)	References
EG	3.0 wt%	Sonication	1×10^{-13}	1×10^{-4}	[48]
EG	2.5 vol%	Solution	1×10^{-15}	1×10^{-2}	[49]
Graphene	0.52 vol%	Solution	1×10^{-15}	1×10^{-2}	[50]

^a Expanded graphite

Table 7.11 Comparison of electrical conductivity of the graphite-filled benzoxazine and phenolic composites [51]

Matrix	Electrical resistivity (mΩ cm)		
	SG	EP	NG
Benzoxazine cured at 180 °C	4.8	2.4	4.6
Benzoxazine cured at 200 °C	4.1	2.2	4.4
Phenolic resin	5.2	2.9	8.8

Table 7.12 Electrical conductivity and percolation threshold of the composites filled with metal particles [52]

Composite	Log (conductivity) of the polymer (S/m)	Log (conductivity) of the composite at maximum (S/m)	Volume fraction of filler at percolation threshold
Epoxy/Copper	-12.8	5.2	0.050
Epoxy/Nickel	-12.8	4.8	0.085
PVC/Copper	-13.5	5.8	0.050
PVC/Nickel	-13.5	4.5	0.040

7.6 Metal Fillers and Their Polymer Composites

Up till now, it is interesting that there has been no study focused on the electrical conductivity of benzoxazine composites filled with metal particles. However, Mamunya et al. [52] studied the effect of metal content and electrical conductivities of the epoxy resin composites and PVC composites with copper and nickel filler. The researcher reported that the percolation threshold depends on the shape and type of spatial distribution. The values of electrical conductivity and percolation threshold are shown in Table 7.12. The difference between the percolation threshold of epoxy/nickel and epoxy/copper is relevant to the particle shape having an effect on the packing density.

It could be noticed that the metal-based fillers render relatively higher conductivity than carbon-based filler materials, whereas carbon-based fillers could render relatively lighter weight than the metal-based [53].

7.7 Potential Applications of Electrically Conductive Polybenzoxazine Composites

The electrically conductive materials can be potentially applied in many fields such as electrostatic materials, conductive adhesives, electromagnetic shielding, printed circuit boards, antistatic clothing, piezoceramics, diodes and transistors. Moreover, they could be used as chemical, biochemical, and thermal sensors, electrical displays, rechargeable batteries and solid electrolytes, ion exchange membrane [54, 55]. Recently, many patents related to the conductive thermosetting have been issued. For example, Sugino et al. [56] invented the electrically conductive, thermosetting materials used as a semiconductor element mounting board. Nakao [57] invented the conductive thermosetting adhesive tape that includes a metallic foil and thermosetting adhesive layer on one side of the metallic foil. Atkin and Beach [58] invented a conductive thermoset material to provide shielding against electromagnetic (EMI) radiation. Chikaoka [59] invented the multilayer piezoelectric element constructed from a plurality of thin piezoelectric layers. Fitts [60] invented a conductive, moldable composite material for

the manufacture of electrochemical cell components comprising a thermosetting resin system and conductive filler.

References

1. Trost T (2006) Electrostatic discharge (ESD)—facts and faults—a review. (A 1995 article in) *Packag Technol Sci* 8(5):231–247
2. Kimura H, Ohtsuka K, Matsumoto A (2011) Curing reaction of bisphenol-A based benzoxazine with cyanate ester resin and the properties of the cured thermosetting resin. *Express polym lett* 5(12):1113–1122
3. ESD-ADV 1.0-1994, Glossary of terms, ESD Association, Rome, NY
4. Al-Saleh HM, Sundararaj U (2009) A review of vapor grown carbon nanofiber/polymer conductive composites. *Carbon* 47:2–22
5. Amarasekera J (2005) Conductive plastics for electrical and electronic applications. *Reinf Plast* 49(8):38–41
6. Markarian J (2005) Increased demands in electronics drive additive developments in conductivity. *Plast Addit Compd* 7(1):26–30
7. Das NC, Yamazaki S, Hikosaka M, Chaki TK, Khastgir D, Chakraborty A (2005) Electrical conductivity and electromagnetic interference shielding effectiveness of polyaniline-ethylene vinyl acetate composites. *Polym Int* 54(2):256–259
8. Huang JC (1995) EMI shielding plastics: a review. *Adv Polym Technol* 14(2):137–150
9. Wilney KI, Vaia RA (2007) Polymer nanocomposites. *MRS Bull* 32(4):314–319
10. Hussain M, Choa Y-H, Niihar K (2001) Fabrication process and electrical behavior of novel pressure-sensitive composites. *Composites Part A* 32:1690–1696
11. Kirkpatrick S (1973) Percolation and conduction. *Rev Mod Phys* 45:574–588
12. Stauffer D (1987) Introduction to percolation theory. Taylor and Francis, London 89
13. Zhang W, Dehghani-Saniy AA, Blackburn RS (2007) Carbon based conductive polymer composites. *J Mater Sci* 42:3408–3418
14. Miyasaka K, Watanabe K, Jojima E, Aida H, Sumita M, Ishikawa K (1982) Electrical conductivity of carbon-polymer composites as a function of carbon content. *J Mater Sci* 17:1610–1616
15. Kitazaki Y, Hata T (1972) *J Adhesion Soc Jpn* 8(3):131–137
16. Johnson KL, Kendall K, Robert AD (1971) Surface energy and the elastic solids. *Proc R Soc London* 324:301–313
17. Sau KP, Chaki TK, Khastgir D (1997) Conductive rubber composites from different blends of ethylene-propylene-diene rubber and nitrile rubber. *J Mater Sci* 32:5717–5724
18. Sau KP, Chaki TK, Khastgir D (1998) Carbon fibre filled conductive composites based on nitrile rubber (NBR), ethylene propylene diene rubber (EPDM) and their blend. *Polymer* 39:6461–6471
19. Wallace GG, Spinks GM, Kane-Maguire LP, Teasdale PR (2009) Conductive electroactive polymers: intelligent polymer systems. CRC Press, U. S. A
20. Chandrasekhar P (2002) Conducting polymers, fundamentals and applications: a practical approach. Kluwer Academic Publishers, Boston
21. Bhadra S, Khastgir D, Singha NK, Lee JH (2009) Progress in preparation, processing and applications of polyaniline. *Prog Polym Sci* 34:783
22. Bhadra S, Singha NK, Khastgir D (2006) Polyaniline by new miniemulsion polymerization and the effect of reducing agent on conductivity. *Synth Met* 156:1148–1154
23. Bhadra S, Chattopadhyay S, Singha Nk, Khastgir D (2007) effect of different reaction parameters on the conductivity and dielectric properties of polyaniline synthesized

- electrochemically and modeling of conductivity against reaction parameters through regression analysis *J Polym Sci Polym Phys* 45:2046–2059
24. Bhadra S, Singha NK, Khastgir D (2007) Dual functionality of PTSA as electrolyte and dopant in the electrochemical synthesis of polyaniline, and its effect on electrical properties. *Polym Int* 56:919–927
 25. Bhadra S, Singha NK, Khastgir D (2007) Electrochemical synthesis of polyaniline and its comparison with chemically synthesized polyaniline. *J Appl Polym Sci* 104:1900–1904
 26. Bhadra S, Khastgir D (2007) Degradation and stability of polyaniline on exposure to electron beam irradiation (structure-property relationship). *Polym Degrad Stab* 92:1824–1832
 27. MacDiarmid AG (1997) Polyaniline and polypyrrole: where are we headed. *Synth Met* 84:27–34
 28. Tiptipakorn S, Suwanmala P, Hemvichian K, Pornputtanakul Y (2012) Effects of electron beam on irradiated polyimide/polyaniline composites. *Adv Mat Res* 550–553:861–864
 29. Tiptipakorn S, Duangchan A, Pornputtanakul Y, Rimdusit S (2012) Thermal characterization of polybenzoxazine/polyaniline nanocomposites. *Proceeding in pure and applied chemistry international conference 2012 (PACCON2012)*:1653–1655
 30. Rimdusit S, Punson K, Dueramae I, Somwangthanroj A, Tiptipakorn S (2011) Rheological and thermomechanical characterizations of fumed silica-filled polybenzoxazine nanocomposites. *Eng J* 15:27–38
 31. Ho KS (2002) Effect of phenolic based polymeric secondary dopants on polyaniline. *Synth Met* 126:151–158
 32. Jia W, Tchoudakov R, Segal E, Joseph R, Narkis M, Siegmann A (2003) Electrically conductive composites based on epoxy resin with polyaniline-DBSA fillers. *Synth Met* 132:269–278
 33. Jia QM, Li JB, Wang LF, Zhu JW, Zheng M (2007) Electrically conductive epoxy resin composites containing polyaniline with different morphologies. *Mater Sci Eng A* 448:356–360
 34. Spitalsky Z, Tasis D, Papagelis K, Galiotis C (2010) Carbon nanotube-polymer composites: chemistry, processing, mechanical and electrical properties. *Prog Polym Sci* 35:357–401
 35. Sengupta R, Bhattacharya M, Bandyopadhyay S, Bhowmick AK (2011) A review on the mechanical and electrical properties of graphite and modified graphite reinforced polymer composites. *Prog Polym Sci* 36:638–670
 36. Sander J, Shaffer MSP, Prasse T, Bauhofer W, Schulte K, Windle AH (1999) Development of a dispersion process for carbon nanotubes in an epoxy matrix and the resulting electrical properties. *Polymer* 40:5967–5971
 37. Alloul A, Bai S, Chen HM, Bai J (2002) Mechanical and electrical properties of a MWNT/epoxy composite. *Compos Sci Technol* 62:1993–1998
 38. Sandler JKW, Kirk JE, Kinloch IA, Shaffer MSP, Windle AH (2003) Ultra-low electrical percolation threshold in carbon-nanotube-epoxy composites. *Polymer* 44:5893–5899
 39. Kim B, Lee J, Yu I (2003) Electrical properties of single-wall carbon nanotube and epoxy composites. *J Appl Phys* 94:6724–6728
 40. Song YS, Youn JR (2005) Influence of dispersion states of carbon nanotube and epoxy composites. *Carbon* 43:1378–1385
 41. Li N, Huang Y, Du F, He X, Lin X, Gao H et al (2006) Electromagnetic interference (EMI) shielding of single-walled carbon nanotube epoxy composites. *Nano Lett* 6:1285–1288
 42. Gojny FH, Wichmann MHG, Fiedler B, Kinloch IA, Bauhofer W, Windle AH, Schulte K (2006) Evaluation and identification of electrical and thermal conduction mechanisms in carbon nanotube/epoxy composite. *Polymer* 47:2036–2045
 43. Thostenson ET, Chou TW (2006) Processing-structure-multi-functional property relationship in carbon nanotube/epoxy composites. *Carbon* 44:3022–3029
 44. Yuen SM, Ma CC, Wu HH, Kuan HC, Chen WJ, Liao SH, Hsu CW, Wu HL (2007) Preparation and thermal, electrical, and morphological properties of multiwalled carbon nanotube and epoxy composites. *J Appl Polym Sci* 103:1272–1278

45. Santos AS, Leite T, Furtado CA, Welter C, Pardini LC, Silva GG (2008) Morphology, thermal expansion, and electrical conductivity of multiwalled carbon nanotube/epoxy composites. *J Appl Polym Sci* 108:979–986
46. Thostenson ET, Ziaee S, Chou TW (2009) Processing and electrical properties of carbon nanotube/vinyl ester nanocomposites. *Compos Sci Technol* 69:801–804
47. Wang YH, Chang CM, Liu YL (2012) Benzoxazine-functionalized multi-walled carbon nanotubes for preparation of electrically-conductive polybenzoxazine. *Polymer* 53(1):106–112
48. Jovic N, Dudic D, Montone A, Antisari MV, Mitric M, Djokovic V (2008) Temperature dependence of the electrical conductivity of epoxy/expanded graphite nanosheet composites. *Scripta Mater* 58:846–849
49. Celzard A, McRae E, Mareche JF, Furdin G, Dufort M, Deleuze C (1996) Composites based on micron-sized exfoliated graphite particles: electrical conduction, critical exponents and anisotropy. *J Phys Chem Solids* 57:715–718
50. Lianga J, Wanga Y, Huang Y, Maa Y, Liua Z, Caib J (2009) Electromagnetic interference shielding of graphene/epoxy composites. *Carbon* 47:922–925
51. Kimura H, Ohtsuk K, Matsumoto A (2012) Performance of graphite filled composite based on benzoxazine resin. II. Decreasing the moulding time of the composite. *Polym Polym Comps* 20(8):717–724
52. Mamunya YP, Davydenko VV, Pissis P, Lebedev EV (2002) Electrical and thermal conductivity of polymer filled with metal powders. *Eur Polym J* 38:1887–1897
53. Khosla A (2010) Electrically conductive, thermosetting elastomeric material and uses therefore. US Patent No. US 20100116527 A1
54. Chandrasekhar P (1999) *Conducting polymers, fundamentals and applications: a practical approach*, Kulwer Academic Publishers, London
55. Skotheim TA, Elsenbaumer RL, Reynolds JR (1998) *Handbook of Conducting Polymer*. Marcel Dekker, Inc, New York
56. Sugino M, Hara H, Meura T (2012) Semiconductor element mounting board. US Patent No. 8,269,332
57. Nakao K (2012) Conductive thermosetting adhesive tape. US Patent No. 20120325518 A1
58. Atkins T, Beach BA (2012) EMI shielding thermoset article. US Patent No. 20120107538 A1
59. Chikaoka Y (1995) Multilayer piezoelectric element. US Patent No. 5406164
60. Fitts BB (2004) Thermosetting composition for electrochemical cell components and methods of making thereof. US Patent No. 6811917 B2

Index

A

Acoustic mismatch, 70
Adhesion, 55, 58, 85, 88, 89, 93, 110, 111
Aggregate, 72, 73, 76
Aldehyde, 29
Alloy, 96–98, 100, 106, 108, 112, 113, 120, 123, 124, 125, 127, 128, 129, 131, 133, 134
Anisotropic, 76
Areal density, 121, 133
Armor, 117, 118, 123, 127, 128, 132
Aspect ratio, 71, 73, 76, 77
A-stage viscosity, 49

B

Ballistic resistance, 118, 120
Benzoxazine resin, 48, 49, 124
Bimodal mixtures, 54
Bulk property, 73, 76

C

Carbon-based materials, 150
Carbon fiber, 150
Carbon nanotube, 150
Carboxylic acid, 40
Cardanol, 108
Cashew nut shell liquid, 108, 113
 Char yield, 11, 15, 23, 29, 37–39, 43, 88, 98, 100, 101, 103, 108, 112
Coefficient of thermal expansion, 8, 13, 125
Composites, 84–86, 89–92, 96, 98, 101, 106, 108, 112
Conductive adhesives, 153
Conductive filler, 141, 142, 150
Conductive path, 141, 142
Copper, 153
Coupling agent, 69

Crosslink density, 15, 30, 31, 33, 38, 41–43, 125, 128
Crosslinked structure, 3
Curing, 86, 98, 101–103, 109, 113
Cyanate, 139

D

Degradation temperature, 7, 15, 23, 37, 38, 41, 88, 100, 108, 128
Delamination, 119, 130
Density, 87, 90, 103, 105
Dianhydride, 40, 42
Dielectric constant, 2, 16, 18
Differential scanning calorimetry analysis, 5
Diglycidyl ether, 30
Dimensional stability, 2, 20
Doping, 143
Dynamic mechanical analysis, 6, 106, 112

E

Elastic modulus, 119, 124, 151
Electrical conductivity, 139, 141–143, 145–147, 149, 151–153
Electron beam, 147
Electronic packaging encapsulant, 68
Electrostatic, 139, 140, 153
Epoxy, 30, 33, 69, 75, 85, 101–105, 108, 113, 123, 129–131, 149, 151–153
Esterification, 102
 Exothermic peak, 6, 13

F

Fickian-type diffusion, 81, 95
Fick's law, 94
Flake, 72, 74, 75
Flame retardance, 29

Flammability, 85, 87, 96, 97, 99, 101
Flexibility, 30, 31, 38, 41
Flexural modulus, 88, 90, 97, 100, 113
Flexural strength, 33

G

Gelation, 104
Gel point, 5
Glass-transition temperature, 2, 9, 24, 30, 32, 33, 35, 36, 38, 39, 41, 42, 44, 55, 58, 68, 88, 101, 106, 107, 113, 124, 128, 136
Graphite, 150, 152

H

Heat capacity, 67, 74
Heat resistance, 15
Hexagonal boron nitride, 67, 72
Highly filled composite, 47, 48, 58, 70, 71, 105
Hydrophobicity, 16, 18
Hydroxyl group, 30, 32, 35, 36, 40, 123, 124

I

Impact velocity, 132
Inherently conductive polymer, 143, 144, 149
Insulative, 140, 143
Interfacial interaction, 58

K

Kevlar fiber, 131
Kinetic, 103, 104

L

Lattice vibrational energy, 70
Lignin, 42
Limiting oxygen index, 7, 98, 99
Liquefying temperature, 5
Loss modulus, 6, 9, 12, 15, 39, 106, 107

M

Mannich bridge, 37
Maximum packing, 87, 105
Mechanical modulus, 2
Mechanical properties, 29, 41
Mechanical strength, 2
Melt viscosity, 2, 4, 9, 23
Metal filler, 153
Microparticles

Miscibility, 33, 35, 36, 38
Moisture absorption, 16, 17, 18
Molding compound, 68, 71, 72, 81
Molecular weight, 30, 32, 33
Mole fraction, 41

N

Nanoparticles, 61
Nickel, 153
NIJ standard, 134
Novolac, 149

P

Packing density, 71–73
Particle packing, 50, 51, 54
Particle size distribution, 71, 73, 81
Path-dependent property, 73
Penetration, 118, 129, 134, 136
Percolation, 73, 74, 76, 77, 141, 142, 149, 151, 153
Phenolic, 29, 30, 36, 44, 85, 97–99, 101, 103, 113
Phonon scattering, 70
Poly(imide-siloxane), 38
Poly(N-vinyl-2-pyrrolidone), 35
Polyacetylene, 143, 145
Polyaniline, 143, 145–147, 149
Polybenzoxazine, 29, 30, 33, 35, 36, 38–40, 42, 43, 68–70, 72, 74, 76, 77, 79, 81, 86–90, 94, 96, 109, 112, 123, 124, 127, 129, 136, 139, 147, 149, 153
Polycaprolactone
Polyester, 37, 41
Polyimide, 38–40
Polypyrrole, 143, 145
Polythiophene, 143, 145
Polyurethane, 30, 32, 34
Potential applications, 43
Prepolymer, 32, 33
Prepreg, 20, 21
Processability, 47–49
Processing window, 49

R

Reactive diluents, 48
Reliability, 68
Rubbery plateau, 35

S

Self-polymerization, 1

- Self-extinguishable, 7
- Solvent-less synthesis, 4, 10
- Stability
 - Storage modulus, 6, 15, 34, 77, 106, 107, 110
- Sunflower oil, 37
- Surface hardness, 58
- Surface resistivity, 140
- Surface roughness, 112
- Synergism, 35, 39, 41
- Synergistic, 56

- T**
- Tan Δ , 15, 17
- Ternary system, 30, 32, 101, 103, 105, 113
- Thermal conductivity, 67–70, 74, 76, 81
- Thermal diffusivity, 67
- Thermal expansion coefficient, 67, 68
- Thermally conductive composite, 77
- Thermal polymerization, 4, 14
- Thermal properties, 29, 30, 35, 37, 38

- Thermal stability, 2, 7, 13, 15, 23
- Thermogravimetric analysis, 7, 108

- U**
- Urethane, 32, 33, 37, 123, 124, 127, 129

- V**
- Viscosity, 87, 89, 102, 113
- Volume resistivity, 139, 140, 149

- W**
- Water absorption, 2, 24, 79, 81, 85, 87, 90, 91, 94, 101
- Water uptake, 29
- Wetting characteristic, 47
- Wood fiber, 86
- Wood polymer composites, 54
- Woodflour, 84, 86–90, 92, 96, 101